UNIVERSITÄT LEIPZIG

REPORT

Institute für Physik
The Physics Institutes

2004

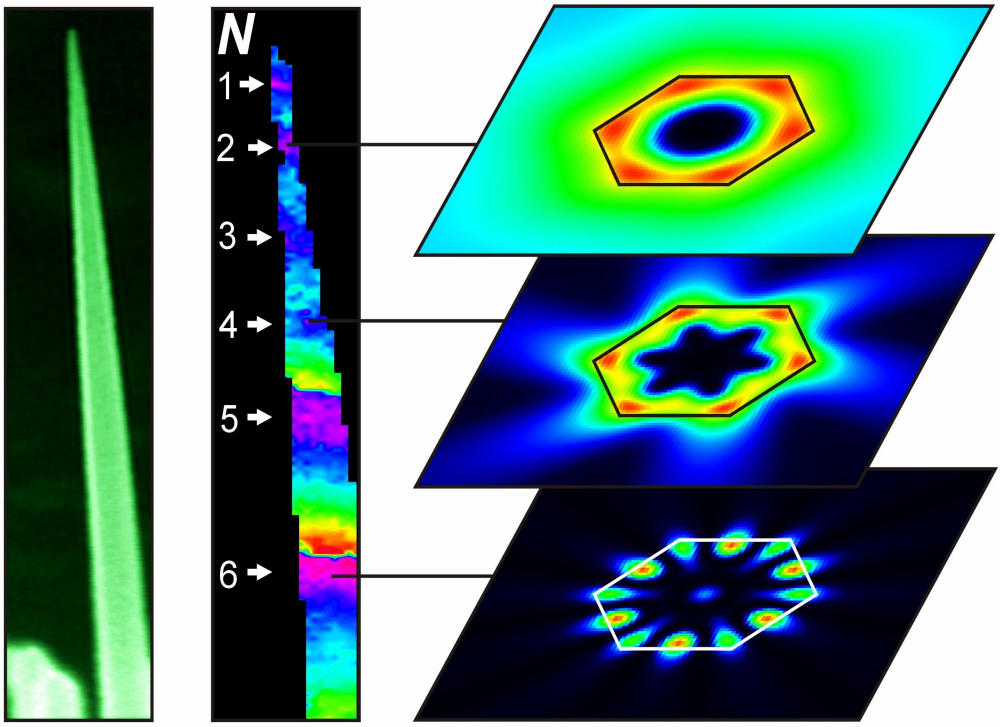

The Physics Institutes of Universität Leipzig, Report 2004
M. Grundmann, ed.
ISBN 3-934178-46-4
Copy Editing & Typesetting: Gregor Zimmermann

Printed in Germany by
MERKUR Druck und Kopierzentrum GmbH, Leipzig

online available at
http://www.uni-leipzig.de/~exph2/report_2004.pdf

Front cover
The smallest whispering galleries for light. *Left*: Scanning electron microscopy image of a ZnO nanoneedle grown with pulsed laser deposition. The bottom width of the needle is 800 nm, the length is 24 µm. The needle has a hexagonal cross section and represents a nanoscopic optical resonator. *Center*: Energy of maximum emission intensity from the so-called 'green' band in false color scale. Spectral modulation is due to whispering gallery resonant modes. *N* denotes the mode number responsible for the emission maximum. *Right*: Numerical simulation (with boundary element method) of the mode pattern of the involved whispering gallery modes for *N*=2,4,6.

Back cover
Conference announcement for 2005.

Institut für Experimentelle Physik I
Institut für Experimentelle Physik II
Institut für Theoretische Physik
Fakultät für
Physik und Geowissenschaften
Universität Leipzig

Institute for Experimental Physics I
Institute for Experimental Physics II
Institute for Theoretical Physics
Faculty of Physics and Geosciences
Universität Leipzig

Report 2004

Addresses

Institute for Experimental Physics I
Linnéstraße 5
D-04103 Leipzig, Germany
Phone: +49 341 9732 551
Fax: +49 341 9732 599
WWW: http://www.uni-leipzig.de/~gasse/nysid_a/inst/exp_1.htm

Institute for Experimental Physics II
Linnéstraße 5
D-04103 Leipzig, Germany
Phone: +49 341 9732 650
Fax: +49 341 9732 668
WWW: http://www.uni-leipzig.de/~exph2/

Institute for Theoretical Physics
Vor dem Hospitaltore 1
D-04103 Leipzig, Germany
Phone: +49 341 9732 420
Fax: +49 341 9732 548
WWW: http://www.physik.uni-leipzig.de/
Mailing address: Augustusplatz 10/11, 04109 Leipzig, Germany

Preface

The three Institutes of Physics of Universität Leipzig present their joint research report covering the year 2004. It documents the scientific progress made in various fields. The year has brought intensified collaboration within and between the Physics Institutes and with the 'outside' world.

Prof. Dieter Geschke from the Polymer Physics Group of Institute for Experimental Physics I retired in 2004. We wish him well in his retirement, in particular that he can enjoy it in fine health. We have made good progress in the search for his successor.

In the Institute for Theoretical Physics, the year 2004 was marked by two decisions that will have far-reaching consequences in the future. They relate to the filling of two open professorships. The University finally approved pursuance of two fields of research that are new to the Institute: *Soft-matter physics* with a strong focus on biophysics and *gravitational physics* with emphasis on the relation to quantum-field theory. For soft-matter physics, the process of hiring was finished in 2004 and we are happy to announce that professor Klaus Kroy (coming from the Hahn–Meitner–Institut, Berlin) took office in March 2005. We look forward to his initiatives. For the position in gravitational physics, negotiations could not yet be finalized since the change in the salary system for professors from 'C'- to 'W'-salaries has increased the administrative effort (and reduced the salaries). However, the negotiations are in their final stage, and we are confident that we can welcome an active new colleague by October 2005.

As of July 2004, Prof. Marius Grundmann coordinates the Network of Excellence SANDiE on 'Self-assembled semiconductor nanostructures for new devices in photonics and electronics' in the 6th framework programme of the EC. The network incorporates 28 partners from Portugal to Russia, including four industrial companies, MPG, CNRS and the A.F. Ioffe-Institute. 9.2 M€ will be spent in the next four years to promote the integration across Europe in the scientific field of self-assembled nanostructures with respect to people (over 150 researchers and 110 PhD students) and the related equipment and infrastructure.

The 3 M€-European Community project on the transport optimization of nanoporous catalysts ('TROCAT') under the guidance of Prof. Jörg Kärger was completed successfully. It is so far the largest EC project completed at Universität Leipzig. The first International Research Training Group ('Internationales Graduiertenkolleg') at the University was established in 2004. It is dedicated to 'Diffusion in Porous Materials'. Under the joint sponsorship of the German and Dutch Science Foundations, DFG and NWO, it brings together professors and young scientists from the Institute for Experimental Physics I, as well as from the Institute for Theoretical Physics and Technical Chemistry, with their partners from the universities of Amsterdam, Delft and Eindhoven.

In the framework of the 'HbfG-Verfahren', a joint proposal of the Faculty of Physics and Earth Sciences and the Faculty of Chemistry and Mineralogy has been successful. We are grateful for the support of the University on all levels for this proposal. A field-emission electron microscope equipped with a focused ion-beam source (FEM–FIB) will open tremendous possibilities in the investigation, preparation and manipulation of nanostructures. The installation of this machine is scheduled for the fall of 2005. In particular, the work within the DFG Research Groups ('Forscherguppen') 404 ('Oxidic Interfaces') and 522 ('Architecture of nano- and micro-dimensional building blocks') will benefit from this versatile tool.

We are very grateful for the support of many funding agencies. Their support is acknowledged in the brief reports. Enjoy browsing through our book and catch some of our scientific spirit. You can do this best, however, by paying us a visit – welcome to Leipzig!

Leipzig, April 2005

F. Kremer
M. Grundmann
K. Sibold
Directors

Contents

1

Structure and Staff of the Institutes

1.1 Institute for Experimental Physics I

1.1.1 Office of the Director

Prof. Dr. Friedrich Kremer (director)
Prof. Dr. Jörg Kärger (vice director)

1.1.2 Physics of Anisotropic Fluids, Physik anisotroper Fluide

Prof. Dr. Friedrich Kremer

Secretary

Karin Girke

Technical staff

PTA Ines Grünwald Dipl. Ing. Jörg Reinmuth
Dipl. Phys. Wiktor Skokow
Dipl. Phys. Uwe Weber

Academic staff

Dr. Jianjun Li
Dr. Rongbiao Wang

PhD candidates

Dipl. Phys. Christof Gutsche
Dipl. Phys. Kati Kegler
Julius Tsuwi Kazungu, M.Sc.
Dipl. Biochem. Mathias Salomo

Dipl. Phys. Anatoli Serghei
Michael Tammer, M.Sc.

Students

Shahrul Kadri Ayop

1.1.3 Physics of Interfaces, Grenzflächenphysik

Prof. Dr. Jörg Kärger

Secretary

Katrin Kunze

Technical staff

Dipl.-Phys. Cordula Bärbel Krause
Dipl.-Ing. Bernd Knorr
Lutz Moschkowitz
Ing. Dagmar Prager

Academic staff

Prof. Dr. Peter Bräuer
PD Dr. Horst Ernst
Prof. Dr. Dieter Freude
Dr. Karen Friedemann
Dr. Petrik Galvosas
Dr. Wilfried Heink
Prof. (i.R.) Dr. Dr. h.c. Harry Pfeifer
Dr. Andreas Schüring
Dr. habil. Frank Stallmach
PD Dr. Brigitte Staudte
PD Dr. Sergey Vasenkov
Dr. Rustem Valiullin

PhD candidates

Dipl.-Phys. Constantijn Blondel
Dipl.-Phys. Andreas Brzank
Dipl.-Phys. Christian Chmelik
Dipl.-Phys. Moises Fernandez
Dipl.-Phys. Johanna Kanellopoulos
Dipl.-Phys. Pavel Kortunov
Dipl.-Phys. Denis Schneider
Dipl.-Phys. Konstantin Ulrich

Students

Tomas Binder
Lars Heinke
Volker Künzel
Sergey Naumov
Markus Wehring

1.1.4 Soft Matter Physics, Physik der weichen Materie

Prof. Dr. Josef A. Käs

Secretary

Claudia Honisch

Technical Staff

Dipl.-Ing. Undine Dietrich
Dipl.-Phys. Bernd Kohlstrunk
Ing. Elke Westphal

Academic Staff

Prof. Dr. Mathias Lösche (on leave of absence)
Prof. Dr. Herbert Schmiedel
Dr. Jochen Guck
Dr. Carsten Selle

PhD candidates

Timo Betz
Claudia Brunner
Susanne Ebert
Allen Ehrlicher
Kristian Franze
Brian Gentry
Jens Gerdelmann
Michael Gögler
Daniel Koch
Bryan Lincoln
Karla Müller
Soyeun Park
Stefan Schinkinger
Thomas Siegemund
David Smith
Björn Stuhrmann
Falk Wottawah

Students

Ann Falk
Cosima Koch
Steffen Lindert
Mireille Martin
Daniel Rings
Maren Romeyke
Frank Sauer
Stefan Surber
Lydia Woiterski
Cornel Wolf

1.2 Institute for Experimental Physics II

1.2.1 Office of the Director

Prof. Dr. Marius Grundmann (director)
Prof. Dr. Tilman Butz (vice director)

1.2.2 Nuclear Solid State Physics, Nukleare Festkörperphysik

Prof. Dr. Tilman Butz

Technical staff

Dipl.-Ing. Bernd Krause
PTA Raimund Wipper

Academic staff

Dr. Dietmar Lehmann
Dr. Tilo Reinert
PD Dr. Wolfgang Tröger
Dr. Jürgen Vogt

PhD candidates

Dipl.-Phys. Frank Heinrich
Dipl.-Phys. Christoph Meinecke
Dipl.-Phys. Frank Menzel
Charlotta Nilsson, M.Sc.
Esam Eldin Tagelsir Ahmed Mohamed, M.Sc.
Dipl.-Phys. Daniel Spemann

Students

Sarah Bühler (Astrophysik, LMU München)
Philipp Eigenmüller (Astrophysik, Tautenburg)
Anja Fiedler
Sven Friedemann
Sebastian Haan (Teilchenphysik, DESY/Zeuthen)
Arnd Hinze (Teilchenphysik, DESY/Zeuthen)
Jan Kohnert (Astrophysik, Tautenburg)
Pedro Hugo Ferreira Natal da Luz
Christian Ostwald
Silvio Petriconi
Stephan Werner

1.2.3 Physics of Dielectric Solids, Physik Dielektrischer Festkörper

Prof. Dr. Dieter Michel

Secretary

Ursula Seibt

Academic staff

apl. Prof. Dr. Rolf Böttcher (Hochschuldozent)
apl. Prof. Dr. Andreas Pöppl
Dr. habil. Horst Braeter
Dr. André Pampel
Dr. Venkatesan Umamaheswari

Technical staff

Dr. Winfried Böhlmann
Dipl.-Ing. Joachim Hoentsch
Dipl.-Phys. Gert Klotzsche
Ursula Heinich

PhD candidates

Emre Erdem
Özlen Ferruh Erdem
Abdoulaye Taye
Nagarajan Vijayasarathi
Anke Weller

Students

Andreas Bunge
Eike Bierwirth
Julia Köhler

External members

Dima Yaskov
Pavel Sedykh
Maria Popova
(PhD Students from St. Petersburg State University)

1.2.4 Semiconductor Physics, Halbleiterphysik

Prof. Dr. Marius Grundmann

Secretary

Gabriele Adami-Kirschey (until 5/2004)
Anja Heck

SANDiE network office

Birgit Wendisch
Dipl.-Phys. Alexander Weber

Technical staff

Dipl.-Phys. Gabriele Benndorf
Ing. Gisela Biehne
Dipl. Ing. Holger Hochmuth
Dipl.-Phys. Jörg Lenzner
PTA Gabriele Ramm
PTA Roswitha Riedel

Academic staff

Dr. Michael Lorenz
PD Dr. Rainer Pickenhain
Prof. Dr. Bernd Rheinländer
Dr. Heidemarie Schmidt

PhD candidates

Dipl.-Phys. Jens Bauer
Mariana Diaconu, M.Sc.
Dipl.-Phys. Daniel Fritsch

Dipl.-Phys. Karsten Goede
Susanne Heitsch, M.Sc.
Dipl.-Phys. Tino Hofmann
Dipl.-Ing. Stefan Jaensch
Dipl.-Phys. Thomas Nobis
Dipl.-Phys. Andreas Rahm
Dipl.-Phys. Rüdiger Schmidt-Grund
Dipl.-Phys. Alexander Weber
Dipl.-Phys. Holger von Wenckstern
Dipl.-Phys. Gregor Zimmermann (from 12/2004)

Students

Chengnui Bekeny
Matthias Brandt
Anke Carstens
Christian Czekalla
Wadinga Fomba
Heiko Frenzel
Marcus Gonschorek
Tobias Gühne
Robert Johne
Hendrik Paetzelt
Marc Schillgalies
Matthias Schmidt
Christian Schulz
Chris Sturm
Swen Weinhold
Gregor Zimmermann

1.2.5 Solid State Optics and Acoustics, Festkörperoptik und -akustik

Prof. Dr. Wolfgang Grill

Secretary

Gabriele Adami-Kirschey

Technical staff

Adelheid Geyer
Hans-Joachim vom Hofe
Dipl. Ing. (FH) Ulrike Teschner

Academic staff

Dr. Tino Hofmann
Dr. Stefan Knauth
Dr. Zbigniew Kojro
Dr. Volker Riede
PD Dr. habil. Mathias Schubert
PD Dr. habil. Reinhold Wannemacher

PhD candidates

Nurdin Ashkenov, M. Sc.
Beri N. Mbenkum, M. Sc.
Carsten Bundesmann
Dipl.-Phys. Jens Jahny
Dipl.-Phys. Oliver Lenkeit
Claas von Middendorff, M. Sc.
Wilfred Ngwa, M. Sc.
Evgeny Twerdowski, M. Sc.

Students

Tsvetan Chavdarov
Mario Saenger
A. Kamanyi
Shouwei Dong
Mingyu Dai
Micha Wiedenmann

1.2.6 Superconductivity and Magnetism, Supraleitung und Magnetismus

Prof. Dr. Pablo Esquinazi

Technical staff

Klaus Grünwald
Dipl.-Krist. Annette Setzer
Monika Steinhardt

Academic staff

Dr. Alberto Bollero Real
Dr. Kyoo-hyun Han
Dr. Roland Höhne
Dr. Hans-Christoph Semmelhack
Dr. Michael Ziese

PhD candidates

Dipl.-Phys. Roberto Ocaña
Dipl.-Phys. Heiko Kempa
Dipl.-Phys. Kristian Schindler

Students

Kristian Schindler
Uwe Schaufuß
Konstantin Ulrich
Andreas Glaser
Roland Salzer
Norman Leps

1.3 Institute for Theoretical Physics

1.3.1 Office of the Director

Prof. Dr. Klaus Sibold (director)
Prof. Dr. Manfred Salmhofer (vice director)

Secretary

Gabriele Menge
Gloria Salzer
Lea Voigt

Library

Elfriede Thiele

1.3.2 Quantum Field Theory, Quantenfeldtheorie

Prof. Dr. Gerd Rudolph

Academic staff

PD Dr. Michael Bordag
Dr. Daniel Grumiller
Dr. Matthias Schmidt
Dr. Dmitri V. Vassilevich

Retired

Prof. em. Bodo Geyer
Prof. em. Armin Uhlmann
Prof. em. Wolfgang Weller

Permanent guests

Doz. Dr. Peter Alberti
Dr. Bernd Crell

PhD candidates

Szymon Charzynski, M.Sc.
Dipl.-Phys. Jörg Eilers
Dipl.-Phys. Stefan Neumeier
Alexei Strelchenko, M.Sc.

Students

Elisabeth Fischer
Nadine Große
Alexander Hertsch
Diana Kaminski
Hedwig Wilhelm
Oliver Witzel

1.3.3 Theory of Elementary Particles, Theorie der Elementarteilchen

Prof. Dr. Klaus Sibold

Academic staff

Dr. Paul Heslop
PD Dr. habil. Roland Kirschner
PD Dr. habil. Arwed Schiller
Dr. Yi Liao

1.3.4 Theory of Condensed Matter, Festkörpertheorie

Prof. Dr. Dieter Ihle (spokesperson)
Prof. Dr. Ulrich Behn
Prof. Dr. Adolf Kühnel (i.R.)

Academic staff

PD Dr. Winfried Kolley

PhD candidates

Dipl.-Phys. Iren Junger
Dipl.-Phys. Micaela Krieger-Hauwede

Students

Fabian Senf
Holger Schmidtchen
Reinhard Vogel

1.3.5 Computational Quantum Field Theory, Computerorientierte Quantenfeldtheorie

Prof. Dr. Wolfhard Janke

Academic staff

Dr. Michael Bachmann
Dr. Elmar Bittner
Dr. Leszek Bogacz
Dr. Peter Crompton
Dr. habil. Adriaan Schakel

PhD candidates

Dipl.-Phys. Andreas Nußbaumer
Dipl.-Phys. Thomas Vogel
Sandro Wenzel, M.Sc.

Students

Rainer Bischof
Goetz Kähler
Anna Kallias
Axel Krinner
Eric Lorenz
Rodrigo Megaides
Reinhard Schiemann
Jakob Schluttig
Stefan Schnabel

1.3.6 Molecular Dynamics / Computer Simulation, Molekü ldynamik / Computersimulation

Academic staff

Dr. rer. nat. habil. Horst Vörtler (speaker)
PD Dr. rer. nat. habil. Siegfried Fritzsche
Prof. Dr. rer. nat. habil. Reinhold Haberlandt
Dr. rer. nat. Andreas Schüring
Dr. rer. nat. Viatcheslav Kormilets (until 4/2004)

PhD candidates

BC Arthorn Loisruangsin
MS Oraphan Saengsawang (starting 10/2004)

1.3.7 Statistical Physics, Statistische Physik

Prof. Dr. Manfred Salmhofer

Academic staff

Dr. Oliver Lauscher

PhD candidates

Walter Pedra (DEA, Ecole Polytechnique, Palaiseau)
Dipl-Phys. Christoph Husemann

Students

Friedmar Schütze
Kay–Uwe Giering

I

Institute for Experimental Physics I

2

Physics of Anisotropic Fluids

2.1 Introduction

In the year 2004 the consolidation of our group continued after the changes in 2003. In the traditional research topics (Broadband Dielectric Spectroscopy and time-resolved Fourier Transform Infrared Spectroscopy) novel and detailed insights were gained into the dynamics of thin (10nm) polymer layers and in the response of (nematic) liquid crystalline elastomers to external mechanical fields. In the experiments with optical tweezers for the first time it could be shown that the force-elongation dependence of *single* DNA-chains of varying length shows systematic deviations from the predictions of the wormlike chain model. Furthermore refined experiments on the interaction between DNA-grafted colloids were carried out and - depending on the direction with respect to the axis between the colloids - the forces parallel and perpendicular to it could be separated and analyzed. This opens completely novel and existing perspectives.

F. Kremer

2.2 Molecular Dynamics in Thin Films of Polymers with Special Architecture

A. Serghei, *F. Kremer*

This projects aims to investigate confinement effects on the dynamic glass transition of polymers having a special architecture. Thin films of hyper-branched polymers (Fig. 2.1a), grafted polymers and star-branched polymers are prepared and their molecular dynamics is investigated in dependence on the confinement size (film thickness). Two questions are addressed. The first one, what role plays the architecture of the macromolecular systems in the deviations of the dynamic glass transition from the bulk behavior observed in thin films. For example, thin layers of hyper-branched polyesters show an increase of the average alpha relaxation rate with decreasing films thickness. This effect appears at much larger thicknesses (Fig. 2.1b) that those reported for linear polymers and therefore must be assigned to the special architecture of these dendritic macromolecules.

The second question, to what extent different methods to investigate the glass transition provide comparable results when applied to thin films. For that, complementary measurements by Broadband Dielectric Spectroscopy, capacitive dilatometry and AC -

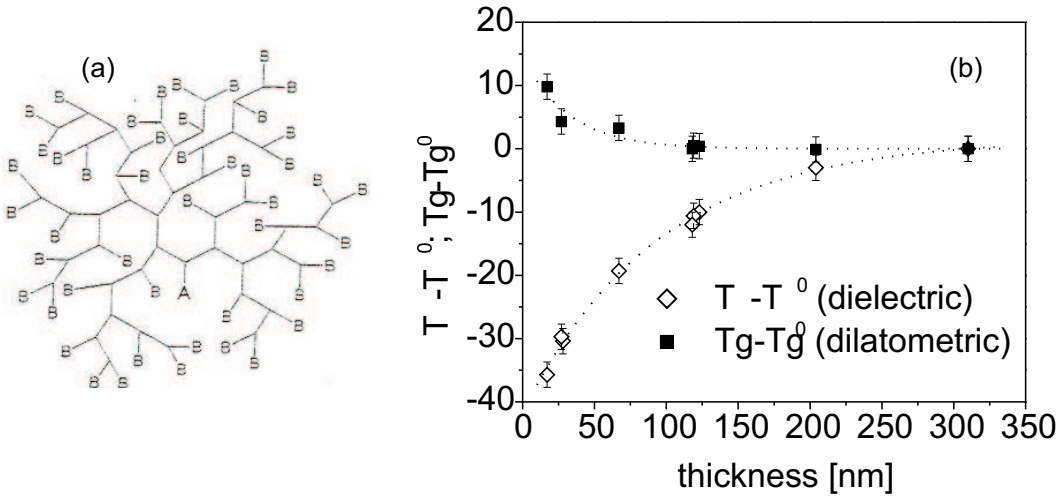

Figure 2.1: a) scheme showing the architecture of hyper-branched polymers b) the maximum temperature position of the alpha relaxation peak (by Broadband Dielectric Spectroscopy, at 0.6 Hz) and the glass transition temperature (by capacitive dilatometry), both normalized in respect to the values corresponding to 310 nm, as a function of film thickness.

calorimetry are employed. In the case of hyper-branched polyesters, the dielectric measurements show a faster dynamic glass transition with decreasing film thickness while simultaneous dilatometric determinations reveal a slight increase of Tg. Such an apparent controversy, reported for linear polymers, too, indicates that dielectric relaxation spectroscopy and dilatometry do not sense the same component of the molecular dynamics in thin polymer films. A combinative approach for the investigation of the dynamic glass transition might help one to get new insights into the mechanism underlying the confinement effects reported since one decade in the literature.

[1] Y.H. Kim, J. Polym. Sci. (A) 36, 1685 (1998).
[2] A. Serghei et al., Eur. Phys. J. E, in press.

2.3 Novel Developments in the Preparation of Thin Polymer Films

A. Serghei, *F. Kremer*

This work attempts to develop novel methods for the preparation of thin polymer films which could allow one to investigate the molecular dynamics of polymers in a one dimensional confinement down to a geometrical constraint comparable with size of the polymer coil (i.e. 10 nm). The method should additionally allow a relative easy adjustment of the interfacial interactions (by treating the surface of the solid electrodes) in order to investigate their role in the shifts of the dynamic glass transition observed in confinement. It should enable also a reliable quantitative determination of the relaxation time distribution in dependence on the confinement size which may facilitate a better understanding of the mechanism underlying the confinement effects. Our current approach is to use ultra flat conductive silicon wafers as hard electrodes, while nanostructures of SiO_x are going to serve as spacers (Fig. 2.2a). After cleaning, contacting and annealing, the

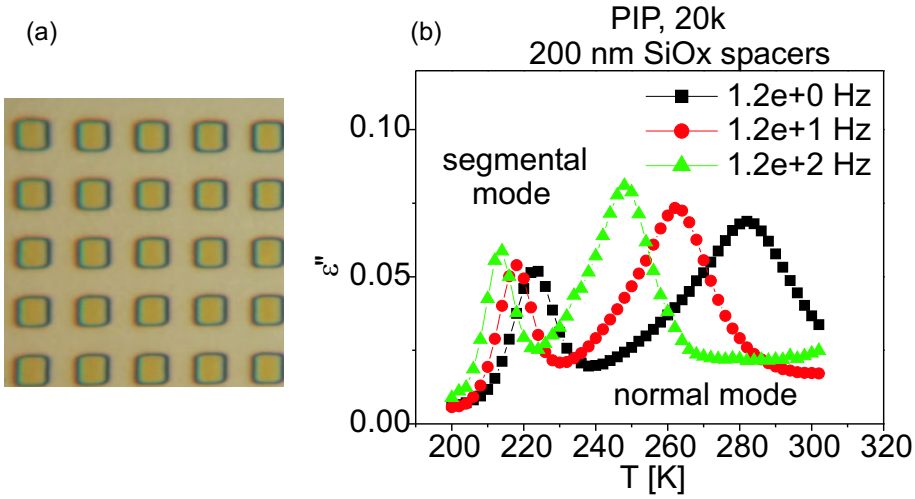

Figure 2.2: a) matrix of nano-spacers (height of 200 nm, width of 5 μm) on the surface of a flat silicon wafer; b) Dielectric loss vs. temperature at different frequencies, as indicated, showing the segmental and the normal mode for a 200 nm thin film of poly-isoprene (Mw=20 Kg/mol).

empty condenser, consisting of two parallel electrodes separated by a matrix of isolating nano-spacers, is filled by capillarity with the material under investigation. The determination of the sample capacity before and after filling provides an additional way to check the thickness of the polymer film. First measurements using nano-structures of 200 nm were proven successfully (Fig. 2.2b), a second sample of 10 nm thickness is currently in preparation.

2.4 Shifts of the Dynamic Glass Transition in Thin Polymer Films: a Possible Mechanism

A. Serghei, *F. Kremer*

The origin of the confinement effects on the dynamic glass transition in thin polymer films observed since one decade in numerous studies is still not elucidated. Moreover, the overview emerging from the data reported in the literature is pretty controversial, since there are many studies indicating no shifts of the glass transition temperature in the confinement of thin films. Here, a possible cause of the Tg deviations is thoroughly investigated: as well-known, a change of the molecular weight distribution, possibly by chain breaking or cross-linking in the presence of oxygen, has definitely an impact on the dynamic glass transition. Since in many studies revealing Tg shifts the sample annealing or the measurements are done in a moderate vacuum or even in ambient air, this possibility cannot be excluded. The first indications of a chain breaking effect which causes above 414 K a reduction of the glass temperature in ambient air (Fig. 2.3) were found in a study investigating a pattern formation in thin films of polystyrene: samples kept in a pure nitrogen atmosphere remains stable while in ambient air they exhibit an enhanced mobility and undergo changes ending up with the formation of a characteristic morphology. Measurements by Broadband Dielectric Spectroscopy, capacitive dilatometry and AC-calorimetry reveal indeed the Tg reductions in ambient air, while the proof of a chain scission effect was provided by IR-spectroscopic measurements. To what extent the re-

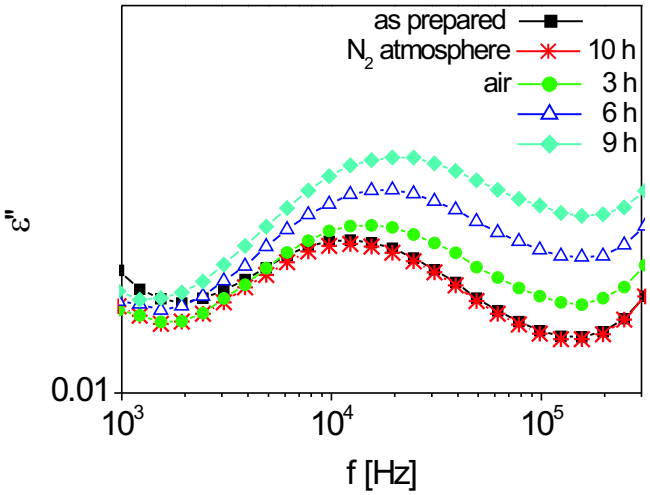

Figure 2.3: Dielectric loss vs. frequency showing the dynamic glass transition of a 86 nm thin PS film at a constant temperature of 414 K, as prepared, in a pure nitrogen atmosphere and in air as a function of time, as indicated.

sults indicating a faster dynamics in thin PS films are caused by chain scissions in the presence of oxygen and especially whether there is a thickness dependence of this effect is currently investigated.

[1] J.A. Forrest, Eur. Phys. J. E 8, 261 (2002).
[2] A. Serghei et al., Phys. Rev. E, in press.

2.5 Molecular Dynamics in Semifluorinated Side-Chain Polyesters as Studied by Broadband Dielectric Spectroscopy

J. Tsuwi, *F. Kremer*

Structural segments consisting of alkyl and perfluoroalkyl groups covalently linked by a C–C bond are well known for their microphase separation resulting in highly ordered bulk structures. The use of such materials for surface modification is numerous because of the resulting low surface free energy. We are employing Broadband Dielectric Spectroscopy to study the molecular dynamics in fluorinated side-chain polyesters.

It is observed that the fluorinated side-chain exhibits two relaxation processes γ and δ-like. The γ process is assigned to librational fluctuations at the terminal position of the side chain while the δ-like process reflects a cooperative motion of the side chain as a whole. Two more processes, β and α , are observed, which are associated with motion of the main chain. The β process is assigned to fluctuations of the dielectrically active carbonyl groups together with the phenyl ring whereas the α relaxation corresponds to the dynamic glass transition process of the polymers. With respect to the flexibility of the main chain, an interesting behavior is seen in the dynamics of the backbone when compared to side chain motion. Based on the analysis of the activation plot, it is concluded that a flexible main chain exhibits faster mobility in direct contrast

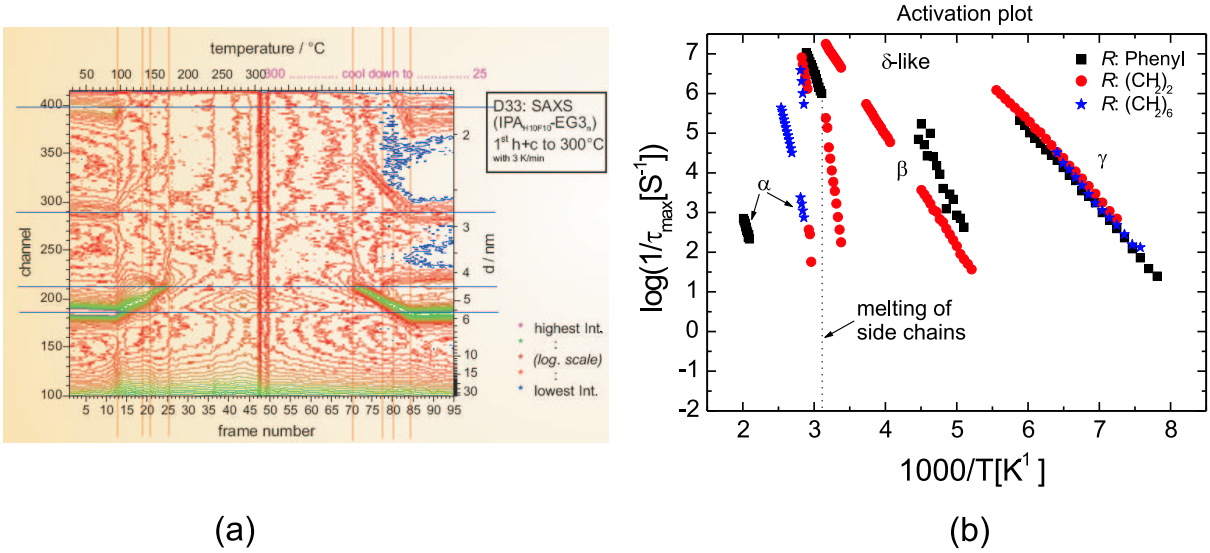

Figure 2.4: (a) Temperature dependent small angle X-ray (t-SAXS) (b) Activation plot showing four relaxation processes γ, β, δ and α in order of their mean relaxation times.

to its side chain motion. On the other hand, the less flexible backbones show the reverse trend. The dielectric results are analyzed in the context of micro-phase separated layered structures, supported by differential scanning calorimetry (DSC) and t-SAXS studies (Fig. 2.4a).

[1] Gottwald A, Pospiech D, et al (2002) Macromol. Chem. Phys. 203 (5-6): 854
[2] Tsuwi J, Appelhans D, Zschoche S, Friedel P, Kremer F (2004) Macrom. 37:6050
[3] Tsuwi J, Appelhans D, et al. (Colloid and Polym., in Press)
[4] Tsuwi J, Pospiech D, et al. (J.Polym. Sci. B: Polym. Phy., in preparation)

2.6 High Frequency Dielectric Studies of Microwave (MW) Enhanced Chemical Reactions

J. Tsuwi, *F. Kremer*

Microwave-assisted chemical reactions (Fig. 2.5) are rapidly gaining interest from polymer chemists. This is because of the fact that it has been proved to greatly increase reaction rates and thereby reducing reaction times from hours to just a few minutes. With MW irradiation, high polymerization yields have been realized in short times and the advantage of non-contact heating compared to convectional heating is highly appreciated.

Controversial discussions have however emerged as to whether there are non-thermal microwave effects during MW-enhanced polymerization or purely thermal processes. In view of this, we carry out high frequency (>10 MHz) dielectric studies on different solvent/monomer/initiator combinations in order to investigate the underlying molecular mechanisms.

[1] Sinnwell S, Ritter H (2005) Macrom. Rapid Comm. 26, 160-163
[2] Iannellil M, Ritter H (2005) Macrom. Chem.Phys. 206, 349-353

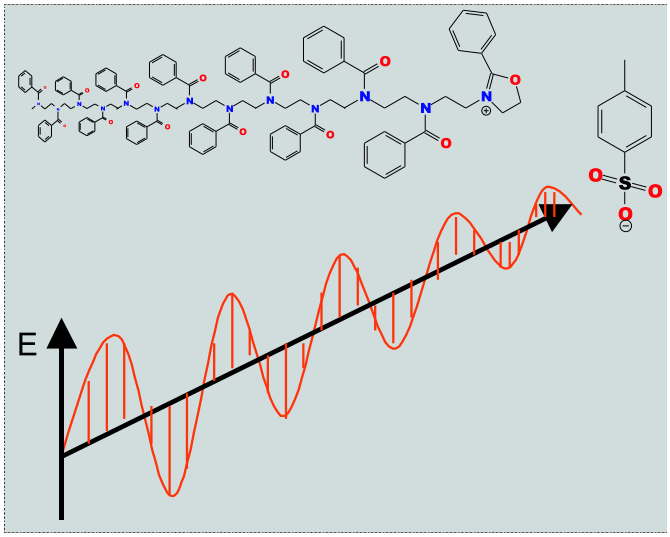

Figure 2.5: Scheme of activation of the reactive site by MW irradiation (Illustration adapted from Macrom. Rapid Comm. 2005, 26, 160)

[3] Wiesbrock F, Hoogenboom R, Schubert US (2004) Macrom. Rapid Comm.25, 1739
[4] Wiesbrock F, Hoogenboom R, Abeln CH, Schubert US (2004) Macrom. Rapid Comm.25, 1895

2.7 Time Resolved FTIR-Spectroscopy on Segmental Reorientation of Nematic Elastomers Under External Mechanical Fields

J. Li, M. Tammer, *F. Kremer*

Fourier transform infrared (FTIR) spectroscopy [1, 2, 4] is an especially suitable method for obtaining molecular level information for liquid crystalline networks. Time resolved FTIR spectroscopy with polarized light is employed to study the segmental orientation and the order parameters of nematic liquid crystalline elastomers (NLCEs, Fig. 2.6, left) with a monodomain structure in response to an external mechanical field [3, 4]. Detailed results about the reorientation of the mesogens, the spacer molecules and the main chain are obtained due to the specifity of the FTIR measurements. Mechanical strain is applied to thin NLCE films parallel and perpendicular to the initial mesogen orientation and the evolution of the orientation and the molecular order parameter with time is obtained for the different molecular moieties after each increase of the elongation ratio. While at parallel strain neither a reorientation nor a significant change of the order parameters takes place for all groups, the molecular units react differently to a strain applied perpendicular to the initial mesogen orientation (Fig. 2.6, right). Below a threshold value of the elongation ratio the orientation and order parameters remain nearly constant. Above this value a continuous reorientation is found for all molecular segments while the order parameters decrease. The network is not stable anymore and flows until the film breaks.

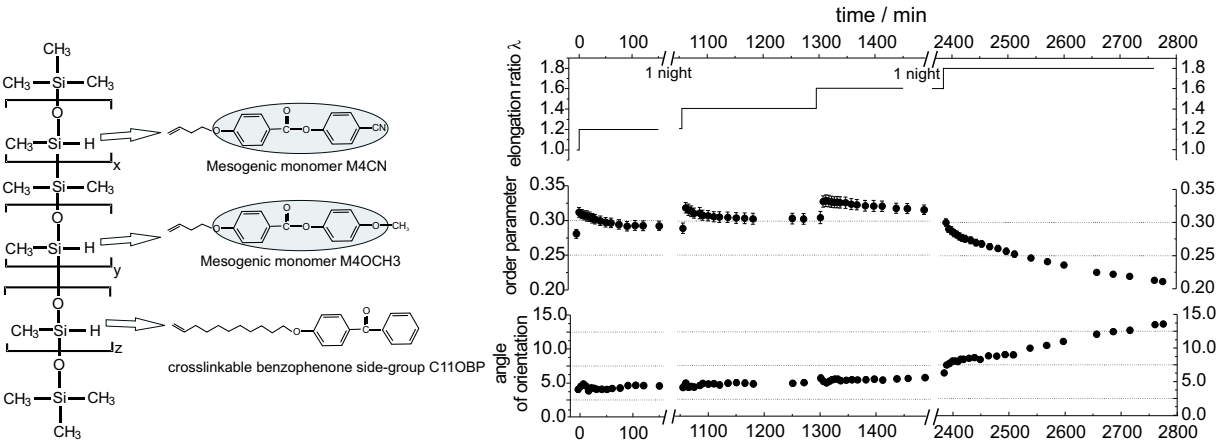

Figure 2.6: Left: NLCE material; Right: Orientation and order parameters for the CC group (mesogens) at perpendicular strain

[1] H.W. Siesler, K. Holland-Moritz, Infrared and Raman Spectroscopy of Polymers, Practical Spectroscopy Volume 4; Marcel Dekker: New York, 1980.
[2] S.V. Shilov, S. Okretic, H.W. Siesler, M.A. Czarnecki, Appl. Spectrosc. Rev. **31**, 125 (1996).
[3] H. Skupin, F. Kremer, S.V. Shilov, P. Stein, H. Finkelmann, Macromolecules, **32**, 3746 (1999).
[4] M. Tammer, J. Li, A. Komp, H. Finkelmann, F. Kremer, Macromol. Chem. Phys. (2005), in press
[5] J. Li, M. Tammer, A. Komp, H. Finkelmann, F. Kremer, Eur. Phys. J. E (2005), submitted

2.8 Dynamic Stress Strain Response in Thin NLCE Films Under External Mechanical Fields

M. Tammer, J. Li, *F. Kremer*

The macroscopic response of thin films of nematic liquid crystalline elastomers (NLCEs) to deformations under a mechanical field is highly anisotropic due to the ordered structure of these materials. Next to the effects like segmental reorientation and change of molecular order parameters investigated by Fourier transform infrared (FTIR) spectroscopy, the stress–strain dependency and its phase relation is of high interest in order to analyze the response of the network. The most remarkable property of NLCEs is the phenomenon of soft elastisity. First experimental results for this theoretical concept were found by Küpfer and Finkelmann [1]. Soft elasticity is defined by a non-linear soft response over a full range of strain and discribed by the theory of nematic-rubber elasticity developed by Warner and Olmsted [2, 3].

In order to measure the force applied to the NLCE sample at the same time as the polarized IR spectra, one end of the film is fixed on a metal spring (Fig. 2.7). The deformation of this callibrated spring is determined by image processing. A detection by optical sensors is planned for dynamic measurements. A first example of a simultaneous FTIR and stress–strain experiment is shown in Fig. 2.8. The angle of orientation and the

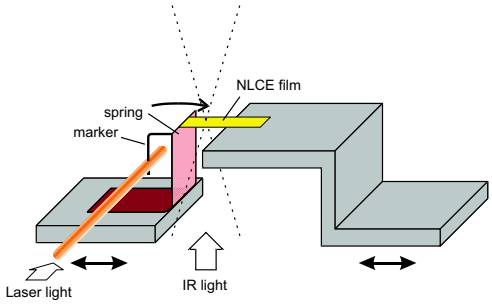

Figure 2.7: Scheme of the force detection setup.

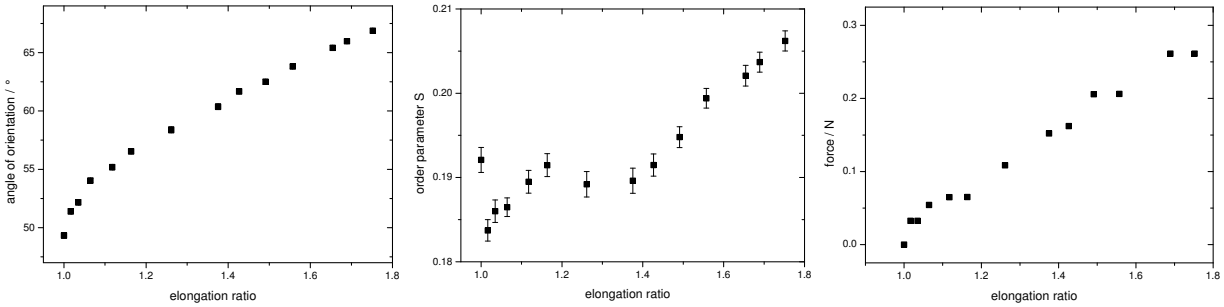

Figure 2.8: Angle of orientation (left) and order parameter (middle) of the CC group (mesogens) at mechanical strain obliquely to the original mesogen orientation; right: force vs. elongation ratio for this NLCE film

molecular order parameter of the mesogens are given together with the force affecting the sample.

[1] J. Küpfer, H. Finkelmann, Macromol. Chem. Phys. **195**, 1353 (1994).
[2] M. Warner, P. Bladon, E.M. Terentjev, J. Phys. II, **4**, 91 (1994).
[3] P.D. Olmsted, J Phys. II, **4**, 2215 (1994)

2.9 Liquid Crystalline Physical Gels: Functional Materials with Controlled Microphase-Separated Structures and Memory States

J. Li, *F. Kremer*

Self-assembly and micrometer scale phase-segregates of the two discrete components, i.e. hydrogen-bonded gelators and conventional LC molecules, results in the generation of LC physical gels. In contrast to chemical gels, the gelation is thermo-reversible. LC physical gels are very promising functional materials in application for their unique features, such as the reversibly memorized states and controlled microphase-separated structures [1, 2].

We study the electro-optic characteristics of these LC physical gels in freely suspended films by means of polarizing microscopy. It is found that during the gelation an anisotropic network of thin birefringent strands phase-separates from the surrounding LC material. The network creates a memory of the 'frozen-in' texture and influences the switching behavior of the ferroelectric phase considerably. Under application of electric fields, the

sample orientation can be switched in the LC microdomains, and after removal of the electric field, the elastic forces restore the memorized local alignment [3].

We demonstrate that proton NMR spectra can provide direct information about order and orientation of the director in the LC physical gels. The results show that small percentages of gel network are sufficient to stabilize the director even in the strong external magnetic field (several Tesla). The critical amount of the gelling agent that is necessary to fix the director orientations is above 3.0 wt%. At lower concentrations, the 2.34 T magnetic field distorts the LC director field. From the NMR spectra, there are no observable differences between the nematic and smectic gel states in 8CB. The order parameter of the 8CB in the gel is not changed significantly from that of the pure mesogen [4].

We show that the Laser Intensity Modulation Method (LIMM) spectra of the hydrogen-bonded FLC gels is able to exhibit spatially resolved polarization distributions and LC director orientation in sandwich cells. Under electric fields, contribution to the resulting distribution caused by the induced polarization due to unwinding the FLC helix has been detected. The influence of hydrogen-bonded network on the polarization distribution is also found when the gel former is increased up to 5.0 wt%. Therein the shape of the measured pyrospectra is completely different to that of other gel samples with lower gel former concentration. Its maximum distribution still locates at the surface of FLC layer which is comparable to the field-free state. These results indicate that the helical structure and director of FLC can be stabilized effectively by the gel network [5].

[1] T. Kato, Science, 295, 2414 (2002)
[2] J. Prigann, Ch. Tolksdorf, H. Skupin, R. Zentel and F. Kremer, Macromolecules 35, 4150 (2002)
[3] J. Li, R. Stannarius, C. Tolksdorf, R. Zentel, Phys. Chem. Chem. Phys, **5**, 916 (2003)
[4] J. Li, D. Geschke, R. Stannarius, Liq. Cryst. **31**, 21 (2004)
[5] J. Li, Geschke, Polym. Adv. Technol., 16, 11 (2005)

2.10 Optical Tweezers as a Tool to Investigate the Elastic Properties of Single DNA Molecules with Different Lenght

M. Salomo, K. Kegler, M. Struhalla, J. Reinmuth, V. Skokow, *F. Kremer*

Optical tweezers are commonly used to manipulate microscopic particles, with applications in cell manipulation, colloid research, manipulation of micromachines and studies of the properties of light beams. With their extraordinary resolution in space (∼2 nm) and force (∼0.050 pN) they became an irreplaceable tool for such purposes. In our project we want to use them to study the elastic properties of single DNA molecules. Therefore we developed an easy and reproducible procedure for the immobilization of single double stranded DNA molecules 1000 to 6000 bp in length obtained by PCR between two micro particles supplying a general approach to address this problem. A fully reversible elastic behaviour is found for the force-extension dependence of ds-DNA for relative elongations up to 50 % as described in the corresponding literature. It is not possible to describe the data for DNA >2000 bp with the wormlike chain model. This might be causal the development of an underlying superstructure of the DNA chains.

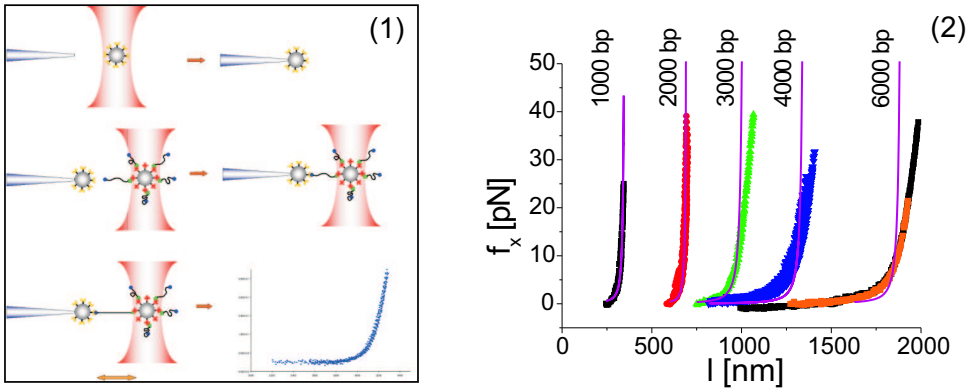

Figure 2.9: Part (1) – Assembly of an "DNA"-bridge: A polystyrene bead modified with A-DIG antibodies was trapped in the optical tweezers (a) and than fixed at a glass micropipette. After this first step a SA labelled particle with immobilized DNA on its surface was trapped and brought closely to the particle that was fixed at the femtotip so that binding between the digoxigenine labelled end of the DNA and the antibodies on the surface of the particle could take place. The single DNA molecule immobilized by this procedure could now be stretched and the occurring forces were documented in a force extension plot. Part (2) – Results of the Force extention measurements: DNAs of lengths between 1000 and 6000 bp were stretched and relaxed several times and the results were recorded in a force extention plot. The curves of the 1000 and 2000 bp DNA could be fitted with the wormlike chain model. Longer DNAs showed deviations from this fit. The reason for this is at the moment not clear.

[1] Allemand JF, Bensimon D, Croquette C; Current Opinion in Structural Biology 13: 266-274 (2003).
[2] Ashkin A; PNAS 94: 4853-4860 (1997).
[3] Baumann CG, Bloomfield VA, Smith SB, Bustamante C, Wang MD, Block SM; Biophysical Journal 78: 1965-1978 (2000).
[4] Baumann CG, Smith SB, Bloomfield VA, Bustamante C; PNAS 94: 6185-6190 (1997).

2.11 Investigating DNA-Binding Proteins with Optical Tweezers

M. Salomo, K. Kegler, M. Struhalla, J. Reinmuth, V. Skokow, *F. Kremer*

Sac7e belongs to a class of small chromosomal proteins identified in the hyperthermophilic archaeon *Sulfolobus acidocaldarius*. It is extremely strongly to the minor groove of DNA, causing a stable to heat, acid and chemical agents and binds sharp kinking of the DNA helix leading to a shortening of the DNA (Fig. 2.10(1)). Our project has the aim to investigate the influence of this DNA-binding protein on a DNA-double helix. We want to use the optical tweezers to measure the dimension of this shortening. Theoretically the protein binds to the DNA every 3 bp leading to a theoretical compaction ratio of ∼1.2. For the experiment a single DNA molecule was immobilized as described previously.

The molecule was than stretched and relaxed several times and force extension plots (Fig. 2.10(2)) were recorded (black curve). Afterwards the Sac7e protein was injected into the cell. During the injection the stretching and relaxing cycles were continued (orange

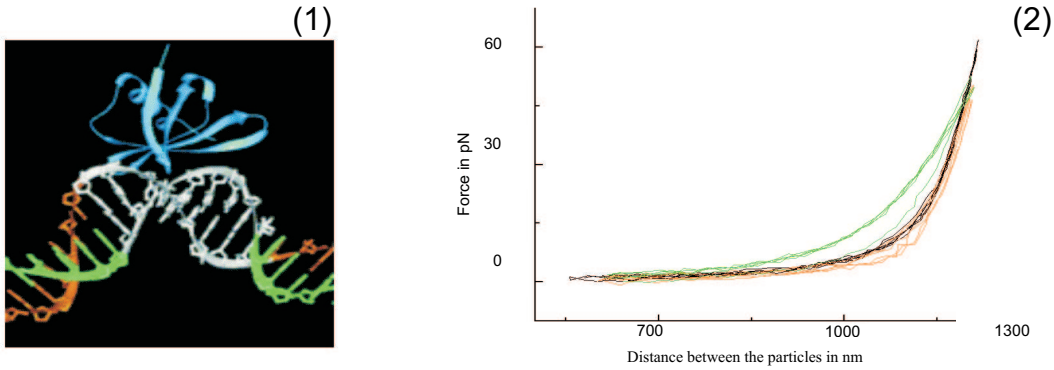

Figure 2.10: Part (1): Model of the binding mechanism of the Sac7d protein (blue) to a DNA helix. Part (2): Result of the binding experiment of Sac7e to a 4000 bp long DNA molecule.

curve). When the protein reached the immobilized DNA the force/extension behaviour of the DNA changed rapidly (green curve). In the moment the protein began to bind the curve released from the plot were no protein was present what has to be interpreted as a shortening of the DNA because of the kinking induced by Sac7e. The achieved shortening of the DNA ranges between 120 and 170 nm that corresponds to a compaction ratio of 1,1–1,17. At higher forces the curve than passes into the plot without protein. That indicates that either the protein is not longer able to stand the applied forces at this moment and releases the DNA from its binding side but remains bound to the DNA or the protein is disrupted from the DNA and binds immediately again when the DNA becomes relaxed.

[1] H. Robinson et al.; Nature 392, 202-205 (1998)
[2] J.G. McAfee et al. ; Bioch. 34, 10063- 10077 (1995)
[3] D. Kulms et al.; Biol. Chem. 378, 545-551 (1997)

2.12 Archaeal Nucleosome Formation by HMfB Protein Studied Using Optical Tweezers

F. Kremer, S.R. Sethu Narayanan, M. Salomo, J. Reinmuth, W. Skokow

HMfB (Fig. 2.11(1)) belongs to a class histone proteins identified in the hyperthermophilic archaeon, *Methanothermus fervidus*. It is extremely stable to heat and acid, and binds strongly to the DNA to form a tetramer complex of nucleosome known as archael nucleosome in contrast to the octamer complex formed by eukaryotic core histones. The aim of this project is to investigate the archaeal nucleosome formation and stability under different salt and buffer conditions to discern the possible *in vivo* mechanisms of nucleosome assembly and dynamics. Plasmid vector carrying HMfB gene was overexpressed in *E.coli* and the protein was purified using affinity (Heparin columns) and gel filtration chromatography. This highly purified HMfB protein was subsequently used to study the nucleosome formation with a double-stranded 4000-bp DNA labelled with biotin and digoxigenin at their 5' end. The DNA was captured between 2 colloids using the previously well-establised protocols in the lab. Briefly, anti-digoxigenin antibody coated

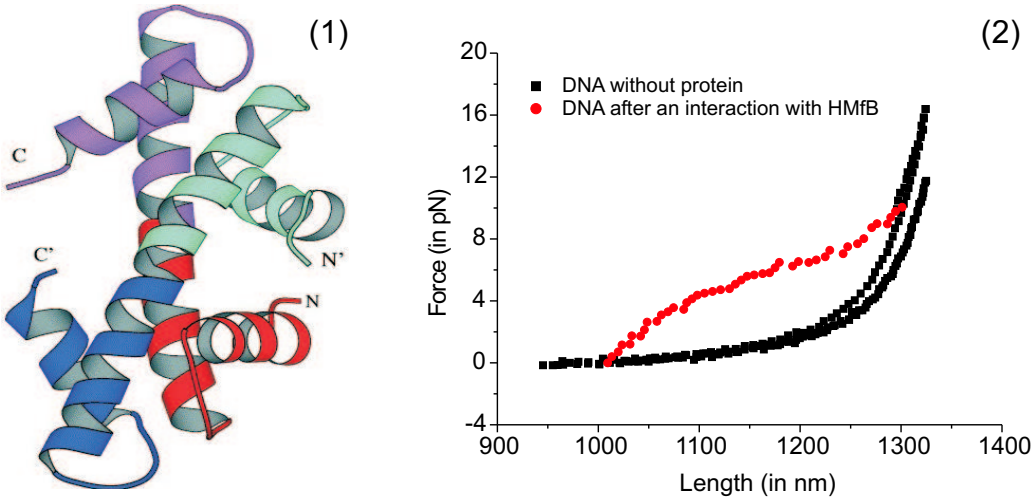

Figure 2.11: Part (1): Ribbon structure of HMfB (69 amino acids long). One monomer is colored cyan (N-terminal, 1 to 35 residues) to blue (C-terminal, residues 36 to 69), and the other monomer is colored orange (N-terminal) to magenta (C-terminal). Part (2): Force-extension curve of 4000bp dsDNA with (red) and without HMfB protein (black).

2.1 μm polystyrene bead was held by using a glass micropipette while the streptavidin coated bead with 100-200 molecules of DNA was held by using the photonic potential. Force-extension data were obtained by image capturing using a CCD video camera and subsequent image analysis using an IDL program. Repeated measurements were carried out for the DNA with and without HMfB protein. The typical force-extension curve obtained with and without HMfB is shown in Fig. 2.11(2). The results suggest that the binding of HMfB to DNA is weak and future experiments will further precisely quantify the strength of this interaction between DNA and HMfB in the piconewton range.

[1] M.L. Bennink et al.; Nat Struct Biol. 8(7):606-10 (2001)
[2] K. Sandman et al.; Meth. Enzymol. 334:116-129 (2001)

2.13 Nano- and Microfluidics Using Optical Tweezers with Fast Single Particle Tracking

C. Gutsche, S.K. Ayop, *F. Kremer*

Optical tweezers with fast single particle tracking are microscopic rheometric tools with nanometer resolution in space and subpico-newton resolution in force. The proposed project has two intentions (i) to contribute to basic questions in colloid- and polymer-research and (ii) to address technological problems of micro- and nanofluidics.In detail the following experiments are realised: 1.) Measurements of the force-distance-dependence between two isolated single colloids of which one is hold by a micropipette and the other by optical tweezers. 2.) Measurement of the flow profile of homogeneous and heterogeneous liquids in small confining geometries like plates with micrometer separation, microchannels, etc. with and without surface modifications (e.g. hydrophobization).

Further planed investigations are: 1.) Measurement of the force-distance-dependence between a single colloid and a wall in the steady state and in fluid flow for coated and

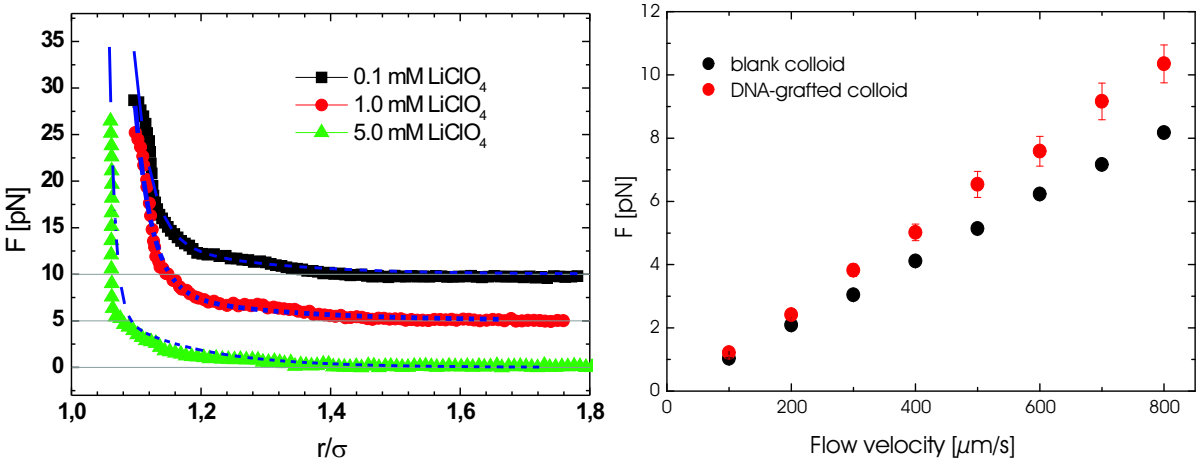

Figure 2.12: Left: Force-distance-dependence for two separated blank colloids (diameter σ : $2,23\,\mu$m) in differing surrounding medium. Right: Flow-resistance vs. velocity of the surounding medium with respect to the colloid hold by optical tweezers. black: blank colloid of diameter $\sigma = 2,1\,\mu$m. red: DNA-grafted colloids. Typically 1000 DNA-chains with a length of 4000 bp are grafted on one colloid.

uncoated surfaces. 2.) Measurement of depletion forces between single colloids in the steady state and in flow for polymer solutions of varying concentration and for polymers of different topology. 3.) A fluctuation analysis of the Brownian motion of a colloid in an optical trap enables one to deduce the local tensor of viscosity. By that inhomogeneous microscopic structures like microchannels or living biological systems can be explored.

This project is funded as part of the DFG-Schwerpunktprogramm “Nano- und Mikrofluide: Von der molekularen Bewegung zur kontinuierlichen Strömung”.

[1] van de Ven, T.G.M., Colloidal Hydrodynamics in *Colloid Science: A series of monographs*, Academic Press (1989)
[2] Crocker, J.C., Grier, D.G., *Physical Review Letters* **77**, 1897-1900 (1996)

2.14 The Interaction Between Single Colloids with and without Grafted DNA as Measured by Optical Tweezers

K. Kegler, *F. Kremer*

Optical Tweezers (OT) are extraordinary microscopic tools with nanometer resolution in 3-D space and subpico-Newton resolution in force. They are used to measure the interaction potential between single pairs of colloids (blank and grafted with (genetically engineered) DNA of varying length (1000 basepairs (bp), 2000 bp, 3000 bp, 4000 bp). To measure the interaction potential the following experimental procedure is used: One particle is trapped by the optical tweezers (OT) and fixed at a glass micropipette (by capillary forces) being mounted on a piezoelectric actuator. A second particle is caught with OT and positioned with respect to the other (Fig. 2.13)

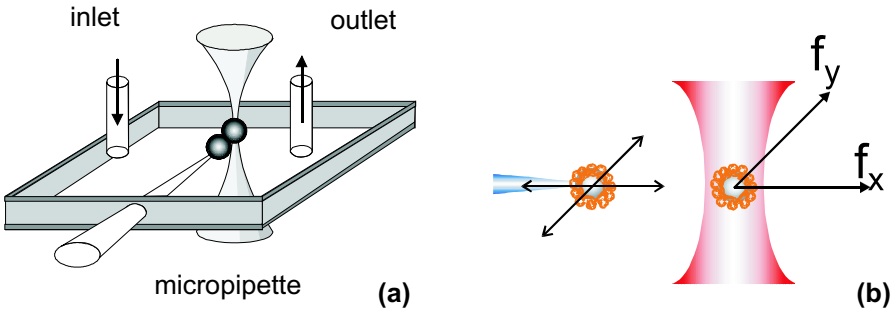

Figure 2.13: Scheme (a) of the sample cell to measure forces between two separated colloids and scheme (b) of the direction of motion.

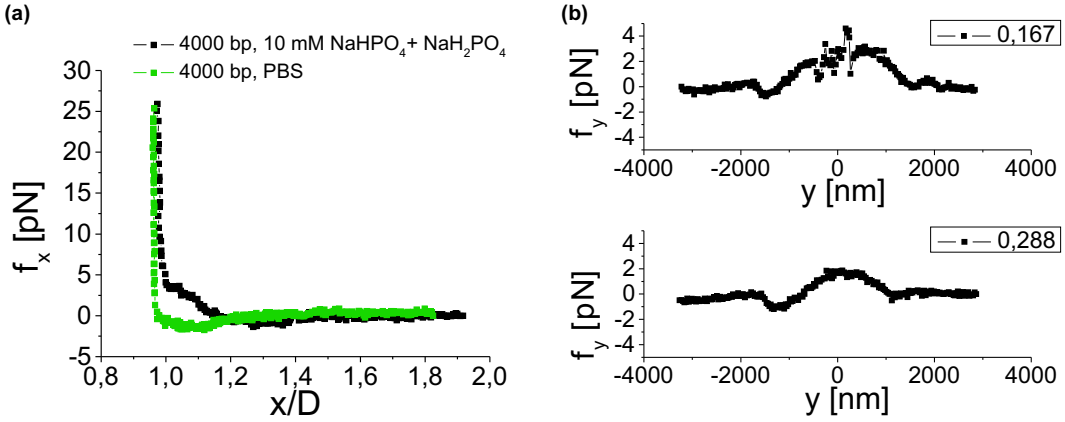

Figure 2.14: (a) The interaction forces of DNA-grafted colloids in different buffers (x-direction [see Fig. 2.13b]), (b) The interaction forces in y-direction (see Fig. 2.13b) of DNA-grafted colloids without (separation between the colloid surfaces: $l = 0,288\,\mu$m) and with ($l = 0,167\,\mu$m) contact.

With this setup we investigate the interaction forces in two dimensions - parallel and perpendicular to the axis between the two colloids (Fig. 2.14). Special emphasis is given to the change of the surrounding media, but as well tribological phenomena will be studied.

This project is supported within the DFG-Schwerpunktprogramm “Nano- und Mikrofluidik: Von der molekularen Bewegung zur kontinuierlichen Strömung”.

[1] Urbakh, M., Klafter, J., Nature 430,525 (2004)
[2] Wu, J., Proc. Natl. Acad. Sci. USA 95, 15169 (1998)

2.15 Funding

Prof. Dr. F. Kremer Optische Pinzette als mikroskopische Sensoren und Aktuatoren zum Studium der Wechselwirkung zwischen einzelnen Biomolekülen SMWK-Projekt 7531.50-02-0361-01/11 (2001-2005)

Prof. Dr. F. Kremer DFG-Teilprojekt im Rahmen des Schwerpunktprogramms “Nano- und Mikrofluidik: Von der molekularen Bewegung zur kontinuierlichen Strömung” DFG-Schwerpunktprogramm 1164, KR 1138/14-1 (2004-2006)

2.16 Organizational Duties

Friedrich Kremer

- Director of the Institute for the institute for experimental physics I

2.17 External Cooperations

Academic

University of Rostock, Germany
C. Schick, H. Huth

Institute for Polymer Research, Dresden
B. Voit, K.-J. Eichhorn, D. Pospiech

Institute for surface modification, Leipzig
M. Ziberi

Institute for organic chemistry and macromolecular chemistry II, Düsseldorf,
H. Ritter

University of Technology, Eindhoven, The Netherlands
U.S. Schubert

University of Freiburg, Germany
H. Finkelmann

Max Plank Institute, Mainz, Germany
R. Zentel

Heinrich-Heine University, Düsseldorf, Germany
H. Loewen

Industry

Novocontrol, Hundsangen, Germany

Comtech GmbH, München, Germany

Freudenberg Dichtungs- und Schwindungstechnik KG, Weinheim, Germany

2.18 Publications

Journals

F. Kremer and R. Stannarius
"Molecular Dynamics of Liquids in confinement"
Bookchapter in "Molecules in Interaction with Surfaces and Interfaces", (Eds.: R. Haberlandt, D. Michel, A. Pöppl and R. Stannarius) (Lect. Notes Physics Vol. 634) Springer-Verlag 2004, pp. 275-300, ISBN 3-540-20539-X

R. Stannarius and F. Kremer
"Liquid Crystals in Confining Geometries"
Bookchapter in "Molecules in Interaction with Surfaces and Interfaces", (Eds.: R. Haberlandt, D. Michel, A. Pöppl and R. Stannarius) (Lect. Notes Physics Vol. 634) Springer-Verlag 2004, pp. 301-336, ISBN 3-540-20539-X

A. Serghei, L. Hartmann, P. Pouret, L. Leger, F. Kremer
"Molecular dynamics in thin (grafted) polymer layers"
Colloid and Polymer Science 282,.946-954 (2004)

J. Tsuwi, D. Appelhans, S. Zschoche, P. Friedel and F. Kremer
"Molecular dynamics in poly(ethene-alt-N-alkylmaleimide)s as studied by Broadband Dielectric Spectroscopy"
Macromolecules 37, 6050-6054 (2004)

W. Ngwa, R. Wannemacher, W. Grill, A. Serghei, F. Kremer and T. Kundu
"Voronoi tessellations in thin polymer blend films"
Macromolecules 37 (5), 1691 (2004)

A. Eremin, H. Nádasi, G. Pelzl, S. Diele, H. Kresse, W. Weissflog, S. Grande
"Paraelectric-antiferroelectric transitions in the bent-core liquid-crystalline materials"
Phys. Chem. Chem. Phys. 6, 1290-1298 (2004)

G. Pelzl, M.W. Schröder, U. Dunemann, S. Diele, W. Weissflog, C. Jones, D. Coleman, N.A. Clark, R. Stannarius, J. Li, B. Das, S. Grande
"The first bent-core mesogens exhibiting a dimorphism B7-SmCPA"
J. Mater. Chem. 14, 2492-2498 (2004)

W. Weissflog, S. Sokolowski, H. Dehne, B. Das, S. Grande, M.W. Schröder, A. Eremin, S. Diele, G. Pelzl, H. Kresse
"Chiral Ordering in the nematic and an optically isotropic mesophase of bent-core mesogens with a halogen substituent at the central core"
Liquid Crystals 31 (7), 923-933 (2004)

R. Wang, H. Schmiedel, B.-R. Paulke
"Isothermal titration calorimetric studies of surfactant interactions with negatively charged, ´hairy´ latex nanoparticles"
Colloid Polym. Sci. 283, 91-97 (2004)

J. Li, D. Geschke, R. Stannarius
"Proton NMR investigation of a hydrogen-bonded liquid crystal gel"
Liquid Crystal 31 (1), 21-29 (2004)

K. Goede, P. Busch, M. Grundmann
"Binding Specificity of a Peptide on Semiconductor Surfaces"
Nanoletters 4 (11), 2115-2120 (2004)

F. Kremer, K. Kegler, C. Gutsche, J. Reinmuth, W. Skokow, M. Salomo, S. Narayanan, M. Struhalla
"Optische Pinzetten zur Untersuchung der Wechselwirkung von Proteinen mit einzelnen DNA-Ketten"
BIOForum (GIT Verlag) 12, p 47 (/2004)

J. Li, D. Geschke
"Pyroelectric inverstigations of a hydrogen bonded ferroelectric liquid crystal gel by LIMM"
Polym. Adv. Technol. 16, 11-18 (2005)

in press

J. Tsuwi, D. Appelhans, S. Zschoche, R-C. Zhuang, P. Friedel, L. Häußler, B. Voit, F. Kremer
"Molecular dynamics in fluorinated side-chain MI copolymers as studied by Broadband Dielectric Spectroscopy"
Colloid and Polymer Science 10/2004, in press

M. Tammer, J. Li, A. Komp, H. Finkelmann, F. Kremer
"FTIR-spectroscopy on segmental reorientation of a nematic elastomer under external mechanical fields"
Macromol. Chemistry Rapid Commun. 12/2004, in press

A. Serghei, H. Huth, M. Schellenberger, C. Schick and F. Kremer
"Pattern formation in thin polystyrene films induced by an enhanced mobility in ambient air"
Phys. Rev. E 2004, in press

A. Serghei, Y. Mikhailova, K.-J. Eichhorn, B. Voit and F. Kremer
"Molecular dynamics of hyper-branched polyesters in the confinement of thin films"
Eur. Phys. J. E 2004, in press

2.19 Graduations

PhD

Dipl.-Phys. Heidrun Schüring
"Mechanische und optische Untersuchungen freitragender smektischer Filme"

Dipl.-Phys. Thomas John
"Experimentelle und theoretische Untersuchungen zur stochastisch getriebenen Elektrokonvektion in nematischen Flüssigkristallen"

Dipl.-Phys. Lutz Hartmann
"Untersuchung der molekularen Dynamik in dünnen Polymerfilmen mittels dielektrischer Spektroskopie"

3

Physics of Interfaces

3.1 Introduction

The highlights in research and education of our group are intimately related to recent progress in the various fields of diffusion measurement, including PFG NMR, interference and IR microscopy. Within the EC-sponsored project TROCAT, under our coordination, nine groups from five countries are jointly exploring the interrelation between molecular diffusion and conversion in heterogeneous catalysis. The so far attained results of both fundamental and industrial relevance were unconceivable without this strong experimental basis within the Magnetic Resonance Centre of our University. We are happy that theses activities are continued within a Network of Excellence of the 6th frame programme of the EC (INSIDE-PORES). With the special focus on diffusion in zeolites, we initiated the establishment of an international (British/French/German) research group ("Internationale Forschergruppe"), jointly sponsored by EPSRC, CNRS and DFG. The activities of this group will be of particular benefit for the International Research Training Group ("Europäisches Graduiertenkolleg") dedicated to "Diffusion in Porous Media", which started to operate in summer term 2004 and comprises groups from our institute and from the institutes of Theoretical Physics and of Chemical Technology of the Faculty of Chemistry and Mineralogy), together with colleagues of the Universities of Amsterdam, Delft and Eindhoven.

J. Kärger

3.2 Fast Magnetic Resonance Imaging and Velocimetry for Liquids under High Flow Rates

P. Galvosas, P.T. Callaghan

Some important properties of fluids are best revealed under condition of flow. Examples include viscosity, elasticity and non-linear dynamic response associated with flow-induced structures. Another intriguing effect is that associated with gradients in surface tension induced by flow, for example where a surfactant migrates to the surface of a moving liquid. This phenomenon is known as the Marangoni effect [1].

Local velocity imaging using NMR [2] enables one to observe this migration and hence the phenomena to which it leads. Indeed, the non-destructive nature of NMR involves

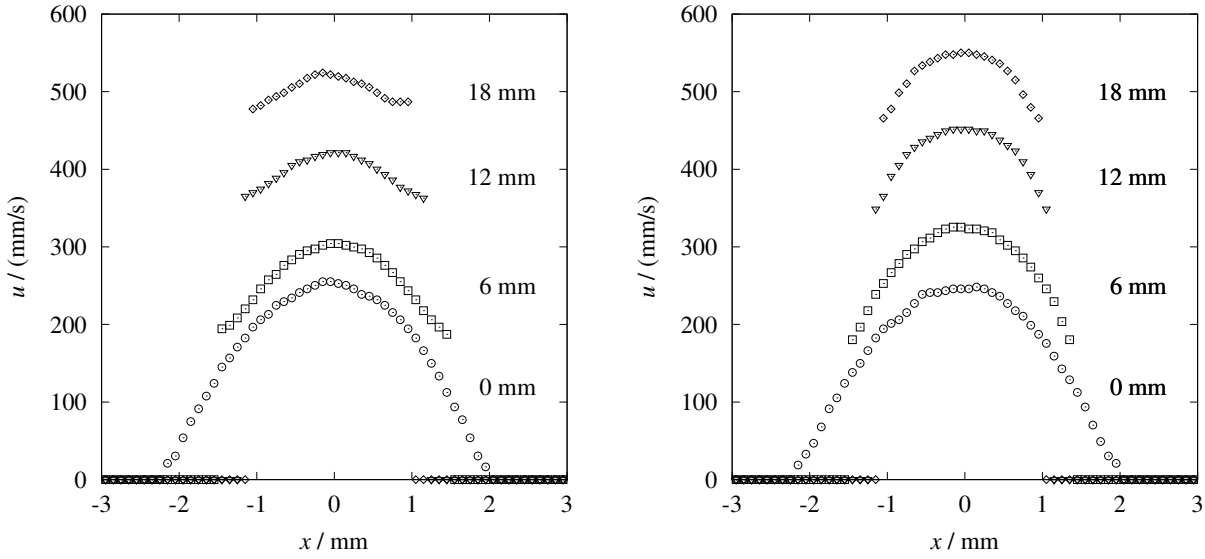

Figure 3.1: Velocity distribution across a liquid jet of water (left) and water with 4 mM lauryl sulfate (right). The distances from the output of the capillary are 0 mm (○), 6 mm (□), 12 mm (▽) and 18 mm (◊).

no perturbation to the flow. Moreover, NMR methods are applicable to non-transparent liquids, in contrast with optical methods. In the experiment described here, a free jet flowing out of a vertical capillary at Reynolds numbers of up to 300 which implies maximum velocities of up to 0.6 m/s is investigated. The impact on the measurements due to the resulting fluctuations in the position of the jet may be greatly reduced using fast imaging techniques combined with a pulsed gradient spin echo sequence [3]. The figures below show velocity profiles at various distances from the output of the capillary for water with and without surfactant. The influence of the surfactant at the surface is clearly obtained. To our knowledge, this is the first investigation of the Marangoni effect by means of NMR.

This work is supported by the New Zealand Foundation for Research, Science and Technology, the Royal Society of New Zealand Marsden Fund, and Centres of Research Excellence Fund.

[1] C. Marangoni, Ann. Phys. **143**, 337 (1871).
[2] P.T. Callaghan, "Principles of Nuclear Magnetic Resonance Microscopy", Oxford University Press, Oxford, (1991).
[3] T.W.J. Scheenen, D. van Dusschoten, P.A. de Jager, and H. Van As, J. Magn. Reson. **142**, 207 (2000).

3.3 Molecular Traffic Control in Porous Nanoparticles

A. Brzank, G. Schütz

We investigate the conditions for reactivity enhancement of catalytic processes in porous solids by use of molecular traffic control (MTC) as a function of reaction rate and grain

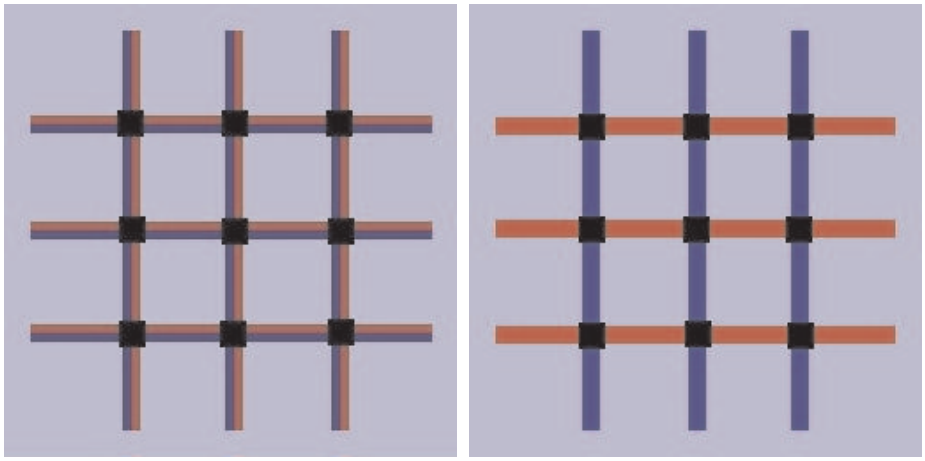

Figure 3.2: REF system (left) with $N = 3$ channels and MTC system (right) of the the same size. In contrast to the REF case, where we allow both types of particles (A and B particles) to enter any channel, in the MTC system A particles are carried through the vertical α channels whereas the B particles diffuse along the horizontal β channels. Black squares indicate catalytic sites where a catalytic transformation $A \to B$ is allowed.

size. Applying dynamic Monte-Carlo simulations and continuous-time random walk theory we consider the NBK lattice model with a quadratic array of channels (Fig. 3.2) modelling reaction diffusion properties of MFL type zeolithes.

Our simulations [1–3] and analytical results [4, 5] describe the MTC effect quantitatively over a wide range of parameters (Fig. 3.3). Moreover, trends which are independent of model details have been identified by analytical calculations and lead to a more positive result than concluded in [2] where no MTC effect at all was reported for short interconnecting channels $L = 1$. For reasonable reactivities and channel lengths the MTC effect vanishes proportionally to $1/N$, i.e., is inversely proportional to the grain diameter. This was shown explicitly for a two-dimensional simulation model, but the reasoning that led to this conclusion extends straightforwardly to a three-dimensional system [5]. Nevertheless, for optimized external process parameters the NBK model exhibits an enhancement

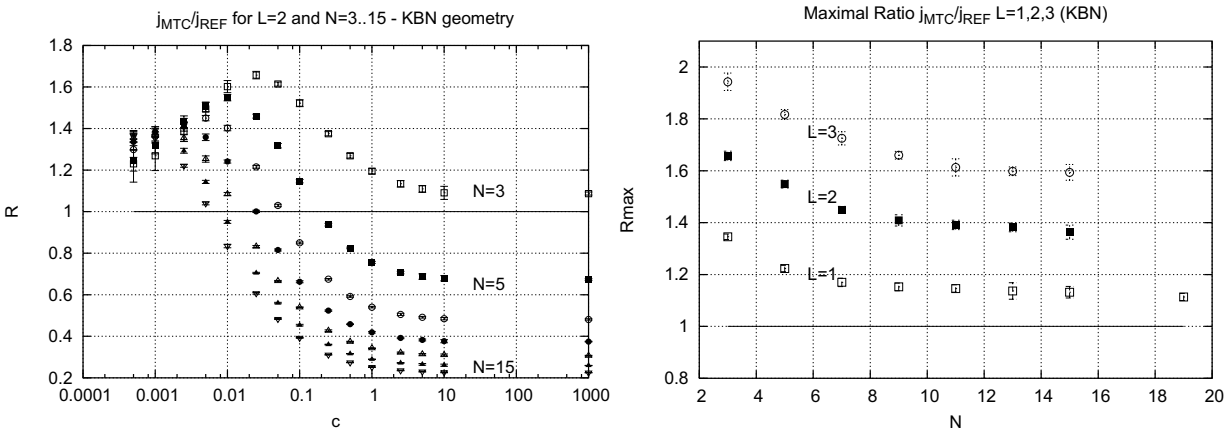

Figure 3.3: Left: Ratio $R(c)$ for different number of channels N and $L = 2$. $R(c)$ is the output current ratio between MTC and reference system as a function of reactivity. Right: Maximal ratio R^* for different L

of the effective reactivity of up to approx. 30 % for small grains and any (even short) channel length and reactivity c. This suggests that MTC may enhance significantly the effective reactivity in zeolitic nanoparticles with suitable binary channel systems and thus may be of practical relevance in applications.

At present we focus on different geometries implementing the idea of MTC trying to find realisations which overcome the negative dependence of the MTC effect as a function of the grain size.

[1] J. Kärger, P. Bräuer, A. Neugebauer, Europhys. Lett. 53 (2001) 8.
[2] P. Bräuer, A. Brzank, J. Kärger, J. Phys. Chem. B 107 (2003) 1821.
[3] A. Brzank, G.M. Schütz, P. Bräuer, and J. Kärger, Phys. Rev. E 69 (2004) 031102.
[4] A. Brzank, G.M. Schütz, Catalysis Today (submitted).
[5] A. Brzank, Sungchul Kwon, Gunter Schütz, Diffusion Fundamentals (submitted).

3.4 Investigations of Dynamical Processes and Transport Phenomena in the Transition Region Gasphase/Adsorbent by Molecular Dynamics Simulations

A. Schüring*, S. Vasenkov, S. Fritzsche*

*Institut für Theoretische Physik

Molecular dynamics simulations are applied to study the influence of crystal boundaries on the overall diffusional transport of molecules in nanoporous crystals. Boundary effects are expected to be of importance if the crystals are small, *i.e.* if the ratio of surface to volume is high. This is the case *e.g.* in catalysis, where relatively small crystals are used, and, furthermore, in currently developed hierarchically ordered porous materials [1] which enable a fast transport of molecules to the active crystals through a mesoporous channel system.

First investigations concentrated on a novel boundary effect observed in Monte-Carlo simulations [2, 3]. Under the conditions of single-file diffusion the concentration profiles of exchanged particles deviate from those observed for normal diffusion (see Fig. 3.4). At the boundaries, the degree of exchange is higher for single-file diffusion compared to normal diffusion while it is lower inside the channel. This corresponds to a faster diffusion at the crystal boundaries. We explain this with two diffuion mechanisms occuring in parallel [4]. Future calculations will consider the dependence of system parameters such as the self-diffusion coefficient, the permeability of the barrier and the sticking probability on the properties of the potential energy of the partiles in the crystal.

[1] Y. Tao and H. Kanoh, J. Am. Chem. Soc. (2003).
[2] P.H. Nelson and S.M. Auerbach, J. Chem. Phys. **110**, 9235 (1999).
[3] S. Vasenkov and J. Kärger, Phys. Rev. E **66**, 0526011 (2002).
[4] A. Schüring, S. Vasenkov and S. Fritzsche, J. Phys. Chem. B, submitted (2005).

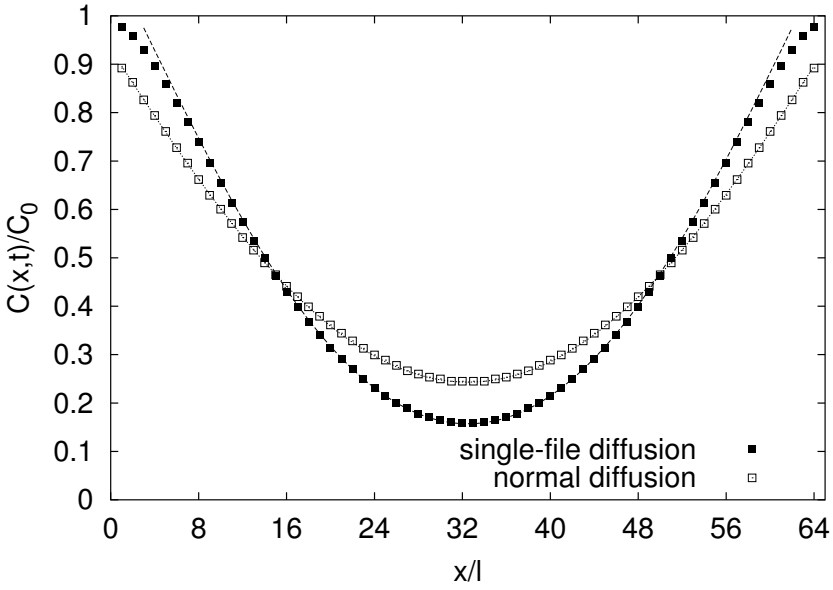

Figure 3.4: Concentration of exchanged particles along the one-dimensional channel.

3.5 Tortuosity Measurements on Formulated Catalyst Samples by PFG NMR

F. Stallmach, S. Crone*

*BASF AG Ludwigshafen, Germany

Pulsed field gradient nuclear magnetic resonance (PFG NMR) monitors averaged molecular displacements (r.m.s. displacements) and the self-diffusion coefficients of the guest molecules in porous materials on time scales, which - depending of the nuclear relaxation times - typically range from a few milliseconds up to seconds. PFG NMR may be used to determine geometric pore structure parameters and contributes to clarify the transport mechanisms of the guest molecules in the porous materials.

In cooperation with the BASF AG we successfully developed and applied a PFG NMR method to selectively measure the tortuosity (τ) of the transport pores in formulated catalyst particles [1]. It is based on measurements of liquid saturated catalyst particles and the comparison of the self-diffusion coefficients in the catalysts D_c and the bulk D_0:

$$\tau = \frac{D_0}{D_c} \geq 1. \tag{3.1}$$

Examples for typical measurement results obtained with fluid saturated formulated catalysts are shown in Fig. 3.5. The catalysts consist of porous zirconium oxid and are used for dehydration reactions [2]. The time dependencies of the mean square displacements of water and cyclooctane, which are used to probe the pore space of the two catalysts, are shown and compared to the corresponding values of the bulk fluids. The parallel shifts of the plotted lines, which are a direct consequence of the tortuosity τ, may be used to distinguish between different catalyst specimens.

[1] F. Stallmach, Habilitation thesis, University of Leipzig (2004).
[2] S. Crone, BASF AG, Private communications (2003/2004).

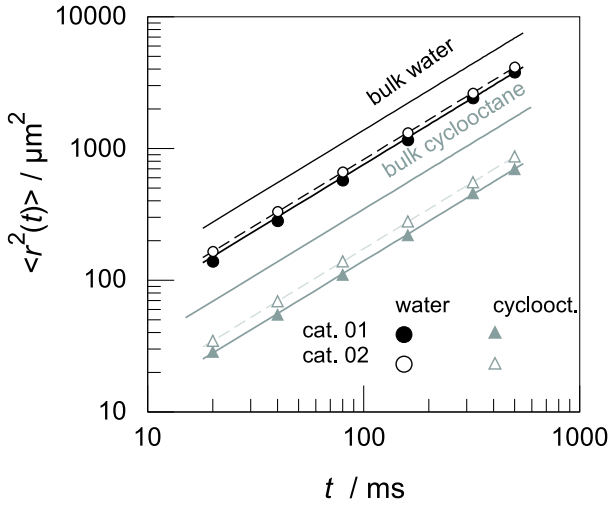

Figure 3.5: Time-dependence of the mean square displacement of water and cyclooctane in bulk and in two catalyst samples. In this log-log plot the parallel shift of the lines represents the tortuosity which is calculated using Eq. (3.1).

3.6 NMR Studies of Water Balance in Concretes with Internal Post-Curing

K. Friedemann, F. Stallmach, J. Kärger

In the ongoing project "Water balance in high performance concretes during internal post-curing with innovative additives" supported by the DFG (Ka 953/17-1), the water balance, the pore water self-diffusion and the transverse relaxation time T_2 in hardening cements of different compositions are investigated [1]. The total content of physically (capillary) bound water, its diffusivity and its transverse relaxation time are critical parameters for internal post-curing processes of cements. They are measured non-destructively by NMR diffusometry and relaxometry, respectively, in order to clarify the mechanism of internal post-curing by additives with temporary delayed release of water.

By CPMG NMR studies of the T_2 relaxation time, which yield qualitatively equivalent information on pore size of these materials as destructive mercury intrusion porosimetry [2], we monitor the amount of physically bound water in the sample, the onset and the progress of hydration (compare also Sect. 3.8) and address tendencies with respect to the final pore size under different post-curing conditions. Spatially resolved PFG NMR diffusion studies are used to determine the self-diffusion coefficient of the physically bound water in different sample locations and to monitor the water transition from the materials added as internal water source for post-curing of the cement matrix.

As an example, Fig. 3.6 shows the water transition from a small alginate sphere (diameter about 3 mm) [3], which contains initially 98 weight-% of water, into a cement matrix with an initial water-cement-ratio of 0.30. The NMR signal intensity at the position of the alginate sphere decreases with increasing hydration time, which means that water is transferred from the alginate to the surrounding cement matrix. The diffusion of this water through the cement matrix is fast, so that there is no built-up of a water concentration gradient. This fast diffusion is confirmed by PFG NMR yielding

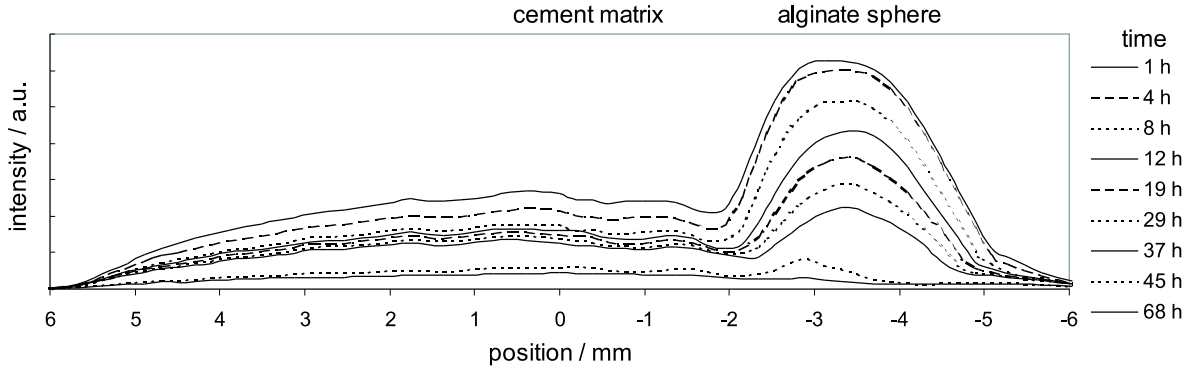

Figure 3.6: Water content of a small alginate sphere imbedded in a cement matrix. The release of water from the alginate with increasing hydration time is shown.

self-diffusion coefficients for the physically bound water, which decrease with increasing hydration time but which are never smaller than $1 \times 10^{-10}\,\mathrm{m^2 s^{-1}}$ during the first 40 hours of hydration [1].

[1] K. Friedemann, F. Stallmach, J. Kärger, NMR-Untersuchungen an hydratisierenden Zementen, LACER **9**. Leipzig, 345-349 (2004).
[2] S. Sharma, F. Casanova, W. Wache, A. Segre, B. Blümich, Magnetic Resonance Imaging **21**, 249-255 (2003).
[3] N. Nestle, Habilitation thesis, University of Leipzig, 2002.

3.7 NMR Diffusion Studies Using Magic Pulsed Field Gradient Ratios with Ultra-High Intensity Field Gradients

P. Galvosas, F. Stallmach, J. Kärger

By evaluating the spin echo attenuation for a generalized 13-interval PFG NMR sequence [1] consisting of pulsed field gradients with four different effective intensities ($F^{p/r}$ and $G^{p/r}$), magic pulsed field gradient (MPFG) ratios for the prepare (G^p/F^p) and the read (G^r/F^r) interval are derived, which suppress the cross term between background field gradients and the pulsed field gradients even in the cases where the background field gradients may change during the z-store interval of the pulse sequence [2]. These MPFG ratios depend only on the timing of the pulsed gradients in the pulse sequence and allow a convenient experimental approach to background gradient suppression in NMR diffusion studies with heterogeneous systems, where the local properties of the (internal) background gradients are often unknown. If the pulsed field gradients are centered in the τ-intervals between the π and $\frac{\pi}{2}$ rf pulses, these two MPFG ratios coincide to

$$\eta = \frac{G^{p/r}}{F^{p/r}} = 1 - 8 \Big/ \left[1 + \frac{1}{3}\left(\frac{\delta}{\tau}\right)^2\right] . \tag{3.2}$$

The predicted suppression of the unwanted cross terms was demonstrated experimentally using time-dependent external gradients which are controlled in the NMR experiment

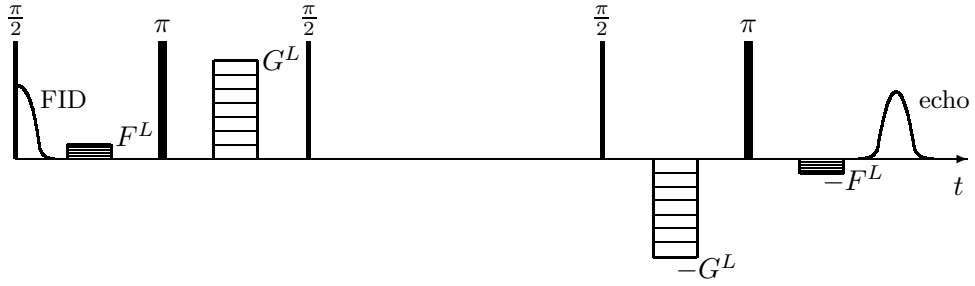

Figure 3.7: Example for the pulsed gradient pattern in the generalized 13-interval sequence. The height ratio of the pulsed gradients (F^L and G^L) drawn and their polarities satisfy the magic pulsed field gradient ratio of Eq. (3.2) for $\tau = 3\delta$, which yields an MPFG ratio of $F^L/G^L = 6.714$ (details see ref. [2]).

as well as spatially dependent internal background gradients generated by the magnetic properties of the sample itself [2].

Fig. 3.7 shows an example for the experimental realization of magic pulsed field gradient ratios. For the special cases considered in Eq. (3.2), the required MPFG ratio are always in the range of $5 \leq -\eta \leq 7$. Thus, such experiments are preferentially performed on NMR spectrometers equipped with ultra-high intensity pulsed field gradient capabilities [3].

This work will be continued and applied for projects in the DFG supported International Research Training Group "Diffusion in Porous Materials".

[1] R.M. Cotts et al., J. Magn. Reson. **83**, 252 (1989).
[2] P. Galvosas, F. Stallmach, J. Kärger, J. Magn. Reson. **166**, 164 (2004).
[3] P. Galvosas, F. Stallmach, G. Seiffert, J. Kärger, U. Kaess, G. Majer, J. Magn. Reson. **151**, 260 (2001).

3.8 NMR and Electrical Resistivity Studies on Self-Hardening Bentonite-Cement Suspensions Used as Geotechnical Barrier Material

W. Schoenfelder*, C. Flechsig*, F. Stallmach

*Institut of Geophysics and Geology, University of Leipzig

Cement bentonite cut-off walls are used for the containment of polluted sites or of old uncontrolled waste landfills. The backfill material more frequently used is the self-hardening cement bentonite mixture, which allows a single phase operation of trench excavations, filling and support of the trench sides. In order to prevent risks to the environment, it is very important to be able to assess hydraulic properties of such walls.

In the frame of a diploma thesis [1], we explored the capabilities of geoelectrical resistivity studies, of low-field NMR relaxometry and PFG NMR diffusometry [2] to characterize the water mobility and pore structure parameters of such bentonite-cement suspensions (BCS). Fig. 3.8 (left) shows the change of the transverse (T_2) relaxation time distribution in such a sample during hardening. From the values of the relaxation times and the areas under these distributions one can conclude that – even after 57 days of hardening –

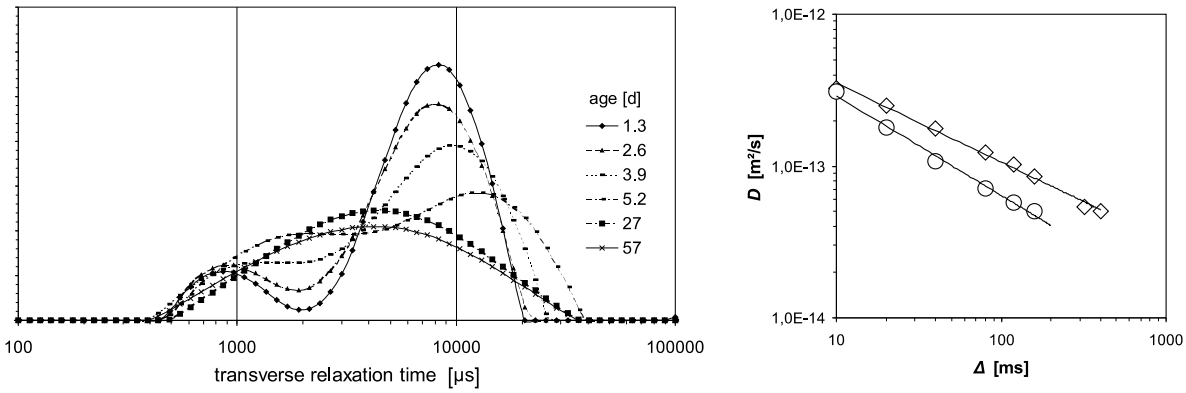

Figure 3.8: Transverse (T_2) relaxation time distribution of a self-hardening bentonite-cement suspension (BCS) during the first 57 days of hardening (left) and time-dependence self-diffusion coefficient in two BCS with different initial water content (right).

the majority of the water is still only physically (capillary) bound and not fixed on clay minerals or silicate hydrates. Nevertheless, the diffusivities of this water are by up to 4 orders of magnitude reduced compared to the self-diffusion coefficient of the free water and decrease slightly with increasing diffusion time (see Fig. 3.8, right).

Together with the time-dependent electrical resistivity studies, which show an increase of electrical resistance during hardening, these NMR results will enter into an advanced pore structure model of the BCS which shall predict hydraulic transport properties of such barrier materials from NMR and electrical properties. This work is continued and currently supported by the DFG via the International Research Training Group "Diffusion in porous materials".

[1] W. Schönfelder, Diploma thesis, University of Leipzig (2004).
[2] F. Stallmach, Habilitation thesis, University of Leipzig (2004).

3.9 Adsorption Hysteresis Probed by NMR Spectroscopy

R. Valiullin, P. Kortunov, J. Kärger

Phase transitions taking place in confined space often display specific features as compared to those in the bulk state. One of such challenging examples is the adsorption hysteresis in mesoporous materials, the origin of which is still controversially discussed in the literature. In the present work, this problem is experimentally addressed with the aid of nuclear magnetic resonance (NMR) spectroscopy, that allowed to follow the details of molecular dynamics in mesopores in region of the adsorption hysteresis [1, 2]. Importantly, dependence of the effective self-diffusion coefficient D_{eff} of intraporous liquid on the gas pressure was found to exhibit a hysteretic behaviour similar to that for the adsorption isotherm. In Fig. 3.9 typical experimental data referring to cyclohexane adsorption in Vycor porous glass are shown. Further investigations of the adsorbate state in pores on microscopical level using the NMR technique may significantly contribute to understanding the hysteresis phenomena under mesoscopic confinements.

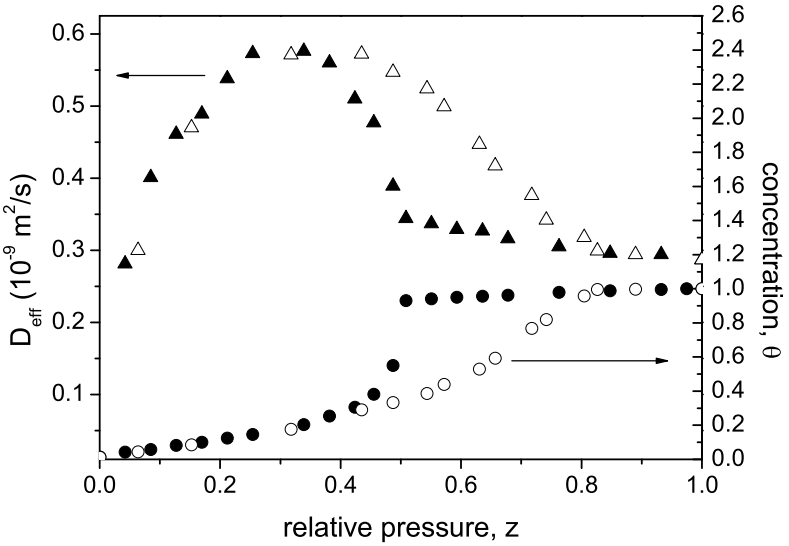

Figure 3.9: The pore filling factor θ (circles) and the self-diffusion coefficients D_{eff} (triangles) for cyclohexane in Vycor porous glass as a function of the relative vapour pressure z measured on the adsorption (open symbols) and the desorption (filled symbols) branches.

This work is supported by the Alexander von Humboldt Foundation.

[1] R. Valiullin, P. Kortunov, J. Kärger, V. Timoshenko, J. Chem. Phys. **120**, 11804 (2004).
[2] J. Kärger, R. Valiullin, S. Vasenkov, New J. Phys. **7**, 15 (2004).
[3] R. Valiullin, P. Kortunov, J. Kärger, V. Timoshenko, Magn. Reson. Imaging, *in press* (2005).
[4] R. Valiullin, P. Kortunov, J. Kärger, V. Timoshenko, J. Phys. Chem. B, *in press* (2005).

3.10 Transport Optimization of FCC Catalysts in the Framework of the EC Project "TROCAT"

P. Kortunov, S. Vasenkov, D. Freude, J. Kärger

This project addresses the problem of finding the routes of the production of fluid catalytic cracking (FCC) catalysts, which lead to improved catalytic performance due to optimization of the transport of reactants and products in these materials. The project consortium includes the University of Athens, CEPSA (Madrid), Grace (Worms), the Heyrovsky Institute Prague, SINTEF (Oslo) and the Stuttgart University. Recent progress in the area of the pulsed field gradient technique of nuclear magnetic resonance (PFG NMR) has made possible the direct observation of molecular migration (diffusion) in microporous catalysts. In the TROCAT project this technique is used to overcome one of the main shortcomings in the optimization of FCC catalyst, i.e. the lack of the optimization with respect to the transport properties.

PFG NMR in combination with classical uptake techniques has been applied to study molecular diffusion in the reference and modified FCC catalysts and in the samples of

reference and modified zeolite Y. This zeolite represents the most important, catalytically active part of FCC formulated catalysts. Investigations of transport properties of the samples were complemented by the characterization of their catalytic and structural properties. The project activities were focused on deactivated (by steaming and by poisoning metals) catalysts. The properties of such catalysts are of primary importance for refineries because they reflect the catalyst properties under typical operating conditions. The results obtained by the consortium have been used to elucidate the relevance of various modes of molecular transport, which are associated with different types of pores in catalyst particles, on the rate of molecular exchange between catalyst particles and their surroundings. Typically, each particle of a formulated FCC catalyst possesses a complex system of pores consisting of micropores located in zeolite crystals and of macro- and mesopores located in the so-called "matrix", which surrounds the crystals. It turned out that for large molecules (in particular for n-octane or still larger n-alkanes) the rate of molecular exchange between catalyst particles and their surroundings, which in many cases determines the overall rate and selectivity of the FCC process, is primarily related to the diffusion for displacements larger than the size of the zeolite crystals located in the particles but smaller than the size of the particles. Under conditions of such diffusion fast molecular exchange between the zeolite crystals and the surrounding macro- and mesopores can be expected. The diffusivity associated with this diffusion mode (i.e. intraparticle diffusivity) may be satisfactorily described as a product of the fraction of guest molecules in the macro- and mesopores of the catalyst particles and their diffusivities. Hence, intraparticle diffusivity does not directly depend on the diffusion coefficient in micropores of zeolite crystals (i.e. intracrystalline diffusivity). This new knowledge allowed us to optimize the transport properties of catalyst particles without changing the zeolitic part of the particles. The latter part is mostly responsible for chemical transformations and can be considered as being optimized already with respect to these transformations. The project results suggest that the intraparticle diffusivity can be increased by making the following parameters larger: (i) the macro- and mesoporosity of catalyst particles; (ii) the macro- and mesopore connectivity; and (iii) the mean size of macro- and mesopores. Using the route (iii) the consortium has prepared modified catalysts showing better catalytic performance as well as higher intraparticle diffusivities in comparison to the reference samples. The results outlined above demonstrate that the transport optimization of FCC catalysts can be based on scientific rather than on the conventional "try and see" approach. The experimental effort has been supported on all stages of the project by simulations of transport in model FCC catalysts.

3.11 Diffusion in Fluid Catalytic Cracking Catalysts on Various Displacement Scales and Its Role in Catalytic Performance

P. Kortunov, S. Vasenkov, J. Kärger

Recent progress in the area of pulsed field gradient (PFG) NMR technique has made possible the direct measurement of diffusivities in industrial FCC catalysts on various displacement scales. This is demonstrated in [1]. The recorded diffusivities are used to evaluate the relevance of various transport modes in the particles of FCC catalysts, such

as diffusion in the micropores of the zeolite crystals located in the particles, diffusion through the surface layer of these crystals and diffusion in the meso- and macropores of the particles, for the rate of molecular exchange between catalyst particles and the surrounding atmosphere. Our results show that for guest molecules which are at least as large as n-octane this rate is primarily determined by the coefficient of intraparticle diffusion. This diffusion coefficient may be satisfactorily described as a product of the fraction of guest molecules in the meso- and macropores of the particles and their diffusivities. Hence, intraparticle diffusivity does not directly depend on the diffusion coefficient in the micropores of the zeolite crystals (i.e. on the intracrystalline diffusivity). In the present work we have directly demonstrated that the intraparticle diffusivity may be increased by increasing the mean size of the macropores in the particles. This opens a possibility to optimize the transport properties of catalysts without changing the zeolitic part of the catalyst particles. The latter part is mostly responsible for chemical transformations and can be considered as being optimized already with respect to these transformations. This work has been done under coordination of Leipzig University, Germany in the framework of the "TROCAT" project (contract G5RD-CT-2001-00520), which is funded by the European Community under the "Competitive and Sustainable Growth" Programme.

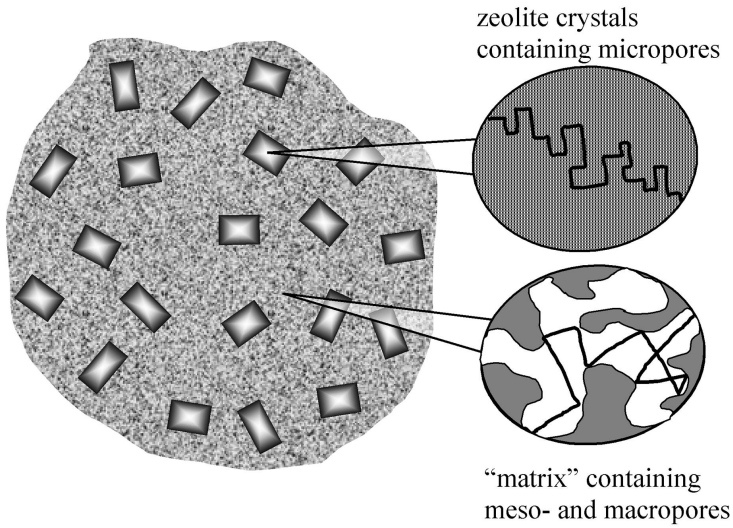

Figure 3.10: Schematic presentation of a particle of a typical FCC catalyst. The winding lines on the right side schematically show trajectories of the guest molecules.

[1] P. Kortunov, S. Vasenkov, J. Kärger, M. Fé Elía, M. Perez, M. Stöcker, G.K. Papadopoulos, D. Theodorou, B. Drescher, G. McElhiney, B. Bernauer, V. Krystl, M. Kocirik, A. Zikánová, H. Jirglová, C. Berger, R. Gläser, J. Weitkamp, E.W. Hansen, Diffusion in Fluid Catalytic Cracking Catalysts on Various Displacement Scales and Its Role in Catalytic Performance, *Chem. Mater.* 2005, in press

3.12 Influence of Defects on the External Crystal Surface on Molecular Uptake into MFI-Type Zeolites

P. Kortunov, S. Vasenkov, C. Chmelik, J. Kärger, D.M. Ruthven, J. Wloch

The interference microscopy technique, which was recently introduced in our laboratory [1], is applied to study transient intracrystalline concentration profiles in ZSM-5 crystals during adsorption and desorption of isobutane [2]. Two different zeolite samples were used, viz. samples of etched and of non-etched ZSM-5 crystals. Etching has been carried out to remove the outer layer of the crystal surface, which may contain large amounts of defects and impurities. Studying the transient concentration profiles in both samples provides unique information on the influence of surface defects on molecular uptake. It is shown that, depending on their type, the defects of the crystal surface can either increase or decrease the rate of adsorption/desorption. The former effect is associated with adsorption/desorption through cracks in the crystal surface. The latter has its origin in the blockage or structural changes of the external crystal surface leading to the appearance of surface transport barriers. Owing to the ability of interference microscopy to gain direct insight into the influence of surface defects on molecular uptake, this technique gives more accurate information on the transport diffusivities in zeolite crystals than the

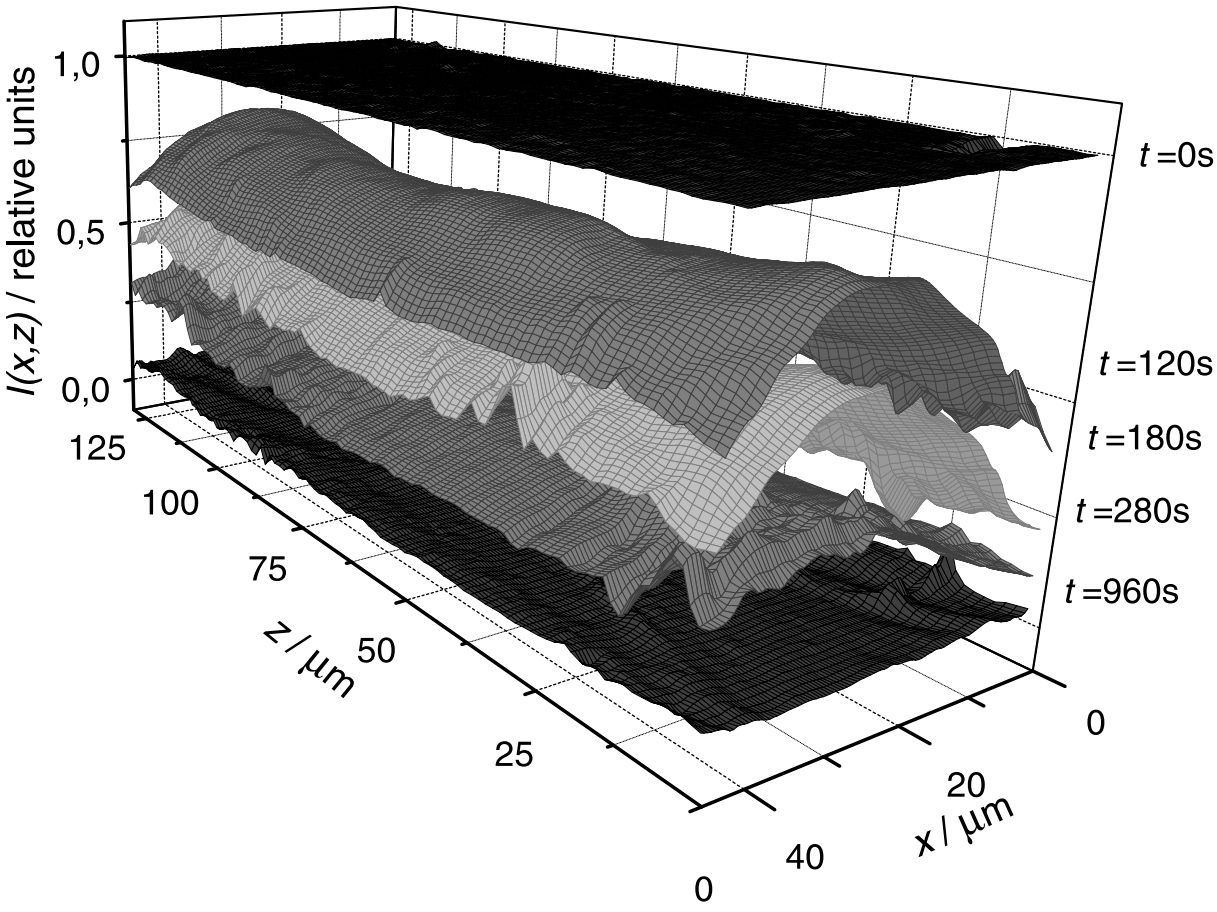

Figure 3.11: Concentration profiles during adsorption of isobutane into etched ZSM-5 crystals

classical uptake methods. Quantitative information on intracrystalline diffusivities has been obtained by fitting the measured concentration profiles by the results of dynamic Monte Carlo simulations [2].

[1] J. Kärger, S. Vasenkov, *Probing Host Structures by Monitoring Guest Distributions* In Host-Guest Systems Based on Nanoporous Crystals, F. Laeri, F. Schüth, U. Simon, M. Wark (Editors) Wiley-VCH, Weinheim, 2003, pp.255-279

[2] P. Kortunov, S. Vasenkov, C. Chmelik, J. Kärger, D.M. Ruthven, Influence of defects on the external crystal surface on molecular uptake into MFI-type zeolites *Chem. Mater.* 16 (2004) 3552

3.13 ^{17}O NMR Studies of the Structure and Basic Properties of Zeolites

H. Ernst, D. Freude, B. Knorr, D. Prager, D. Schneider

Multiple-quantum magic-angle spinning and double rotation NMR techniques were applied in the high field of 17.6 T to the study of oxygen-17 enriched zeolites A, LSX and sodalites with the ratio Si/Al = 1. A monotonic correlation between the isotropic value of the chemical shift and the Si–O–Al bond angle α (taken from X-ray data) could be found. It was confirmed that individual linear correlations exist between the isotropic ^{17}O chemical shift $\delta(^{17}\mathrm{O})$ and the s-character ρ of the oxygen hybrid orbitals for the hydro- and hydroxysodalites, the zeolites (with Si/Al = 1) Na-A (hydrated) and Na,K-LSX (hydrated, dehydrated). Corresponding linear dependencies can be found if the isotropic chemical shifts $\delta(^{17}\mathrm{O})$ are plotted against the Si-Al-distances in the Si–O–Al bridges. The increase in $\delta(^{17}\mathrm{O})$ by the adsorption of water and cation exchange can be separated from the effect of the bond angle α on the ^{17}O chemical shift.

The dehydration of the zeolites LSX causes ^{17}O NMR chemical shift changes by the superimposed effects of the well-known changes of the Si–O–Al bond angles and the effect of polarization of the framework by the adsorbed water molecules. The total effect is about 8 ppm, whereas the angular corrected effect amounts about 4 ppm. The low field shift due to the adsorption interaction is relatively small (ca. 2.2 ppm) for formic acid.

Ion exchange of the hydrated zeolites generates stronger chemical shift effects. The increase of the basicity of the oxygen framework of the zeolite LSX is reflected by a downfield shift of ca. 10 ppm going from the lithium to the cesium form, and the substitution of sodium by thallium in the zeolite A causes a shift of 34 ppm for the O3 signal.

^{17}O DOR NMR spectra are superior to ^{17}O 3QMAS NMR spectra with respect to the resolution by a factor of two. The application of the FAM2 excitation does not improve resolution or intensity in the ^{17}O 3QMAS NMR spectra. The signal-to-noise ratio of DOR and 3QMAS NMR spectra is comparable, whereas that of 5Q MAS NMR spectra is lower by more than one order of magnitude, and the spectral window is lower by a factor of five. This limits the application of the 5QMAS technique to the ^{17}O NMR. The residual linewidths of the signals in the ^{17}O DOR and ^{17}O 5QMAS NMR are caused by a distribution of the Si–O–Al angles in the zeolites.

3.14 *In situ* Studies of the ^{1}H and ^{13}C MAS NMR *n*-Butene Conversion on H-Ferrierite

H. Ernst, D. Freude, A.G. Stepanov

In situ spectroscopy of the temperature-dependent conversion of $n-$but-1-ene on H-ferrierite in a batch reactor offers information about the mechanism of isomerization and

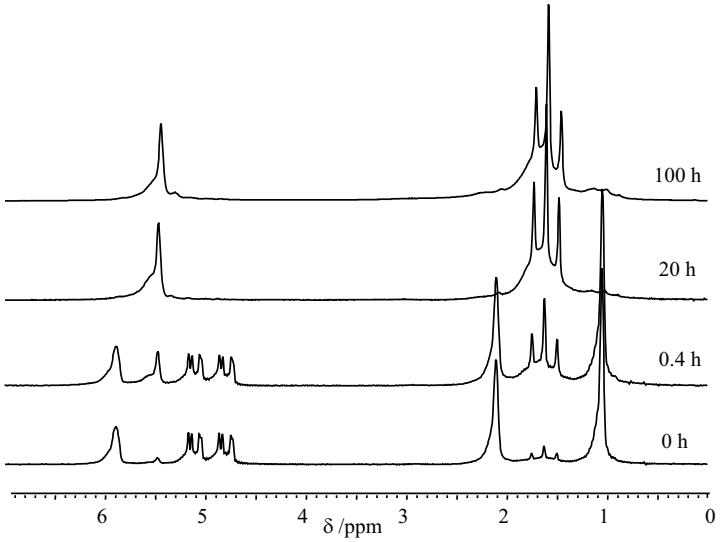

Figure 3.12: ^{1}H MAS NMR spectra of the zeolite H-FER loaded with [1-^{13}C]-$n-$but-1-ene1 at 300 K in dependence on the reaction time.

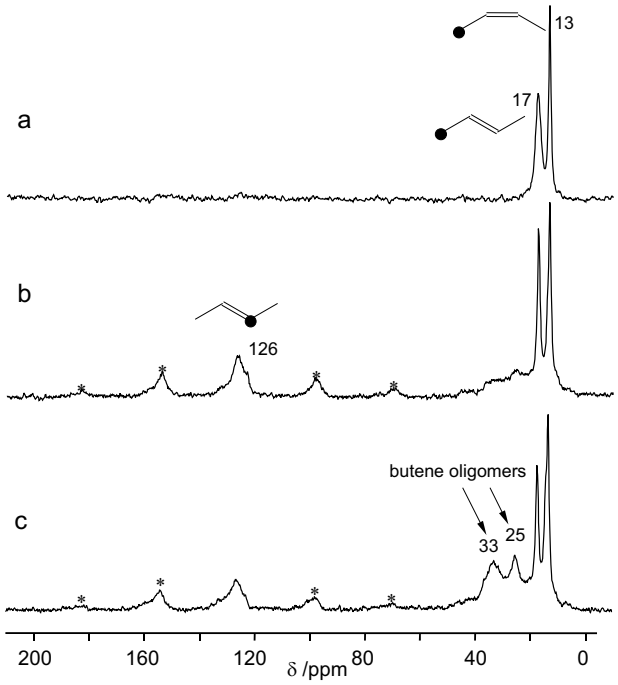

Figure 3.13: ^{13}C CP/MAS NMR spectra of the zeolite H-FER loaded with [1-^{13}C]-$n-$but-1-ene 1. (a) zeolite kept for 15 min at 300 K; (b) zeolite kept for one week at 300 K; (c) zeolite kept for 1 h at 373 K and then measured at 300 K.

the formation of carbonaceous deposits, which is important also for processes in a flow reactor. The following successive steps in the olefin conversion at increasing temperature of the reaction were distinguished: a double bond shift reaction affording *n*−but-2-enes; scrambling of the selective ^{13}C-label in *n*−but-2-enes, oligomerization (dimerization), conjunct polymerization, formation of condensed aromatics, formation of simple aromatics. Selective ^{13}C-label scrambling in *n*−but-2-ene and oligomerization as well as the absence of *iso*-butene among the products of *n*−but-1-ene isomerization, provide evidence for a bimolecular pathway of *n*−but-1-ene isomerization on a fresh zeolite.

3.15 In situ Studies of the Mechanism of Heterogeneously Catalyzed Reactions by Laser-Supported High-Temperature MAS NMR

H. Ernst, D. Freude, J. Kanellopoulos, D. Prager, D. Schneider

Surface sites capable of donating protons or accepting electrons from adsorbed molecules are essential for heterogeneous catalysis. Magic-angle-spinning nuclear magnetic resonance spectroscopy (MAS NMR) has been successfully applied to the study of the interaction between acid sites in zeolites and base molecules and to the catalytic conversion of organic molecules. The *in situ* technique became the most important tool for such studies. A new technique making use of a laser beam makes it possible to switch from room temperature, at which the reaction is too slow to be measured, to temperatures up to 800 K, at which the reaction takes place within a few seconds.

Activation energies of the proton transfer have been obtained under the assumption of a constant value of the pre-exponential factor in the Arrhenius plot to 102 kJ mol^{-1} for zeolite 85 H-Y (Si/Al = 2.4) and 93 kJ mol^{-1} for zeolite 92 H-Y (Si/Al = 3.1). In this case, the variation of the Si/Al ratio, which causes a change of the deprotonation energy of the bridging hydroxyl groups, can explain the differences of the exchange rate. However, a variation of the pre-exponential factor by steric effects like the existence of non-framework aluminum species cannot be excluded.

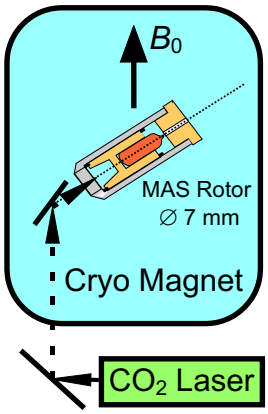

Figure 3.14: Experimental setup.

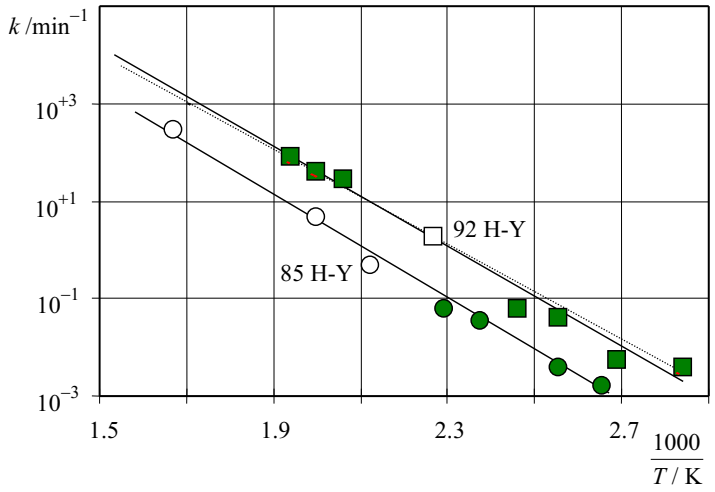

Figure 3.15: Arrhenius plot of the H-D and H-H exchange rates for benzene molecules in the zeolites 85 H-Y and 92 H-Y. The values which are marked by open or full circles and squares were measured by laser heating or conventional heating, respectively.

3.16 Long-Time Scale Molecular Dynamics of Constrained Fluids Studied by NMR

F. Grinberg

Soft matter systems like liquid crystals, polymers, colloids or biomembranes are characteristic of the orientational molecular order on the meso- and macroscopic length scales. Individual or collective molecular motions in these substances tend to range over many time decades. This in turn gives rise to extremely slow spin relaxation mechanisms in the range of milliseconds and longer. The most illustrative examples can be found with the confined liquid crystals [1] widely used in the electro-optical devices. Another example is given by elastomers in which ultra-slow chain relaxation modes are associated with the presence of chemical cross-links [2].

Addressing molecular dynamics of complex fluids by the NMR techniques raise a problem of decomposing numerous overlapping stochastic processes contributing to spin relaxation in the same frequency or time ranges. In our work we investigate the effects produced by nano- to micrometer scale constraints on dynamical and structural properties of organised fluids using a combination of several NMR techniques: stimulated echo studies [1], 2D-exchange spectroscopy [3], temperature and frequency dependent measurements of the relaxation rates [3, 4] and diffusion studies with help of Pulsed Field Gradient NMR [5]. Experimental data are supported by the Monte-Carlo simulations.

In confined liquid crystals, the cavity constraints are found to strongly affect molecular collective and non-collective orientational fluctuations both below and above the nematic-isotropic transition. The correlation length of the surface-induced order is determined. In elastomers, ultraslow chain relaxation modes with correlation times of the order of a few milliseconds were monitored by measuring the dipolar-correlation effect on the stimulated echo [2]. The mean squared fluctuation of the residual dipolar coupling constant shows a strong dependence on the cross-link density of rubber materials and suggests a new contrast parameter for NMR mapping [6].

Acknowledgements: I cordially thank Prof. R. Kimmich and Prof. M. Vilfan for fruitful multi-year co-operation. A big part of the experiments was performed in the Sektion Kernresonanzspektroskopie, Universität Ulm. Financial support by the Deutsche Forschungsgemeinshaft (DFG) and the Ministerium für Wissenschaft, Forschung und Kunst Baden-Württemberg is gratefully acknowledged.

[1] F. Grinberg, M. Vilfan, E. Anoardo. In "NMR of Ordered Liquids", E.E. Burnell and C.A. de Lange (Eds.), Kluver Academic Publishers, Dordrecht, 2003.
[2] F. Grinberg. In Handbook of Modern Magnetic Resonance, G. Webb, Ed., Kluwer Academic Publishers, Dordrecht, 2005.
[3] F. Grinberg. In NATO SCIENCE SERIES "Magnetic Resonance in Colloid and Interface Science", J. Fraissard and O. Lapina (Eds.), Kluver, Dordrecht, 2002.
[4] R. Kimmich. "NMR: Tomography, Diffusometry, Relaxometry", Springer, Heidelberg, 1997.
[5] J. Kärger. In "Diffusion-Fundamentals 1" (www.uni-leipzig.de/diffusion/pages/contributions.html), 2005.
[6] F. Grinberg, M. Heidenreich and W. Kuhn, J. Magn. Reson., **159**, 87, (2002).

3.17 Normal Diffusion in an Aluminophosphate under Different Transport Conditions: A Molecular Dynamics Study

J. Gulin-Gonzalez*, A. Schüring, S. Fritzsche, S. Vasenkov, J. Kärger

*Universidad de Ciencias Informáticas (UCI), La Habana, Cuba

One of the most striking problems in the study of the diffusion processes in microporous materials is the frequent discrepancy between the values of diffusivities measured by conventional uptake methods and microscopic methods [1]

While the uptake experiments observe macroscopic properties of mass transport, the microscopic techniques monitor diffusion processes on displacement scale much smaller than the crystalline size. For this reason, macroscopic phenomena such as transport barriers on a crystal surface or intergrowth effects have a limited influence in the diffusivities obtained by microscopic methods.

The aim of this research is to perform an extensive MD study of the molecular diffusion in $AlPO_4$-5 microporous material in presence of surface barriers. We attempt a description of the molecular exchange in different "experimental" conditions, focusing on the analysis in the extreme transport conditions: desorption-limited transport and diffusion-limited transport.

Simulations were carry out for a particle which performs normal diffusion in $AlPO_4$-5. Different site occupancy ($\theta = 0.25, 0.50$ and 0.75), and two temperatures, 200 and 300 K were considered. A time step of 10 fs was used in the simulations. The equilibrium of the system was achieved in all cases within a time < 1 ns. After the equilibration, production runs of 10^4 ns were performed.

The behaviour of the profiles in the marginal sites shows the influence on the diffusion of the surface barriers. At the same temperature and loading only the length of the channel

can affect the transport conditions in the system. For $\theta = 0.25$ and $L = 13.744\,\text{nm}$ (a very thin membrane) and at both temperatures simulated the profiles are very flat indicating an homogenous concentration of molecules independent of the position inside the channel. In these conditions, the influence of the surface barrier is critical, that is, the desorption in the marginal sites is the determining factor on the molecular transport. This case corresponds to the desorption-limited transport condition. When L is increased the profiles trend to the classical shape for a normal diffusion regime. For longer channel ($L = 217.188\,\text{nm}$), the exchange of labelled molecules in the sites localized in the centre of the channel is practically void, suggesting that in this condition the intracrystalline diffusion limited the molecular transport in the zeolite.

Taking into account the relative value of $\alpha L/D$ ratio (α is the permeability and D is the self-diffusion coefficient), different conditions are possible: for a shorter channel, lower loading and at both temperatures (200 and 300 K) the desorption-limited transport is observed, this condition can be extended to the case of $L = 27.148\,\text{nm}$. After this, we have different situations to produce intermediate transport conditions, this means, a similar influence of both boundaries and intracrystalline diffusion on transport: low loading ($\theta = 0.25$), long channel and $T = 200\,\text{K}$, $\theta = 0.50$, $L > 27.148\,\text{nm}$ and $T = 300\,\text{K}$, and $\theta = 0.75$, $L < 27.148\,\text{nm}$ and $T = 300\,\text{K}$. For$L > 27.148\,\text{nm}$, the diffusion-limited transport is observed.

Finally, the values of α and D obtained by macroscopic method (numerical solution of Fick's second law) and microscopic method (TST for α and Einstein equation for D) are in good agreement.

[1] J. Kärger, *Diffusion under Confinement*, Verlag der Sächsischen Akademie der Wissemchaften zu Leipzig – In Komission bei D. Hirzel Stuttgart/Leipzig, Band 128, Heft 6 Germany, 2003.

[2] J. Crank, *The Mathematics of Diffusion*, Claredon Press, Oxford, 1956.

3.18 Funding

Prof. Dr. D. Freude, Dr. H. Ernst
Untersuchung der Protonen-Beweglichkeit in H-Zeolithen mit PFG NMR und MAS NMR im Temperaturbereich bis 800 K.
DFG-Projekt FR 902 / 12-1 und FR 902 / 12-2

Prof. Dr. D. Freude, Dr. H. Ernst
Anwendungen der Doppelrotations- und Multiquanten-Messtechnik für Hochfeld-NMR-Untersuchungen an ^{17}O-Kernen in porösen Festkörpern.
FR 902 / 16-1 und FR 902 / 16-2

Prof. Dr. D. Freude
Alkan- und Alken-Aktivierung in der heterogenen Säurekatalyse. Insitu-^{13}C und ^{1}HMAS NMR-Untersuchungen der Kinetik des Isotopen-Scramblings (^{13}C, ^{2}H im Reaktionsverlauf.
FR 902 / 15-1

Prof. Dr. J. Kärger
Molecular diffusion in nanoporous materials.
DFG-CNRS-Project KA 953/14-1, KA 953/14-2

Prof. Dr. J. Kärger
Reaktion und Diffusion in Single-File Netzwerken: Computersimulationen und statistisch-thermodynamische Untersuchungen.
DFG-Projekt KA 953/15-1

Prof. Dr. J. Kärger, Dr. habil. F. Stallmach
Fourier-Transform-PFG-NMR mit starken Feldgradientenimpulsen zur selektiven Selbstdiffusionsmessung.
DFG-Projekt KA 953/16-1

Prof. Dr. J. Kärger
Wasserbilanz in Hochleistungsbeton.
DFG-Projekt KA 953/17-1

Prof. Dr. J. Kärger
Studying Zeolitic Diffusion by Interference and IR Microscopy.
DFG-Projekt KA 953/18-1 within the International Research Group "Diffusion in Zeolites"

Prof. Dr. J. Kärger, PD Dr. Sergey Vasenkov
Bestimmung mikroskopischer Kenngrößen der Molekültranslation in Schüttungen nanoporöser Partikel mittels PFG NMR und Monte-Carlo-Simulationen."
DFG-Projekt KA 953/19-1

Prof. Dr. J. Kärger
Development of new ceramics.
EC-Project GRD1-1999-11207

Prof. Dr. J. Kärger
New dealumination routes to produce transport-optimised catalysts for crude oil conversion.
EC-Project GRD2-2000-30364

Prof. Dr. J. Kärger, Dr. habil. F. Stallmach
Diffusion optimation of microporous membranes and particle batches.
EC-Project HPMD-CT-2000-00029

Prof. Dr. J. Kärger, Dr. F. Stallmach
PFG NMR investigations on technical catalysts.
BASF AG

Dr. F. Stallmach, Prof. Dr. J. Kärger
NMR and MRI studies of aquifer rock.
UFZ Halle-Leipzig GmbH

Prof. Dr. J. Kärger
Confinement Effects on Diffusion and Reaction in Zeolites, Studied by Dynamic MC Simulations, PFG NMR and Interference/IR Microscopy.
DFG-Graduiertenkolleg 1056/1 within the International Research Training Group "Diffusion in Porous Materials"

Dr. habil. Frank Stallmach
Fluid Transport in Porous Rocks and Sediments from Near-Surface Aquifers Studied by NMR and MRI.

DFG-Graduiertenkolleg 1056/1 within the International Research Training Group "Diffusion in Porous Materials"

Prof. Dr. Dieter Freude
Combined NMR Studies of Diffusion and Reaction.
DFG-Graduiertenkolleg 1056/1 within the International Research Training Group "Diffusion in Porous Materials"

3.19 Organizational Duties

Jörg Kärger

- Ombudsman of Leipzig University
- Membership in the Programme Committee "Magnetic Resonance in Porous Media" (Ulm 2002, Paris 2004), "Fundamentals of Adsorption" (Sedona, Arizona, USA, 2004), International Zeolite Conference (Capetown 2004) and in the permanent DECHEMA committees Zeolites and Adsorption
- Membership in Editorial Boards: Microporous and Mesoporous Materials (European Editor), Diffusion Fundamentals (Online Journal, Editor), Adsorption
- Referee: Phys. Rev., Phys. Rev. Lett., Europhys. Lett., J. Chem. Phys., J. Phys. Chem., Langmuir, Micropor. Mesopor. Mat., PCCP, J. Magn. Res.
- Project Reviewer: Deutsche Forschungsgemeinschaft, National Science Foundation (USA)

Dieter Freude

- Project Reviewer: Deutsche Forschungsgemeinschaft
- Membership in Editorial Boards: Solid State NMR, Diffusion Fundamentals (Online Journal, Editor)
- Referee: Chem. Phys. Lett., J. Chem. Phys., J. Phys. Chem., J. Magn. Res., Solid State NMR

Brigitte Staudte

- Referee: Micropor. Mesopor. Mat.

Sergey Vasenkov

- Referee: J. Am. Chem. Soc., Micropor. Mesopor. Mat.

Frank Stallmach

- Referee: J. Magn. Res., Micropor. Mesopor. Mat., Phys. Rev. Lett.

3.20 External Cooperations

Academic

Acad. Sci. Czech. Republ., Inst. Macromol. Chem., Czech Republic,
Prof. Konak, Prof. Stepanek

Acad. Sci. Czech. Republ., Heyrovsky-Inst. Phys. Chem., Czech Republic,
Dr. Kocirik, Dr. Zikanova

Delft University, Inst.Chem. Tech., Delft, Niederlande
Prof. Kapteijn

Institut de Recherches sur la Catalyse, CNRS, Villeurbanne, France
Dr. Jobic

Institut Francais du Petrole, Malmaison, France
Dr. Methivier

KFA Jülich GmbH, Forschungszentrum, Inst. Biotechnol., Jülich, Germany
Dr. Schoberth

Max Planck Institut für Kohlenforschung, Mülheim, Germany
Dr. Schmidt, Prof. Schüth

Max Planck Institut für Metallforschung, Stuttgart, Germany
Dr. Majer

Russian Acad. Sci., Boreskov Inst. Catalysis, Siberian Branch, Novosibirsk, Russia
Dr. Stepanov

TU München, Lehrstuhl Technische Chemie 2, Germany
Dr. Kornatowski, Prof. Lercher

Università di Sassari, Dipartimento Chimica, Sassari, Italy
Prof. Demontis, Prof. Suffritti

Universiät Eindhoven, Schuit Institute, Eindhoven, Niederlande
Prof. van Santen

Universität Erlangen Nürnberg, Dept. Chem. Engin., Erlangen, Germany
Prof. Emig, Prof. Schwieger

Universität Hannover, Dept. Phys. Chem., Hannover, Germany
Prof. Caro, Prof. Heitjans

Universität Leipzig, Institut für Analytische Chemie, Leipzig, Germany
Prof. Berger

Universität Leipzig, Institut für Technische Chemie, Leipzig, Germany
Prof. Einicke, Prof. Papp

Universität Leipzig, Institut für Medizinische Physik und Biophysik, Leipzig, Germany
Prof. Arnold, Prof. Gründer

Universität Leipzig, Instiut für Pharmazeutische Technolgie, Leipzig, Germany
Prof. Süß

Universität Leipzig, Wilhelm Ostwald Institut für Physikalische & Theoretische Chemie, Leipzig, Germany
Dr. Hunger, Dr. Knoll

Universität Regensburg, Inst. Biophysik & Physikalische Biochemie, Regensburg, Germany
Prof. Brunner

Universität Stuttgart, Institut für Technische Chemie, Stuttgart, Germany
Prof. Hunger, Prof. Weitkamp

University Athens, Dept Chem. Engn., Athens, Greece
Prof. Theodorou

University of Maine, Dept. Chem. Engin., USA
Prof. Ruthven

Industry

Air Prod & Chem Inc, Allentown
Dr. Coe, Dr. Zielinski

BASF, Ludwigshafen
Dr. Müller

Cepsa, Madrid
Dr. Perez

Grace, Worms
Dr. McElhiney

Resonance Instruments Ltd., Witney, UK
J. McKendry

SINTEF, Oslo
Prof. Stöcker

Tricat, Berlin
Dr. Tufar, Dr. Lutz

3.21 Publications

Journals

Kortunov P., Vasenkov S., Chmelik C., Karger J., Ruthven DM., Wloch J.
Influence of defects on the external crystal surface on molecular uptake into MFI-type zeolites.
Chem. Mat. 16 (2004): 3552-3558.

Rauscher M., Selvam T., Schwieger W., Freude D.
Hydrothermal transformation of porous glass granules into ZSM-5 granules.
Micropor. Mesopor. Mater. 75 (2004) 195-202.

Bauer F., Ernst H., Hirsch D., Naumov S., Pelzing M., Sauerland V., Mehnert R.
Preparation of scratch and abrasion resistant polymeric nanocomposites by monomer grafting onto nanoparticles, 5(a) - Application of mass Spectroscopy and atomic force microscopy to the characterization of silane-modified silica surface.
Macromol. Chem. Phys 205 (2004) 1587-1593.

Gröger S., Geschke D., Kärger J., Stallmach F., Konak C.
Co-micellization investigated by pulsed field gradient-NMR spectroscopy.
Macromol. Rapid. Commun. 25 (2004) 1015-1018.

Bauer F., Chen WH., Ernst H., Huang SJ., Freyer A., Liu SB.
Selectivity improvement in xylene isomerization.
Micropor. Mesopor. Mater. 72 (2004) 81-89.

Valiullin R., Kortunov P., Kärger J., Timoshenko V.
Concentration-dependent self-diffusion of liquids in nanopores: A nuclear magnetic resonance study.
J. Chem. Phys. 120 (2004) 11804-11814.

Schüring A., Fritzsche S., Haberlandt R., Vasenkov S., Kärger J.
Modeling molecular diffusion in channel networks via displacements between the channel segments.
Phys. Chem. Chem. Phys. 6 (2004) 3676-3679.

Bräuer P., Fritzsche S., Kärger J., Schütz G., Vasenkov S.
Diffusion in Channels and Channel Networks,
In molecules in interaction with surfaces and interfaces, R. Haberlandt, D. Michel, A. Pöppel, R. Stannarius (Editors) Springer, Heidelberg, 2004

Kärger J., Papadakis C.M., Stallmach, F.
Structure-Mobility Relations of Molecular Diffusion in Interface Systems,
In Molecules in Interaction with Surfaces and Interfaces, R. Haberlandt, D. Michel, A. Pöppel, R. Stannarius (Editors) Springer, Heidelberg, 2004

Brzank A., Schütz G.M., Bräuer P., Kärger J.
Molecular traffic control in single-file networks with fast catalysts
Phys Rev E 69 (2004) No. 031102.

Nestle N., Galvosas P., Zimmermann C., Stallmach F., Kärger J.
Direct investigation of the fate of NAPL contaminations in a hydrating cement matrix by means of magnetic resonance techniques.
Environ. Sci. Technol. 38 (2004) 880-885.

Galvosas P., Stallmach F., Kärger J.
Background gradient suppression in stimulated echo NMR diffusion studies using magic pulsed field gradient ratios.
J. Magn. Reson. 166 (2004) 164-173.

Geier O., Snurr R. Q., Stallmach F., Kärger J.
Boundary effects of molecular diffusion in nanoporous materials: A pulsed field gradient nuclear magnetic resonance study.
J. Chem. Phys. 120 (2004) 367-373.

Gane P., Ridgway C., Lehtinen E., Valiullin R., Furó I., Schoelkopf J., Paulapuro H., and Daicic J.
On the comparison of NMR cryoporometry, mercury intrusion porosimetry and DSC thermoporosimetry in characterizing pore size distributions of compressed fine ground calcium carbonate structures
Ind. Eng. Chem. Res. 43, 7920 (2004)

Valiullin R., Vargas-Krusa D., Furo I.
Liquid-liquid phase separation in micropores
Curr. Appl. Phys. 4, 370 (2004)

in press

Pampel A., Fernandez M., Freude D., Kärger, J.
New Options for Measuring Molecular Diffusion in Zeolites by MAS PFG NMR
Chem. Phys. Lett., in press

Vasenkov S., Kärger J.
Long-range diffusion in beds of nanoporous particles: Pitfalls and potentials,
Magnetic Resonance Imaging 2005, in press

Kortunov P., Vasenkov S., Kärger J., Fe Elía M., Perez M., Stöcker M., Papadopoulos G. K., Theodorou D., Drescher B., McElhiney G., Bernauer B., Krystl V., Kocirík M. , A. Zikánová, H. Jirglová, C. Berger, R. Gläser, J. Weitkamp, E.W. Hansen
Diffusion in Fluid Catalytic Cracking Catalysts on Various Displacement Scales and Its Role in Catalytic Performance, Chem. Mater. 2005, in press

Kortunov P., Vasenkov S., Kärger J., Fe Elía M., Perez M., Stöcker M., Papadopoulos G. K., Theodorou D., Drescher B., McElhiney G., Bernauer B., Krystl V. ,Kocirík M., Zikánová A. , Jirglová H., Berger C., Gläser R., Weitkamp J., Hansen E.W.
Diffusion in Fluid Catalytic PFG NMR study of transport properties of FCC catalysts
Magnetic Resonance Imaging 2005, in press

Vasenkov S., Kortunov P.
PFG NMR measurements of tortuosity factors for diffusion in meso- and macropores of FCC catalysts
Diffusion Fundamentals. 2005, in press.

Valiullin R., Kortunov P., Kärger J., Timoshenko V. Surface self-diffusion of organic molecules adsorbed in porous silicon
J. Phys. Chem. B, in press

Valiullin R., Kortunov P., Kärger J., Timoshenko V.
Concentration-dependent self-diffusion of adsorbates in mesoporous materials
Magn. Reson. Imaging, in press

submitted

Simon J.-M., Bellat J.-P., Vasenkov S., Kärger J.
Sticking Probability on Zeolites
J. Phys. Chem. B, submitted

3.22 Guests

Dr. Taro Ito/Sapporo
Juni 2004

Dr. Krysztof Banas/ University of Krakov, as a Marie-Curie Fellow of the EC
January-August 2004

Dr. Federico Brandani/ University of Aquila, as a Marie-Curie Fellow of the EC
January-August 2004

Dr. Alexander Stepanov/ Novosibirsk
March-August 2004

Dr. Jorge Gulin-Gonzalez/ University of Habana, as an Alexander von Humdoldt fellow
September-December 2004

Dipl.-Phys. Aleksey Khokhlov/ Bauman Moscow State University, as an Awardee of the Russian Federation President
November-December 2004

4

Soft Matter Physics

4.1 General Scientific Goals - Polymers and Membranes in Cells

Studies of soft matter physics on the scale of nanometers to tens of microns, i.e., on the scale of proteins and cells, in complex multifunctional biological matter - often far from equilibrium and frequently behaving in a highly nonlinear manner - are the next big challenge for materials science. Our division is based on the idea that a complete understanding of molecular and cell biological systems calls forth a new type of fundamental physics, biological physics, which can describe biological soft matter with active elements and which is adaptive to multipurpose. Over the last decade there has been tremendous progress in molecular biology. Nevertheless, this progress will only impact the design and development of new materials if a novel combination of nanosciences and soft matter physics is developed - bridging biology and engineering. This synergetic research in physics, chemistry, engineering and biology simultaneously advances our fundamental knowledge-base and provides novel applications in biomedicine and materials science.

The need for novel soft matter physics is exemplified in the actin cytoskeleton. The actin cytoskeleton, a compound of highly dynamic polymers and active nano-elements inside biological cells, mechanically senses a cell's environment and generates cellular forces sufficiently strong to push rigid AFM-cantilevers out of the way. These forces are generated by molecular motor-based nano-muscles and by polymerization through mechanisms similar to Feynman's hypothetical thermal ratchet. Active polymer networks are described by a new type of polymer physics since nano-sized molecular motors overcome the inherently slow, often glass-like Brownian polymer dynamics resulting in novel self-organization and rapid switching through dynamical instabilities.

Light has been used to observe cells since Leeuwenhoek's times; however, we use the forces caused by light described by Maxwell's surface tensor to feel cells. The optical stretcher exploits the nonlinear, thus amplified response of a cell's mechanical strength to small changes between different cytoskeletal proteomic compositions as a high precision cell marker that uniquely characterizes different cell types. Consequentially, the optical stretcher detects tumors and their stages with accuracy unparalleled by molecular biology approaches. This precision allows us to isolate adult stem cells. Stem cells are cells which have not yet differentiated into specialised tissues such as skin, brain or muscle. They

promise a new class of regenerative medicine, which could repair apparently permanent damage such as heart disease or Parkinson's.

Stem cells are currently extracted from aborted human foetuses, an issue which has led to controversy and opposition in many parts of the world. An alternative source is the isolation of stem-cell-like cells from adults, e.g. from blood. Scientists have known for some time that adult stem cells exist. However the only way to separate them involved contaminating the cells with molecular markers, making the use for medical purposes questionable. The optical stretcher technique for the first time uses a physical characteristic of each cell - its stretchiness or elasticity - instead of its biological make-up, to decide whether or not it's a stem cell. Stem cells don't need a rigid "cytoskeleton" to hold them in shape, which makes them stretchier than normal cells. The optical stretcher uses a powerful beam of infrared laser light to stretch and measure cells one by one. The optical stretcher differs from an existing tool known as optical tweezers in which the light is focused to a sharp point to grab hold of a cell. In contrast, the optical stretcher does not use focused light. This allows laser beams up to 2 W, strong enough to detect stretching, to be used without killing the cell. The optical stretcher uses the refractive index of the cell to generate stretching forces. As the laser beam enters the cell, its momentum changes, reverting back again as it exits at the other end. These momentum changes exert equal and opposite forces on the cell at the entry and exit points, which stretch the cell in the direction of the laser beam. The optical stretcher can already test 3,600 cells per minute. This is not yet fast enough for industrial production of millions of stem cells, but it promises a viable future alternative to the use of human embryos.

The optical stretcher promises more immediate benefits elsewhere, in the diagnosis and staging of cancer. Cancer cells tend to de-differentiate, losing their rigid cytoskeleton. Just as with stem cells, the optical stretcher can be used to identify this characteristic. Of all the physical properties of a cell, elasticity is the one which varies most dramatically between normal and cancerous cells. This makes stretching the most sensitive method known for identifying cancer. Just 50 tumour cells within a sample are required for the optical stretcher to test for cancer, contrasting with traditional methods which need 10,000 to 100,000 cells. With such small samples, doctors will be able to test where traditional biopsies are dangerous or even impossible. More importantly, the optical stretcher can yield crucial information on the spread of cancer. The softer the cancer cells, the more likely they are to travel through the body and produce secondary tumours (known as metastases). Traditionally, doctors have had to check nearby lymph nodes for cancer cells. However, the optical stretcher can determine, just by measuring cells from the primary tumour, whether or not the cancer is likely to be spreading. Secondary tumours can be difficult to find, and women with breast cancer often undergo precautionary mastectomy or whole-body chemotherapy. The optical stretcher will allow many women to avoid the emotional and physical side-effects of such unnecessary treatment. The optical stretcher is already fast enough to be useful in clinical diagnosis of cancer. We believe that this high speed and the equipment's low cost could even herald a shift towards cancer prevention. Dentists, for example, could swab their patients for mouth cancer cells even before a solid tumour develops. A clinical prototype of the optical stretcher is currently being developed together with the Dresden-based company Gesim and the TU Dresden. The Berlin branch of the biotech-company Evotec plans to use the stretcher as diagnosis tool in a joint venture with MIT, the In-

stitute Pasteur, the University of Singapore, and us. Concepts for the use in regenerative therapies are investigated together with the Leipzig-based company Neuroprogen in case of Parkinson disease and with the Leipzig-based company Euroderm in case of tissue engineering.

In addition to probing cytoskeletal structure, optical gradient forces can also influence cytoskeletal activity allowing us to manipulate neuronal growth. The specific opto-molecular interactions are complex since cells, which cannot modulate diffusion by the parameters found in the Einstein equation (temperature, viscosity, molecular size), exhibit rich multifaceted behavior including ballistic transport and anomalous diffusion.

4.2 Active Polymer Networks

D. Smith, F. Ziebert, W. Zimmermann, B. Gentry, J. Käs

The molecular motor myosin II has not only the well-known force generating functions in structures such as muscle cells; it can fluidize entangled actin networks by superseding reptation dynamics with myosin-induced filament sliding. This illustrates how molecular motors can overcome conventional polymer dynamics and generate an active material with a new switchable viscoelastic behavior. Up to 40 % of a cell's energy (i.e. ATP) turnover fuel this active, energy-dissipating states of the actin cytoskeleton illustrating the importance for a cell's material properties.

All eukaryotic cells rely on self-assembly of protein filaments to form an intracellular cytoskeleton. The necessity of motility and reaction to stimuli additionally requires pathways that serve to reversibly change cytoskeletal organization. While temperature-driven disordering is, from the viewpoint of physics, the most obvious method for dissolving complex cellular structures, such an approach would exceed the physiologically viable temperature range. This motif is exemplified in the de-hybridization of DNA, which is temperature-induced in PCR, but achieved by molecular motors in cells. We report another fundamental mechanism whereby changes in the activity of the molecular motor myosin II induce order-disorder transitions in reconstituted cytoskeletal actin-myosin networks. Bulk activity of the motors, which causes sliding of individual filaments [1], maintains a dynamically disordered network. During depletion of the ATP supply, an increasing fraction of molecular motors becomes inactive, crosslinking actin filaments to small clusters. The remaining active motors combined with continually increasing cross-linking foster further growth of these clusters, resulting in a variety of ordered macro-molecular structures such as asters, networks resembling neuronal architectures, and condensed super-precipitates. Experiments with photo-activated motors demonstrate the quick reversible restoration of the disordered state. This nonequilibrium pathway to switch between order and disorder is much faster than any structural changes driven by Brownian motion in thermodynamic equilibrium. This ability for rapid, isothermal motor-induced transitions between different degrees of self-organization indicates that molecular motors, in general, may substantially contribute to dynamic cellular organization.

[1] D. Humphrey, C. Duggan, D. Saha, D. Smith and J. Käs, Active fluidization of polymer networks through molecular motors, Nature, **416** 413- 416 (2002)

[2] Smith D, Ziebert F, Humphrey D, Duggan C, Zimmermann W, Käs J. Molecular motors in cells: a rapid switch of biopolymer organization. Science, submitted.

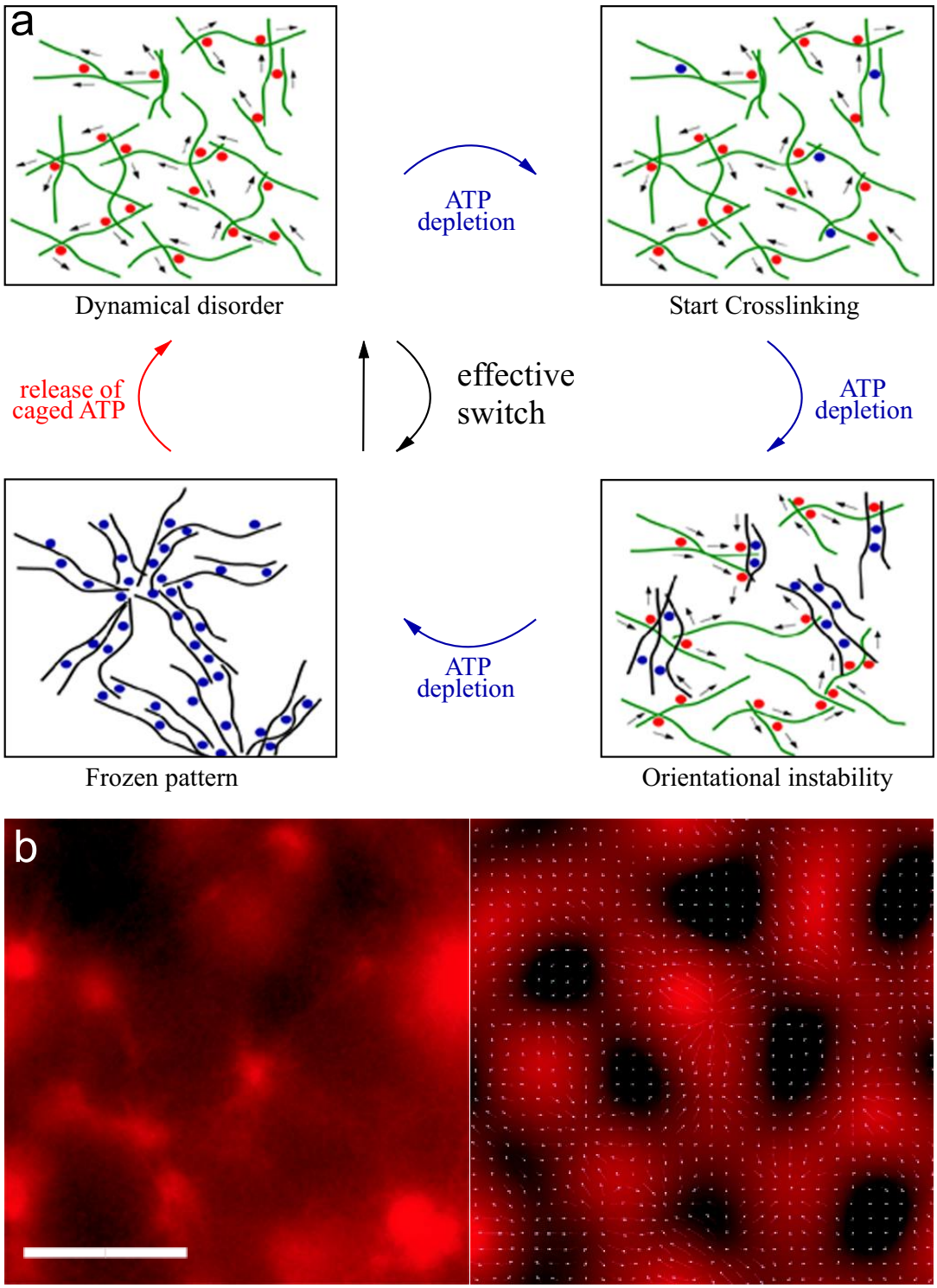

Figure 4.1: Nonlinear instabilities allow rapid switching between ordered and disordered states in active polymer networks.

[3] For background see also: J. Käs, H. Strey and E. Sackmann, Direct imaging of reptation for semiflexible actin filaments, Nature, **368**, 226-229 (1994); Nedelec, F.J., Surrey, T., Maggs, A.C. & Leibler, S. Self-organization of microtubules and motors, Nature **389**, 305-308 (1997)

4.3 SFM-Based Cell Microrheology

S. Park, C. Brunner, K. Franze, J. Gerdelmann, A. Ehrlicher, D. Koch, M. Gögler, K. Shih, J. Käs

Viscoelastic changes of the lamellipodial actin cytoskeleton are a fundamental element of cell motility. Thus, the correlation between the local viscoelastic properties of the lamellipodium (including the transitional region to the cell body) and the speed of lamellipodial extension is studied for normal and malignantly transformed fibroblasts. Using our newly developed SFM-based microrheology technique, we found different mechanical properties between the lamellipodia of malignantly transformed fibroblasts (H-ras transformed and SV-T2 fibroblasts) and normal fibroblasts (BALB 3T3 fibroblasts). The average elastic constants, K, in the plateau regime of SV-T2 fibroblasts (0.63±0.44 kPa) and of H-ras transformed fibroblasts (0.57±0.47 kPa) are significantly lower than that of BALB 3T3 fibroblasts (1.35±1.02 kPa). The analysis of time-lapse phase contrast images shows that the decrease in elastic strength for malignantly transformed fibroblasts is correlated with an enhanced motility of the lamellipodium. The measured mean speeds are 6.1±4.5 μm/h for BALB 3T3 fibroblasts, 13.1±4.2 μm/h for SV-T2 fibroblasts, and 26.2±11.5 μm/h for H-ras fibroblasts. Furthermore, the elastic strength K increases towards the cell body in many instances. This observation is complementary with the actin fluorescence images which show a decreased actin density at the leading edge of a lamellipodium. The correlation between the enhanced motility and the decrease in viscoelastic moduli points towards the 'Elastic Brownian Ratchet model' for driving lamellipodia extension (Mogilner and Oster, 1996).

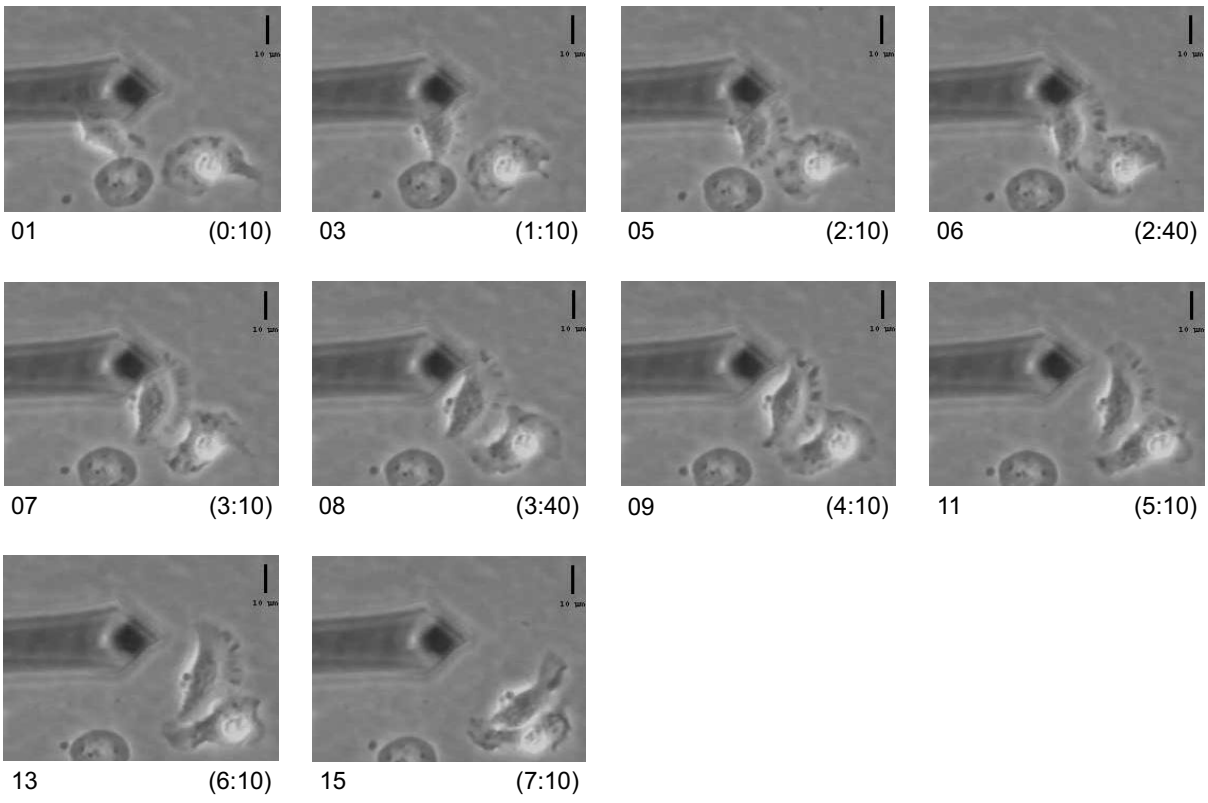

Figure 4.2: Biological Cell probed by an SFM

Furthermore, we present direct measurements of the forward forces generated at the leading edge of the lamellipodium, the cell body, and lamellar fragments of fish keratocytes. We positioned an elastic spring, the cantilever of a scanning force microscope (SFM) in front of a moving cell, which pushed the cantilever out of its path. We measured forward forces between 1-8 nN without visibly affecting the cells. A load dependence behaviour was not observed for opposing forces up to at least 15 nN, where the cells were strongly deformed. Further increase caused the cells to stop due to structural damage.

[1] R. Mahaffy, C.K. Shih, F.C. MacKintosh, and J. Käs, Quantitative analysis of the viscoelastic properties of thin regions of fibroblasts using atomic force microscopy, Biophys. J., **86**, 1777-1793 (2004)
[2] S. Park, R. Cardenas, J. Käs, and C.K. Shih, Cell motility and local viscoelasticity of fibroblasts, Biophys. J., in press (2005)
[3] C. Brunner, A. Ehrlicher, B. Kohlstrunk, D. Knebel, J. Käs, and M. Goegler, Propulsive forces of fast moving biological cells, Phys. Rev. Lett., submitted
[4] For background see also: R. Mahaffy, C.K. Shih, F. C, MacKintosh, and J. Käs, Scanning probe-based, frequency-dependent microrheology of polymer gels and biological cells, Phys. Rev. Lett., **85**(4), 880-883 (2000)

4.4 Optical Deformability as a Cell Marker

F. Wottawah, S. Schinkinger, B. Lincoln, S. Ebert, F. Sauer, J. Käs, J. Guck

A step stress deforming suspended cells causes a passive relaxation, due to a transiently cross-linked isotropic actin cortex underlying the cellular membrane. The fluid-to-solid transition occurs at a relaxation time coinciding with unbinding times of actin cross-linking proteins. Elastic contributions from slowly relaxing entangled filaments are negligible. The symmetric geometry of suspended cells ensures minimal statistical variability in their viscoelastic properties in contrast with adherent cells and thus is defining for different cell types. Mechanical stimuli on time scales of minutes trigger active structural responses.

The relationship between the mechanical properties of cells and their molecular architecture has been the focus of extensive research for decades. Especially the cytoskeleton, an internal polymer network, determines a cell's mechanical strength and morphology. This cytoskeleton evolves during the normal differentiation of cells, is involved in many cellular functions, and is characteristically altered in many diseases, including cancer. We demonstrate here that we can exploit this link between function and elasticity to distinguish between different cells using a microfluidic optical stretcher, a two-beam laser trap optimized to serially deform single suspended cells by optically induced surface forces. In contrast to previous cell elasticity measurement techniques, statistically relevant numbers of single cells can be measured in rapid succession through microfluidic delivery, without any modification or contact. We find that optical deformability is sensitive enough to monitor the subtle changes during the progression of mouse fibroblasts and human breast epithelial cells from normal to cancerous and even metastatic state. The surprisingly low numbers of cells required for this distinction reflects the tight regulation of the cytoskeleton by the cell. This suggests using optical deformability as an inherent cell marker for basic cell biological investigation and diagnosis of disease.

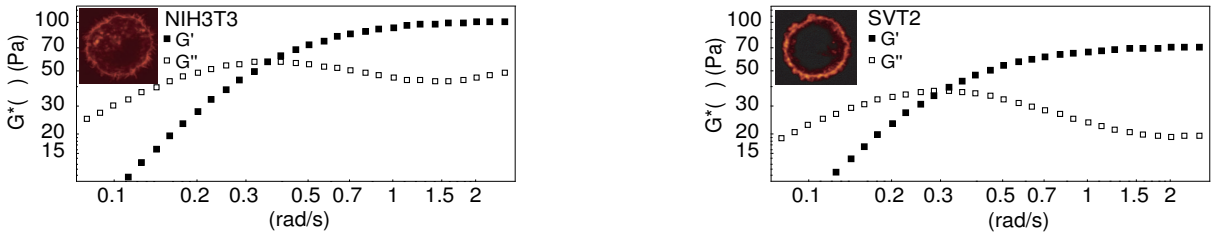

Figure 4.3: Rheological data of a normal (left) and a cancerous (right) cell

[1] F. Wottawah, S. Schinkinger, B. Lincoln, R. Ananthakrishnan, M Romeyke, J. Guck, J. Käs, Optical rheology of biological cells, Phys. Rev. Lett., 94(9), 98103 (2005)

[2] J. Guck, H. Erickson, R. Ananthakrishnan, D. Mitchell, M. Romeyke, S. Schinkinger, F. Wottawah, B. Lincoln, J. Käs, S. Ulvick, and C. Bilby. Optical Deformability as Inherent Cell Marker for Malignant Transformation and Metastatic Competence. Biophys. J. 88:5 (2005)

[3] For background see also: J. Guck, R. Ananthakrishnan, T.J. Moon, C.C. Cunningham and J. Käs, Optical deformability of soft dielectric materials, Phys. Rev. Lett., 84(23), 5451-5454 (2000); J. Guck, R. Ananthakrishnan, T.J. Moon, C.C. Cunningham and J. Käs, The Optical Stretcher - A Novel, noninvasive tool to manipulate biological materials, Biophys. J., 81 767-784 (2001)

4.5 Light Guidance Properties of Cell

K. Franze, J. Grosche, S.N. Skatchkov, S. Schinkinger, D. Schild, O. Uckermann, K. Travis, A. Reichenbach, J. Guck

The retina of the vertebrate eye is inverted with respect to optical function. Light has to pass through a significant thickness of scattering tissue before it reaches the light-sensitive photoreceptor cells. Without additional functionality, this architecture would critically reduce the eye's sensitivity especially in scotopic vision. Given the small acceptance angle of rod photoreceptor cells responsible for low-light-level vision, any significantly scattered photon would be lost for detection. Here we show that the retina contains living optical fibers that guide light from the vitreous body through the scattering layers of the neuronal retina and to the photoreceptor cells, all with minimal loss. These optical fibers are identified as Müller cells, which are radial glial cells and span the entire thickness of the retina. Measurements evaluate the transmission and scattering properties of Müller cells both in their natural matrix, using retinal whole-mounts, and as isolated cells, using a modified dual-beam laser trap. The experiments are supported by theoretical modeling. This finding ascribes a new optical function to glial cells in the retina and enables a more complete understanding of the retina as an optimally-integrated optical system.

[1] K. Franze, J. Grosche, S.N. Skatchkov, S. Schinkinger, D. Schild, O. Uckermann, K. Travis, A. Reichenbach, J. Guck, Spotlight on Glial Cells: Living Optical Fibers in the Vertebrate Retina, Nature, submitted

4.6 Optically Guided Neuronal Growth

A. Ehrlicher, T. Betz, D. Koch, B. Stuhrmann, M. Goegler, J. Käs

The highly dynamic, active properties of the actin cytoskeleton require that it is a reaction-diffusion based system which allows quick assembly and disassembly. Guided by this basic property of the cytoskeleton we are therefore using delicate light-induced gradient forces to control biochemical cellular processes (in sharp contrast to the established technique of optical tweezers, which holds entire cellular structures with strong gradient forces). Control over neuronal growth is a fundamental objective in neuroscience, cell biology, developmental biology, biophysics, and biomedicine, and is particularly important for the formation of neural circuits in vitro, as well as nerve regeneration in vivo. We have shown experimentally that we can use weak optical forces to guide the direction taken by the leading edge, or growth cone, of a nerve cell. In actively extending growth cones, a laser spot is placed in front of a specific area of the nerve's leading edge, enhancing growth into the beam focus and resulting in guided neuronal turns as well as enhanced growth. The power of our laser is chosen so that the resulting gradient forces are sufficiently powerful to bias the actin polymerization-driven lamellipodia extension, but too weak to hold and move the growth cone. We are therefore using light to control a natural biological process, in sharp contrast to the established technique of optical tweezers which uses large optical forces to manipulate entire structures. Our results therefore open a new avenue to controlling neuronal growth in vitro and in vivo with a simple, non-contact technique. We have shown that weak optical dipole forces can be used to bias the molecular process of cell motility so that we can guide neuronal growth. Since we influence lamellipodia extension, a process essential for all motile cells, optical guidance may be extended as a general cell guidance method, and may provide an investigative tool to understand the underlying processes of cell motility. Moreover, we hope that optical guidance will allow us to form controlled neuronal structures in vitro, and we can also imagine that optical guidance could find applications in nerve repair in vivo.

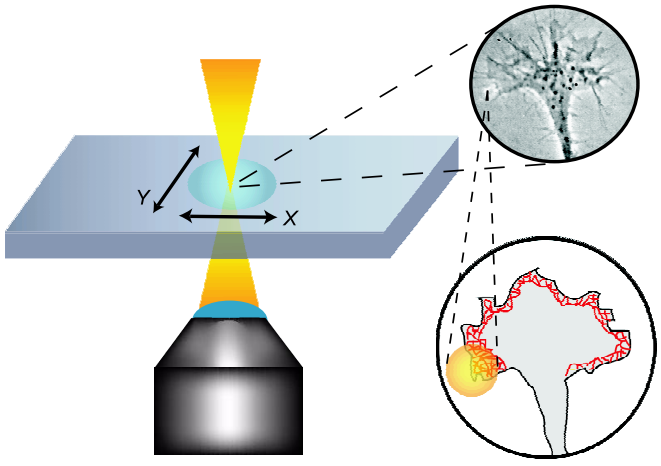

Figure 4.4: Experimental setup for the optical guidance of growing neurons. A laser spot (diameter = 2 - 16 μm, power = 20 - 120 mW, λ= 800 nm) was placed with partial overlap in front of an actively extending growth cone. The overlap area was chosen in the direction of the preferred growth and to cover the actin cortex, which directly underlies the plasma membrane and drives the advancement of the leading edge of the nerve.

[1] A. Ehrlicher, T. Betz, B. Stuhrmann, D. Koch, V. Milner, M. Raizen and J. Käs, Guiding neuronal growth with light, PNAS, 99(25) 16024-16028 (2002)
[2] For background see also: E.J. Furnish, W. Zhou, C.C. Cunningham, J. Käs, and C.E. Schmidt, Increased actin severing via gelsolin overexpression enhances neurite outgrowth, FEBS Lett., 508 282 - 286 (2001)

4.7 Signal Transduction Investigated by Nano-Probes

D. Martin, M. Forstner, F. Rückerl, A. Falk, L. Woiterski, S. Surber, C. Selle

Single particle tracking on phase separated Langmuir phospholipid monolayers reveals transient confinement of diffusing probe beads to the phase boundaries, leading to a transition from two- to one-dimensional diffusion. The confinement is explained by a dipole-dipole interaction between domains of the liquid condensed phase and the diffusion probe. Since similar interactions are expected between lipid rafts and membrane proteins, the experiments are extended to cellular scales with numerical simulations, showing an order of magnitude reduction of the long term diffusion coefficient.

The diffusion of nano-particles in monolayers in the presence of condensed lipid domains has been investigated by Monte Carlo simulations. Due to an excess dipolar moment density, the domains exhibit an electric dipole field. A change of this radial field, from single dipole to semi infinite domain characteristics, has been shown for increasing radii. A significant influence of this dependence on the motion of the particle has been found. For small domains (R=1 μm) the motion was confined to the domain boundary. In contrast, larger domains (R=10 μm) induced a temporary change of the diffusion only.

[1] M.B. Forstner, D.S. Martin, A.M. Navar, J. Käs, Simultaneous Single Particle Tracking and Fluorescence Microscopy on Inhomogenous Lipid Monolayers, Langmuir, in press (2003)
[2] D. Martin, M. Forstner and J. Käs, Apparent subdiffusion inherent to single particel tracking, Biophys. J., in press (2002)
[3] For background see also: M. Forstner, J. Käs and D. Martin, Single lipid diffusion in Langmuir monolayers, Langmuir, 17(3), 567-570 (2001)

4.8 Interaction of Functionalized Nanoparticles with β-Amyloid Peptides

H. Schmiedel, W. Härtig, T. Siegemund

The general purpose of the project is the explanation of the structure and the physicochemical properties of nanoparticles acting as carriers of active ingredients in the treatment of neurodegenerative deseases such as Alzheimer disease (AD). One hallmark of brains in AD is the appearance of extracellular plaques consisting of amyloid-beta-peptide aggregates (Aβ, usually comprising 40 - 42 amino acids). Polymer nanoparticles with different size, surface and hydrophobicity (see e.g. [1]) were shown to penetrate the blood-brain barrier and might interact with the Aβ plaques. Coated nanoparticles will be chosen for the in vitro interactions between Aβ- aggregates and some of their specific

ligands. This study includes nanoparticles surface-labelled with: 1. β-sheet breaking low-molecular-mass substances, 2. Aβ-specific antibodies and 3. Aβ itself (with appropriate spacers). Due to the interdisciplinary character of the project largely different methods are applied to study the interaction of functionalized nanoparticles with Aβ-aggregates. SANS [2] (Small Angle Neutron Scattering) measurements are performed to derive the structure of the active layers coating the nanoparticles. QELS (Quasi Elastic Light Scattering) and ITC (Isothermic Titration Calorimetry) measurements are used to support the SANS results. The distribution of the nanoparticles and their released model drugs targeting fibrillar Aβ in the brains of transgenic mice with age-dependent β-amyloidoses are studied by light and electron microscopy including multiple fluorescence labelling and confocal laser scanning. First electron microscopic data on the delivery of the Aβ-binding model compound thioflavin-T after injection of nanoparticles with encapsulated thioflavin into the hippocampus of wild-type mice were published [3]. Nanoparticles optimized by the physico-chemical methods mentioned above are tested for drug targeting in animal models and might result in carriers for medical applications.

[1] B.-R. Paulke, W. Härtig, G. Brückner. Synthesis of nanoparticles for brain cell labelling in vivo. Acta Polymerica 43 (1992) 288-291.
[2] H. Schmiedel, P. Jörchel, M. Kiselev, G. Klose. Determination of structural parameters and hydration of unilamellar POPC/C12E4 vesicles at high water excess from neutron scattering curves unsing a novel method of evaluation. J. Phys. Chem. B 105 (2001) 111-117.
[3] W. Härtig, B.-R. Paulke, C. Varga, J. Seeger, T. Harkany, J. Kacza. Electron microscopic analysis of nanoparticles delivering thioflavin-T after intrahippocampal injection in mouse: implications for targeting β-amyloid in Alzheimer's disease. Neurosci. Lett. 338 (2003) 174-176.

4.9 Funding

Prof. Dr. J.A. Käs:
Alexander von Humboldt Foundation, Euro 2.0 Mio, 2002 - 2005, "Molecular structure and function of biopolymer networks, characterized by novel laser trapping tools, nanorheology and single polymer microscopy"

Prof. Dr. J.A. Käs:
Donation to the Softmatter Physics Division from Ms. M. Duda/ 40,000.00 Euro

Prof. Dr. J.A. Käs:
"Laser Directed Growth Cone Motility: A Study on How Optomolecular Mechanisms Influence Cytoskeletal Activity"
DFG-Project KA 1116/ 3-1

Prof. Dr. J.A. Käs, Dr. C. Selle:
"Untersuchung der Diffusion von Nanosonden in inhomogenen Monoschichten als Modell für diffusiven Transport in Lipidmembranen"
DFG-Project KA 1116/ 4-1

Prof. Dr. H. Schmiedel (jointly with Dr. W. Härtig, P.-Flechsig-Institut für Hirnforschung):
Wechselwirkung beschichteter Nanopartikel mit Amyloid-Peptiden/ Interaction of functionalized nanoparticles with β-amyloid peptides
BMBF, 03DUO3LE (from 1/2003, within Bereich Neutronenstreuung)

4.10 Organizational Duties

Joseph A. Käs

- Berufungskommission, Theoretische Biopysik
- Berufungskommission, Nachwuchsgruppe, MPI für angewandte Mathematik in den Wissenschaften
- Berufungskommission, Quantengravitation
- Berufungskommission, Nachfolge Geschke
- Advisory committee for soft matter physics, NASA, USA
- Prize committee, "Freundlichste Auslaenderbehoerde", Alexander von Humboldt Foundation
- CNRS review committee, Institute Curie, Paris
- Organizing committee, Summer School for Soft Matter Physics 2004, Iran
- Journal review: Nature, Physical Review Letters, Physical Review E, Biophysical Journal, Biophysica and Biochemica Acta, Biochemistry, Proceedings of the National Academy of Science, European Biophysical Journal, Langmuir
- Grant review: National Science Foundation, Div. of Materials Research; National Science Foundation, Div. of Cellular Organization; National Science Foundation, Div. of Computational Biology; National Science Foundation, Div. of Physics, Special Programs; Deutsche Forschungs Gesellschaft, Alexander von Humboldt Foundation, Deutsche Studienstiftung, Centre National de Reserche

4.11 External Cooperations

Academic

Prof. Dr. Harry Swinney
Center for Nonlinear Dynamics, Austin, Texas

Prof. Dr. Jean-Francois Joanny
Institute Curie, Paris

Prof. Dr. Jacques Prost
ESPCI, Paris

Prof. Dr. Marie-France Carlier
Cea Saclay, France

Prof. Dr. Walter Zimmermann
University of Saarbruecken

Prof. Dr. Reinhardt Lipowsky
MPI for Colloids and Interfaces, Potsdam-Golm

Industry

GeSim GmbH, Dresden

Evotec GmbH, Berlin

Euroderm GmbH, Leipzig

Neuroprogen GmbH, Leipzig

FAUN GmbH, Leipzig

jpk Instruments, Berlin

Nimbus GmbH, Leipzig

4.12 Publications

Journals and books

Selle C, Rückerl F, Martin DS, Forstner MB, Käs JA. Measurement of Diffusion in Langmuir Monolayers by Single-Particle-Tracking. Physical Chemistry Chemical Physics.; 6(24), 5535-5542 (2004)

Daniel Koch, Timo Betz, Allen Ehrlicher, Michael Gögler, Björn Stuhrmann, Josef Käs, Optical control of neuronal growth, Proceedings of SPIE Vol.5514, 428-436, (2004)

B. Lincoln, H.M. Erickson, S. Schinkinger, F. Wottawah, D. Mitchell, S. Ulvick, C. Bilby, and J. Guck. Deformability-Based Flow Cytometry. Cytometry 59A:203-209 (2004)

S. Schinkinger, K.A. Travis, F. Wottawah, B. Lincoln, and J. Guck. Feeling for Cells with Light. Proceedings SPIE: Optical Trapping and Optical Micromanipulation 5514, 170-178 (2004).

F. Wottawah, S. Schinkinger, B. Lincoln, R. Ananthakrishnan, M. Romeyke, J. Guck, J. Käs, Optical rheology of biological cells, Phys. Rev. Lett., 94(9), 98103 (2005)

J. Guck, H. Erickson, R. Ananthakrishnan, D. Mitchell, M. Romeyke, S. Schinkinger, F. Wottawah, B. Lincoln, J. Käs, S. Ulvick, and C. Bilby. Optical Deformability as Inherent Cell Marker for Malignant Transformation and Metastatic Competence. Biophys. J. 88:5 (2005).

S. Park, R. Cardenas, J. Käs, and C.K. Shih, Cell motility and local viscoelasticity of fibroblasts, Biophys. J., in press (2005)

T. Betz, J. Teipel, D. Koch, W. Härtig, J. Guck, J. Käs and H. Giessen, Excitation beyond the monochromatic laser limit: Simultaneous 3-D confocal and multiphoton microscopy with a tapered fiber as white-light laser source, J Biomed Optics, in press (2005)

K. Travis, K. Sokolov, J. Guck. Scattering from Single Nanoparticles: Mie theory revisited. Lecture Notes in Physics in press, (2005).

F. Wottawah, S. Schinkinger, B. Lincoln, S. Ebert. K. Müller, F. Sauer, K. Travis, and J. Guck. Characterizing Single Suspended Cells by Optorheology. Acta Biomat. in press, (2005)

R. Wang, H. Schmiedel, B.-R. Paulke:
Isothermal Titration Calorimetric Studies of Surfactant Interactions with negatively charged, 'hairy' Latex Nanoparticles, Colloid Polym. Sci 283 (2004) 91-97

P. Berghuis, M. Dobszay, K.M. Sousa, G. Schulte, P.P. Mager, W. Härtig, T.J. Görrcs, Y. Zilberter, P. Ernfors, T. Harlkany:
Brain-derived neurotrophic factor controls functional differentiation and microcircuit formation of selectively isolated fast-spiking GABAergic interneurons, Eur. J. Neurosci. 20 (2004) 1290-1306.

Conference contributions, talks, posters

Prof. Dr. J. Käs
Conference "Mathematical Aspects of Material Science", Castle Ringberg, Munich/ Max-Planck Institute for Mathematics in the Sciences
February 2004 (invited talk)

Prof. Dr. J. Käs
Invitation DPG-spring conference
Regensburg
March 2004 (invited talk)

Prof. Dr. J. Käs
International Winterschool "Physics of the Cell", Institute Curie, Paris
Les Houches, France
March 2004 (invited talk)

Prof. Dr. J. Käs
Summer school on "Soft and Biological Matter", organized by Institute for Advanced Studies in Basic Sciences (IASBS) and the University of Leipzig (Soft Matter Physics Division)
Zanjan, Iran
June 2004 (talk)

Prof. Dr. J. Käs
Workshop "Physics and Biology: A Material Science Approach", Institut Curie
Paris, France
July 2004 (invited talk)

Prof. Dr. J. Käs
Heraeus summer school "Dynamik in dünnen Schichten und Grenzflächen",
Otto-von-Guericke Universität Magdeburg
September, 2004 (invited talk)

Prof. Dr. J. Käs
Symposium on "Single Cell Mechanics", MIT
Boston, USA (invited talk)
October 2004

Prof. Dr. J. Käs
Workshop on "Struktur und Dynamik von Polymeren in einschränkenden Geometrien unterschiedlicher Topologie"
Großbothen
December 2004 (invited talk)

Dr. J. Guck
Annual Meeting of the German Physical Society, Section Biological Physics
Regensburg, Germany (invited talk)
March 2004

Dr. J. Guck
Colloids Seminar (Prof. Maret), Universität Konstanz
Konstanz, Germany (invited talk)
March 2004

Dr. J. Guck
DPG-Jahrestagung 2004
Regensburg
March 2004 (poster)

Dr. J. Guck
Summerschool "Soft and Biological Physics"
Institute for Advanced Studies in Basic Sciences
Zanjan, Iran (lecture series, T)
June 2004

Dr. J. Guck
Conference on Optical Trapping and Micromanipulation (SPIE Annual Meeting)
Denver, USA (invited talk)
August 2004

Dr. J. Guck
Annual Conference of the European Life Science Organization (ELSO 2004)
Nice, France (invited talk)
October 2004

Dr. J. Guck
Symposium on Single Cell Mechanics, MIT
Boston, USA (invited talk)
October 2004

Dr. J. Guck
5th Dresden Fall Seminar on "Fluid Dynamics",
MPI for Physics of ComplexSystems
Dresden, Germany (invited talk)
November 2004

Dr. C. Selle:
48th Annual Meeting Biophysical Society
Baltimore, MD.,
February 2004 (poster)

Dr. C. Selle:
DPG-Jahrestagung 2004
Regensburg
March 2004 (poster)

Dr. C. Selle:
103. Bunsentagung
Dresden,
May 2004 (talk)

Dr. C. Selle:
Soft and Biological Soft Matter, International Summer School, 5 lectures Zanjan/ Iran
June 2004 (invited talk)

Dr. C. Selle:
Statistical Physics Of Complex Fluids, A STATPHYS 22 satellite meeting, Zanjan, Iran,
June 2004 (talk)

Dr. C. Selle:
Biophysical Society Discussion Meeting,
Asilomar, CA.,
October 2004 (poster)

W. Härtig, H. Schmiedel, T. Siegemund, R. Wang, B.-R. Paulke, K. Pranzas, H. Eckerlebe
SANS Study of Negatively Charged Hairy Latex Particles, Proceedings Condensed Matter Physics with Neutrons at the IBR-2 Pulsed Reactor Dubna (2004) 66-70

W. Härtig, B.-R. Paulke, J. Grosche, J. Seeger, C. Varga, H. Schmiedel, T. Siegemund, T. Harkany, H. Tanila, J. Kacza
Nanoparticles delivering β-amyloid-binding thioflavins into the mouse hippocampus - Electron microscopic analysis after photoconversion. Poster 6.4. auf dem 3rd Biotechnology Symposium of the University of Leipzig. 19.5.2004, Abstract-Band, S. 171

W. Härtig, B.-R. Paulke, J. Grosche, J. Seeger, H. Schmiedel, T. Siegemund, T. Harkany, H. Tanila, J. Kacza
Targeting of β-amyloid deposits with thioflavins released from nanoparticles in transgenic mice. Program-No. 124.8.2004 Abstract Viewer/Iterinary Planner. Washington, DC: Society for Neuroscience, 2004.

T. Siegemund, B.-R. Paulke, H. Schmiedel, J. Grosche, A. Hoffmann, T. Harkany, H. Tanila, J. Kacza, W. Härtig
Thioflavins delivered from nanoparticles targeting β-amyloid in transgenic mice. Poster 058 auf dem 3rd Leipzig Research Festival for Life Sciences 2004, 10.12.2004, Abstract-Band, S. 67.

4.13 Graduations

Diploma

Claudia Brunner
Active Biomechanics of Biological Cells
01.03.2004

Karla Müller
Polymer Physics of the Cytoskeleton - the Impact of Additional Actin Monomers On Cell Elasticity Measured with the Optical Stretcher
15.01.2004

M.Sc. (Physics)

Florian Rückerl
Diffusion of Nanoparticles in Two-Dimensional Potential Landscapes
15.01.2004

4.14 Guests

Yunbi Lu
School of Medicine Zhejiang/ Hangzhol, since October 2004

Cosima Koch
Technische Universität Wien, since September 2004

II

Institute for Experimental Physics II

5

Nuclear Solid State Physics

5.1 Introduction

The working horse in the nuclear solid state physics division is the LIPSION accelerator laboratory. Our research interest focuses on ion beam analysis and modification (e.g. proton beam writing) in the fields of material and life sciences. In addition, time differential perturbed angular correlation (TDPAC) experiments are carried out with emphasis on biomolecules at the TDPAC-laboratory and at the isotope separator ISOLDE at CERN, Geneva.

T. Butz

5.2 The High-Energy Ion Nanoprobe LIPSION

T. Butz, D. Lehmann, H.N. da Luz, C. Meinecke, F. Menzel, T. Reinert, D. Spemann, W. Tröger, J. Vogt

The high-energy ion nanoprobe LIPSION at the University of Leipzig has been operational since October, 1998 (Fig. 5.1). Its magnetic quadrupole lens system, arranged as a separated Russian quadruplet, was developed by the Microanalytical Research Centre (MARC), Melbourne and has a symmetrical demagnification factor of about 130. The single-ended 3 MV SINGLETRON^{TM} accelerator (High Voltage Engineering Europa B.V.) supplies H^+ and He^+ ion beams with a beam brightness of approximately $20\,A{\cdot}rad^{-2}m^{-2}eV^{-1}$. Due to this high brightness, the excellent optical properties of the focusing system of the nanoprobe and the suppression of mechanical vibrations by founding the bed-plates of accelerator and probe in greater depths separately from the surroundings, lateral resolutions below 100 nm for the low current mode (STIM) and 30 nm at a current of 10 pA (PIXE) were achieved routinely. A beam diameter of 41 nm was achieved. The UHV experimental chamber is equipped with electron, X-ray, and particle detectors to detect simultaneously the emitted secondary electrons (Ion Induced Secondary Electron Emission, SE), the characteristic X-rays (Particle Induced X-Ray Emission, PIXE), as well as the backscattered ions (Rutherford Backscattering Spectrometry, RBS) and - in case of thin samples - the transmitted ions (Scanning Transmission Ion Microscopy, STIM, and Scanning Transmission Ion Micro-Tomography, STIM-T). A newly installed optical microscope allows sample positioning and inspection during measurement. The

Figure 5.1: LIPSION laboratory

magnetic scanning system moves the focused beam across the sample within a scan field of adjustable extent. The data collection system MPSYS (MARC Melbourne) collects and stores the spectra of the several techniques at any beam position (Total Quantitative Analysis, TQA). In addition, optional windows can be set in the spectra for real-time elemental mapping. The pictures are viewed and printed as two-dimensional colour-coded intensity distributions.

The installation of an active compensation system of stray magnetic fields using Helmholtz-coils (see Fig. 5.1) yields compensation factor in excess of 100 and proved very useful. The installation of an irradiation platform designed for single ion bombardment of living cells allows first patterned irradiations and hit verification tests.

Current work in nuclear nanoprobe performance is focused on:

1. A new target chamber with a UHV-x,y,z-translation stage and eucentric goniometer was developed and built; the chamber can also be converted into a new irradiation platform for living cells with microscope access from the rear. This will be installed in 2005.

2. The old data acquisition system was replaced by the new MicroDAS MARC (Melbourne)

3. Computer controlled ion beam writing

4. Installation of faceted RBS- and X-Ray-detectors on the new target chamber

Accelerator Statistics 2004:

operating hours: 1560 h
maintenance and conditioning: 280 h

5.3 Analysis of Proteins by Particle Induced X-Ray Emission

H.N. da Luz, A. Vogel*, O. Schilling*, W. Meyer-Klaucke*, D. Spemann, W. Tröger
*EBML Outstation Hamburg, Universität Leipzig

The development of a standard PIXE procedure dedicated to the metal analysis in proteins is of great interest for biochemists. The use of PIXE allows to use the known sulphur content of a protein sample as an internal standard to determine the metal to protein ratio. In order to achieve this aim, the LIPSION microprobe facility at the Leipzig University was used with a 2.25 MeV scanning proton micro-beam for the investigation of several test systems with known metal concentrations and stoichiometries. The scanning mode with a focused proton beam of low current has the following advantages compared with the use of a broad beam PIXE analysis (i. e. beam diameter of approximately 1 mm):

1. the spatial resolution reveals any sample inhomogeneities and allows to identify external contaminations of the sample or the supporting foil

2. the low currents in combination with the scanning reduce drastically the heating and the evaporation of volatile elements of the sample.

STIM and RBS were performed to select the best technique for areal density determination of the protein samples. With the present set-up STIM proved to be less sensitive to sample thickness inhomogeneities. Radiation damage was evaluated in real proteins, such as glyoxalase II and no effects were noticed for currents up to 500 pA. Glyoxalase II served also to demonstrate the ability of PIXE to determine the metal stoichiometry even for protein concentrations of 60 μM (see Fig. 5.2). The zinc phosphodiesterase and the flavorubredoxin lactamase domain were also analyzed. The use of PIXE, combined with

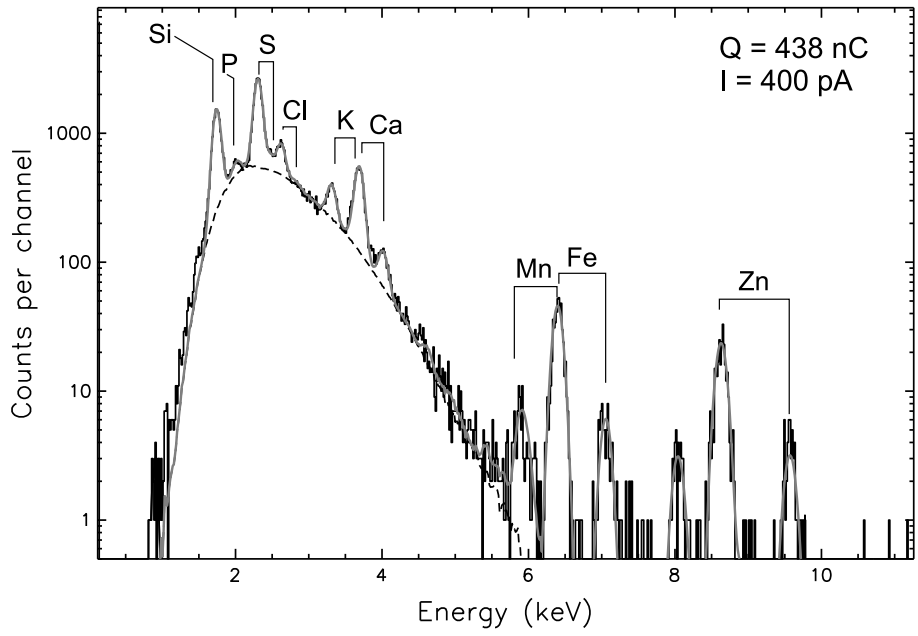

Figure 5.2: PIXE spectrum of glyoxalase II.

STIM for areal density determination, turned out to be a very powerful technique in protein analysis, allowing for stoichiometry determinations of very small sample quantities without any further chemical preparation.

5.4 Antibody Meets Microbeam – or How to Find Neurofibrillary Tangles

M. Morawski*, T. Reinert, C. Meinecke, T. Arendt*, T. Butz

*Paul-Flechsig-Institut für Hirnforschung, Universität Leipzig

In biomedical research the distributions of physiologically or pathologically active elements around or in a certain structure (e. g. tangles, plaques or different cell types) are often of great interest. Therefore, μPIXE analyses are applied to yield quantitative and spatially resolved concentration images of the elements of interest. However, the localisation of the structures to be examined is sometimes scarcely practicable or even impossible. In this study we propose a method of localising the areas of interest for μPIXE analysis. The method is based on the application of a suitable antibody tagged with a single elemental marker (e. g. Ni, Co, Cd, Ag or Au). The antibody then binds selectively to the structures of interest. The elemental marker is detectable via μPIXE, thus, showing finally the structure of interest via the bound antibody (Fig. 5.3). The versatility of the antibodies in combination with the easily applied marker facilitates the localisation of a variety of structures in both light microscopy and μPIXE-imaging. The method was tested on several cellular and subcellular structures in the brain. We have compared the elemental concentrations of two consecutive slices, one stained with Ni-enhanced antibody, the other unstained control, to test the feasibility of trace elemental analysis for particular

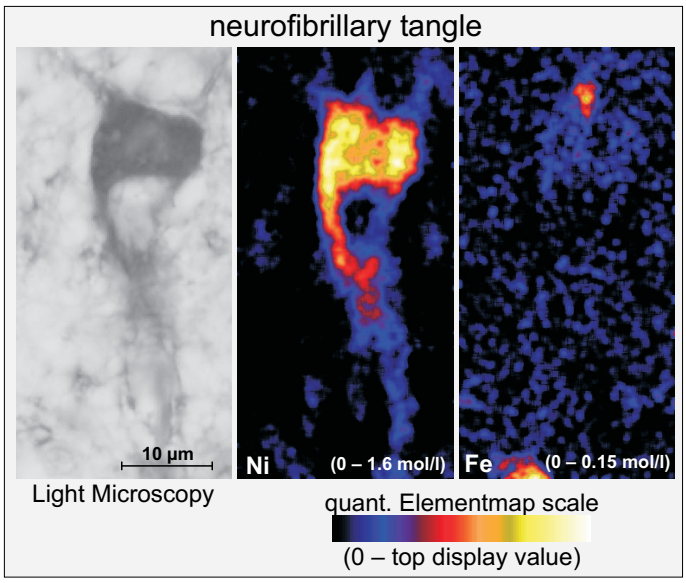

Figure 5.3: Light- and nuclear microscopy (μPIXE for trace element analysis) of a neurofibrillary tangle. After localising the aggregated τ-protein (the tangle) via the Ni-enhanced immunohistochemistry, the concentrations of other elements (e. g. iron) can be analyzed to investigate a possible correlation.

elements in spite of the immunohistochemical structure identification. However, it has to be stated that the proposed technique will not work for freely diffusing elements (like Na, Cl, K and Ca) whose concentrations can be altered by wet sample preparation.

The results show that for spatially resolved analysis of elements (e.g. P, Fe, Cu, Zn) using μPIXE the immunohistochemistry, enhanced with a specific metal (Ni), is a suitable and versatile tool to assist the localisation and differentiation of particular structures not only in the brain but in every biological tissue where antibodies are available. The principle was demonstrated with nickel. Other elements are feasible as well if X-ray line overlaps have to be avoided. For example cobalt, cadmium, gold and silver are applicable. With a suitable (overlap-free) metal enhancer detection limits below 50 μmol/l (< 1 μg/g) are achievable.

5.5 Determination of Trace Elements in the Human *Substantia Nigra*

M. Morawski*, C. Meinecke, T. Reinert, A.C. Dörffel*, P. Riederer†, T. Arendt*, T. Butz

*Paul-Flechsig-Institut für Hirnforschung, Universität Leipzig

†Klinische Neurochemie, Abt. Psychiatrie, Universität Würzburg

"The gain in brain is mainly in the stain" was for a long time a key sentence for research in neurodegenerative disease. However, for a quantification of the element concentrations (especially iron) in brain tissue, standard staining methods are insufficient. Nuclear microscopy (μPIXE) allows a quantitative elemental analysis of brain tissue with a subcellular spatial resolution.

Histochemical and biochemical determinations of total iron content in brain regions from idiopathic Parkinson's disease have exhibited an increase of iron in parkinsonian *substantia nigra* (*SN*) *pars compacta* (*pc*) but not in the *pars reticulata* (*pr*), however without a clear cellular classification. For the first time, we have differentially investigated the intra- and extraneuronal elemental concentrations (especially iron) of the human *substantia nigra pars compacta* versus *pars reticulata* with detection limits in the range of 50 μmol/l. Thus, we could compare the neuronal iron concentration in human brain sections of healthy and parkinsonian brain tissue. Clear differences in the iron concentration and distribution could be disclosed. Additionally, we could show *in situ* that the increased intraneuronal iron content is linked to neuromelanin (see Tab. 5.1).

Griffiths' questions about "the cellular and subcellular distributions of iron" and his statement that they "are also uncertain" can now be answered in more detail. In the numerous studies most attention is drawn to non-neuronal cells in order to explain the iron content in *SN*. Here, we could show that even the neurons in the *SN* contain a non negligible amount of iron, which underlies the same shift typically described under PD pathological conditions. Furthermore, we could show that the neurons of the *SN pars reticulata* accumulate more iron. A possible explanation is: the highly increased activation of microglia leads to a loss of extracellular matrix thereby decreasing the iron binding capacity which releases more free iron to the *SN pars reticulata*. A detailed study about this subject is currently underway.

Table 5.1: Iron concentration in a control and in a parkinsonian *subsantia nigra*.

Iron concentration /(mmol/l)			
localization		Control	Parkinson's disease
SN	Total (*pc*+*pr*)	9.3 ± 1.2	15.5 ± 3.0
pc	Total	7.8	14.3
	Extraneuronal	6.2 ± 1.3	8.5 ± 1.7
	Intraneuronal	15.2 ± 3.2	25.0 ± 6.6
	Melanin	20.5 ± 3.8	41.4 ± 5.6
pr	Total	10.7	16.7
	Extraneuronal	7.6 ± 1.0	13.8 ± 6.7
	Intraneuronal	8.1 ± 1.4	14.8 ± 7.3
	Melanin	–	–

5.6 Skin as a Barrier to Ultra-Fine Particles

Y. Tong, T. Reinert, U. Anderegg*, M. Sticherling*, J. Vogt, T. Butz

*Klinik and Poliklinik für Dermatologie

Micronised TiO_2 particles used in sunscreens as physical UV filters are suspected to pass through the horny *stratum corneum* into vital skin layers via intercellular channels, hair follicles, and sweat glands. But this penetration is undesirable because of its possible impact on human health. For example, the particles can activate the immune system and accumulations of these particles in the skin can decrease the threshold for allergies [1]. The function of the *stratum corneum* as a barrier against dermal uptake of ultrafine particles was the subject of several investigations, which came to different conclusions concerning the penetration depth of the particles [2, 3]. Most of these studies used the method of tape stripping, which does not yield reliable depth profiles, contrary to the spatially resolved methods using thin cross-sections such as electron microscopy or ion beam analytical techniques such as PIXE, RBS, ERDA, STIM and SEI. Within the European project NANODERM, supported by the European Commission, at Leipzig ion beam analyses on freeze dried cross-sections of skin which was exposed to different TiO_2 containing formulations were carried out. First, we used porcine skin with different types of formulations and skin pretreatments (e. g. wetting, defatting or partially removing the *stratum corneum*). The results showed that pig skin is a good barrier against nanoparticles. The applied TiO_2 remained on the skin surface or pentrated just into the first few micrometers of the horny *stratum corneum*. Traverses in the PIXE-maps indicate that in some rare cases a small amount of the TiO_2 penetrates into the vital *startum granulosum*. However, no indications for a penetration into the *dermis* were found up to now. Interestingly enough, there is a deep penetration into the hair follicles (Fig. 5.4).

In 2004 we investigated human skin to test its barrier function. As expected from the initial studies, healthy skin is a good barrier. In collaboration with partners in Kraków we also carried out autoradiography experiments with micro-emulsions using radiolabelled TiO_2 particles which yielded similar results. We will also test the barrier function of impaired human skin (e. g. psoriatic skin).

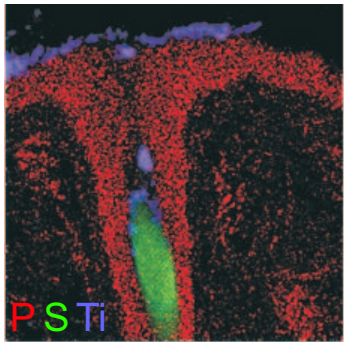

Figure 5.4: Three element image of phosphorus, sulphur and titanium of a skin section with follicle (400 µm×400 µm). Apart from the skin surface, there are also TiO_2 particles deep in the follicle.

[1] B. Granum, P.I. Gaarder, E.-C. Groeng, R.-B. Leikvold, E. Namork and M. Løvik, Toxicology Letters 115 (2001) 171-181.
[2] F. Pflücker, V. Wendel, H. Hohenberg, E. Gärtner, T. Will, S. Pfeiffer, R. Wepf and H. Gers-Barlag, Skin Pharmacol Appl Skin Physiol 14 (2001) 92-97.
[3] M.-H. Tan, C.A. Commens, L. Burnett and P.J. Snitch, Australasian Journal of Dermatology 37 (1996) 185-187

5.7 Irradiation of Living Human Cells with High Energetic Protons

A. Fiedler, T. Reinert, J. Tanner, T. Butz

The high-energy ion nanoprobe LIPSION is currently under development in order to broaden its applications into the field of radiobiology, especially for studies of low dose effects of ionizing radiation. A first irradiation platform for test irradiation has already been constructed and tested for radiobiological studies [1, 2]. Based on previous studies with X-rays which focused on interleukin-1α and integrin-β_1 as fast cellular response (endpoints) to X-ray irradiation [3], we tested the response of primary human fibroblasts and HeLa-cells to 2 MeV protons. Additionally, we investigated the expression of apoptose markers, the expression of heat the shock protein HSP70 and the induction of DNA double strand breaks (γH2AX).

The studies on the expression of interleukin-1α and integrin-β_1 showed neither a significant dependence on the applied dose nor direct effects of proton bombardment. We obtained similar results for the induction of apoptose. Even at higher doses apoptose was scarcely seen, whereby HeLa-cells were more affected by proton irradiation than fibroblasts. The proton irradiation induced expression of HSP70 in fibroblasts could be seen mainly as spot-wise agglomerations in the cytoplasm. However, the pattern of the affected cells did not correspond to the irradiation pattern. There were also HSP70-positive cells outside the irradiation area. This behaviour, a cell response due to cell-to-cell communication but not due to a direct impact of radiation, is known as bystander effect. Whether our findings are related to the bystander effect or not has to be studied in more detailed. The immunohistochemical staining of the phosphorylated histone H2AX (γH2AX) is a suit-

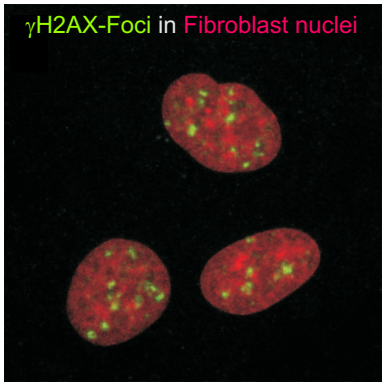

Figure 5.5: Laser scanning microscopic image of three fibroblast nuclei immunohistochemically stained anti γH2AX (green) as a marker for DNA double strand breaks induced by α-irradiation.

able marker for irradiation induced DNA double strand breaks. Tests with α-particles from a ^{241}Am source showed clear foci (Fig. 5.5). The 2 MeV protons did also induce γH2AX. However, their localization did not coincide with the irradiation pattern (regular dots and lines). The appearance was diffuse. This is mainly due to the lower ionization density of 2 MeV protons compared to several MeV α-particles or heavier ions. Therefore, the double strand breaks appear to be induced rather by secondary effects (e. g. radiation induced reactive oxygen species) than by a direct interaction of the protons with the DNA.

[1] T. Reinert, A. Fiedler, J. Škopek, J. Tanner, J. Vogt, T. Butz, Nucl. Instr. and Meth. B 219–220 (2004) 77.
[2] A. Fiedler, J. Škopek, T. Reinert, J. Tanner, J. Vogt, J. Österreicher, L. Navratil, T. Butz, Radiat. Res. 161 (1) (2004) 95.
[3] J. Österreicher, J. Škopek, J. Jahns, G. Hildebrandt, J. Psutka, J.M. Tanner, J. Vogt, T. Butz, Acta Histochem. 105(3) (2003) 223.

5.8 Proton Beam Writing

F. Menzel, D. Spemann, S. Petriconi, J. Lenzner, T. Butz

Proton beam writing (PBW) is a new lithographic method with high potential for applications in microoptics, micromechanics, and microfluidics. Within the framework of the research group "Architecture of nano and microdimensional building blocks" (FOR 522) this technique was established at the LIPSION nanoprobe. In recent experiments real 3-dimensional structures were produced in the negative photoresist SU-8 (Fig. 5.6a) and PBW was tested at the positive resist PMMA. Furthermore, first experiments concerning Ni plating were carried out with the objective of creating metal microstructures using resist structures as templates. In order to prepare, handle, and develop the UV sensitive resists, the chemistry laboratory was equipped with yellow light, spin coater, and hot plate. A dedicated beam scanning program for the new MicroDAS data acquisition system was written and tested, which gave us the possibility to produce arbitrarily shaped structures (Fig. 5.6b). Furthermore, a new target chamber and a very precise sample manipulation stage, which are already constructed and will be assembled soon, will allow us to produce structures with even better edge definition.

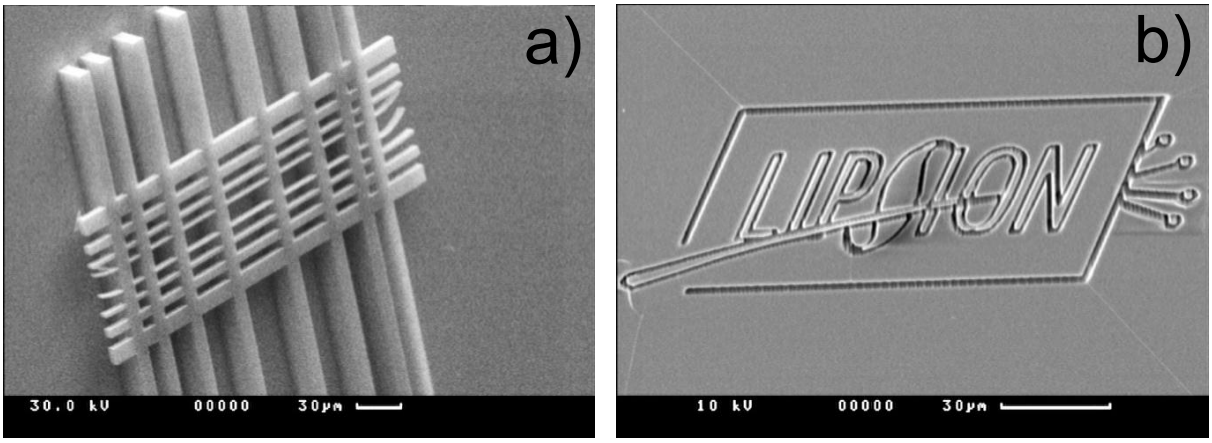

Figure 5.6: REM image of (a) a 3-dimensional structure produced in SU-8 by proton beam writing (PBW) and (b) the LIPSION logo in PMMA resist.

5.9 Ion Beam Analysis of (Mg, Mn, Fe, Co, Ni, Cd)$_x$Zn$_{1-x}$O and ZnO:(Li, Al, P, Ti, Cu, Ga, Sb) Thin Films Epitaxially Grown on c- and a-Plane Sapphire

D. Spemann, H. Hochmuth, E.M. Kaidashev, M. Diaconu, H. Schmidt, M. Lorenz, J. Vogt, T. Butz

ZnO thin films, nominally undoped, doped with Li, Al, P, Ti, Cu, Ga, and Sb and alloyed with Mg, Mn, Fe, Co, Ni, and Cd grown epitaxially on c- and a-plane sapphire by pulsed laser deposition (PLD) were investigated. In order to correlate the optical, electrical and magnetic properties, e.g. the band gap energy and carrier concentration, to the elemental composition, the films were analysed by Rutherford Backscattering Spectrometry (RBS), Particle Induced X-ray Emission (PIXE), and Particle Induced γ-ray Emission (PIGE) using He^+ and H^+ ion beams.

It was found that the element transfer from the PLD target to the film differs significantly for the individual doping and alloying elements, with concentration ratios between film and target ranging from 4 % for Li and Cd to 400 % for Ga (see Fig. 5.7). In general, the films exhibited a metal to oxygen ratio of 1:1, only the ZnO:Li films were slightly oxygen deficient.

Furthermore, the crystalline quality of the films was investigated using ion channeling. The nominally undoped ZnO films which were deposited with low-temperature interlayers for lower lateral stress showed a normalized minimum RBS yield of c_{min}=3.3 % under channeling conditions. Whereas the incorporation of isovalent alloying atoms into the ZnO films leads to a slight degradation of the crystalline quality only, doping degrades the crystalline quality remarkably, even at low dopant concentrations (see Fig. 5.8). This indicates that the dopant atoms do not reside on regular Zn lattice sites (for one ZnO:Li film this could be proven by the Li-RBS yield under channeling conditions) and/or that the incorporation of a dopant atom leads to a locally strained lattice around the atom, possibly associated with a trapped defect or impurity atom. Both crystalline distortions lead to an increased backscattering yield under channeling conditions.

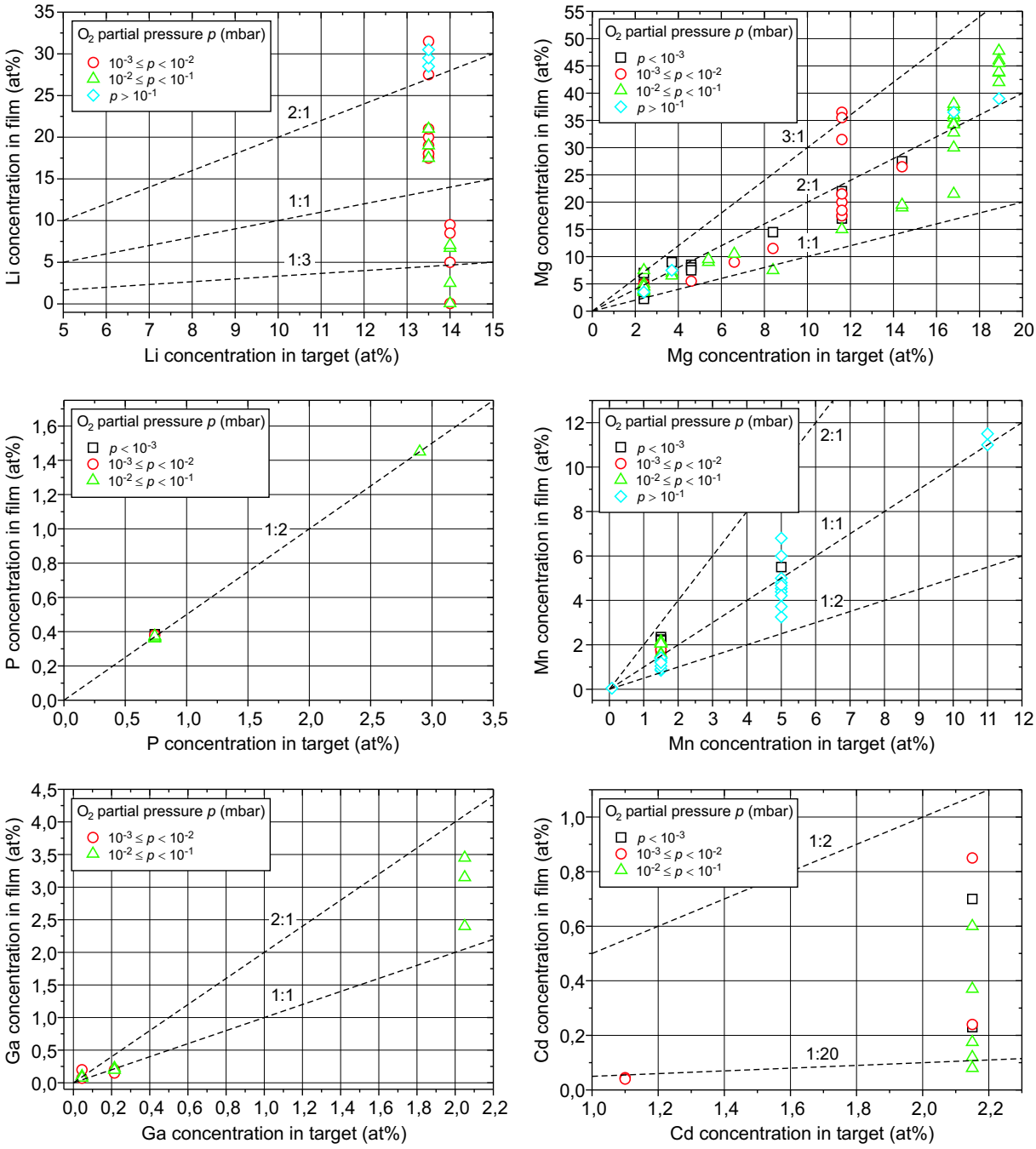

Figure 5.7: Element transfer of Li, Mg, P, Mn, Ga, and Cd from the PLD target to the ZnO film at different oxygen partial pressures. The dashed lines represent a element transfer $c_{\mathrm{X}}^{\mathrm{film}}$:$c_{\mathrm{X}}^{\mathrm{target}}$ as indicated.

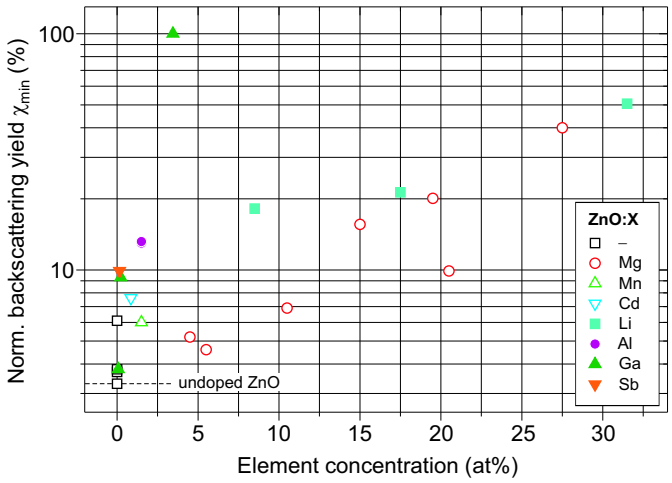

Figure 5.8: Normalized minimum yield $\chi_{\min}$ from ZnO-based films doped or alloyed with various elements at different concentrations. In general, the crystalline quality degrades with increasing concentration, but to a different extent for doping and alloying elements. Whereas alloying (Mg, Mn, and Cd) leads to a slight degradation of the crystalline quality only, the incorporation of doping atoms (Li, Al, Ga, and Sb) results in a significant degradation of the crystalline quality even at low dopant concentrations.

5.10 Ferromagnetism in Graphite and Amorphous Carbon Films Induced by Proton Irradiation

D. Spemann, K.-H. Han, R. Höhne, P. Esquinazi, A. Setzer, U. Schaufuß, T. Butz

Ferromagnetic ordering in highly oriented pyrolytic graphite samples and amorphous carbon films was created by high energy proton irradiation using broad ion beams and microbeams. Simultaneously, the impurity content was checked using Particle Induced X-ray Emission (PIXE). Due to the excellent sensitivity of better than 0.5 μg/g of PIXE for metallic impurities like Fe, it was possible to exclude the possibility of metallic impurities as a cause of the observed ferromagnetism. This work was done in close co-operation with the division of Superconductivity and Magnetism. More details can be found in their report.

5.11 Elemental Depth Profiling in Cu(In, Ga)Se_2 Solar Cells using micro-PIXE on a bevelled section

D. Spemann, K. Otte, M. Lorenz, T. Butz

Solar cells based on Cu(In,Ga)Se_2 (CIGS) absorber layers are one of the most promising thin film solar materials and stand on the edge of a profitable industrial realization. Photovoltaic conversion efficiencies of up to 19.2 % have been achieved. Mechanically flexible thin film solar cells based on CIS absorbers deposited on polyimide foils by the Solarion company were investigated in the ion beam laboratory LIPSION of the University of

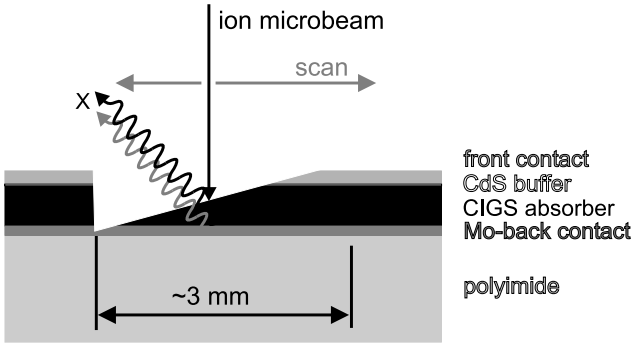

Figure 5.9: Schematic of a bevelled section of a CIGS solar cell.

Leipzig by means of Rutherford Backscattering Spectrometry (RBS) and Particle Induced X-ray Emission (PIXE) using a 2.25 MeV proton microbeam.

From these measurements the composition of the absorber as well as the lateral homogeneity and the film thicknesses of the individual layers could be determined under some reasonable assumptions. Quantitative depth profiling of the individual elements was performed by microPIXE measurements on a bevelled section of a CIGS solar cell consisting of the following layers: polyimide / Mo / CIGS / CdS / ZnO (see Fig. 5.9). The bevelled section was prepared at the Leibniz-Institute for Surface Modification (IOM) Leipzig using ion beam etching with 500 eV nitrogen ions.

The observed yields from Cu, In, Ga, Se, and Cd were used to calculate the composition of the CIGS absorber as a function of depth (see Fig. 5.10). For this purpose, the elemental concentrations were extracted along the bevelled section using appropriate yield calculations for each depth interval. As can bee seen, small concentration-depth-gradients of Cu, In, Ga, and Se in the CIGS absorber layer were found. Furthermore, the extracted elemental profiles show a remarkable amount of Cd in the order of 5 at% in the absorber layer leading to an overall composition of $Cu_{0.96\pm0.03}In_{0.52\pm0.03}Ga_{0.46\pm0.02}Se_{1.89\pm0.06}Cd_{0.18\pm0.02}$. This could not be revealed by standard RBS/PIXE analysis on these samples without the

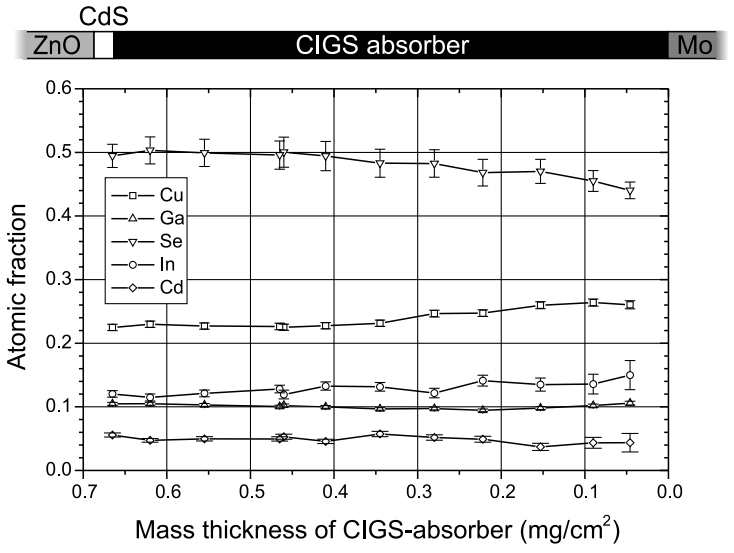

Figure 5.10: Composition of the CIGS absorber as a function of depth.

use of a bevelled section because of its insufficient depth profiling capabilities. Since, due to the massive overlap of the S-K_α-lines ($E_X = 2.307\,\text{keV}$) with the intense Mo-L_α-lines ($E_X = 2.292\,\text{keV}$) from the back contact layer, a depth profiling of S is not possible with PIXE on these samples it cannot be concluded from the PIXE data whether the Cd in the absorber layer is metallic or in the form of CdS. However, since SNMS depth profiling measurements show similar concentration-depth-profiles of Cd and S, Cd seems to be present in the form of CdS within the absorber layer. The reason why CdS can be found throughout the whole absorber layer at a nearly constant concentration level is unclear up to now and subject of further investigations.

5.12 First 3D – RBS Characterisation of SiO_2 Microstructures

C. Meinecke, J. Vogt, T. Butz

In the course of the DFG project "Architecture of nano- and microdimensional building blocks" we will investigate nanoscopic structures with the method of ion beam analysis Rutherford backscattering spectrometry. In cooperation with the Semiconductor Physics group (HLP) we analysed the composition of microdimensional Bragg-reflectors, which were produced in the HLP group. Therefore the ion beam was focused down to below 1 µm to resolve the microdimensional resonators. Due to this high spatial resolution it was possible to determine the elemental composition of the Bragg-reflector and the thickness of the Bragg-layer. The micro-dimensional optical resonators consist of a glass fiber coated with zirconium dioxide (ZrO_2). A scheme of the experimental setup is given in Fig. 5.11a.

The composition and thickness of the ZrO_2 film as well as its homogeneity were analysed by means of µRBS. The glass fiber with a diameter of approximately 10 µm was measured under different angles (see Fig. 5.11b). From the measurements a three-dimensional image of the Bragg-reflector including spatially resolved information of the homogeneity and thickness of the ZrO_2 shell was obtained. Additionally, the morphology of the sample was investigated by scanning transmission ion microscopy (STIM). First, µRBS-spectra

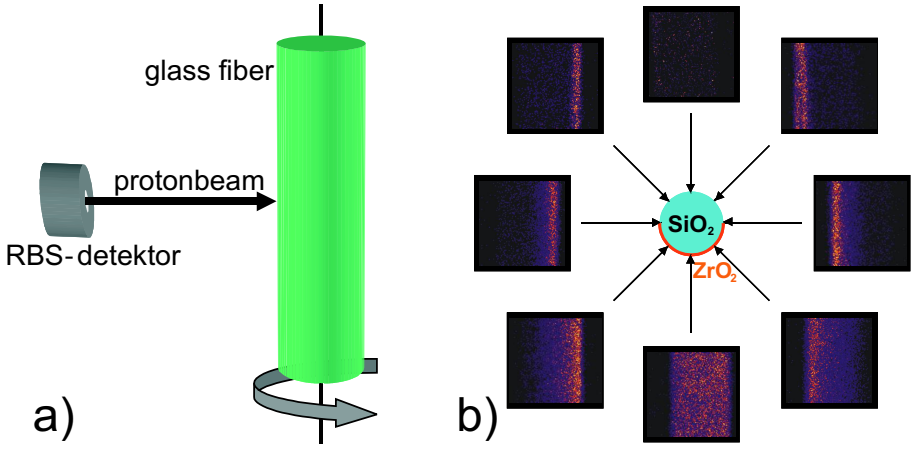

Figure 5.11: (a) sketch of sample, proton beam, and RBS-detector arrangement. (b) sketch of the sample with RBS maps (size 20 µm×20 µm) taken at indicated areas.

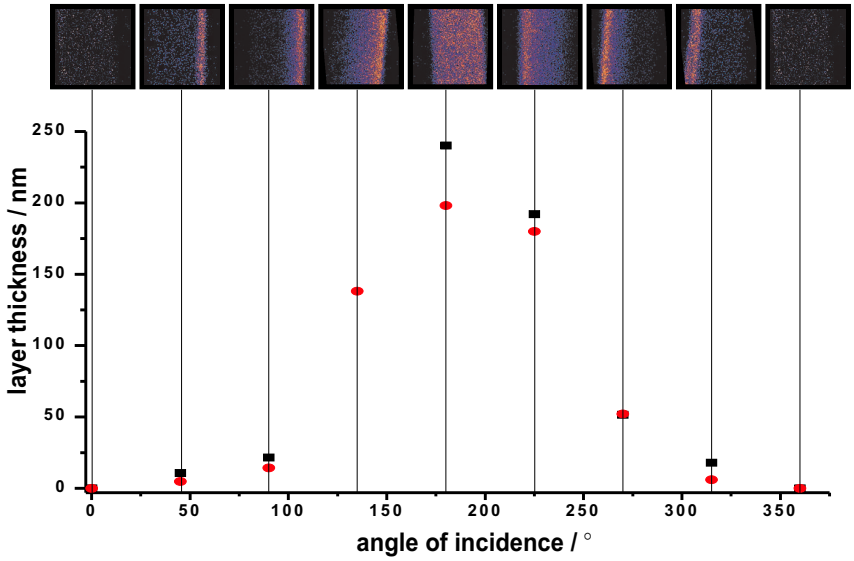

Figure 5.12: Layer thickness of the Bragg-reflector versus the angle of the incident proton beam. The black squares indicate the thickness, which was determined when the layer is in front of the sample (facing the beam). The red points indicate the thickness when the layer is at the backside of the sample (180 ° shifted), that means that the proton beam has to pass the glass fiber before it hits the ZrO_2 layer.

for this non-planar microstructure were simulated with the design parameters. Then, the ZrO_2 film thickness was varied until simulated and measured μRBS-spectra were in agreement. In Fig. 5.12 is shown the layer thickness versus the angle of the incident proton beam.

5.13 TDPAC-Laboratory

W. Tröger, S. Friedemann, F. Heinrich, T. Butz

Nuclear probes are used to study the interaction of metals with biological macromolecules like, e.g., DNA and proteins. Many life processes are based on such interactions. The structure and dynamics of metal sites in biomolecules are important in determining the functional efficiency of these macromolecules. In order to study those metal sites close to physiological conditions a highly sensitive spectroscopic method is required, like Time Differential Perturbed Angular Correlation (TDPAC). Here, a radioactive atom is placed at the site of interest and by correlating the emitted γ-quanta in space and on a nanosecond time scale local structural information is provided. These investigations allow a deeper insight into the detoxification processes, switches, adaptivity and rigidity of metal sites in electron transfer proteins, and also the development of new radiopharmaceuticals in cancer therapy. Two modern 6-detector-TDPAC spectrometer are installed permanently at the Solid State Physics Lab of the ISOLDE on-line isotope separator at CERN. This outstation of the Leipzig TDPAC Laboratory is dedicated for TDPAC experiments with rather short-lived TDPAC isotopes, like ^{111m}Cd or ^{199m}Hg, ^{204m}Pb with half-lifes less than 70 minutes.

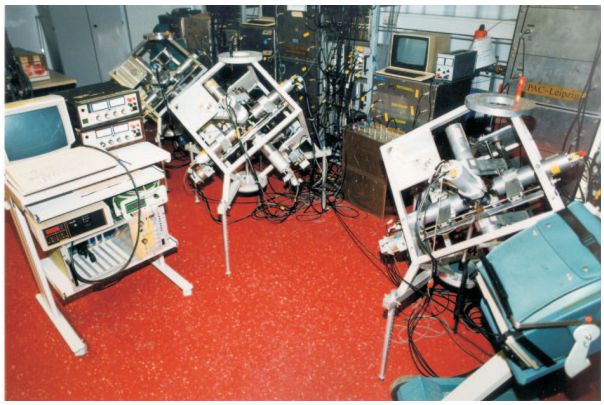

Figure 5.13: View of the TDPAC laboratory at Leipzig with three modern TDPAC-Cameras ("silver cubes").

5.14 ^{204m}Pb: A New Isomeric TDPAC probe

W. Tröger, S. Friedemann, F. Heinrich

Recently, the lead isotope ^{204m}Pb ($t_{1/2}$ = 67 min) became available for TDPAC measurements at the online separator ISOLDE at CERN, Geneva (TDPAC - Time Differential Perturbed Angular Correlation). This isotope is well suited for dynamic studies due to the long life time of the intermediate state (τ_N= 382 ns), which allows for an excellent frequency resolution. In first experiments the NQIs of a large number of inorganic ^{204m}Pb(II)-compounds like Pb salts and Pb oxides have been determined (e.g. see Fig. 5.14). These compounds serve as model compounds for life sciences. Additional experiments on biological molecules have been performed, e.g. of Pb-Penicillamine, the type-II metal binding site in Azurin (see Fig. 5.15) and of a lead binding catalytic DNA which might serve as a metal sensor.

Besides the ^{204m}Pb isotope production at ISOLDE much effort was spent to optimize the production of this isotope at the ISL facility (ISL - Ionenstrahllabor) at the Hahn-Meitner-Institute in Berlin. There, a lead target is irradiated with protons to produce ^{204}Bi ($t_{1/2}$ = 11,4 h) which is used for a ^{204}Bi/^{204m}Pb generator. We developed a special target holder for the Pb irradiation which reduces drastically the production of unwanted radioisotopes in the lead target as well as in the target holder. Furthermore, the separation

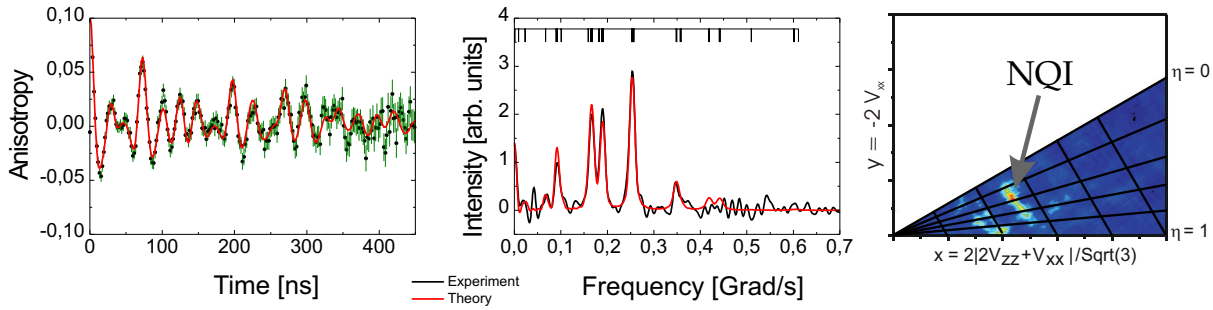

Figure 5.14: Left: The TDPAC spectrum of $Pb_3(PO_4)_2$, a model compound for biological molecules. A single NQI, i. e. only one binding site of the Pb, was observed. Middle: Cosine Transform of the TDPAC spectrum. Right: Cross Correlation Analysis of the Cosine Transform.

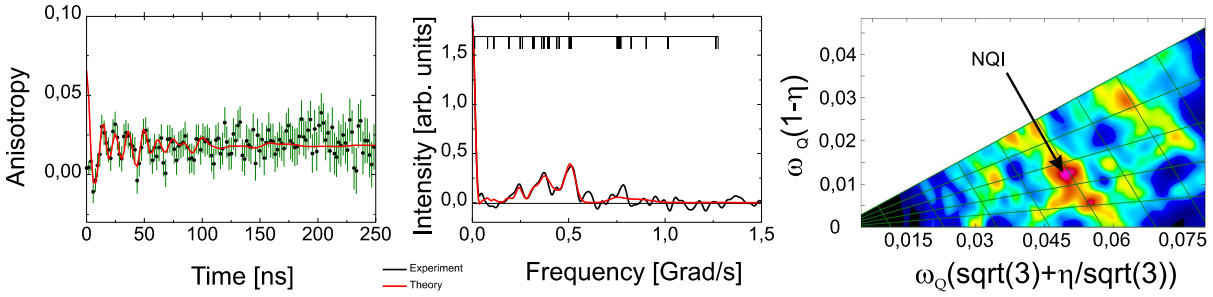

Figure 5.15: Left: TDPAC spectrum of Pb-Azurin (wt). Middle: Cosine Transform of the TDPAC spectrum. Right: Cross Correlation Analysis of the Cosine Transform.

of ^{204m}Pb from ^{204}Bi in the ion exchanger column was was significantly improved by the use of a High Performance Liquid Chromatography unit.

5.15 Ab initio Calculations of the Electric Field Gradient in Molecules

F. Heinrich, W. Tröger

Electric field gradients (EFG) at the nucleus of a nuclear probe can be measured via the nuclear quadrupole interaction by various methods, e.g. NMR or time differential perturbed angular correlation spectroscopy (TDPAC). Usually, the interpretation of the

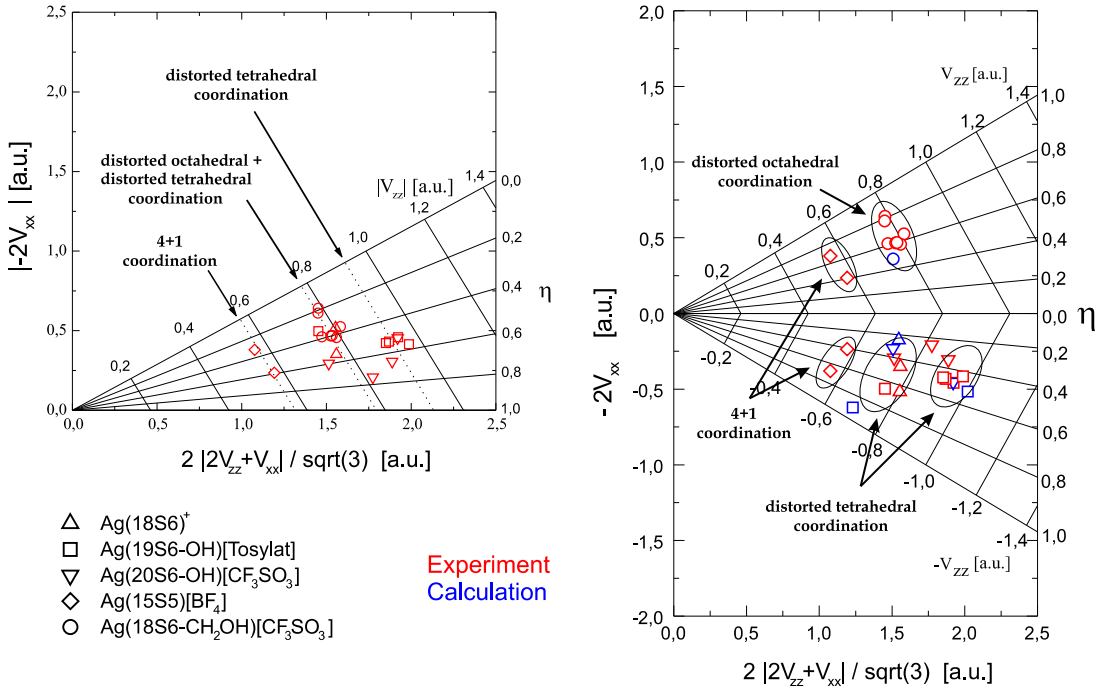

Figure 5.16: By means of EFG calculations with the Amsterdam Density Functional package (ADF) an experimentally found fingerprint system (left figure) which associates the measured EFG with an Ag-S-coordination geometry could be validated and extended (right figure). Since the sign of the EFG is not known experimentally, both possibilities are plotted.

experimental data is done by comparison of the experimental EFG with well-known EFGs of model compounds. Ab initio calculations of the EFG represent an alternative to validate proposed chemical geometries of metal binding sites.

Our investigations are focused on the calculation of EFGs of molecules of different families such as mercaptides, thio-crown ethers (see Fig. 5.16) and metal centers of blue copper proteins. We successfully reproduced EFGs in small and medium-sized molecules such as mercaptides and thio-crown ethers. These calculations are the basis to calculate EFGs in macromolecules and to solve open questions of ligand coordination in metal centers of proteins.

5.16 Funding

3D-Ionenstrahlanalytik zur morphologischen und stofflichen Charakterisierung nano- und mikrodimensionaler Strukturbauelemente und "Ionenstrahl-Micromachining"
Prof. T. Butz
DFG Bu 594/19-1
within Forschergruppe FOR 522
Architecture of nano- and microdimensional building blocks

CELLION: Studies of cellular response to targeted single ions using nanotechnology
Prof. Dr. T. Butz
EU-Project:MRTN-CT-2003-503923

ESRF: Aufbau eines SRPAC Spektrometers zur Untersuchung der Koordination und Dynamik von Nickel-Zentren in biologischen Systemen
Priv.-Doz. Dr. W. Tröger, Prof. T. Butz
BMBF, 05KS40LA/3

NANODERM – Quality of Skin as barrier to ultra-fine particles
Prof. T. Butz
EU-Project, QLK4-CT-02678

Koordinationstudien mit TDPAC an makrozyklischen AG-Kronen und -Käfigen: Molekulare Integrität von ^{111} Ag-Radiopharmaka
Priv.-Doz. Dr. W. Tröger
Deutsche Forschungsgemeinschaft, Tr327/5-2

Radioactive Metal Probes as Diagnostic Tools in Biomolecules
Priv.-Doz. Dr. W. Tröger, Prof. T. Butz
Deutsche Forschungsgemeinschaft, Tr327/8-1

ISOLDE: Aufbau eines volldigitalen, nutzerfreundlichen PAC-Spektrometers
Priv.-Doz. Dr. W. Tröger, Prof. T. Butz
BMBF, 05KK4OL1/4

5.17 Organizational Duties

Tilman Butz

- Member of the committees "Forschung mit nuklearen Sonden und Ionenstrahlen" (BMBF), and "International Symposium on Nuclear Quadrupole Interactions"
- Vorsitzender des wissenschaftlichen Beirates des Instituts für Oberflächenmodifizierung e.V., Leipzig
- Vertrauensdozent der Studienstiftung des deutschen Volkes
- Sprecher der Ortsgruppe Leipzig des deutschen Hochschulverbandes
- Co-tutor for students of Tautenburg (astrophysics), LMU München (astrophysics), DESY/Zeuthen (particle physics)
- Reviewer: DFG, Studienstiftung des deutschen Volkes, US Immigration Service, CNRS (France)
- Referee: J. of Physics C, Phys. Rev. B, Chem. Reviews, Phys. Rev. Lett., J. Biol. Inorg. Chem., Israeli Science Foundation, Alexander von Humboldt Foundation, Nucl. Instr. and Meth. Phys. Res. B, Hyperfine Interactions

Wolfgang Tröger

- Referee: Hyperfine Interactions, Z. Naturforsch. A

Tilo Reinert

- Referee: Nucl. Instr. and Meth. Phys. Res. B

Daniel Spemann

- Referee: Nucl. Instr. and Meth. Phys. Res. B

Frank Menzel

- Referee: Nucl. Instr. and Meth. Phys. Res. B

Christoph Meinecke

- Referee: Nucl. Instr. and Meth. Phys. Res. B

5.18 External Cooperations

Academic

CENBG, Bordeaux, Prof. PH. Moretto

CERN, Genf, ISOLDE Collaboration

Chalmers Technical Highschool, Göteborg

CSIRO, Exploration and Mining, Sydney, Dr. C. Ryan

EMBL Outstation Hamburg, Dr. W. Meyer-Klauke, Dr. A. Vogel, O. Schilling

FRM, Garching, Prof. E. Wagner, Dr. U. Wagner

FU Berlin, Prof. U. Abram

Gray Cancer Institute, London, Prof. B. Michael

GSI Darmstadt, Dr. D. Dobrev, Dr. B. Fischer

HMI, Berlin, Dr. D. Alber, Dr. H. Haas

IIF Leipzig, K. Franke

INFN-LNL, Legnaro-Padova, Prof. P. Mittner

Institute of Physics, Kraków

Institute of Nuclear Technology, Sacavém, Dr. T. Pinheiro

IOM Leipzig, Dr. K. Zimmer, Dr. J. Gerlach

KVL, Kopenhagen, Prof. R. Bauer, Dr. E. Danielsen, Dr. L. Hemmingsen

Massenseperator-Kollaboration Bonn-Göttingen

MLU Halle-Wittenberg, Dr. J. Tanner

MPI for Demographic Research, Rostock, A. Fabig

MPI für Biochemie, Martinsried, Prof. R. Huber, Dr. A Messerschmidt

MPI für Mikrostrukturphysik, Halle/S., Dr. J. Heitmann

MPI für Polymerforschung, Mainz, Prof. W. Knoll

Panjab University, Dr. P. Sidhu

Paul-Flechsig-Institut, Prof. T. Arendt, M. Morawski

Prähistorische Staatssammmlung München, Dr. R. Gebhard

PSI Villigen, Schweiz, Prof P.A. Schubiger

The University of Melbourne, Microanalytical Research Centre

TU Wien, Prof. K. Schwarz, Prof. P. Blaha

Universidade de Aveiro, Portugal, Prof. V.S. Amaral

Universitat Autonoma de Barcelona, Dr. Á. Leiva-Presa, Dr. M.Capdevila, Prof. P. González-Duarte

Université de Montreal, Prof. S. Roorda

Universität Hannover, Arbeitskreis Prof. P. Behrens

Universität Hannover, Arbeitskreis Prof. C. Vogt

Universität Leipzig, Prof. R. Hoffmann

Universität Mainz, Dr. H. Decker

Universität Zürich, Prof. Vašak, Dr. P. Faller, Prof. R. Alberto

Universitätskliniken Leipzig, PD Dr. G. Hildebrandt, Prof. M. Sticherling

University of Illinois, Prof. Y. Lu, J. Liu

Industry

Infineon Technologies Dresden GmbH & Co. OHG

Solarion GmbH

Dechema, Dr. E. Zschau, Self-employed expert in materials research

5.19 Publications

Journals

T. Butz.
On nuclear quadrupole interaction "families".
Hyperfine Int. 151/152: 49-76, (2003)

R. Böhme, D. Spemann, K. Zimmer
Surface characterization of backside-etched transparent dielectrics.
Thin Solid Films 453-454: 127-132 (2004).

P. Esquinazi, R. Höhne, K.-H. Han, A. Setzer, D. Spemann, T. Butz.
Magnetic carbon: An explicit evidence on ferromagnetism induced by proton irradiation.
Carbon 42(7): 1213-1217 (2004).

D. Spemann, E.M. Kaidashev, M. Lorenz, J. Vogt, T. Butz.
Ion beam analysis of epitaxial (Mg, Cd)$_x$Zn$_{1-x}$O and ZnO:(Li, Al, Ga, Sb) thin films grown on c-plane sapphire.
Nucl. Instr. Meth. B 219-220: 891-896 (2004).

D. Spemann, R. Deltschew, M. Lorenz, T. Butz.
Ion beam analysis of functional layers for Cu(In,Ga)Se$_2$ solar cells deposited on polymer foils.
Nucl. Instr. Meth. B 219-220: 693-698 (2004).

D. Spemann, K.-H. Han, P. Esquinazi, R. Höhne, T. Butz.
Ferromagnetic microstructures in highly oriented pyrolytic graphite created by high energy proton irradiation.
Nucl. Instr. Meth. B 219-220: 886-890 (2004).

E. Guzmán, H. Hochmuth, M. Lorenz, H. von Wenckstern, A. Rahm, E.M. Kaidashev, M. Ziese, A. Setzer, P. Esquinazi, A. Pöppl, D. Spemann, R. Pickenhain, H. Schmidt, M. Grundmann.
Pulsed laser deposition of Fe-, Cu-, and Fe, Cu-doped ZnO thin films.
Annalen der Physik 13(1-2): 57-58 (2004).

M. Hetterich, B. Daniel, C. Klingshirn, P. Pfundstein, D. Litvinov, D. Gerthsen, K. Eichhorn, D. Spemann.
Lattice parameter and elastic constants of cubic Zn$_{1-x}$Mn$_x$Se epilayers grown by molecular-beam epitaxy.
phys. stat. sol. (c) 1(4): 649-652 (2004).

J. Kvietkova, D. Daniel, M. Hetterich, M. Schubert, D. Spemann.
Optical properties of ZnSe and $Zn_{0.87}Mn_{0.13}Se$ epilayers determined by spectroscopic ellipsometry.
Thin Solid Films. 455-456: 228-230 (2004).

T. Reinert, A. Fiedler, J. Škopek, J. Tanner, J. Vogt, T. Butz.
Single ion bombardment of living cells at LIPSION.
Nucl. Instr. Meth. B 219-220 77-81(2004).

F. Menzel, T. Reinert, J. Vogt, T. Butz.
Investigations of percutaneous uptake of ultrafine TiO_2 particles at the high energy ion nanoprobe LIPSION.
Nucl. Instr. Meth. B 219-220 82-86 (2004).

A. Fiedler, J. Skopek, T. Reinert, J. Tanner, J. Vogt, J. Österreicher, L. Navratil, T. Butz.
First Irradiation Experiments with Living Cells at LIPSION.
Radiation research Vol. 161 1 95-96 (2004)

K.-H. Han, D. Spemann, P. Esquinazi, R. Höhne, V. Riede, T. Butz.
Magnetic signals of proton irradiated spots created on highly oriented pyrolithic graphite surface.
J. Magn. Magn. Mater. 272-276: 1190-1191 (2004)

R. Höhne, K.-H. Han, P. Esquinazi, A. Setzer, H. Semmelhack, D. Spemann, T. Butz.
Magnetism of pure, disordered carbon films prepared by pulsed laser deposition.
J. Magn. Magn. Mater. 272-276: e839 (2004).

D. Spemann, M. Lorenz, T. Butz, K. Otte.
Ion beam analysis of $CuInSe_2$ solar cells deposited on polyimide foils.
Anal. Bioanal. Chem. 379: 622-627 (2004).

J. Kvietkova, D. Daniel, M. Hetterich, M. Schubert, D. Spemann, D. Litvinov, D. Gerthsen.
Near-band-gap dielectric function of $Zn_{1-x}Mn_xSe$ thin films determined by spectroscopic ellipsometry.
Phys. Rev. B 70: 045316 (2004).

C. Bundesmann, M. Schubert, A. Rahm, D. Spemann, H. Hochmuth, M. Lorenz, M. Grundmann.
Infrared dielectric function an phonon modes of Mg-rich cubic $Mg_xZn_{1-x}O$ ($x > 0.67$) thin films on sapphire (0001).
Appl. Phys. Lett. 85: 905 - 907 (2004).

V. Gottschalch, G. Leibinger, G. Benndorf, H. Herrenberger, D. Spemann.
Intrinsic carbon doping of (AlGa)As for (InGa)As laser structures ($\lambda \approx 1.17$ mm).
J. Cryst. Growth 272: 642-649 (2004).

V. Gottschalch, G. Leibinger, D. Spemann.
X-Ray Investigation of the intrinsic Carbon-Incorporation during the MOVPE Growth of $Al_xGa_{1-x}As$.
Z. Anorg. Allg. Chem. 630: 1419-1422 (2004).

In Press

T. Butz, D. Spemann, K.-H. Han, R. Höhne, A. Setzer, P. Esquinazi.
The role of nuclear nanoprobes in inducing magnetic ordering in graphite.
Hyperfine Interactions

R. Höhne, P. Esquinazi, K.-H. Han, D. Spemann, A. Setzer, U. Schaufuß, V. Riede, T. Butz, P. Streubel, R. Hesse.
Ferromagnetic structures in graphite and amorphous carbon films produced by high energy proton irradiation.
Proc. 16th Int. Conf. on Soft Magnetic Materials

M. Diaconu, H. Schmidt, H. Hochmuth, M. Lorenz, G. Benndorf, J. Lenzner, D. Spemann, A. Setzer, K.-W. Nielsen, P. Esquinazi, M. Grundmann.
UV optical properties of ferromagnetic Mn-doped ZnO thin films grown by PLD.
Thin Solid Films

D. Spemann, K. Otte, M. Lorenz, T. Butz.
Elemental depth profiling in Cu(In, Ga)Se_2 solar cells using microPIXE on a bevelled section.
Nucl. Instr. Meth. B

D. Spemann, P. Esquinazi, R. Höhne, K.-H. Han, A. Setzer, M. Diaconu, H. Schmidt, T. Butz.
Magnetic carbon: A new application for ion microbeams.
Nucl. Instr. Meth. B

F. Menzel, D. Spemann, J. Lenzner, J. Vogt, T. Butz.
Proton beam writing using the high energy ion nanoprobe LIPSION.
Nucl. Instr. Meth. B

H. Natal da Luz, D. Spemann, W. Meyer-Klaucke, W. Tröger.
Analysis of proteins by Particle Induced X-ray Emission.
Nucl. Instr. Meth. B

M. Morawski, C. Meinecke, T. Reinert, T. Butz, A.C. Dörffel and T. Arendt.
Determination of trace elements in the human substantia nigra.
Nucl. Instr. Meth. B

M. Morawski, T. Reinert, C. Meinecke, T. Arendt, T. Butz.
Antibody meets the microbeam – or how to find neurofibrillary tangles.
Nucl. Instr. Meth. B

Annual Reports

T. Butz (Editor)
NFP - Scientific Activities.
In: M. Grundmann (Ed.)
The Physics Institutes of Universität Leipzig, Report 2003, ISBN 3-934178-33-2 (2003)

Conference Contributions

Erste Stoffanalysen an ZnO-Mikrodrähten und RBS–Simulationen von Mikrostrukturen. (T.)
C. Meinecke, F. Menzel, D. Spemann, J. Vogt, T. Butz.
1. FOR522-Statusseminar, Leipzig Feb. 2004

Eigenschaften von Li-, Sb-, und P-dotierten ZnO-Dünnfilmen. (T.)
H. von Wenckstern, C. Bundesmann, S. Heitsch, G. Benndorf, D. Spemann, E.M. Kaidashev, M. Lorenz, M. Schubert, M. Grundmann.
Frühjahrstagung der DPG, Regensburg, 8.–12.03.2004.

Magnetic Carbon: An explicit evidence on ferromagnetism induced by proton irradiation. (T.)
P. Esquinazi, *D. Spemann*, R. Höhne, A. Setzer, K.-H. Han, T. Butz.
Frühjahrstagung der DPG, Regensburg, 8.–12.03.2004.

Bestimmung der intra- und extraneuronalen Eisenkonzentration im Gehirn mittels Ionenstrahlanalytik. (P.)
C. Meinecke, M. Morawski, T. Reinert, T. Arendt, T. Butz.
Frühjahrstagung der DPG, Regensburg, 8.–12.03.2004.

Optische Charakterisierung von ZnO:P- und ZnO:Li, N-PLD-Dünnfilmen. (P.)
S. Heitsch, C. Bundesmann, E.M. Kaidashev, H. von Wenckstern, D. Spemann, M. Schubert, G. Benndorf, M. Lorenz, M. Grundmann.
Frühjahrstagung der DPG, Regensburg, 8.–12.03.2004.

$Mg_xZn_{1-x}O$-Mischkristalle für UV-Bragg-Reflektoren. (P.)
A. Carstens, R. Schmidt-Grund, H. Hochmuth, B. Rheinländer, D. Spemann, M. Lorenz, M. Grundmann.
Frühjahrstagung der DPG, Regensburg, 8.–12.03.2004.

Composition-dependent structural and optical material parameters of $Zn_{1-x}Mn_xSe$ epilayers grown by molecular-beam epitaxy. (P.)
M. Hetterich, B. Daniel, P. Baumann, C. Klingshirn, P. Pfundstein, D. Litvinov, D. Gerthsen, K. Eichhorn, D. Spemann.
Frühjahrstagung der DPG, Regensburg, 8.–12.03.2004.

Preparation of Mn-doped ZnO thin films for spintronics. (P.)
E. Guzmán, H. Hochmuth, M. Lorenz, D. Spemann, H. von Wenckstern, R. Schmidt-Grund, P. Busch, A. Setzer, P. Esquinazi, H. Schmidt, M. Grundmann.
Frühjahrstagung der DPG, Regensburg, 8.–12.03.2004.

Optical properties of $Zn_{1-x}Mn_xSe$ studied by spectroscopic ellipsometry. (P.)
J. Kvietkova, D. Daniel, M. Hetterich, M. Schubert, D. Spemann, D. Litvinov, D. Gerthsen.
Frühjahrstagung der DPG, Regensburg, 8.–12.03.2004.

Determination of trace elements in brain tissue. (P.)
C. Meinecke, M. Morawski, T. Reinert, T. Arendt, T. Butz.
3. Biotechnologie-Tag der Universität Leipzig 19.05.2004

Magnetic microstructures in carbon created by proton beam writing. (Inv. T.)
D. Spemann, P. Esquinazi, R. Höhne, K.-H. Han, A. Setzer, M. Diaconu, H. Schmidt, T. Butz.
1st International Workshop on Proton Beam Writing, Singapore, 18.–22.07.2004.

First results of proton beam writing at LIPSION. (T.)
F. Menzel, D. Spemann, T. Reinert, J. Lenzner, T. Butz.
1st International Workshop on Proton Beam Writing, Singapore, 18.–22.07.2004.

Morphologische und stoffliche Charakterisierung mit der Hochenergie-Ionen-Nanosonde LIPSION. (T.)
T. Butz, C. Meinecke, M. Morawski, T. Reinert, M. Schwertner, D. Spemann, J. Vogt.
13. Arbeitstagung Angewandte Oberflächenanalytik, Dresden 2004

Irradiation of living cells with high energetic protons. (P.)
A. Fiedler, T. Reinert, J. Tanner, T. Butz.
33rd Annual Meeting of the European Society for Radiation Biology

Einzelionenbeschuss lebender Zellen. (T.)
T. Reinert, A. Fiedler, J. Tanner, T. Butz.
Verbundtreffen "Forschung mit Nuklearen Sonden und Ionenstrahlen"

Elemental depth profiling in Cu(In, Ga)Se_2 solar cells using microPIXE on a bevelled section. (P.)
D. Spemann, K. Otte, M. Lorenz, T. Butz.
9. International Conference on Nuclear Microprobe Technology and Applications, Cavtat, Kroatien, 13.–17.09.2004.

Determination of trace elements in the human substantia nigra. (T.)
C. Meinecke, M. Morawski, T. Reinert, T. Arendt, T. Butz.
9. International Conference on Nuclear Microprobe Technology and Applications, Cavtat, Kroatien, 13.–17.09.2004.

Antibody meets the microbeam – or how to find neurofibrillary tangles. (T.)
M. Morawski, *T. Reinert*, C. Meinecke, T. Arendt, T. Butz.
9. International Conference on Nuclear Microprobe Technology and Applications, Cavtat, Kroatien, 13.–17.09.2004.

3D-RBS-characterisation of microstructures. (P.)
C. Meinecke, J. Vogt, T. Butz.
9. International Conference on Nuclear Microprobe Technology and Applications, Cavtat, Kroatien, 13.–17.09.2004.

Magnetic carbon: A new application for ion microbeams. (Inv. T.)
D. Spemann, P. Esquinazi, R. Höhne, K.-H. Han, A. Setzer, M. Diaconu, H. Schmidt, T. Butz.
9. International Conference on Nuclear Microprobe Technology and Applications, Cavtat, Kroatien, 13.–17.09.2004.

Proton beam writing using the high energy ion nanoprobe LIPSION. (T.)
F. Menzel, D. Spemann, J. Lenzner, J. Vogt, T. Butz.
9. International Conference on Nuclear Microprobe Technology and Applications, Cavtat, Kroatien, 13.–17.09.2004.

Analysis of proteins by Particle Induced X-ray Emission. (T.)
H. Natal da Luz, D. Spemann, W. Meyer-Klaucke, W. Tröger.
9. International Conference on Nuclear Microprobe Technology and Applications, Cavtat, Kroatien, 13.–17.09.2004.

Proton beam writing using the high energy ion nanoprobe LIPSION. (T.)
F. Menzel, D. Spemann, T. Reinert, J. Lenzner, T. Butz.
2. FOR522-Statusseminar und Herbstschule, Wörlitz Okt. 2004

Stoffanalysen an ZnO-Mikrodrähten und RBS-Simulationen von Mikrostrukturen. (T.)
C. Meinecke, F. Menzel, D. Spemann, J. Vogt, T. Butz.
2. FOR522-Statusseminar und Herbstschule, Wörlitz Okt. 2004

5.20 Graduations

Diploma

Sven Friedemann
^{204m}Pb: Die Wiederentdeckung einer isomeren TDPAC-Sonde in der Festkörperphysik.
Diplomarbeit, Universität Leipzig (2004).

M.Sc.

Pedro Hugo Ferreira Natal da Luz
Determination of Metal-to-protein Stoichiometries in Metalloproteins by Particle Induced X-ray Emission.
Master Thesis, University Leipzig (2004).

5.21 Guests

Dipl.-Biol. M. Morawski
Paul-Flechsig-Institut für Hirnforschung
10 weeks

Prof. Dr. X. Ni
Shanghai Institute of Applied Physics, China
2 months

Dr. W. Meyer-Klaucke, Dipl.-Biol. O. Schilling
EBML Outstation Hamburg
1 week

Christina Rögge
Universität Hannover
1 week

Prof. Yongpeng Tong
Shanghai Institute of Applied Physics, China
10 months

Prof. Dr. G. Sun, Prof. Dr. Z. Zhou
Beijing Institute of Petrochemical Technology, China
6 weeks

6

Physics of Dielectrics Solids

6.1 Introduction

The research of the *Physics of Dielectric Solids Group* is directed to the study of structure and dynamics of dielectric solids by means of stationary and pulsed magnetic resonance spectroscopy as nuclear magnetic resonance (NMR), nuclear-nuclear double resonance, electron paramagnetic resonance (EPR), and electron-nuclear double resonance (ENDOR) in a broad region of frequencies and temperatures.

One of the objectives is the investigation of the microscopic mechanism of phase transitions and the local and collective dynamics associated therewith in ferroelectrics and ferroelastics with commensurately and incommensurately modulated structures, orientational glass phases and of systems with nanometer particle size. The peculiar properties of ferroelectrics and ferroelastics under invstigation are treated under the aspect of material science. Substantial experience is available for the investigation of ferroelectric perowskites.

Another topical direction of research is the investigation of the peculiar properties of nanostructured materials. These studies include the electronic structure, the spatial structural arrangement and local dynamics of adsorbed molecules interacting with the internal surfaces of nanostructured porous solids (zeolites). In this context in particular nanoparticles of crystalline solids and nanoclusters in solid matrices are investigated.

For the experimental investigations a comprehensive NMR and EPR instrumentation is available supplemented by dielectric methods. The instrumental and methodological development of magnetic resonance for an advanced application on the field of research is continuously carried out.

D. Michel

6.2 Incorporation of Chromium into Hexagonal $BaTiO_3$ Studied by Multifrequency Electron Paramagnetic Resonance (EPR) Study

R. Böttcher, E. Erdem, H.T. Langhammer*, T. Müller*, H.-P. Abicht*

*Fachbereich Physik and Chemie, Martin-Luther-Universität Halle-Wittenberg

The stability range of the hexagonal phase can be extended to room temperature both by firing in reducing atmospheres (oxygen-deficient h-$BaTiO_3$) and by doping with some acceptor-type 3d transition metal elements like Cr, Mn, Fe, Ni, or Cu. This is the reason for our investigation of the incorporation of chromium into hexagonal $BaTiO_3$ and the determination of its valence state. Because of the large difference of the effective ionic radii between Ba^{2+} (161 pm) and Ti^{4+} (60.5 pm) the incorporation of chromium ions with the three- or tetravalent charge states onto the Ti sites in h-$BaTiO_3$ is very probable. The charge state of the ion determines its electron spin quantum numbers S unambiguously. Cr^{3+} is a $(3d)^3$ ion with S = 3/2 whereas the free ion Cr^{4+} has S=1. Electron paramagnetic resonance (EPR) permits the determination of the charge state, and the electronic ground state of the paramagnetic ion as well as its different incorporation sites in a solid. Through intensity measurements by means of EPR the occupancy fractions for Cr^{3+}-ions at the Ti(1) and Ti(2) sites are estimated. Up to now no EPR investigations on chromium in h-$BaTiO_3$ are known in the literature whereas the Cr-EPR spectra of the other modifications are excessively analysed. In this paper we present powder and single-crystal EPR spectra of chromium doped h-$BaTiO_3$ measured in three different microwave-frequency bands, determine the spin-Hamiltonian parameters and discuss the incorporation of the Cr^{3+} ions and the charge compensation. $BaTiO_3$ ceramics doped with 2 mol chromium contain tetragonal and hexagonal phase parts which percentage strongly depends on impurities,

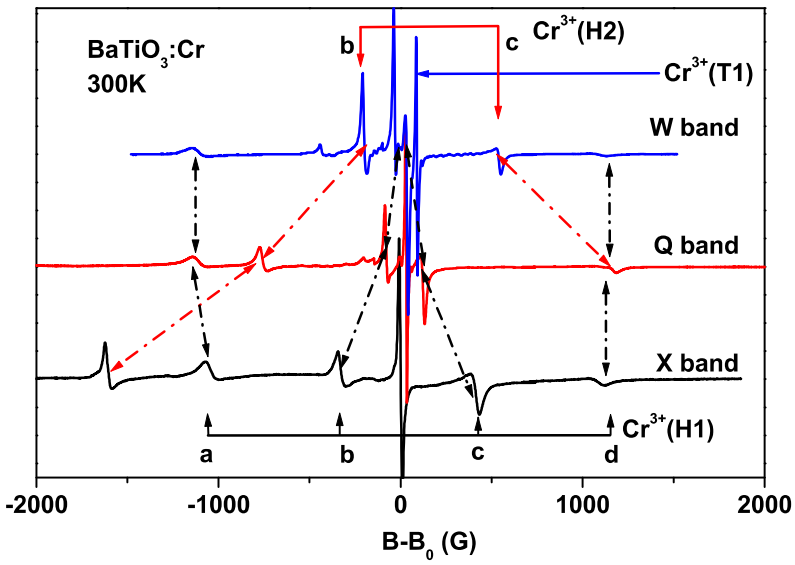

Figure 6.1: Room temperature EPR spectra of the sample with a nominal composition of $BaTiO_3$ + 0.04 BaO + 0.01 Cr_2O_3, sintered at 1400 °C and measured in the X band (9.1 GHz), Q band (34.0 GHz), and W band (94.0 GHz) with $B_0 = h\upsilon/g_{||}\beta$. $g_{||}$ was taken from the H1 spectrum. Different transitions are marked by letters, related transitions by arrows.

stoichiometry and sintering conditions. At room temperature this material reveals three axially symmetric EPR spectra which are assigned to Cr^{3+} ions (Fig. 6.1). They are substituted at Ti^{4+} lattice sites in tetragonally and trigonally distorted octahedra which reflect their tetragonal and hexagonal crystal surroundings. In contrast to manganese-doped hexagonal $BaTiO_3$ in which the Mn^{4+} ion (S=3/2) only substitutes at the Ti(1) lattice site in the corner-sharing octahedra, both the Ti(1) and the Ti(2) (face-sharing octahedra) sites are occupied by Cr^{3+}-ions. By variation of the preparation conditions (sinter temperature and excess of BaO) their occupation probabilities with Cr^{3+} can be changed in a broad range. Only 30 % of the added chromium is incorporated in the grains as Cr^{3+}-ions whereas the remnant is in the EPR-silent tetravalent charge state or in Cr-rich secondary phases segregated at grain boundaries, pores and triple points.

6.3 Size Effect in Chromium Doped $PbTiO_3$ Nanopowders Observed by Multifrequency EPR

E. Erdem, R. Böttcher, H.-J. Gläsel*, E. Hartmann*

*Leibniz-Institut für Oberflächenmodifizierung, Leipzig

In our multifrequency (X, Q, and W band) electron paramagnetic resonance (EPR) study of chromium-doped $PbTiO_3$ micro- and nanopowder samples three paramagnetic Cr^{3+} centers (C1, C2, C3) with different axial fine structure (FS) parameters are identified, with one of them (C1) being compatible with former measurements on crystalline and ceramics samples carried out in the X band. The superposition model by Newman and Urban was applied to translate the FS data into local displacements inside the distorted oxygen octahedra of the $PbTiO_3$ lattice. When going to nanopowder samples, except C1 center the other centers are no longer detectable. The size-dependent EPR spectra of the C1 centers may be described by an axial spin-Hamiltonian whose size-dependent FS parameter D is considered to be Gaussian distributed. By simulation of the spectra the

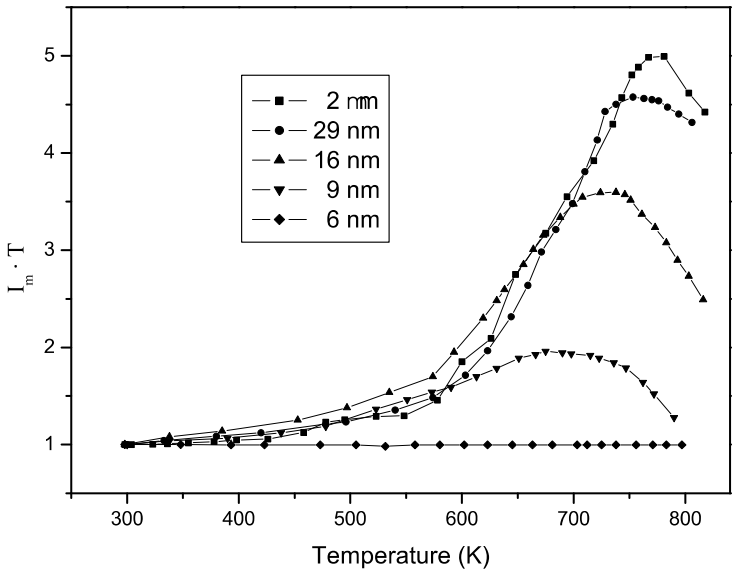

Figure 6.2: $I_m \cdot T$ versus T plots for different size of CPP prepared nanopowders.

values D and their dispersions ΔD were estimated in dependence on the mean particle size d_m. In $PbTiO_3$ nanopowders with mean particle size d_m in the vicinity of the critical size (d_{cr}) for the size-driven tetragonal-to-cubic phase transition additionally to the C1 spectrum a new one (C4) appears, consisting of one EPR line with an isotropic g-factor. The C4 spectrum is assigned to Cr^{3+} ions incorporated into paraelectric cubic nanoparticle with diameters $d < d_{cr}$ and is considered to be an indicator of the size-driven phase transition.

Furthermore by means of temperature-dependent EPR measurements of the cubic intensity I_m the shift of the Curie temperature in dependence on the mean particle is determined (see Fig. 6.2). Details of this study can be found in [1–6]. This work is supported by the DFG.

[1] Erdem E, Böttcher R, Semmelhack HC, Gläsel HJ, Hartmann E. phys. stat. sol. (b) 2003; 239: R7.
[2] Erdem E, Böttcher R, Semmelhack HC, Gläsel HJ, Hartmann E, Hirsch D. J. Mater. Sci. 2003; 38: 3211.
[3] Erdem E, Böttcher R, Weller A, Gläsel HJ, Hartmann E. Phys. Rev. B (submitted in 2005).
[4] Erdem E, Böttcher R, Gläsel HJ, Hartmann E. Mag. Res. Chem. (in press)
[5] Erdem E, Böttcher R, Gläsel HJ, Klotzsche G, Hartmann E, Michel D. Ferroelectrics (in press).
[6] Erdem E, Böttcher R, Gläsel HJ, Klotzsche G, Hartmann E, Michel D. Advances in Solid State Physics (in press).

6.4 Evaluation of Lattice Site and Valence of Manganese in Hexagonal $BaTiO_3$ by Electron Paramagnetic Resonance (EPR)

R. Böttcher, H.T. Langhammer*, T. Müller*, H.-P. Abicht*

*Fachbereich Physik and Chemie, Martin-Luther-Universität Halle-Wittenberg

Manganese-doped barium titanate ceramics consist of parts of 3C- and 6H-stacked crystallites depending on the doping level. Manganese is incorporated at Ti sites in both crystallographic surroundings which is reflected in well-distinguishable EPR spectra. Whereas the EPR spectra of the 3C-stacked crystallites (air-sintered samples) exhibit the well-known behaviour (major defect $Mn_{Ti}{}^{4+}$ with hfs sextet at g = 4.35, minor defect $Mn_{Ti}{}^{2+}$ with hfs sextet at g = 2.00), hexagonal Mn-doped $BaTiO_3$ shows the new H1 EPR spectrum of $Mn_{Ti}{}^{4+}$ (S = 3/2) with four fs lines around g = 2.00. The analysis of the spectrum in the X and Q band shows that $Mn_{Ti}{}^{4+}$ is only incorporated at Ti(1)-sites of the hexagonal lattice (exclusively corner-sharing octahedra). Samples which were annealed under heavily reducing conditions are completely retransformed into the 3C modification. Their EPR spectra exhibit two different hfs sextet lines at $g_{eff} = 6.00$ and g = 2.00 which are caused by $Mn_{Ti}{}^{2+}$. The lines near g = 2.00 are attributed to isolated $Mn_{Ti}{}^{2+}$ centers whereas the other ones are caused by neutral $Mn_{Ti}{}^{2+}$ -V_O associates.

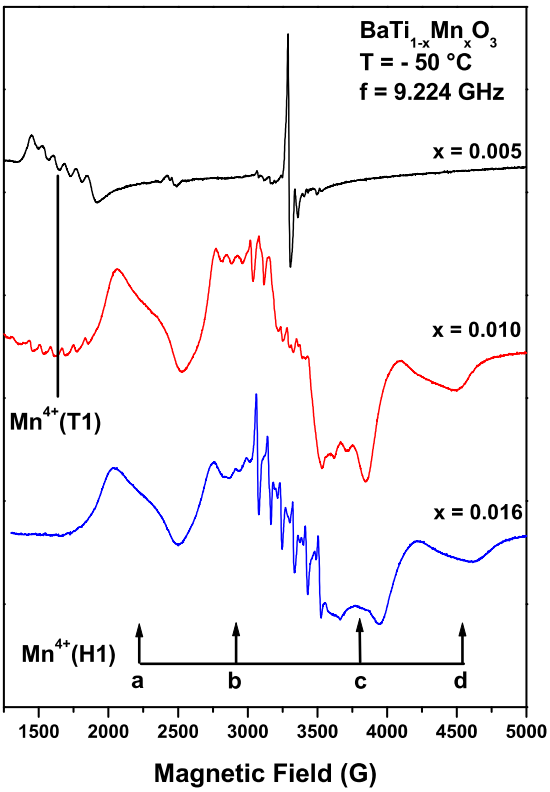

Figure 6.3: X band EPR spectrum of $BaTi_{1-x}Mn_xO_3$ samples with different concentrations of x (0.005, 0.010, 0.016). The samples were annealed in air at 1200 °C and their spectra recorded at −50 °C.

6.5 EPR, ENDOR, and ESEEM Studies of Active Sites in Heterogeneous Catalysts

A. Pöppl, V. Umamaheswari, G. Vijayasarthi

A major research topic of our group is the study of active surface sites in heterogeneous catalysts by electron paramagnetic resonance (EPR) spectroscopy [1–3]. To apply EPR methods to such systems the catalytically active sites have to be either paramagnetic species by themselves (eg. paramagnetic transition metal ions) or paramagnetic probe molecules have to be adsorbed on the studied diamagnetic surface sites (eg. acid centers and transition metal ion species).

The first approach has been used to characterize V(IV) species in molybdophosphate catalysts and to study the immobilization of catalytically active V(IV) complexes on various solid surface supports (SiO_2, Al_2O_3, AlF_3). The grafting of tetrakis(dimethylamido)-vanadium(IV) precursor complexes and the subsequent exchange of the dimethylamido ligands by phosphorous and vanadium(V) containing ligands was studied in detail by a combined application of several EPR techniques at low temperatures. Besides continuous wave multifrequency EPR spectroscopy at X, Q, and W band pulsed electron nuclear double resonance (ENDOR) as well as hyperfine sublevel correlation (HYSCORE) spectroscopy have been used to measure the weak superhyperfine (shf) interactions between the unpaired electron spin at the metal ion and the nuclear spins in the ligand molecules (^{1}H, ^{14}N, ^{31}P, ^{51}V) or in the surface support (^{27}Al, ^{19}F). These shf interactions are the key

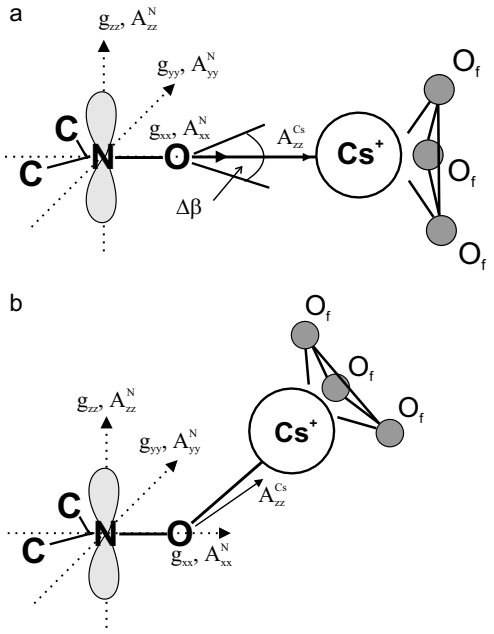

Figure 6.4: Structural models of the DTBN-Cs(I) adsorption complexes zeolite CsNaY (with the framework oxygen of the zeolite indicated by O_f): (a) complex geometry A with a bond length $R_{O-Cs} = 0.25$ nm and $\beta_{bond} = 180°$; (b) complex structure B with $R_{O-Cs} = 0.21$ nm and $\beta_{bond} = 137°$.

information in the structural analysis of such immobilized paramagnetic transition metal ion complexes. Alternatively, nitric oxide (NO) and di-tert-butyl nitroxide (DTBN) probe molecules were employed to characterize Lewis acid sites and Cu(I) cations in various zeolite materials. The geometrical and electronic structures of the resulting adsorption complexes with alkali and transition metal cations could be again determined by a combined application of advanced EPR methods. An attractive example for the application of modern EPR methods for the study of surface sites in microporous materials is the investigation of the adsorption of DTBN in Cs exchanged Y zeolites. ^{133}Cs HYSCORE spectroscopy has been employed to characterize the structure of adsorption complexes of DTBN with cesium cations in zeolite CsNaY. The experimental HYSCORE data proved the direct coordination of the adsorbed DTBN molecules to the Cs(I) ions and revealed unambiguously the existence of two different types of adsorption complexes. Evaluation of the orientation selective ^{133}Cs HYSCORE spectra provided the ^{133}Cs hyperfine coupling tensors and thus information about the geometrical structure of those complexes. For one type of adsorption complexes a complex geometry was obtained where the Cs(I) ion is located within the molecular mirror plane of the DTBN radical with an oxygen - cesium cation bond length of 0.25 nm (complex structure A). For this the isotropic Cs hyperfine coupling was found to be negative. The second Cs(I)-DTBN complex is characterized by a bent structure (complex structure B). With an isotropic ^{133}Cs hyperfine coupling of 9 MHz the unpaired electron spin density in this Cs(I)-DTBN complex localized at the Cs ion was determined as 0.36. This work is supported by the DFG and Fonds der Chemischen Industrie.

[1] A. Pöppl, M. Gutjahr, T. Rudolf: Paramagnetic Adsorption Complexes in Zeolites as Studied by Advanced Electron Paramagnetic Resonance Techniques; in “Molecules in

Interaction with Surfaces and Interfaces", Eds. Haberlandt, Michel, Pöppl, Stannarius; Springer-Verlag, Berlin, Heidelberg (2004), pp 189 - 220.
[2] M. Gutjahr, J. Hoentsch, R. Böttcher, O. Storcheva, K. Köhler, A. Pöppl, J. Am. Chem. Soc. **126**, 2905 (2004).
[3] V. Umamaheswari, A. Pöppl, M. Hartmann, J. Mol. Catal. A: Chemical, **223**, 123 (2004).

6.6 Synthesis and Characterisation of One Dimensional Ferroelectrics with Perovskite Structure

A. Weller, R. Böttcher, H.-J. Gläsel*, E. Hartmann*

*Leibniz-Institut für Oberflächenmodifizierung, Leipzig

Advances toward nanoscale electronics have created interest in the effects of particle size on the properties of oxidic perovskite substance (ABO_3). These materials are employed for their dielectric, piezoelectric, eletrostrictive, pyroelectric, and electro-optic properties. Understanding how the crystal structure and the state of polarization are influenced by particle size is important to the performance of these ferroelectric materials in many applications. Our work aims to understand how nanoscaling influences the ferroelectric properties and to determine the critical size where a ferroelectric nanostructure no longer behaves like the bulk material. This project in the frame of the Forschergruppe 522 focuses on the synthesis and characterisation of perovskite nanotubes made by template method. Masked Whatman anodisc membranes (200 nm pores) served as templates and are dipped into a solution of monomeric metallo-organic precusor from barium (lead) oxide, titanicum (IV) isopropoxide and methacrylic acid. After calcining the templates are removed and the powder sample of the nanotubes are characterized, Crystallographic characterization is performed with X-ray diffraction (XRD), electron microscopy and FT-Raman spectroscopy. EPR investigations of paramagnetic 3d-ions incorporated into the perovskite lattice at Ti-sites and dielectric measurements in a broad frequency band give a deep insight in the change of the dielectric properties of nanotubes in dependence of the aspect ratio. This work is supported by the DFG.

6.7 NMR and Dielectric Investigations on Ethylene Glycol Molecules Adsorbed in Zeolites

Ö.F. Erdem, D. Michel

The application of ^{1}H NMR spectroscopy to the characterisation of the behaviour of molecules adsorbed in zeolites is often limited due to the poor spectral resolution. A notable enhancement in resolution of the spectra is achieved when random local magnetic fields due to susceptibility effects are partially averaged out by the application of magic angle spinning (MAS) techniques. This allows to clearly differentiate between molecules within the zeolite cages and those ones adsorbed at the outer surface of the zeolite grains as well as to study the dynamics of the different species. For this purpose selective measurements of the proton longitudinal relaxation times were carried out for various pore filling

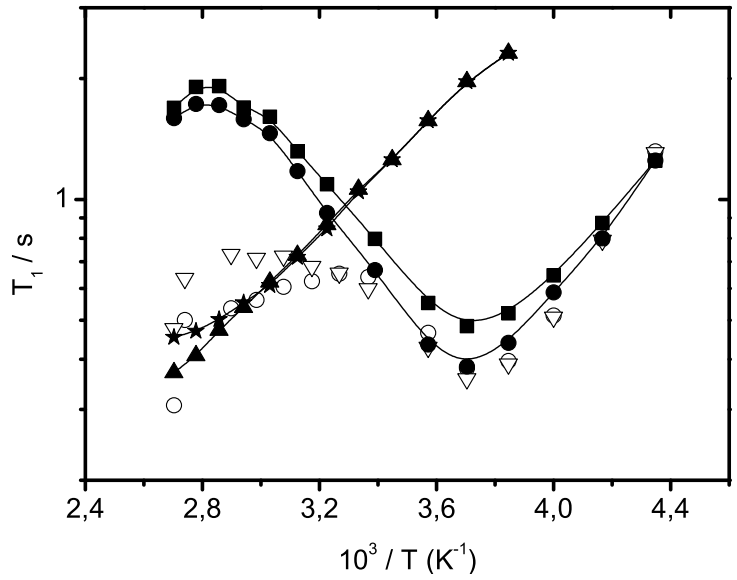

Figure 6.5: Temperature dependence of T_1 (500 MHz, MAS frequency of 3 kHz) for EG molecules which are not adsorbed inside the supercages of NaX (pore filling factor $\Theta = 1.8$) show a relatively high mobility (OH group (solid squares), CH_2 group (solid circles)), i.e. minima of T_1 at lower temperatures. Measurements for $\Theta = 1.0$ (OH group (open circles), CH_2 group (open triangles)) and for EG adsorbed inside the supercages of NaX for $\Theta = 0.5$ (OH group (solid triangles), CH_2 group (solid stars)) clearly indicate the different behavior: the minima appear at high temperatures above the temperature range of these measurements. The solid lines are guides for the eyes.

degrees of the NaX zeolites (see Fig. 6.5). Large differences were found in the thermal mobility when the pore filling degree is varied. For the molecules inside the supercages, a dynamic heterogeneity occurs and this may be related to the competing influences of interactions between molecules and internal surfaces and molecule-molecule interactions within a network of intermolecular hydrogen bonds. We have also measured temperature dependent dielectric relaxation (by means of broadband dielectric spectroscopy in a frequency regime between 10^{-3} Hz and 10^{9} Hz) of ethylene glycol adsorbed in NaX zeolites with a complete and half loading of the zeolite cages. For both cases, the temperature dependence of the relaxation rate follows an Arrhenius-type behavior. Even for the samples with full loading of the NaX supercages, i.e. ca. 10 molecules adsorbed inside a supercage, the experimental data do not reveal deviations from this behavior which would indicate the influence of a glass transition.

6.8 NMR Studies on $BaTiO_3$ Nanoparticles

G. Klotzsche, D. Michel

^{137}Ba NMR measurements allows to study small changes of the local symmetry at the Ba site and to elucidate collective properties such as structural phase transitions. NMR powder spectra of the central line transitions ($m = +\frac{1}{2} \Leftrightarrow m' = -\frac{1}{2}$) were measured at various d.c. magnetic fields (B = 11.7 T, 17.6 T) and simulated using second order perturbation theory of the quadrupolar interaction to estimate the quadrupolar coupling constant $|e^2qQ/h|$.

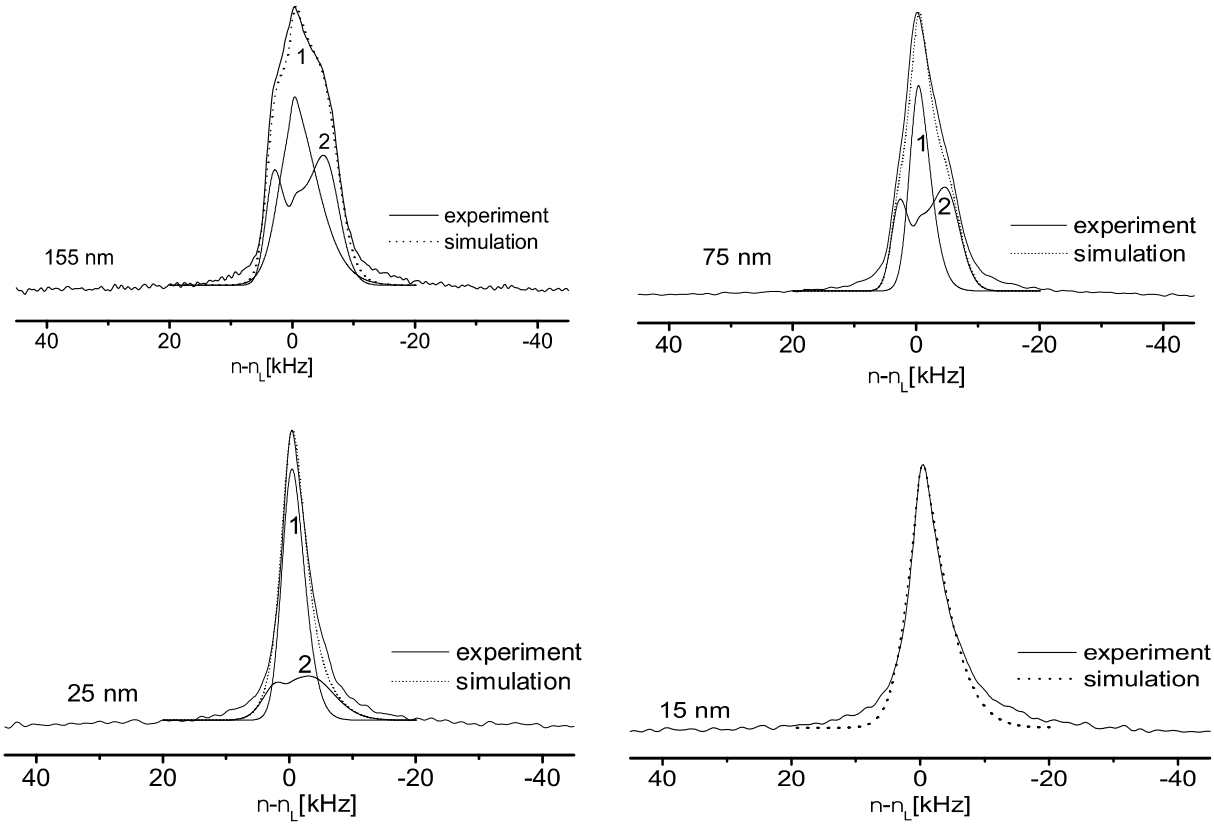

Figure 6.6: Central transition ^{137}Ba NMR spectra in $BaTiO_3$ powder sample with an average diameter d_m. The spectra were measured at 300 K (in the tetragonal phase) and at a d.c. magnetic field of B = 17.6157 T. Apart from the scaling proportional to 1/B, the same line shapes were measured at B = 11.744 T. The lines 1 and 2 denote the simulated NMR powder spectra. The sum of the simulated spectra is denoted by dots. The intensity ratio of the two simulated spectra is denoted by $p_{1,2} = p_{line1} : p_{line2}$.
a) d_m = 155 nm; $p_{1,2} = 1 : 1$, Line ***1***: $<C_Q> = 2.2$ MHz, $\Delta C_Q = 1$ MHz. Line ***2***: $<C_Q> = 2.65$ MHz, $\Delta C_Q = 0.5$ MHz.
b) d_m = 75 nm; $p_{1,2} = 1 : 1.2$, Line ***1***: $<C_Q> = 1.6$ MHz, $\Delta C_Q = 0.7$ MHz. Line ***2***: $<C_Q> = 2.55$ MHz, $\Delta C_Q = 0.5$ MHz.
c) d_m = 25 nm; $p_{1,2} = 2.2 : 1$, Line ***1***: $<C_Q> = 1.6$ MHz, $\Delta C_Q = 0.7$ MHz. Line ***2***: $<C_Q> = 2.6$ MHz, $\Delta C_Q = 0.8$ MHz.
d) d_m = 15 nm; one line simulated with $<C_Q> = 2.2$ MHz, $\Delta C_Q = 1.1$ MHz.

Typical spectra for nanoparticles (i.e. samples with an average grain size in the range between 15 nm $\leq d_m \leq$ 250 nm) are shown in Fig. 6.6. The influence of the grain size on the ^{137}Ba NMR spectra is clearly reflected in the spectra measured at ca. 300 K (tetragonal phase). The typical powder pattern of the central line for the samples with mean particle sizes of 155, 55, and 25 nm may be explained by a superposition of two tetragonal contributions with different values $<C_{Q,k}>$ and $\Delta C_{Q,k}$ for the quadrupole constants and the distribution widths, respectively. One line shape component for the nanoparticles shows the typical line shape for the tetragonal phase ($<C_{Q,2}> \approx 2.6$ MHz) and a relatively small distribution of the quadrupole constant ($\Delta C_{Q,2} \approx 0.5$ MHz). This situation leads to the conclusion that one part of the sample possesses a tetragonal symmetry with small distortions. The other component obviously

belongs to regions where the mean quadrupole coupling constant is smaller (2.2 MHz - 1.6 MHz, depending on the particle size) and where a relatively broad distribution occurs.

The simulation of the NMR spectra is nicely consistent with the structural model for fine $BaTiO_3$ particles derived from the EPR data: A weakly distorted tetragonal core is surrounded by a highly distorted shell where the local symmetry can be only characterized by a strong distribution of the internal electrical fields (electric field gradients). The fraction of the distorted regions increase when the particle diameters are reduced from 155 nm to 25 nm. But at 25 nm still a tetragonal ordered part occurs (fraction less than 50 %). For the sample with the smallest diameters (15 nm) the strongly distorted component dominates and it was not possible to find a tetragonal center. This supports a conclusion where an ordered tetragonal phase disappears when the mean diameters are close and smaller than this size. This work is supported by the DFG.

6.9 Pulsed Field Gradients in Combination with Magic Angle Spinning NMR - Novel Prospects for Studying Heterogeneous Materials

A. Pampel, D. Michel

Part of the research program of our group is also the investigation of systems with restricted geometry and restricted mobility such as liquid-crystalline phases, biological systems or zeolites. We are applying a multidisciplinary approach using mainly Solid

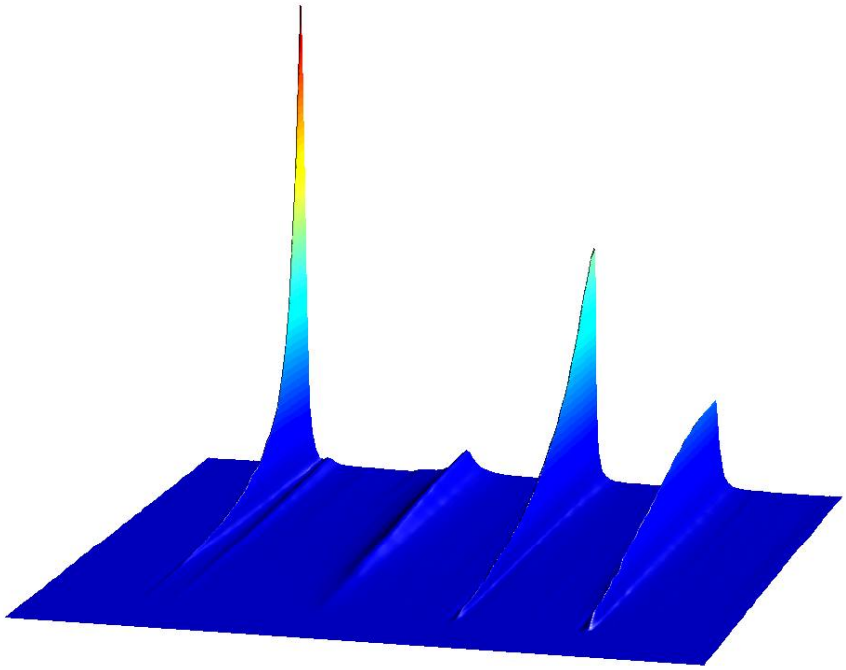

Figure 6.7: Spin-echo attenuation (gradient strength vs. signal intensities) of the spectroscopically resolved signals of ethane, water, butane and benzene adsorbed in NaX zeolite.

State NMR spectroscopy to reveal structural and dynamical aspects of such systems. NMR spectroscopy has definite advantages over diffraction techniques in the structure elucidation of such systems. These advantages, however, are frequently offset by resonance broadening mechanisms, which are caused by the anisotropic NMR parameters. Therefore, for this research we are using methods, which have been developed for the High-resolution NMR spectroscopy of solids. As a novel technique for investigation of such system we have introduced the combination of pulsed Field Gradient NMR and HR MAS NMR spectroscopy. The PFG MAS technique allows the determination of diffusion coefficients, even in a complicated environment like a membrane or zeolitic structures, which contains many components. Albeit the gain in resolution, the rather weak gradients strengths available in HR MAS probes limit the types systems that can be studied. Recently, we have introduced a novel approach that overcomes this restriction increasing the gradient strength by a factor of 5. As an application we have recently simultaneously observed the diffusion of four organic molecules adsorbed in NaX zeolite. This work is being done in cooperation with Prof. Jörg Kärger (Institute Experimental Physics I).

6.10 Investigation of Conformational Changes of Simple Molecules Sorbed in Zeolites by Proton HR MAS NMR Spectroscopy

A. Pampel, W. Böhlmamn, D. Michel

Aim and scope

The applicability of high-resolution ^{1}H NMR spectroscopy to molecules adsorbed in porous materials is in general strongly limited due to the poor resolution. The line broadening is not only caused by the restricted molecular mobility and the interaction with paramagnetic impurities but originates also from the presence of random local magnetic fields within the polycrystalline materials[1]. Local inhomogeneous magnetic fields mainly result from the polarization of the polycrystalline grains in the zeolite powder in the strong externally applied magnetic fields. In a good approximation these susceptibility effects can be described if the grains in the polycrystalline material with a size of some micrometers are considered as an ensemble of randomly distributed magnetic dipole moments. A notable enhancement in resolution of the spectra may be achieved when the induced static local magnetic fields are averaged out by the application of magic angle sample spinning (MAS) [1–3]. On this basis highly resolved spectra may be measured, and it is the aim of this work to use ^{1}H NOESY NMR experiments and other two-dimensional (2D) NMR methods to characterize structural changes in the course of adsorption but also to study the internal mobility of the molecules. Besides this the experimental requirements of this work will be described.

2D ^{1}H NOESY NMR. Molecular conformation

Standard NOESY pulse sequences are applied and the cross-relaxation rates σ_{ij} between the different nuclear spins i, j in the adsorbed molecule are calculated from the cross-peak intensities in the 2D NOESY spectra taken at different mixing times. Then it is possible to estimate the ratio of cross-relaxation rates by integrating the intensities of

the cross-peaks for various mixing times. The dipole-dipole cross-relaxation rates σ_{ij} are given by

$$\sigma_{ij} = \frac{1}{20}(\frac{\mu_0}{4\pi}\gamma_i\gamma_j\hbar)^2\frac{1}{r_{ij}^6}[6J_{ij}(2\omega) - J_{ij}(\omega)] = \frac{F(\omega)}{r_{ij}^6} \tag{6.1}$$

with the proton Larmor frequency ω and the magnetogyric ratio $\gamma_i = \gamma_k = \gamma$ of the protons in a fixed distance r_{ij} and the reduced spectral density function $J_{ij}(\omega)$ which in general may be the sum

$$J_{ij}(\omega) = \sum_k \frac{2p_k\tau_k}{1 + (\omega\tau_k)^2} \tag{6.2}$$

of contributions with different correlation times τ_k and weighting factors p_k. For the further discussion the shape of the reduced correlation function will not of essential, if the quantity $J_{ij}(\omega)$ can be considered to be the same for some proton spin pairs in the molecule and if we discuss only the ratios of these suitable cross-relaxation rates involved in the analysis. Consequently, we may only concentrate on the dependence of the quantities σ_{ij} on the factor $1/r_{ij}^6$ and compare the distance ratio derived from this analysis:

$$\frac{\sigma_{ij}}{\sigma_{kl}} = (\frac{r_{kl}}{r_{ij}})^6 \Rightarrow r_{kl} = \sqrt[6]{\frac{\sigma_{ij}}{\sigma_{kl}}}r_{ij}. \tag{6.3}$$

For the further discussion one "standard" distance r_{ij} is used as internal reference which is evaluated from other structural data. The problem was here to achieve a higher accuracy in the estimation of intramolecular distances that allows further conclusions about conformational changes of the adsorbed olefins in comparison to molecules in the gaseous phase [4, 5].

Homonuclear and heteronuclear cross-relaxation

Molecular motion Using an internal reference distance also the quantity F(ω) may be obtained and in combination with other heteronuclear relaxation rate measurements the spectral density function $J_{ij}(\omega)$ is estimated. A good approximation is achieved if Eq. (6.2) is given by a superposition of two terms. At room temperature the values of the respective correlation times are $1.8 \cdot 10^{-9}$ s and $2.7 \cdot 10^{-12}$ s if on average one butene-1 molecule is sorbed in a supercage of NaX zeolites. The first value corresponds to the mean life time of a molecule in a large cavities in a nice agreement with the results of PFG-NMR diffusion measurements [6]. The shorter correlation time is typical for an (anisotropic) librational motions of a molecule at an adsorption sites which are known from previous work known to be accessible Na^+ cations in the large cavities. This work was supported by the DFG.

[1] U. Schwerk, D. Michel, and M. Pruski, J. Magn. Reson. 119, 157-64 (1996)
[2] D.L. VanderHart, Magnetic Susceptibility High Resolution NMR of Liquids and Solids (John Wiley Sons, New York, 1996)
[3] J. Roland and D. Michel, Magn. Reson. Chem. 38, 587 (2000)
[4] D. Michel, A. Pampel, W. Böhlmann, J. Roland Investigation of conformational changes of simple 1-butene sorbed in zeolites by proton HR MAS NMR spectroscopy, Proceedings of the 14th International Zeolite Conference, Cape Town, South Africa, (2004) 1746 - 1750, Ed. By E. van Steen, L.H. Callanan, M. Claeys, and C.T.O'Connor

[5] D. Michel, A. Pampel, J. Roland Investigation of conformational changes of organic molecules sorbed in zeolites by proton magnetic resonance spectroscopy J. Chem.Phys. 119 (2003) 9242-9250
[6] D. Michel, W. Böhlmann, J. Roland, S. Mulla-Osman, Study of Conformation and Dynamics of Molecules Adsorbed in Zeolites by ^{1}H NMR, Lect. Notes Phys. 634, 217-274 (2004)

6.11 NMR Studies on Crystals with Structurally Incommensurately Modulated Phases

D. Michel, A. Taye, J. Petersson*

* Department of Physics, University of Saarland

Several crystals exhibit a structural phase transition from a high temperature paraelectric (N) phase into a structurally incommensurately (IC) modulated phase, where at least one local physical quantity is modulated in such a way that the characteristic wave vector q_i is not a rational multiple of the reciprocal lattice vectors of the N phase. Since the modulation does not fit to the underlying basic structure, the translational symmetry of the lattice is broken. As a consequence, the initial phase of the modulation wave is arbitrary, and the IC structure is continuously degenerate with respect to a phase shift. Because of the energetic degeneracy of the structure with respect to a shift of the initial

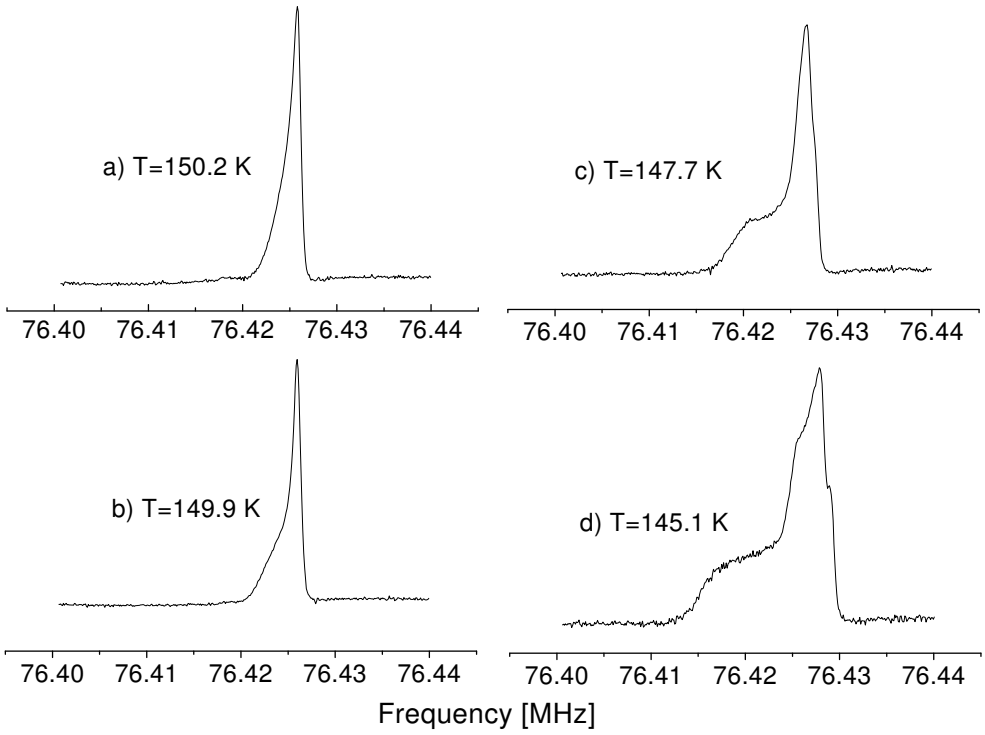

Figure 6.8: ^{35}Cl NMR line shape of the central transition lines of BCPS at different temperatures in a static magnetic field of $B_0 = 17.6\,T$ using a Bruker AVANCE 750 NMR spectrometer. A progressive broadening of the lines is observed from $T_i \approx 150.2\,K$ to $T \approx 145.1\,K$ in the in-commensurate phase.

phase of the modulation wave, special low-energy excitations termed "phasons" may be present in incommensurate systems.

In the last years a joint research program was realized in which the dynamics of the incommensurate (IC) modulation was investigated for various one-dimensionally incommensurately modulated crystals near the transition to the normal high temperature phase at the temperature T_i. Using nuclei with nuclear quadrupole moments as local probe, nuclear magnetic resonance (NMR) line shape and spin-lattice relaxation have shown to be very sensitive to study the order parameter dynamics and slow elementary excitations in crystals with IC phases. All results could be described consistently in terms of a static modulation in the IC phase without any indication for "floating" or large scale fluctuations of the modulation wave. The critical exponents derived from the NMR line shape and the relaxation times T_1 very nicely fit to the universality class of the 3d-XY model. For Rb_2ZnBr_4 and Rb_2ZnCl_4 crystals the characteristic frequency of the critical dynamics of the order parameter (OP) slows down to a frequency range which has been estimated to lie between 2-10 MHz. In this particular case one can derive the characteristic frequency of the critical dynamics of the OP above T_i and of the phason below T_i from the Larmor frequency dependence of ^{87}Rb NMR relaxation times T_1. The relatively broad temperature range where the critical dynamics was observed may be explained using the self-consistent phonon theory and the renormalization-group theory. We can conclude, that the critical region can be large if the dispersion of the soft mode is small (very "soft" mode) and/or if the anharmonic interaction constant is large. Taking parameters appropriate to these compounds we obtain results which are in good agreement with the experimental data, e.g. the width of the critical region is $\Delta T \approx 30 - 50\,K$ for RZB/RZC.

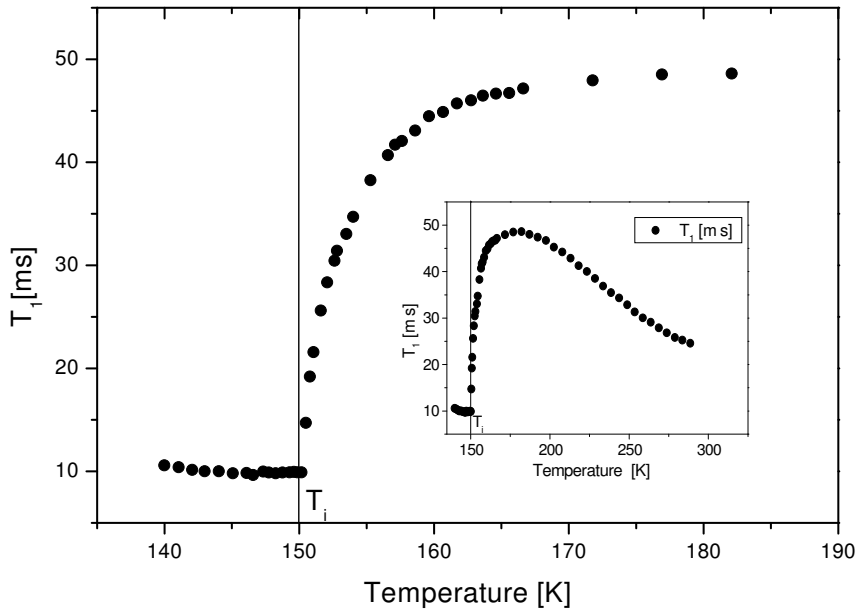

Figure 6.9: Temperature dependence of the ^{35}Cl NMR spin-lattice relaxation time T_1 in a single crystal of BCPS measured in the normal phase above T_i and at the higher frequency edge singularity in the incommensurate phase below T_i. The measurements were run at the central line in a static magnetic field of $B_0 = 17.6\,T$ using a Bruker AVANCE 750 NMR spectrometer. The limits of experimental error in the T_1 measurements are estimated to be $\pm$ 5 %, the temperature can be controlled with an accuracy of $\pm$ 0.1 K.

Recently, the validity of this conclusion was also confirmed for the particular IC system of bis(4-chlorophenyl)sulphone ($(ClC_6H_4)_2SO_2$, abbreviated here as BCPS). For BCPS the IC phase appears in a very broad temperature range from 150 K apparently down to 0 K. The static character of the modulation in the IC phase is confirmed by ^{35}Cl NMR line near the phase transition form the normal into the IC phase (Fig. 6.8) where high quality BCPS single crystals were used. In ^{35}Cl NMR spin-lattice rate measurements a large critical contribution to the relaxation rate T_1 can be detected. It can be described by a critical exponent which is nicely in agreement with the predictions of the 3d-XY model too. This work is supported by the DFG.

6.12 Melting-Freezing Phase Transition of Gallium and $NaNO_2$ Embedded in Porous Glasses and in Opals

D. Michel, B.F. Borisov*, E.V. Charnaya*, D. Yaskov*, C. Tien†, C.S. Wur†, Y.A. Kumzerov‡

*Institute of Physics, St. Petersburg State University, Russia

†Department of Physics, National Cheng Kung University, Tainan, Taiwan

‡A.F. Ioffe Physico-Technical Institute RAS, St. Petersburg, Russia

The main topics of this work include
- the study of phase transitions in confined geometry, in particular melting and freezing of metallic gallium nanoparticles and of $NaNO_2$ embedded into porous matrices and
- to investigate the influence of size effects on the mobility in confined liquids.

Samples of porous glasses (with pore diameter of 3.5 to 200 nm) and synthetic opals (regular spheres of silica) were used as matrices.

The melting-freezing phase transition of gallium confined within Vycor glass was studied by NMR and acoustic techniques. A pronounced depression of the freezing and melting phase transition temperatures and a hysteresis in the melting-freezing processes were found and discussed. NMR studies on liquid confined gallium revealed a noticeable decrease in the Knight shift and a drastic acceleration in gallium spin-lattice relaxation. These changes depend on the size and the geometry of the pores. The relaxation measurements were used to estimate the thermal correlation times of the Ga atoms in the confined geometry and to relate them with atomic diffusion.

Recently, we have performed ^{14}N NMR and acoustic measurements on $NaNO_2$ embedded into porous glass and in mesoporous materials of type MCM and SBA. To investigate the dynamics of embedded $NaNO_2$, ^{23}Na-NMR spin-lattice relaxation measurements have been made at various Larmor frequencies. Results are shown in Fig. 6.10. The relaxation times T_1 for ^{23}Na in $NaNO_2$ confined within a porous glass is shorter (open symbols) than for the bulk material (full symbols) near the ferroelectric phase transition and the apparent "minimum" is shifted to lower temperatures. According to the preliminary measurements shown in Fig. 6.10, to the parallel studies on $NaNO_2$ in mesoporous materials MCM-41 and SBA-15 and to the results of the previous work on polycrystalline material and on larger particles, this "minimum of T_1" can related to the collective motion of the NO_2^- ions. Hence, we may suggest that the relaxation rate $1/T_1$ is strongly influenced

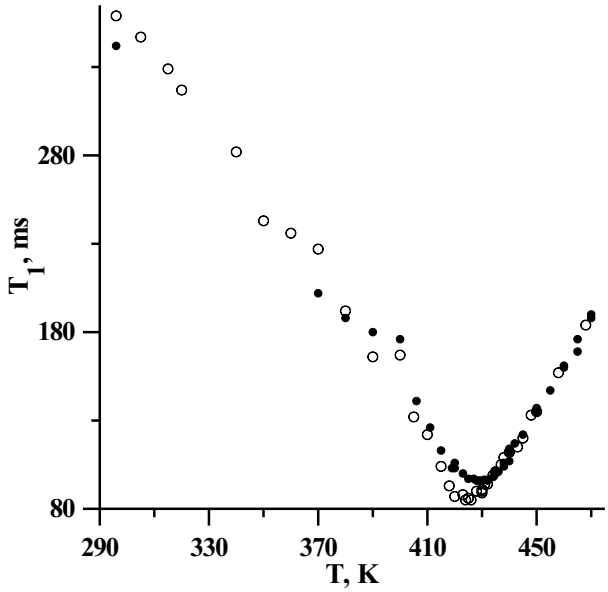

Figure 6.10: ^{23}Na-NMR longitudinal relaxation times T_1 for $NaNO_2$: porous glass (open symbols) and bulk material (full symbols). The measurements were run in a magnetic field of $B = 9\,\mathrm{T}$

by a critical contribution, i.e. a contribution which can be directly related with the ferroelectricity in this material and which allows direct conclusions about the phase transition. This work is supported by the Euler program of the DAAD.

6.13 Self-Association Processes of Short-Chain Anionic Surfactant in Silica Dispersions from ^{13}C NMR

M.V. Popova*, Y.S. Tchernyshev*, D. Michel

*Physical Institute, St. Petersburg State University

Structural properties of the ionic surfactant potassium nonanoate in aqueous solutions with pH values of 2 and 6 containing a silica dispersion (SiO_2) were investigated by means of ^{13}C MAS NMR techniques. It is shown that the chemical shifts σ and the spin-lattice relaxation times T_1 of separate segments of the hydrophobic chain reflect rather sensitively the process of surfactant adsorption on a solid surface as well as the self-association of the surfactants in the bulk solution. The values and the character of the changes of $\Delta\sigma$ and T_1 are mainly determined by the surface charge, which is generally assumed to change with the initial pH value of the aqueous silica dispersion. Most sensitive to the surface charge are the ^{13}C NMR parameters of the first and second carbon atoms in the hydrophobic chain of the surfactant molecules. In a system with pH = 2, the greatest dependence of these parameters on the surfactant concentration was observed. Comparing the NMR parameters for the surfactant-water-silica systems with similar parameters found for aqueous surfactant solutions [1], it is shown that at low surfactant concentrations in a solution (1.5 to 3 weight %) with pH = 6, the surfactant molecules are oriented parallel to the surface. They are mainly adsorbed due to a hydrophobic interaction with the

surface. In the same range of concentration, for systems with pH = 2 the adsorption occurs primarily on hydroxyl groups with the formation of hydrogen bonds between these groups and the polar head groups of the surfactant molecules. The adsorbed molecules then are oriented normal to the surface. At concentrations between 10 to 20 weight %, which considerably exceed the CMC value, the chemical shifts and relaxation times in both ternary systems are approximately equal to the values measured in solution because of the molecular exchange process between the adsorbed state and the bulk solution [2]. This work is supported by the Euler program of the DAAD.

[1] M.V. Popova, Y.S. Tchernyshev, D. Michel, NMR Investigation of the Short-chain Ionic Surfactant-Water Systems, Langmuir 20 (2004) 632 - 636
[2] M.V. Popova, Y.S. Tchernyshev, D. Michel, Self-association processes of short-chain anionic surfactant in silica dispersions from ^{13}C NMR, Colloids and Surfaces A: Physicochem. Eng. Aspects 243 (2004) 139 - 145

6.14 Funding

Strukturaufklärung nanokristalliner Ferroelektika mit Perowoskitstruktur durch Hochfeld-EPR-Spektroskopie
Investigation of nanocrystalline ferroelectrics with pervoskite structure by means of high-field-EPR spectroscopy (im Rahmen des Schwerpunktprogrammes 1051)
R. Böttcher: DFG, Bo 1080/6-3

Synthese und Charakterisierung eindimensionaler Ferroelektrika mit Perowskitstruktur
Synthesis and characterisation of one dimensional ferroelectrics with perovskite structure (im Rahmen der Forschergruppe 522)
R. Böttcher, E. Hartmann: DFG, Bo 1080/8-1

Hochfeld-ESR Spektroskopie von monomerem und dimerem Stickstoffoxid-Komplexen in Zeolithen
High field EPR spectroscopy of monomer and dimer nitric oxide complexes in zeolites (im Rahmen des Schwerpunktprogrammes 1051)
A. Pöppl, M. Hartmann: DFG, PO 426/2-3

Synthese und Strukturaufklärung von Vanadium-Phosphat-Systemen mittels ENDOR- und ESEEM-Spektroskopie
Synthesis and determination of the structure of vanadium-phosphate systems by means of ENDOR and ESEEM spectroscopy
A. Pöppl, K. Köhler: DFG, PO 426/3-1

Experimental proof of the predictions of renormalization theory on the critical exponents in systems with incommensurately structurally modulated phases
D. Michel: DFG, Mi 390/21-1

High-Resolution NMR Spectrometer with a Proton Resonance Frequency of 750 MHz
D. Michel: DFG, Mi 390/5-3

Phase transitions in metals and ferroelectrics embedded into porous glasses and other porous matrices
D. Michel, E.V. Charnaya: DAAD, Leonhard-Euler programme

NMR studies of short-chain surfactants in a heavy water solutions
D. Michel, V.I. Chizhik: DAAD, Leonhard-Euler programme

New materials for the information technology
R. Böttcher, D. Michel, J. Banys: Joint research project supported by Humboldt-Stiftung

6.15 Organizational Duties

Dieter Michel

- Vorsitzender des Verwaltungsrates des Studentenwerkes Leipzig
- Vorsitzender der Haushaltkommission de Universität Leipzig
- Mitglied der Sächsischen Akademie der Wissenschaften
- Mitglied des Internationalen Komitees der Groupement Ampere
- Mitglied des Internationalen Komitees der EENC (European Experimental Nuclear Magnetic Resonance Conferences)
- Mitglied des Internationalen Komitees der EMF (European Meeting on Ferroelectricity)
- Mitglied des Internationalen Komitees der IMF (International Meeting on Ferroelectricity)
- Mitglied des Beirates des Mathematisch - Naturwissenschaftlichen Fakultätentages der Bundesrepublik Deutschland
- Vertrauensdozent des Evangelischen Studienwerkes Villigst
- Gutachter der Zeitschriften Physical Review, Physical Review Letters, Journal of Chemical Physics, Journal of Physics: Condensed Matter, Zeitschrift für Naturforschung, physica status solidi

Rolf Böttcher

- Gutachter der Zeitschriften Physical Review, Journal of Physics: Condensed Matter, Langmuir, Journal of Magnetic Resonance

Andreas Pöppl

- Gutachter der Zeitschriften Journal of Magnetic Resonance, Journal of American Chemical Society, Physical Chemistry Chemical Physics, Chemical Physics Letters

André Pampel

- Gutachter der Zeitschrift Biophysical Journal, Journal of the American Chemical Society

Emre Erdem

- Member of International EPR Society (IES)

6.16 External Cooperations

Academic

Institut für Oberflächenmodifizierung - IOM Leipzig (Dr. E. Hartmann)

Universität Kaiserslautern, Fachbereich Chemie, Technische Chemie (Dr. M. Hartmann)

Technische Universität München, Anorganisch-chemisches Institut (Prof. K. Köhler)

The Weizmann Institute of Science, Department of Physical Chemistry, Rehovot, Israel (Prof. D. Goldfarb)

University of Vilnius, Radiophysics Department (Prof. J. Banys)

University of Wroclaw, Institute of Experimental Physics (Prof. Z. Czapla)

University of Opole, Institute of Mathematics (Prof. V.A. Stephanovich)

Max-Delbrück-Centrum für Molekulare Medizin Berlin-Buch (Dr. R. Reszka)

Universität des Saarlandes, Saarbrücken (Prof. J. Petersson)

St. Petersburg State University (Prof. E.V. Charnaya, Prof. B.N. Novikov, Prof. V.I. Chizhik)

Ioffe Institute of the RAS, St. Petersburg (Prof. J.A. Kumzerov)

Kirensky Institute of Physics of the Sibirian Branch of the Russian Academy of Sciences, Krasnoyarsk (Prof. I.P. Aleksandrova, Dr. J. Ivanov)

A. Mickiewicz University of Poznan (Prof. S. Jurga)

Universität Leipzig, Fakultät für Biowissenschaften, Pharmazie und Psychologie (Prof. A. Beck-Sickinger)

Martin-Luther-Universität Halle-Wittenberg: Department of Physics (Dr. H.T. Langhammer, Prof. Dr. H. Schneider, Prof. H. Beige) School of Pharmacy, Institute for Pharmaceutics (Prof. R.H.H. Neubert, Prof. S. Wartewig)

Technische Universität Darmstadt, Institut für Materialwissenschaften (Prof. H. Fuess)

Universität Leipzig, Fakultät für Chemie und Mineralogie, Institut für Technische Chemie (Prof. H. Papp, Dr. O. Klepel)

6.17 Publications

Journals and books

C. Freysoldt, A. Pöppl, J. Reinhold
Influence of Coligands on the EPR Hyperfine Coupling Constants of the Cu(I)-NO System - A Theoretical Study
J. Phys. Chem. A 108 (2004) 1582-1588

H.T. Langhammer, T. Müller, R. Böttcher, V. Müller, H.-P. Abicht
Copper-doped hexagonal barium titanatee ceramics
J. Eur.Ceramic Soc. 24 (2004) 1489-1492

M.V. Popova, Y.S. Tchernyshev, D. Michel
NMR Investigation of the Short-chain Ionic
Langmuir 20 (2004) 632-636

M. Gutjahr, J. Hoentsch, R. Böttcher, O. Storcheva, K. Köhler, A. Pöppl
A Q- and X-Band Pulsed Electron Nuclear Double Resonance Study of the Structure and Location of the Vanadyl Ions in the Cs Salt of Heteropolyacid $PVMo_{11}O_{40}$
J. Am. Chem. Soc. 126 (2004) 2905-2911

R. Haberlandt, D. Michel, A. Pöppl, R. Stannarius (eds.)
Molecules in Interaction with Surfaces and Interfaces
Lect. Notes Phys. 634 (Springer Verlag Berlin Heidelberg 2004)
ISBN 3-540-20539-X Springer-Verlag Berlin Heidelberg New York

A. Taye, D. Michel
NMR line shape analysis in the incommensurate phase of bis(4-chlorophenyl)sulfone
phys. stat. sol. (b) 6 (2004) 1333-1342

D. Michel, A. Pampel, W. Böhlmann, J. Roland
Investigation of conformational changes of simple 1-butene sorbed in zeolites by proton HR MAS NMR spektroscopy
Proceedings of the 14^{th} International Zeolite Conference, Cape Town, South Africa, 2004, 1746-1750, Ed. By E. van Steen, L.H. Callanan, M. Claeys, and C.T. Connor

W. Böhlmann, S. Mulla-Osman, D. Michel
^{1}H and ^{13}C NMR studies of long chain hydrocarbons adsorbed on MCM-41 and Zeolite NaX
Proceedings of the 14^{th} International Zeolite Conference, Cape Town, South Africa, 2004, 1823-1829, Ed. By E. van Steen, L.H. Callanan, M. Claeys, and C.T. Connor

D. Michel, W. Böhlmann, J. Roland, S. Mulla-Osman
Study of Conformation and Dynamics of Molecules Adsorbed in Zeolites by ^{1}H NMR
Lect. Notes Phys. 634 (2004) 217-274

A. Vinu, V. Murugesan, W. Böhlmann, M. Hartmann
An Optimized procedure for the Synthesis of AISBA-15 with Large Pore Diameter and High Aluminum Content
J. Phys. Chem. B 108 (2004) 11496-11505

A. Pampel, K. Zick, H. Glauner, F. Engelke
Studying Lateral Diffusion in Lipid Bilayers by Combining a Magic Angle Spinning NMR Probe with a Microimaging Gradient System
J. Am. Chem. Soc. 126 (2004) 9534-9535

T. Bräuniger, P.K. Madhu, A. Pampel, D. Reichert
Application of fast amplitude-modulated pulse trans for signal enhancement in static and magic-angle-spinning $^{47,49}Ti$-NMR spectra
Sol. Stat. Nucl. Magn. Reson. 26 (2004) 114-120

D. Michel, S. Mulla-Osman, G. Völkel, Z. Czapla
Order-Disorder of TMA Ions and Phase Transitions in Tetramethylammonium Calcium Chloride (TMCC) Studied by NMR
Integrated Ferroelectrics 62 (2004) 243-248

D. Michel, A. Taye, J. Petersson
Critical Dynamics in BCPS at the N-IC Phase Transition
Ferroelectrics 302 (2004) 163-166

M.V. Popova, Y.S. Tchernyshev, D. Michel
Self-association processes of short-chain anionic surfactant in silica dispersions from ^{13}C NMR
Colloids and Surfaces A: Physicochem. Eng. Aspects 243 (2004) 139-145

O. Klepel, W. Böhlmann, E.B. Ivanov, V. Riede, H. Papp
Incorporation of tungsten into MCM-41 framework
Microporous and Mesoporous Materials 76 (2004) 1205-112

V. Umamaheswari, A. Pöppl, M. Hartmann
Electron spin resonance spectroscopy of Cu(I)-NO complexes in copper exchanged zeolites
J. Mol. Catalysis A: Chemical 223 (2004) 123-128

E. Guzman, H. Hochmuth, M. Lorenz, H. von Wenckstern, A. Rahm, E.M. Kaidashev, M. Ziese, A. Setzer, P. Esquinazi, A. Pöppl, D. Spemann, R. Pickenhain, H. Schmidt, M. Grundmann
Pulsed laser deposition of Fe- and Fe, Cu-doped ZnO thin films
Ann. d. Phys. 13 (2004) 57-58

A. Vinu, K.U. Nandhini, V. Murugesan, W. Böhlmann, V. Umamaheswari, A. Pöppl, M. Hartmann
Mesoporous FeAlMCM-41: an improved catalyst for the vapor phase tert-butylation of phenol
Appl. Catal. A General 265 (2004) 1-9

A. Taye, D. Michel
Phason and Amplitudon Dynamics in the Incommensurate Phase of Bis(4-chlorophenyl)sulphone (BCPS)
Phys. Rev. B, *accepted* (2004)

H.A. Scheidt, A. Pampel, L. Nissler, R. Gebhardt, D. Huster
Investigation of the membrane localization and distribution of flavonoids by high-resolution magic angle spinning NMR spectroscopy
Bioch. Biophys. Acta Biomembranes 1663 (2004) 97-107

A. Pöppl, M. Gutjahr, T. Rudolf
Paramagnetic Adsorption Complexes in Zeolites as Studied by Advanced Electron Paramagnetic Resonance Techniques
Lect. Notes Phys. 634 (2004) 185-215

A. Pampel, F. Volke
Studying Lyotropic Crystalline Phases Using High-Resolution MAS NMR Spectroscopy
Lect. Notes Phys. 634 (2004) 440-464

6.18 Graduations

PhD

Abdoulaye Taye
Zum statischen und dynamischen Verhalten von Systemen mit strukturell inkommensurablen Phasen: ^{35}Cl-NMR-Untersuchungen an Bichlorophenylsulfon

International cooperation:
Maria Popova
PhD thesis (candidate of science) at St. Petersburg State University, chair of Prof. Dr. V.I. Chizhik

Diploma

Andreas Bunge
Festkörper-NMR-Untersuchungen membranassoziierter Peptide

Eike Bierwith
NMR Studies on Ferroelectrics in Confined Geometry

Peter Rhone
Cooperation with Institut für Troposphärenforschung Leipzig (Dr. D. Althausen, Prof. Dr. J. Heintzenberg)

Pavel Sedyhk
Dima Yaskov
(Magister theses at the St. Petersburg State University, chair of Prof. Dr. E. Charnaya, Prof. Dr. B. Novikov)

6.19 Guests

A large number of guests have visited our group in 2004 about which we cannot report here in detail. This includes short-time visits of numerous guests from abroad, e.g. from Israel, France, Lithunia, Poland, Syria, Vietnam, the Russian Federation (St. Petersburg, Kazan), the United States. Mrs. Dr. Natalya Grunina (St. Petersburg state University) has received a support from the DAAD to realize 3 month's postdoc-stay in our group.

7

Semiconductor Physics

7.1 Introduction

The Semiconductor Physics Group has enjoyed in 2004 scientific success as well as the attraction of major funding. Our results on whispering gallery modes with low mode numbers down to $N = 1$ have been featured in Physical Review Focus[1]. A related image of pulsed laser deposition grown ZnO nanoneedles (Fig. 7.1a) is on the APS 2005 calendar. Our investigation of peptide attachment on semiconductor surfaces has been published in Nano Letters and was chosen for the cover of the November issue of this magazine

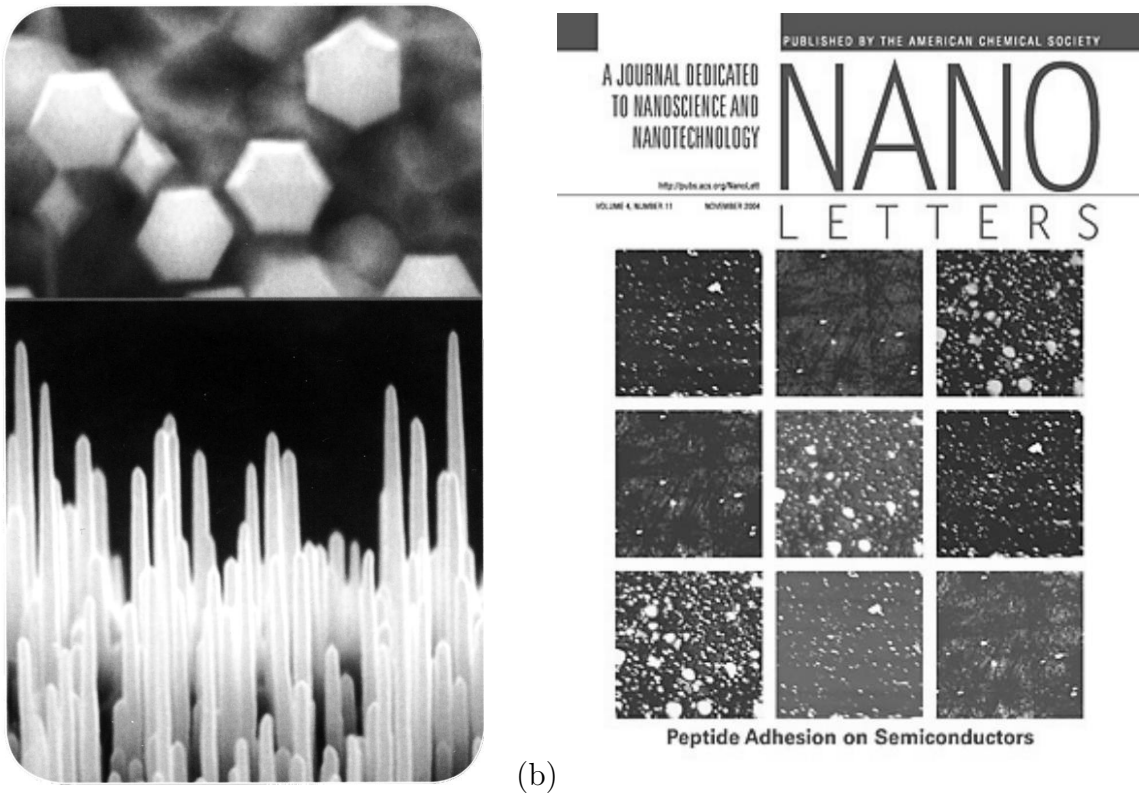

(a) (b)

Figure 7.1: (a) Scanning electron image of ZnO nanoneedles featured on APS Calendar 2005. (b) Cover of Nano Letters 4(11) (2004) with AFM images of peptide attachment.

[1] http://focus.aps.org/story/v14/st10

(Fig. 7.1b). Significant progress has been made with regard to the understanding and manipulation of the electrical properties of ZnO thin films and ZnO Schottky diodes. Further information about our research activities can be found in the following brief reports or in the references given below. Please check the related links on our WWW site[2]; we happily provide you reprints on request.

At the end of March, the Conference TCO2004 took place at the University. It was jointly organized by Prof. Marius Grundmann and Dr. Alexander Braun of Solarion GmbH, Leipzig and supported by BMBF and DFG. More than one hundred scientists came together and followed thirteen invited lectures about transparent conductive oxides and their epitaxy, physical properties, industrial applications and related manufacturing equipment. Many participants joined the lab tours offered at the University and Solarion GmbH.

The European Network of Excellence SANDiE began in July. SANDiE is the acronym for 'Self-Assembled semiconductor Nanostructures for new Devices in photonics and Electronics'. The Universität Leipzig coordinates this joint, four-year project of 28 European Partners from Portugal to Russia and hosts the Network Office. SANDiE will lead to an integration of research on self-assembled nanostructures, as well as integration of the related people and resources on an European level. The kick-off meeting brought all Partners together in Leipzig and, apart from the first assembly meeting, the welcome dinner at Auerbach's Keller is favorably remembered.

We became a member of the European Thematic Network on ZnO for UV optoelectronics (SOXESS). We were able to strengthen our scientific cross-border relationships. We enjoyed an increase in cooperation through sample exchange, visits of our distinguished guests and conference attendance. We look forward to intensify these ties in 2005.

M. Grundmann

7.2 MgZnO Nanowire Arrays on Sapphire Grown by High-Pressure Pulsed-Laser Deposition

M. Lorenz, E.M. Kaidashev, A. Rahm, T. Nobis, J. Lenzner, G. Wagner, D. Spemann, H. Hochmuth, M. Grundmann

$Mg_xZn_{1-x}O$ nanowires with Mg-content x from 0 to 0.2 have been grown by high-pressure pulsed-laser deposition (PLD) on gold-covered sapphire single crystals [1]. The PLD process allows for a unique wide-range control of morphology, diameter, and composition of the $Mg_xZn_{1-x}O$ nanowires. The diameter of single ZnO wires could be varied between about 50 and 3,000 nm, and the Mg content x of $Mg_xZn_{1-x}O$ wire arrays was controlled via the PLD gas pressure [1]. The microscopic homogeneity of Mg-content is displayed in Fig. 7.2(b) by cathodoluminescence (CL) imaging of the excitonic peak energy. The fluctuation of CL peak energy between individual wires is about an order of magnitude smaller than the alloy broadening, as shown in Fig. 7.2(c) and (d).

This work is supported by the DFG within FOR 522 (Gr 1011/11-1).

[2] www.uni-leipzig.de/∼hlp

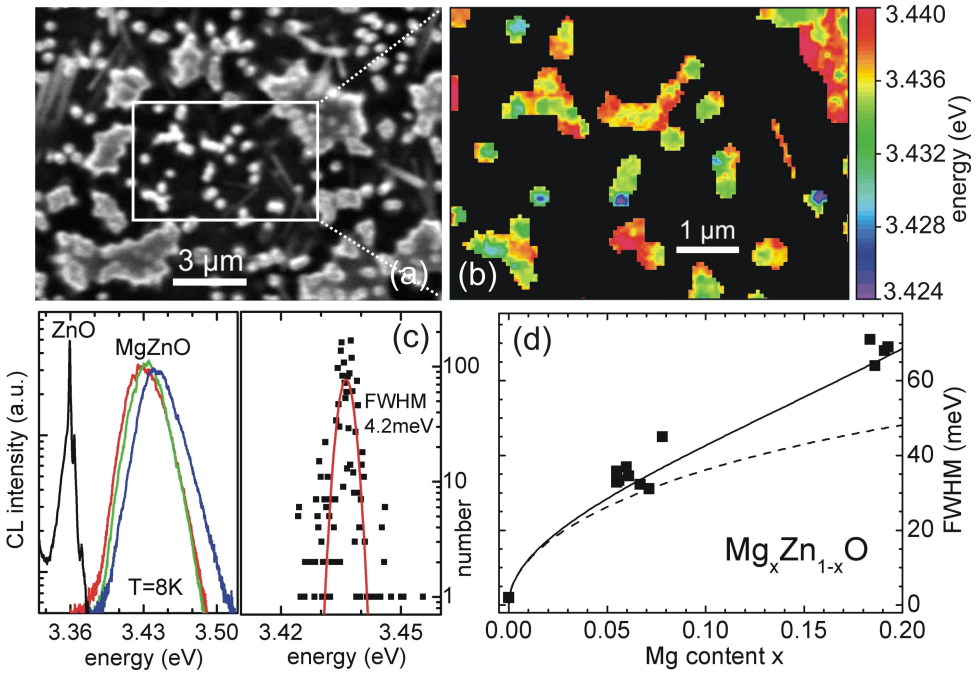

Figure 7.2: Lateral homogeneity of Mg content in a $Mg_xZn_{1-x}O$ nanowire array: (a) SEM image, the white rectangle indicates the area of the CL scan image of the excitonic peak energy (b). (c) shows a selection of three typical CL spectra as used for (b), together with a spectrum of a ZnO nanowire, and the histogram of CL peak energies with Gaussian fit. (d) shows FWHM of CL spectra at $T = 8\,\mathrm{K}$ of individual wires vs. Mg concentration (obtained from energy of the CL peak maximum). The dashed and solid curves in (d) are the theoretical alloy broadening for ZnO and MgZnO exciton parameters, respectively.

[1] M. Lorenz, E.M. Kaidashev, A. Rahm, T. Nobis, J. Lenzner, G. Wagner, D. Spemann, H. Hochmuth, M. Grundmann, Appl. Phys. Lett. **86** 2005, 143113

7.3 Whispering Gallery Modes in Nanosized Hexagonal Resonators

T. Nobis, E.M. Kaidashev, A. Rahm, M. Lorenz, M. Grundmann

Concerning sound waves, the whispering gallery effect is a common and well-known phenomenon. We analyzed the formation of such whispering gallery modes (WGMs) for visible light. The investigated resonator structures are hexagonal zinc oxide (ZnO) nanoneedles, whose diameter is tapered from about 800 nm at the bottom down to zero at the top (see Fig. 7.3a). In this nano-regime, WGMs had been explored little so far.

For a theoretical understanding of hexagonal WGMs, Maxwell's equations have to be solved numerically. However, a descriptive plane wave model (PWM) has been deduced [1] that considers the light to circulate inside the cavity as shown in the inset of Fig. 7.3a. Exploiting the process of total internal reflection, constructive interference leads to an enforcement of certain wavelengths that approximate the resonant modes of the cavity.

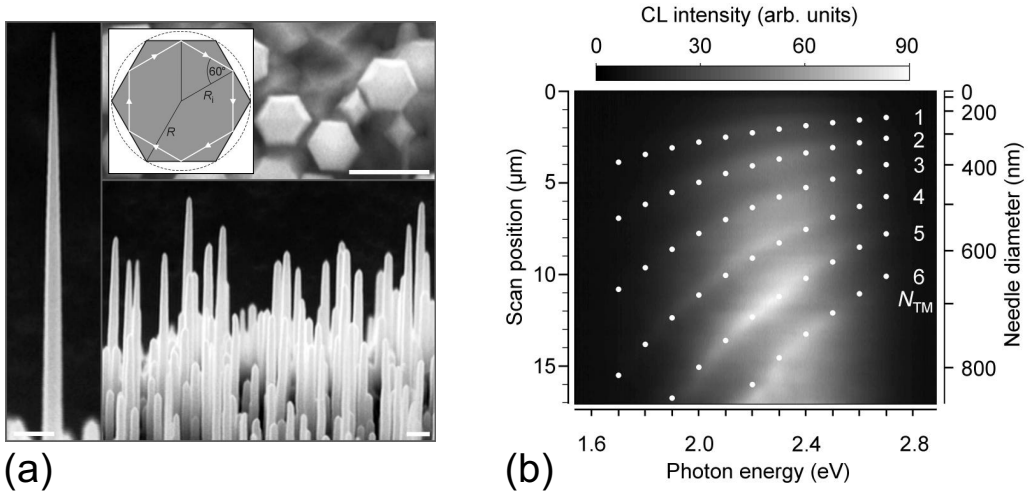

Figure 7.3: (a) SEM-images (top view and side views) of ZnO nanoneedles. (Scalebars = $2\,\mu$m.) Inset: Schematic of the 2-dim. hexagonal resonator. (b) CL linescan along the axis of a nanoneedle. Dots mark theoretical resonance energies of TM-polarized WGMs.

We performed cathodoluminescence (CL) spectroscopy exciting the broad green luminescence band of ZnO around $E = 2.3\,\text{eV}$ to optically detect WGMs. In the presence of a cavity, the green band is modulated such that maxima can be distinguished, each referring to a certain resonant WGM energy. A set of modulated CL spectra recorded along the longitudinal axis of a nanoneedle is shown in Fig. 7.3b. With the CL intensity given in gray scales, the bright regions in Fig. 7.3b represent resonant WGMs. When the diameter of the needle is decreased, all resonances systematically shift to higher energies. Even at the very top of the needle CL-intensity modulations indicate the occurrence of low order WGMs. Theoretical resonance energies of TM-polarized WGMs for mode numbers $N = 1$ to 6 due to the PWM are additionally shown in Fig. 7.3b. They fit the experimental data in good agreement. Hence, for the first time the whispering gallery effect for visible light could be resolved within the nano-regime for small mode numbers down to $N = 1$. Detailed information is given in [2]. Extensive numerical modeling and polarization-resolved spectroscopy are under way.

This work was supported by DFG within FOR 522 (Gr 1011/11-1)

[1] J. Wiersig, Phys. Rev. A **67**, 023807 (2003)
[2] T. Nobis *et al.*, Phys. Rev. Lett. **93**, 103903 (2004)

7.4 Two-Dimensional ZnO:Al Nanosheets and Nanowalls Obtained by Al_2O_3-Assisted Carbothermal Evaporation

A. Rahm, G.W. Yang*, M. Lorenz, T. Nobis, J. Lenzner, G. Wagner, M. Grundmann
*permanent address: Zhongshan University, P.R. China

The control of the dimensionality and shape of nanostructures to attain various building blocks and novel nanosized effects is highly desirable for applications of nanomate-

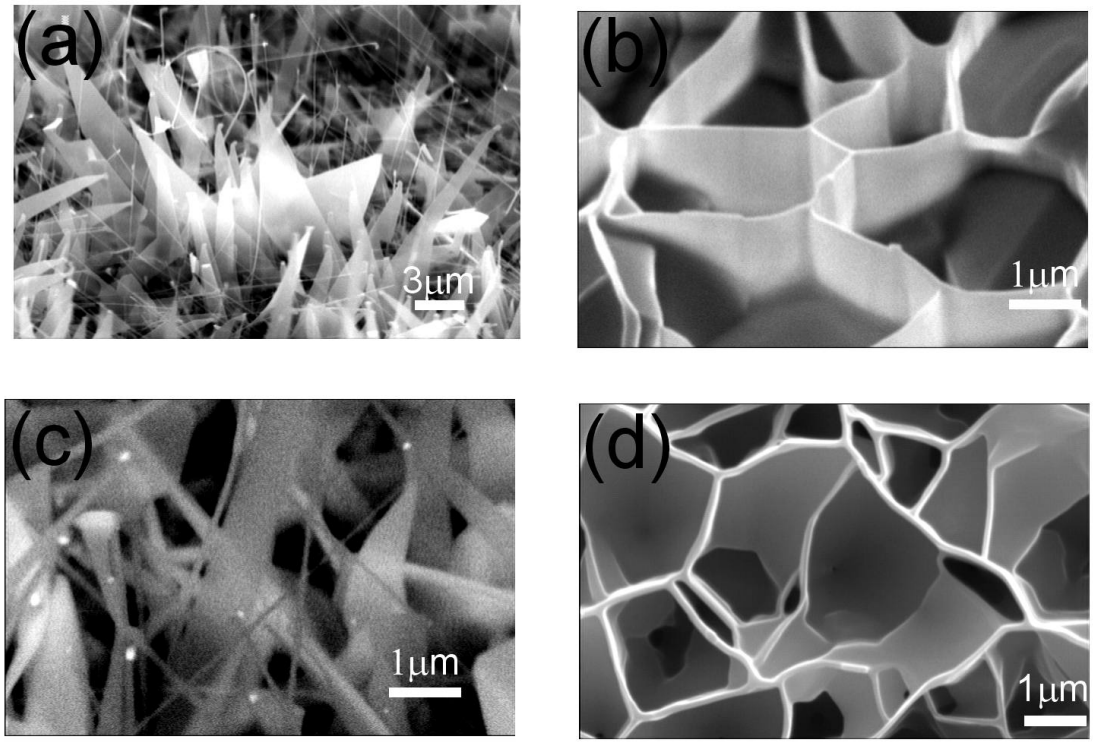

Figure 7.4: SEM images of ZnO:Al nano-sheets: (a) 45° view, (c) backscattered electron contrast; nano-honeycomb structures: (b) 45° view, (d) 90° view.

rials. Only a few studies pay attention to two-dimensional (2D) ZnO nanostructures so far. Here, free-standing, 2D ZnO nanosheets (Fig. 7.4a) and branched honeycomb-like nanowalls (Fig. 7.4b,d) have been grown together with one-dimensional nanothreads on gold covered a-plane sapphire and GaN templates on silicon substrates (from A. Dadgar and A. Krost, Universität Magdeburg) using Al_2O_3 assisted carbothermal evaporation of ZnO [1]. In X-ray diffraction 2Θ-ω scans, two orientations, ZnO(0001) and ZnO($10\overline{1}1$), of the two-dimensional nanosheets were detected, in contrast to the purely c-axis oriented honeycomb structures. Temperature-dependent cathodoluminescence shows bound exciton and donor-acceptor pair recombinations with a linewidth of 2.1 meV at 10 K. This peak width is comparable to values known for pure ZnO nanowire and PLD ZnO thin films. EDX and TEM investigations reveal gold droplets on top of the grown 2D structures and hence the formation of the novel Al-doped ZnO nanostructures is due to a vapor-liquid-solid growth mechanism. The gold droplets can also be seen in the contrast of backscattered electrons in the electron microscope (Fig. 7.4c). We attribute the specific 2D growth behavior to a growth rate promotion due to the Al_2O_3 in the source [2].

This work was supported by the DFG within FOR 522 (Gr 1011/11-1).

[1] M. Lorenz, J. Lenzner, E.M. Kaidashev, H. Hochmuth, M. Grundmann, Ann. Phys. **13** (2004) 39

[2] A. Rahm, G.W. Yang, M. Lorenz, T. Nobis, J. Lenzner, G. Wagner, M. Grundmann, Thin Solid Films, *in press*

7.5 MOVPE Growth Study of Free-Standing GaAs Nanowires

J. Bauer*, V. Gottschalch*, H. Herrnberger†, G. Wagner‡, J. Lenzner, M. Grundmann

*Institut für Anorganische Chemie, Universität Leipzig

†Leibniz-Institut für Oberflächenmodifizierung Leipzig

‡Institut für Mineralogie und Kristallographie, Universität Leipzig

The fabrication of free-standing GaAs-nanowires using metal organic vapor phase epitaxy (MOVPE) was previously investigated by Hiruma *et al.* [1]. Therefore the vapor-liquid-solid (VLS) approach was applied which was discovered in 1964 by Wagner *et al.* [2] to describe the growth of Si-NWs. The decomposition paths and the growth mechanism itself are not understood in detail until today.

We used Si(111), Ge(111) and GaAs$(\bar{1}\bar{1}\bar{1})_{\mathrm{As}}$ as substrate materials. To prepare these substrates with gold droplets, we applied the droplet formation due to annealing of thin gold films. This technique is favourable to investigate the NW growth in dependence of the diameter. We studied the influence of the growth conditions (temperature, precursor partial pressures, total reactor pressure, and growth duration) important to fabricate GaAs-NWs with MOVPE. We used a commercial MOVPE-apparatus AIX200 (AIXTRON AG) in low-pressure mode. Trimethylgallium served as group-III precursor. Arsine and tertiarybutyl-arsine were applied as group-V source materials. The dependence of the NW's length l on its diameter d can be described by a potential law: $l = f \cdot d^{\gamma}$. So the diameter dependence of the MOVPE parameters on the NW growth can be discussed by using the both parameters f and γ. The choice of group-V source partial pressure allows a variation of the parameter γ from a positive to a negative value with increasing pressure. Using the partial pressure at $\gamma = 0$, a diameter independent NW growth can be achieved (Fig. 7.5). Time dependent investigations showed a linear behaviour of the NW growth, which can be expressed by the parameter f. Therefore, a diameter-dependent growth rate could be determined. The NWs' real structure was investigated using transmission

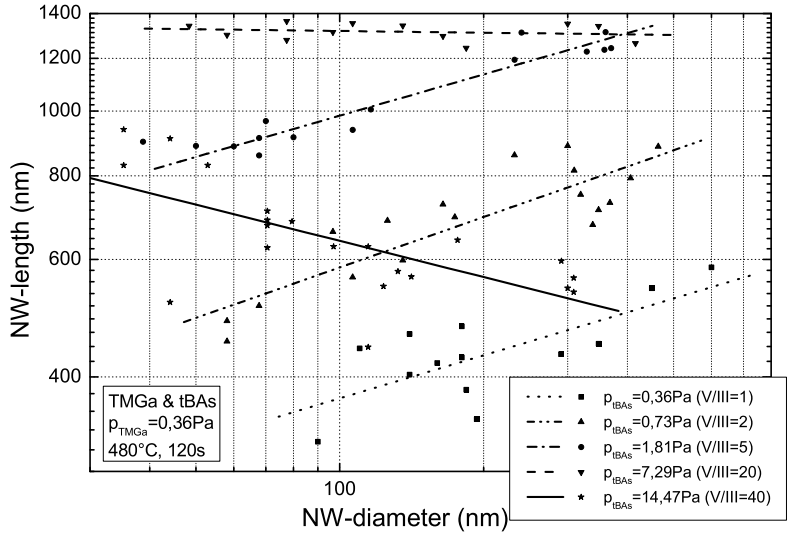

Figure 7.5: Effect of arsine partial pressure on the GaAs-NW growth with respect to the diameter. At V/III≈20 the NW growth is diameter independent.

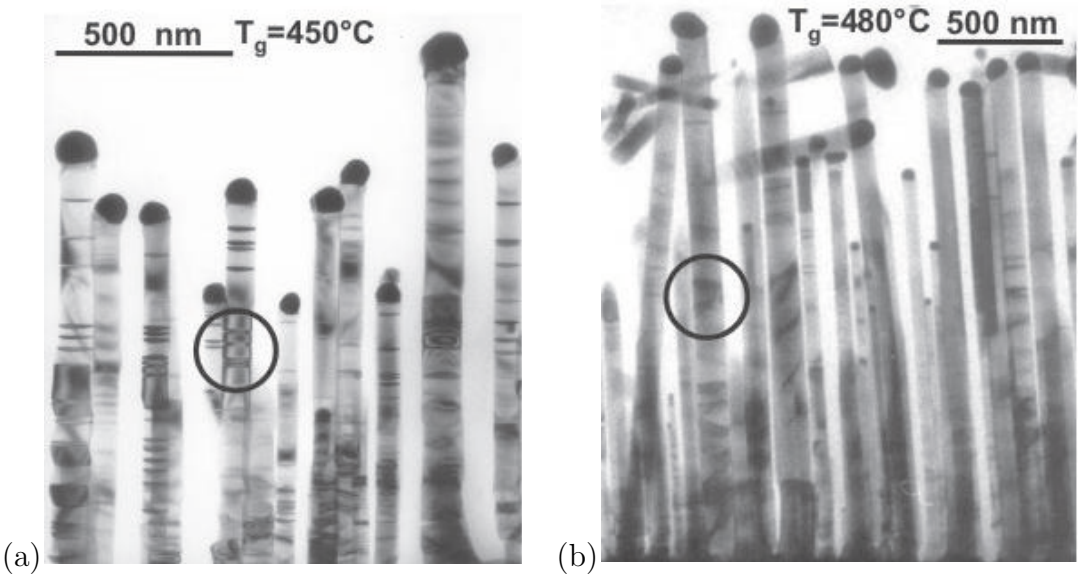

Figure 7.6: TEM-bright field view (beam direction perp. NW-axis) of GaAs nanowires grown with MOVPE at (a) $T = 450\,^{\circ}\mathrm{C}$ and (b) $T = 480\,^{\circ}\mathrm{C}$. At higher growth temperatures a smaller number of twins forms.

electron microscopy and transmission electron diffraction. We identified twin sections along the $[\bar{1}\bar{1}\bar{1}]_{\mathrm{As}}$-growth direction. The twin formation can be reduced by increasing the growth temperature (Fig. 7.6).

[1] K. Hiruma *et al.*, Appl. Phys. Lett. 59, 431 (1991)
[2] R.S. Wagner *et al.*, Appl. Phys. Lett. 4, 89 (1964)

7.6 Preparation of $A^{III}B^{V}$ Micro-Tubes with Strained GaAs Quantum Wells Grown by MOVPE

H. Paetzelt*, V. Gottschalch*, J. Lenzner, H. Herrnberger†, J. Bauer*, G. Benndorf, G. Wagner‡, M. Grundmann

*Institut für Anorganische Chemie, Universität Leipzig
†Leibniz-Institut für Oberflächenmodifizierung Leipzig
‡Institut für Mineralogie und Kristallographie, Universität Leipzig

Multilayer structures consisting of a GaAs buffer layer, AlAs sacrifical layer, (InGa)As strain layer, (AlGa)As bottom barrier, GaAs quantum well with a layer thickness of 3 . . . 1.5 nm and a (BAlGa)As strained top barrier were epitaxially grown on a GaAs (100)-oriented substrate by metal-organic vapour-phase epitaxy. These structures are able to form micro-tubes when the sacrifical AlAs layer is material-selectivly etched with hydrofluoric acid [1].

The pseudomorphic $In_xGa_{1-x}As$ layer with a mole fraction of about x=0.37 was used to grow a lattice-mismatched thin film with a maximum compressive strain to GaAs. The

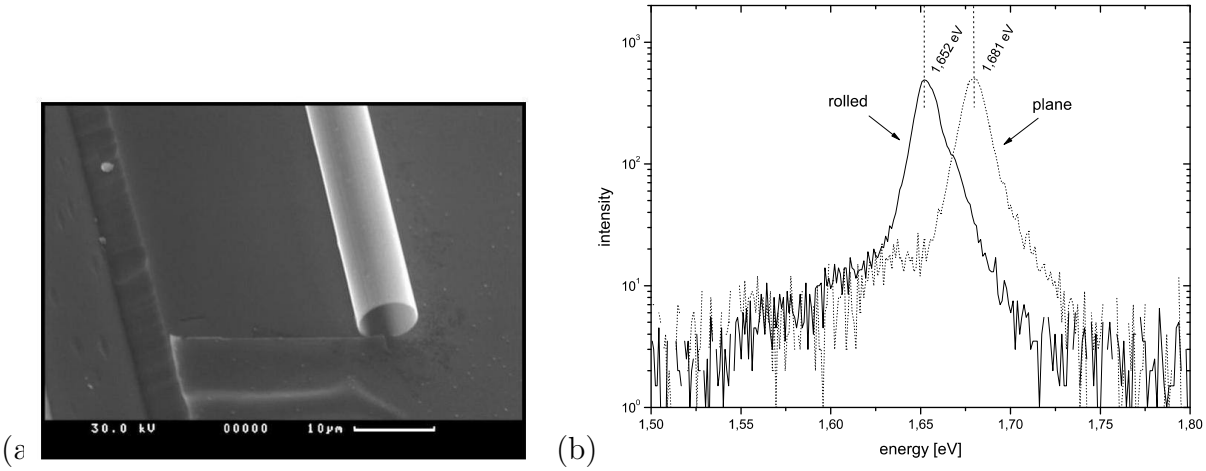

Figure 7.7: (a) SEM image of a tube formed along ⟨110⟩. (b) Cathodoluminescence spectra at $T = 10\,\mathrm{K}$. The peak shift is $\Delta E = 29\,\mathrm{eV}$,

boron incorporation in (AlGa)As was used to perform a tensil strain in the top layer and to study the effect on the surface and the rolling properties of the tube. After lithographical preparation, the AlAs sacrifical layer was materialselectivly etched with HF:H_2O (1:2) and the strained multilayer systems rolled up along the ⟨100⟩ direction from a starting edge. The ⟨100⟩ direction is preferred for the roll-up process, but with a special technique we are also able to produce tubes in ⟨110⟩ direction. The realized structures were imaged by scanning electron microscopy (Fig.7.7a) and compared to a theoretical strain relaxation model which uses the continuum theory to calculate the diameter of the tube.

We studied the optical properties of the embedded QW using room- und low-temperature (4K) photoluminescence spectroscopy to characterize the planar system and cathodoluminescence spectroscopy at 10.2 K (Fig.7.7b) for the planar and rolled system. By measuring the peak shift of the GaAs quantum well caused by uniaxial strain [2], we were able to characterize the strain type and compared it to the theoretical quantum well bandgap energies.

[1] Prinz *et al.*, Physica E 6, 828 (2000).
[2] Jain *et al.*, Semicond. Sci. Technol. 11, 641 (1996)

7.7 MgZnO/ZnO Hetero- and Double Heterostructures Grown by Pulsed Laser Deposition

S. Heitsch, G. Zimmermann, C. Schulz, H. Hochmuth, G. Benndorf, H. Schmidt, T. Nobis, M. Lorenz, M. Grundmann

Zinc oxide is a promising material for the preparation of lasers working in the UV spectral range. To realize laser structures, quantum wells (QW) are used because their emission properties can be controlled by their geometry. In ZnO QWs the large exciton binding energy could even be enhanced above the LO phonon energy to reduce scattering effects

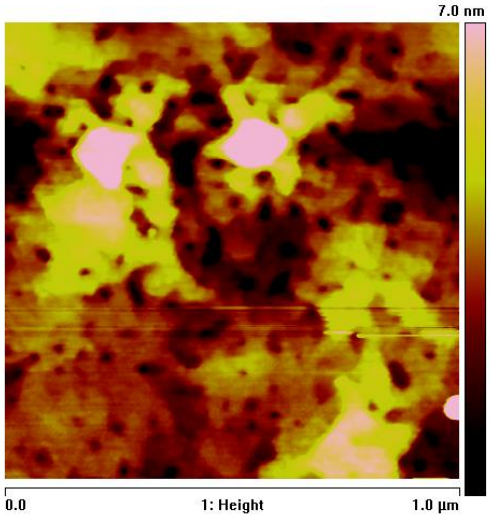

Figure 7.8: AFM image of the surface of a MgZnO/ZnO HS with nominal 6 nm ZnO

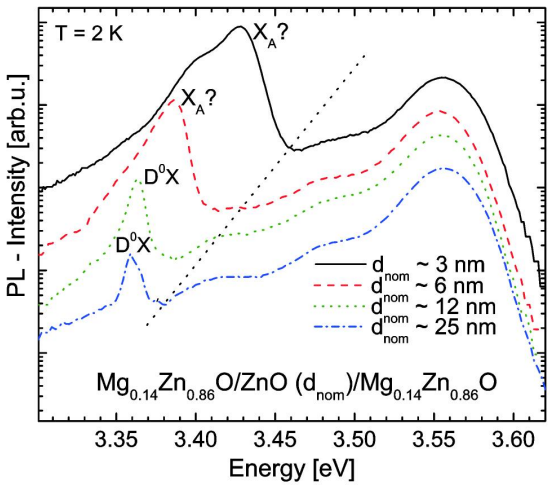

Figure 7.9: PL spectra of MgZnO/ZnO DHS with different nominal ZnO thicknesses

and use excitonic lasing processes. As barrier material for such QW, MgZnO is suitable because the bandgap of ZnO increases by alloying it with MgO.

We have investigated MgZnO thin films (thickness $\sim$ 300 nm), MgZnO/ZnO heterostructures (HS), and MgZnO/ ZnO/MgZnO-double heterostructures (DHS) by means of AFM, cathodoluminescence (CL, at 12 K), and photoluminescence (PL) spectroscopy (at 2 K). All samples were grown by pulsed laser deposition on *a*-plane sapphire substrates.

PL investigations of the MgZnO thin films prove the blue shift of the MgZnO bandgap with increasing Mg content of the films. While cathodoluminescence measurements show their laterally homogeneous emission properties, AFM images reveal their rough surfaces which prevent smooth interfaces in HS. Accordingly, ZnO layers with nominal thicknesses of $\leq$ 6 nm grown on MgZnO thin films do not form films but star-like structures at the surfaces of the HS (Fig. 7.8). Only for thicker ZnO layers their structure is film-like. This means that, under the present growth conditions, in DHS with nominal ZnO thicknesses of $\leq$ 6 nm no usual quantum well structures are formed, but small, nm-sized ZnO structures which are packed in MgZnO.

The PL of such structures is shown in Fig. 7.9. On the right hand side of the dotted line PL stemming from the MgZnO layers of the DHS is observed. On the left hand side of the dotted line the PL from the ZnO layer is visible. With decreasing nominal ZnO layer thickness d_{nom} its intensity increases and the peak position shifts to higher energies. These two facts point to the presence of localization and confinement effects in the DHS. In DHS with $d_{\mathrm{nom}} \geq 12$ nm, the ZnO PL can be ascribed to defect bound excitons. Temperature-dependent PL measurements between 4.4 and 300 K suggest the recombination of localized excitons to be the origin of the ZnO PL in DHS with $d_{\mathrm{nom}} \leq 6$ nm. Their emission energy is blue shifted up to 50 meV with respect to the emission of free excitons in bulk ZnO.

This work is supported by the DFG within the Forschergruppe 404 'Oxidische Grenzflächen' (Gr 1011/14-1).

7.8 Alloy Broadening in $Mg_xZn_{1-x}O$ Thin Films

C. Schulz, S. Heitsch, T. Nobis, J. Lenzner, M. Lorenz, M. Grundmann

In order to make MgZnO thin films and quantum well (QW) structures applicable for technical purposes, it is necessary to grow sufficiently homogeneous layers exhibiting intensive and narrow luminescence lines. Therefore, the optimal growth parameters have to be found. By changing the Mg-content of the material, it is intended to tune the bandgap energy of the MgZnO-crystal. A disorder effect connected with an increase of the Mg-content is the so-called alloy broadening of luminescence features.

We used spatially resolved cathodoluminescence (CL) spectroscopy at $T = 10\,\mathrm{K}$ to investigate the luminescence properties of MgZnO samples (thin films and single QW-structures) grown with pulsed laser deposition (PLD) on a-plane sapphire substrates under different growth conditions. On each sample, we recorded the CL-spectra at various lateral positions and determined the spectral position and FWHM of the dominating peak (donor bound exciton recombination). Fig. 1(a) shows the FWHMs with respect to the peak energy pointing out the influence of alloy-broadening on the MgZnO luminescence. The alloy broadening theory [1] explains the composition dependence of the line widths in ternary materials with the random occupation of cation sites in the lattice by one of the two cationic elements. Assuming a linear dependence of E_g on the Mg mole fraction x [2], the calculation yields the root-like curve plotted in Fig. 7.10a which represents a theoretical minimum for the width of the D_0X-transition. The experimental data are in good agreement with the theory since no measured values lie significantly below the curve.

Figure 7.10b shows the effect of the O_2 partial pressure in the PLD-process on the FWHMs and peak energies of two series (open circles in Fig. 7.10a) of MgZnO thin films. To compare the measured data concerning their line widths, the ratio w of experimental value and theoretical minimum of FWHM due to alloy broadening is given. A tendency to narrower CL-peaks of lower energy and less lateral fluctuation at enhanced O_2 pressures is recognizable indicating thin films of better quality.

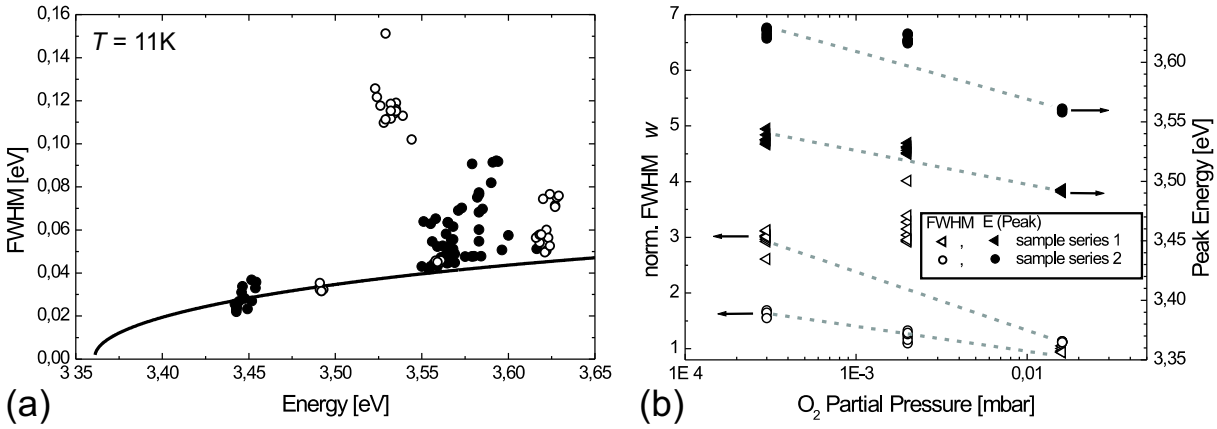

Figure 7.10: (a) Experimental data (dots) and theoretical minimum (line) of FWHM of dominating CL peak of MgZnO samples vs. peak energy. (b) influence of O_2 pressure on the ratio $w = FWHM_{\mathrm{exp}}/FWHM_{\mathrm{all.broad.}}$ (open symbols) and peak energy (filled symbols).

[1] E.F. Schubert et al., Phys. Rev. B **30**, 813 (1984)
[2] M. Lorenz et al., Appl. Phys. Lett., *in press*

7.9 ZnO Thin Films with High Cathodoluminescence Yield for Scintillator Applications

M. Lorenz, H. Hochmuth, J. Lenzner, T. Nobis, G. Zimmermann, H. Schmidt, M. Grundmann

Epitaxial ZnO thin films were grown by pulsed laser deposition (PLD) in N_2 or N_2O or O_2 background gas on MgO-buffered a-plane sapphire [1]. The excitonic room-temperature cathodoluminescence (CL) intensity, the carrier concentration and the Hall mobility showed well defined maxima for films grown at PLD gas pressures of ca. 1 mbar N_2, N_2O, and O_2. However, despite the comparable high CL intensities of the ZnO films grown in the three different background gases, their surface roughness varied considerably [2]. Films with rough surface showed a broadening and splitting of the room-temperature CL peak into maxima at 3.19 and 3.26 eV, which could be due to either grain morphology or spatial variation of the electronic defect structure. Laterally homogenous PLD ZnO thin films with diameter of 32 mm are currently tested as innovative scintillation detectors by El-Mul Technologies Ltd., Yavne, Israel.

This work was supported by the BMBF within FKZ 03WKI09 and 03N8708.

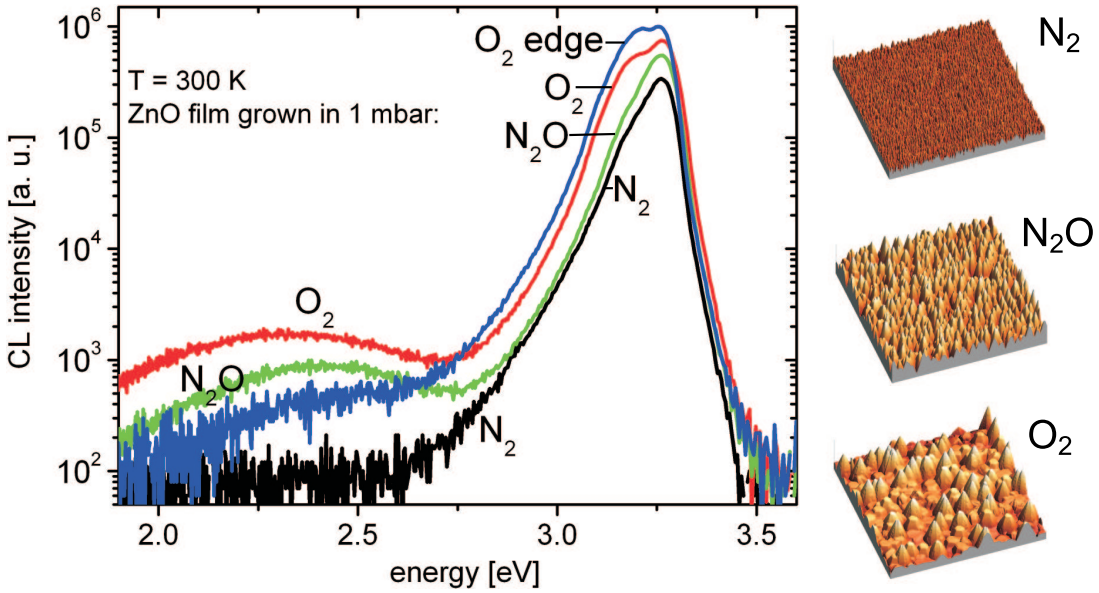

Figure 7.11: CL spectra (300 K) and AFM scan images ($10 \times 10\,\mu m^2$) of ZnO films on a-plane sapphire grown by PLD in 1 mbar N_2, N_2O, or O_2 background gas. Average roughness is 10 nm (N_2), 66 nm (N_2O), and 125 nm (O_2).

[1] H. Hochmuth, M. Lorenz, M. Grundmann, German patent application No. P 10 2004 048 378.7 of 01.10.2004.

[2] M. Lorenz, H. Hochmuth, J. Lenzner, T. Nobis, G. Zimmermann, M. Diaconu, H. Schmidt, H. von Wenckstern, M. Grundmann, Thin Solid Films 2005, *in press*.

7.10 Crystalline Nanostructure of PLD ZnO and MgZnO Thin Films on Sapphire

M. Lorenz, H. Hochmuth, H. von Wenckstern, H. Schmid*, W. Mader*, M. Grundmann
*Institut für Anorganische Chemie, Universität Bonn

Epitaxial ZnO and $Mg_xZn_{1-x}O$ ($0 \leq x \leq 1$) thin films were grown by pulsed laser deposition (PLD) on sapphire with and without MgO buffer layer, respectively. Transmission electron microscopy (TEM) was used to visualize the crystalline nanostructure of the films. Fig. 7.12 shows TEM cross sections of epitaxial ZnO thin films grown at about 600°C at an oxygen partial pressure of (a) 1.6×10^{-2} and (b) 8×10^{-4} mbar. Prior to the ZnO film deposition, a laterally homogeneous, approx. 10 nm thick single crystalline MgO buffer layer was grown as a diffusion barrier. Fig. 7.12a shows nicely the decreasing density of dislocation lines in the ZnO film from the interface to the film surface due to relaxation of the initial misfit. The orientational relationship in growth direction is $[0001]_{ZnO} \parallel [111]_{MgO} \parallel [0001]_{sapphire}$ and in plane $[01\bar{1}0]_{ZnO} \parallel [112]_{MgO} \parallel [\bar{2}110]_{sapphire}$. Figure 7.12c,d show TEM cross sections of a $Mg_{0.37}Zn_{0.63}O$ thin film grown at approx. 700°C on c-sapphire. Figure 7.12c shows strong strain contrast in the sapphire substrate, which is due to the misfit to the MgZnO film. Moreover, the MgZnO film shows in the initial 50 nm MgZnO and probably also MgO crystallites in different orientation, Fig. 7.12d. Above this polycrystalline nucleation layer, epitaxially grown columnar MgZnO crystallites dominate the film structure.

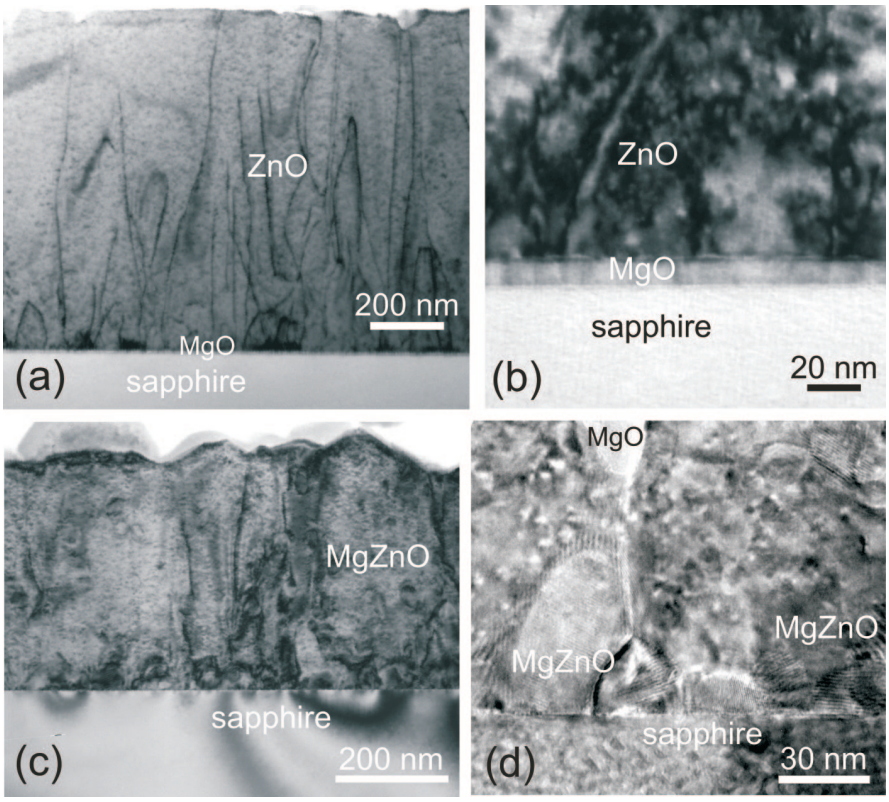

Figure 7.12: (a,b) TEM bright field cross sections of ZnO films on MgO buffer layer on c-sapphire showing dislocation lines, (c,d) TEM bright field cross sections of a $Mg_{0.37}Zn_{0.63}O$ thin film showing nanosized crystallites and strain contrast near the interface.

7.11 SPM Characterization of ZnO Thin Films and Nanostructures

G. Zimmermann, J. Bauer*, H. Schmidt, M. Grundmann

*Institut für Anorganische Chemie, Universität Leipzig

Different scanning probe microscopy (SPM) techniques are used to measure properties of PLD-grown ZnO thin films and nanostructures with nm-resolution and *without* unintentional alteration/damaging of the samples [1].

Conventional scanning force microscopy (SFM) proves useful to relate surface quality with growth conditions and thus to optimize the growth process for special-purpose thin films, e.g. quantum well heterostructures and scintillators (see Sects. 7.7 and 7.9). Using this technique we also obtain exact geometrical information on ZnO nanostructures. An example is given in Fig. 7.13.

Electronic properties are measured using the current-sensing scanning force microscopy (csSFM/cAFM). In this setup a voltage is applied between the sample's backside and the tip (Fig. 7.14). This allows to obtain I–V curves of nanostructures, e.g. single nanorods [2], as well as to determine changes of conductivity over areas up to $90 \times 90\,\mu$m.

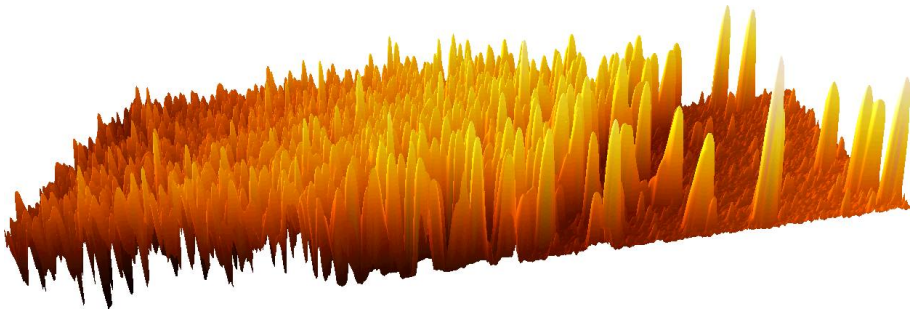

Figure 7.13: SFM micrograph of ZnO nanorods. The scan area is $20 \times 10\,\mu$m and the average height is about 1µm

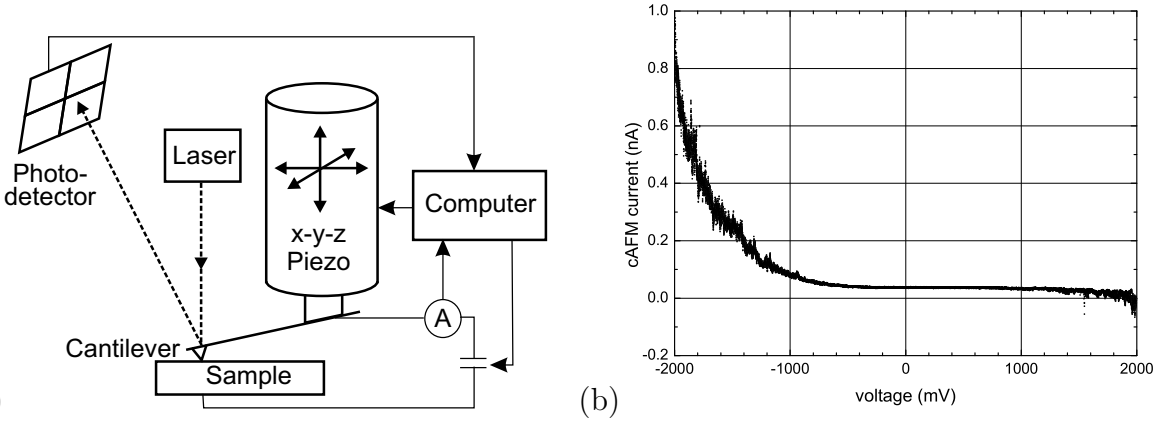

Figure 7.14: (a) Setup of a current sensing SFM. Althoug the data sets are taken simultaneously, structural and electrical characterization are independent. (b) $I - V$ characteristics of an intrinsically carbon doped p-type GaAs nanowire on a silicon doped n-type GaAs substrate.

[1] G. Zimmermann, Diplomarbeit, Universität Leipzig 2004.
[2] W.I. Park *et al.*: Appl. Phys. Lett. **82** (24), 4358 (2003), DOI: 10.1063/1.1584089

7.12 EPR Study on $Zn_{1-x}Mn_xO$ Thin Films

M. Diaconu, H. Schmidt, A. Pöppl

The valence state and the site symmetry of Mn ions in $Zn_{1-x}Mn_xO$ thin films were determined by X-band electron paramagnetic resonance (EPR) measurements. The $Zn_{1-x}Mn_xO$ thin films, with $0.001 < x < 0.1$, were grown by pulsed laser deposition on *c*-plane sapphire substrates and are of interest for spintronic applications [1]. We found that the Mn ions are in trigonal site symmetry with 2+ valence state, isovalently replacing the Zn^{2+} ions in the wurtzite lattice. Kim et al. [3] observed that the crystallinity of $Zn_{1-x}Mn_xO$ thin films on *c*-sapphire is best for $x = 0.05$.

We define a parameter, $\varepsilon_V = \frac{a^2 \cdot c - a_0^2 \cdot c_0}{a_0^2 \cdot c_0}$, which accounts for the distortion of the hexagonal ZnO lattice by Mn substitution, $a_0 = 0.3249\,\text{nm}$ and $c_0 = 0.5206\,\text{nm}$ are the values of the lattice parameters for undoped ZnO single crystals (JCPDS card No. 36-1451) and a and c are the lattice parameters of the specific ZnMnO sample.

In Fig. 7.15 we compare the Mn^{2+} fine structure parameter D obtained from EPR spectra for thin films and single crystals as a function of the distortion parameter. The fine-structure parameter D is equal for single crystals and PLD-grown thin films with a Mn content of about $x = 0.05$. So we assume that around $x = 0.05$ the thin films ideally possess the crystalline quality of unstrained $Zn_{1-x}Mn_xO$ single crystals (the empty circle value is taken from [2]).

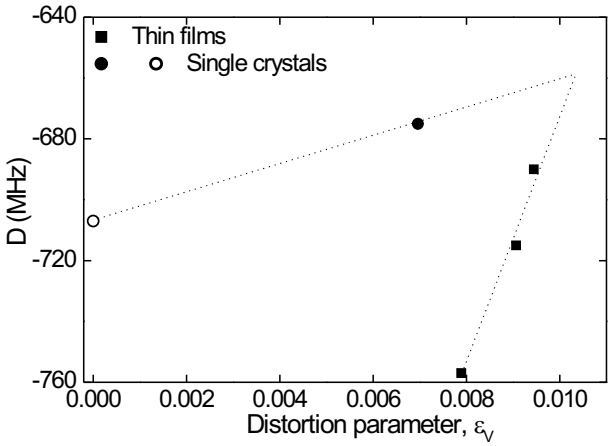

Figure 7.15: EPR fine-strucure parameter D for thin films and single crystals as a function of the distortion parameter ε_V defined in the text.

[1] M. Diaconu, H. Schmidt, H. Hochmuth, M. Lorenz, G. Benndorf, J. Lenzner, D. Spemann, A. Setzer, K.W. Nielsen, P. Esquinazi, and M. Grundmann, Thin Solid Films, *in press.*
[2] A. Hausmann and H. Huppertz, J. Phys. Chem. Sol. **29**, 1369 (1968).
[3] S.S. Kim, J.H. Moon, B.T. Lee, O.S. Song, and J.H. Je, J. App. Phys. **95**, 454 (2004).

7.13 Coercivity Mechanism in Ferromagnetic $Zn_{1-x}Mn_xO$ Films

H. Schmidt, M. Diaconu, H. Hochmuth, M. Lorenz, A. Setzer, P. Esquinazi, K.-W. Nielsen*, R. Gross*, M. Grundmann

*Walter-Schottky-Institut, München

Mn-alloyed ZnO films with a thickness of ca. 1 µm have been grown by pulsed laser deposition on *c*-plane sapphire substrates. The microstructure of the epitaxially grown films is columnar with a growth condition dependent column diameter ranging from 30 to 250 nm.

We observe a correlation between the coercive field and the column diameter in semi-insulating, weak ferromagnetic Mn-alloyed ZnO thin films. As shown in Fig. 7.16, at room temperature the maximal coercive field amounts to 234 Oe for a critical column diameter of 140 nm. The occurrence of a critical column diameter does not depend on measurement temperature or Mn content and offers a new opportunity for tailoring soft magnetic materials based on Mn-alloyed ZnO for ferromagnetic piezoelectrics.

We suggest to explain the observed coercivity mechanism in the Mn-alloyed thin films by Brown's micromagnetic model [2] because there is a competition between the anisotropy and exchange interaction energy in ferromagnetic, polycrystalline materials.

This work is partially (H.S., M.D., H.H.) supported by BMBF (FKZ03N8708).

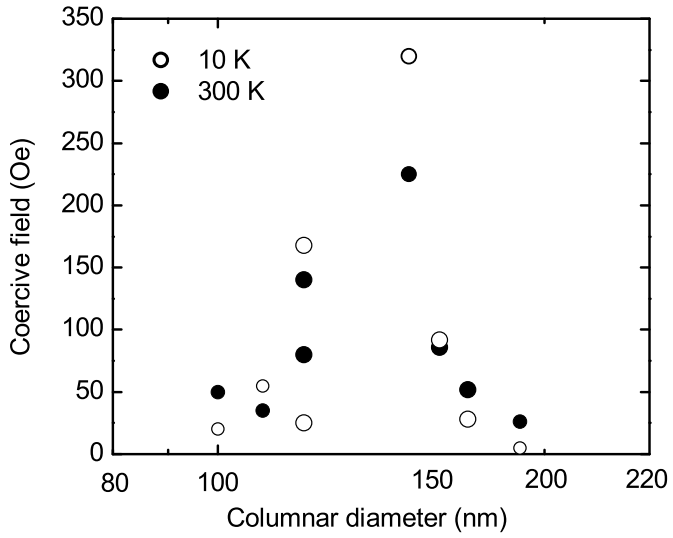

Figure 7.16: Coercive field as a function of column diameter at 10 K (open circles) and at 300 K (filled circles) for Mn contents between 3 at% (smaller circles) and 10 at% (larger circles). The diameter is given on a logarithmic scale.

[1] M. Diaconu *et al.*, submitted to Phys. Rev. B.
[2] G. Bertotti, *Hysteresis in Magnetism* (Academic Press, San Diego, 1998).

7.14 Measured and Simulated CV Profiles of Quantum Dots

M. Gonschorek, H. Schmidt, M. Grundmann

We simulated the temperature dependent capacitance-voltage (CV) profiles which have been measured on n-conducting GaAs Schottky diodes with an embedded InGaAs quantum dot ensemble containing about 10^7 quantum dots. That work is of importance for future applications of voltage-induced charge storage and decharging of quantum dots in quantum computers.

The strain and doping dependent energy band structure of the GaAs/InGaAs/GaAs heterostructure (Fig. 7.17a) has been determined by a selfconsistent solution of the Poisson and Schrödinger equation. At 75 K, the electron ground state E1 and two excited states E2 and E3 lie below the quasi-Fermi level. From the simulation of the measured 1-kHz CV-profile (Fig. 7.17b), it becomes clear that at 75 K about 3 electrons are bound in every quantum dot of the quantum dot ensemble, whereas at room temperature only the spin-degenerated ground state E1 lies below the Fermi level. Therefore, at room temperature only 2 electrons are bound in every quantum dot.

The experiments have been performed by M. Geller and A. Marent (TU Berlin) and are supported by NoE SANDiE. We are grateful to the Ioffe Institute, St. Petersburg, for providing the samples.

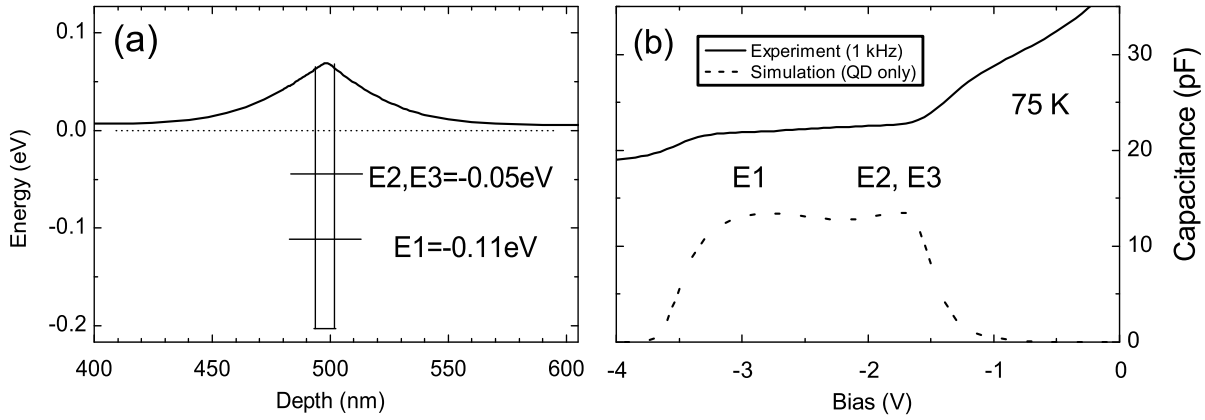

Figure 7.17: (a) Calculated energy band diagram of an unbiased n-GaAs Schottky diode ($n = 3.3 \times 10^{16}\,\mathrm{cm}^{-3}$) with an InGaAs quantum dot ensemble positioned at a depth of 500 nm. (b) 1 kHz-CV profile measured at 75 K on the sample structure represented in (a). The contribution from the bound quantum dot states to the measured CV data is clearly visible in the voltage range from –1.0 to –3.5 V.

7.15 Concentric a-Si/SiO$_x$ Bragg-Reflectors

R. Schmidt-Grund, T. Gühne, B. Rheinländer, V. Gottschalch, T. Nobis, A. Rahm, M. Grundmann

Lateral confinement for coaxial micro-resonator light emitters improves the ratio of the number of the axial resonant modes to the number of the spontaneous emitting lateral

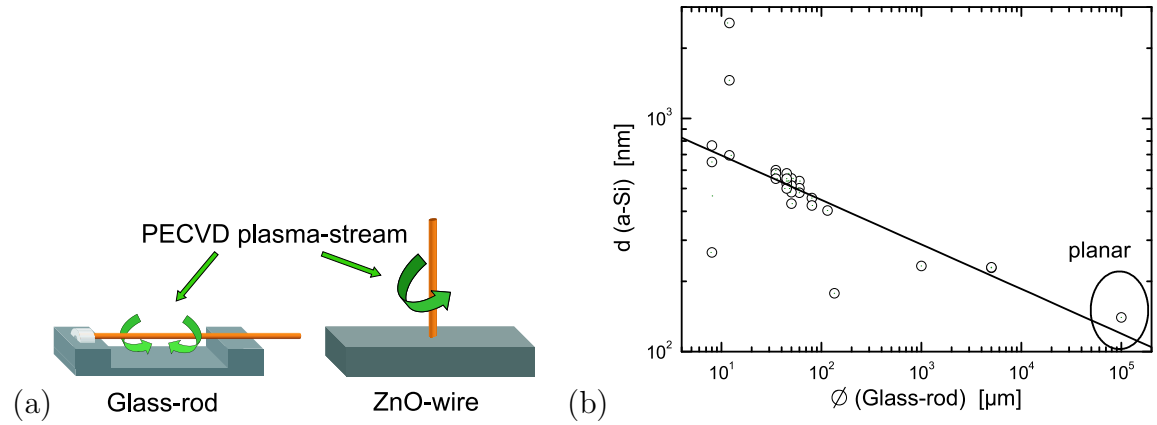

Figure 7.18: (a) Deposition-properties for the glass-rods and ZnO-wires. (b) Dependence of the a-Si layer thickness on the diameter of the glass-rod.

modes. High reflectivity a-Si/SiO_x Bragg-reflectors are attractive for the improvement of optical confinement in micro-structured resonators [1, 2]. Concentric a-Si and SiO_x single-layers else as a-Si/SiO_x Bragg-reflectors with a small number N of layer pairs, typically $N = 4.5$, were deposited using plasma-enhanced chemical vapor deposition (PECVD) on glass-rods (diameters between 5 and 5000 μm) and free-standing ZnO-wires (diameters between 0.5 and 5 µm) (Fig. 7.18a). The reflectivity of the a-Si/SiO_x Bragg-reflectors was measured using a confocal micro-reflectometer (μR) with a spatial resolution set to 4 μm and spatially resolved spectroscopic ellipsometry (μE) technique [2]. For the glass-rods, the deposition-rate was found to depend on the diameter of the rod (Fig. 7.18b). For the ZnO-wires, the deposition-rate was found to be 1.3 times larger in comparison to those on planar structures. On both structures, the glass-rods and the ZnO-wires, deposition of Bragg-reflectors was possible (Fig. 7.19a and b, respectively). While for the Bragg-reflector deposited on the glass-rod the zero order bragg-band is visible in the μR spectral range, the thicknesses of the layers of the Bragg-reflector deposited on the ZnO wire are larger and therefore in the μR spectral range the first order bragg-band is visible.

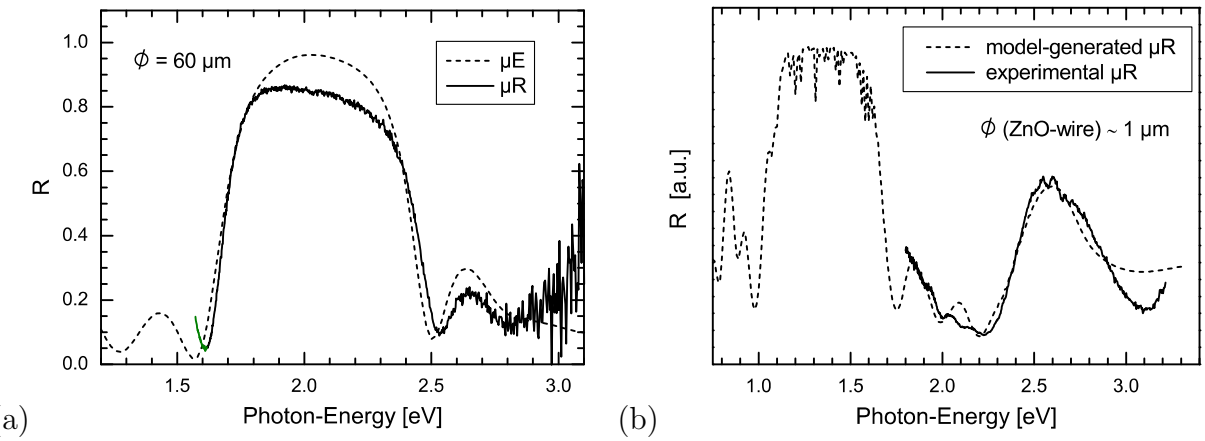

Figure 7.19: (a) Reflectivity of a a-Si/SiO_x Bragg-reflector deposited on a glass-rod with diameter of 60 µm (green: experimental μR, red: generated from the μE model analysis). (b) Reflectivity of a a-Si/SiO_x Bragg-reflector deposited on a ZnO wire with diameter of approximately 1 µm (green: experimental μR, red: generated from a layer model).

This work was supported by the Deutsche Forschungsgemeinschaft within FOR 522 (RH 28/4-1).

[1] V. Gottschalch, R. Schmidt, B. Rheinländer, D. Pudis, S. Hardt, J. Kvietkova, G. Wagner, and R. Franzheld, Thin Solid Films **416**, 224 (2002).
[2] R. Schmidt-Grund, T. Nobis, V. Gottschalch, B. Rheinländer, H. Herrnberger, and M. Grundmann, Thin Solid Films *in press*.

7.16 VUV Ellipsometry of Rocksalt MgZnO

R. Schmidt-Grund, A. Carstens, M. Schubert, B. Rheinländer, H. Hochmuth, M. Lorenz, C.M. Herzinger*, M. Grundmann

*J.A. Woolam Co., Lincoln, USA

For ternary rocksalt $Mg_xZn_{1-x}O$ films, optical properties were determined using spectroscopic ellipsometry. The $Mg_xZn_{1-x}O$ ($0.68 \leq x \leq 1$) layers with a thickness of typically 500 nm have been deposited by pulsed laser deposition on sapphire substrates. For the $Mg_xZn_{1-x}O$ layers, the dielectric functions were determined using a critical point (CP) model dielectric function (MDF) and a cauchy (CA) MDF approach [1, 2]. In the dielectric function, structures due to the free exciton transition (binding energy E_{xb}), the fundamental bandgap (E_0 and $E_0+\Delta_{so}$, Δ_{so} is the spin-orbit-splitting energy), and the E_1 and E_2 transitions were found. Increasing the Mg-content, E_0 shifts to higher energies by showing a small bowing, whereas E_1 increases linear and E_2 reveals no considerable energyshift (Fig. 7.20a). E_{xb} increases linearly and Δ_{so} decreases linearly from approximately $\Delta_{so} = 120$ meV for $x = 0.678$ to $\Delta_{so} = 50$ meV for $x = 1$ (Fig. 7.20b). The below-bandgap refractive index was found to decrease with a small bowing for increasing x (Fig. 7.21). Between the wurtzite- and the rocksalt-phase of the alloy system E_0 possess a discontinuity of approximately 1 eV. We attribute this effect to the change of the Zn and Mg coordination in the crystals from fourfold in the wurtzite-phase to sixfold in the rocksalt-phase, which leads to different types of band-structures and therefore of different values of the bandgap. Similar to the behavior of E_0, the refractive index reveals a discontinuity between the wurtzite- and the rocksalt-phase of the alloy system.

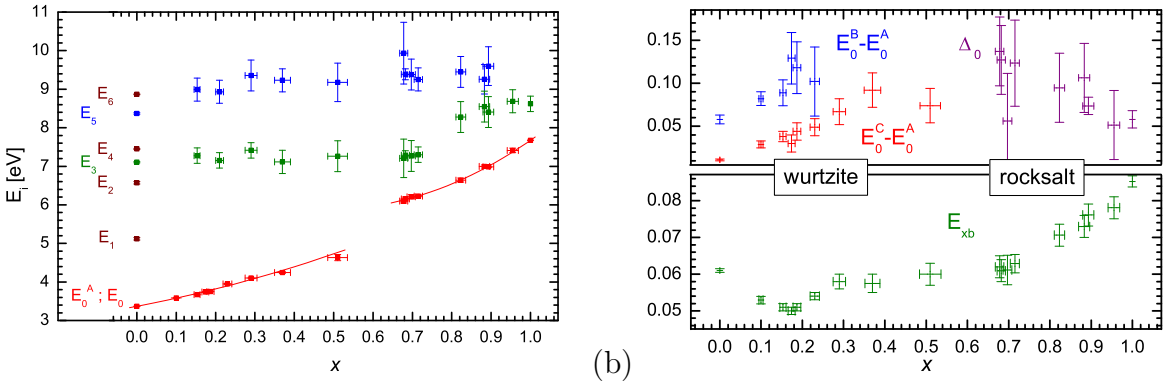

(a) (b)

Figure 7.20: (a) $Mg_xZn_{1-x}O$ band-to-band transition energies vs. Mg-content x obtained from ellipsometry data analysis. (b) Energies E_{xb} and Δ_{so} vs. Mg-content x. Data for the wurtzite part were taken from [1, 2].

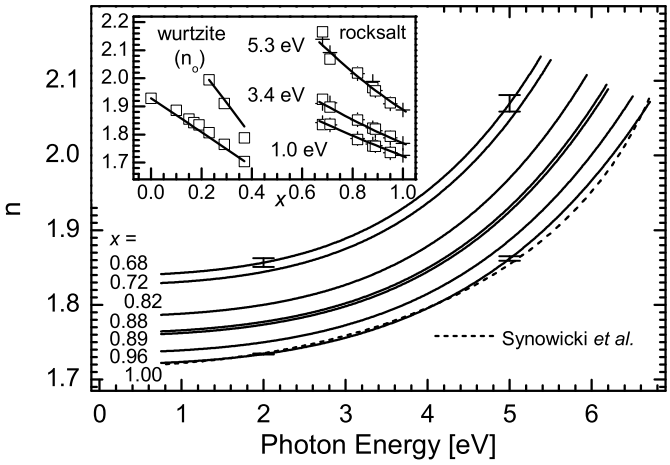

Figure 7.21: $Mg_xZn_{1-x}O$ index of refraction n. For comparison, data reported by Synowicki *et al.* for $x = 1.0$ are included [3]. The inset depicts n for individual photon energies calculated from the best-fit CP-MDF (open squares), the CA-MDF fit for each sample individually (crosses), and for all samples simultaneously (solid lines). Data for the wurtzite part were taken from [1].

This work was supported by the Bundesministerium für Bildung und Forschung within the "Wachstumskern Innocis" (FK 03WKI09), and the Deutsche Forschungsgemeinschaft GR1011/10-1 within SPP 1136, and SCHUH1338/4-1 within FOR404.

[1] R. Schmidt *et al.*, Appl. Phys. Lett. **82**, 2260 (2003).
[2] R. Schmidt-Grund, M. Schubert, B. RheinlÄander, D. Fritsch, H. Schmidt, E.M. Kaidashev, M. Lorenz, C.M. Herzinger, and M. Grundmann, Thin Solid Films **455-456**, 500 (2004).
[3] R.A. Synowicki and T.E. Tiwald, Thin Solid Films **455-456**, 248 (2004).

7.17 Temperature-Dependent Bandgap Energies and Optical Constants of ZnO

R. Schmidt-Grund, N. Ashkenov, M. Schubert, W. Czakai, G. Benndorf, H. Hochmuth, M. Lorenz, M. Grundmann.

We report the temperature dependencies of the fundamental band-to-band transition energies and the below-bandgap refractive index in ZnO. Spectroscopic ellipsometry data, taken from a (0001)-oriented ZnO thin film at temperatures between 300 K and 829 K, and for photon energies from 1.25 eV to 3.335 eV, are analyzed by using model dielectric function approaches, augmented by excitonic continuum and free exciton contributions. A strong and linear red-shift of the three wurtzite-type Γ-point transition energies is observed (E_A, E_B, E_C in Fig. 7.22a). The increase of the valence band splitting energies upon temperature is indicative for an increase of the quasi-cubic model crystalfield splitting energy Δ_{cf} caused by thermal deformation of the crystal structure (Fig. 7.22b). Results of photoluminescence studies between 4.4 K and 300 K are used to supplement the high-temperature bandgap data (Fig. 7.22a). For ZnO, the phonon dispersion must be considered appropriately in order to model the temperature dependence of the fundamental band-to-band transition energy. By applying the two-oscillator model, we obtain

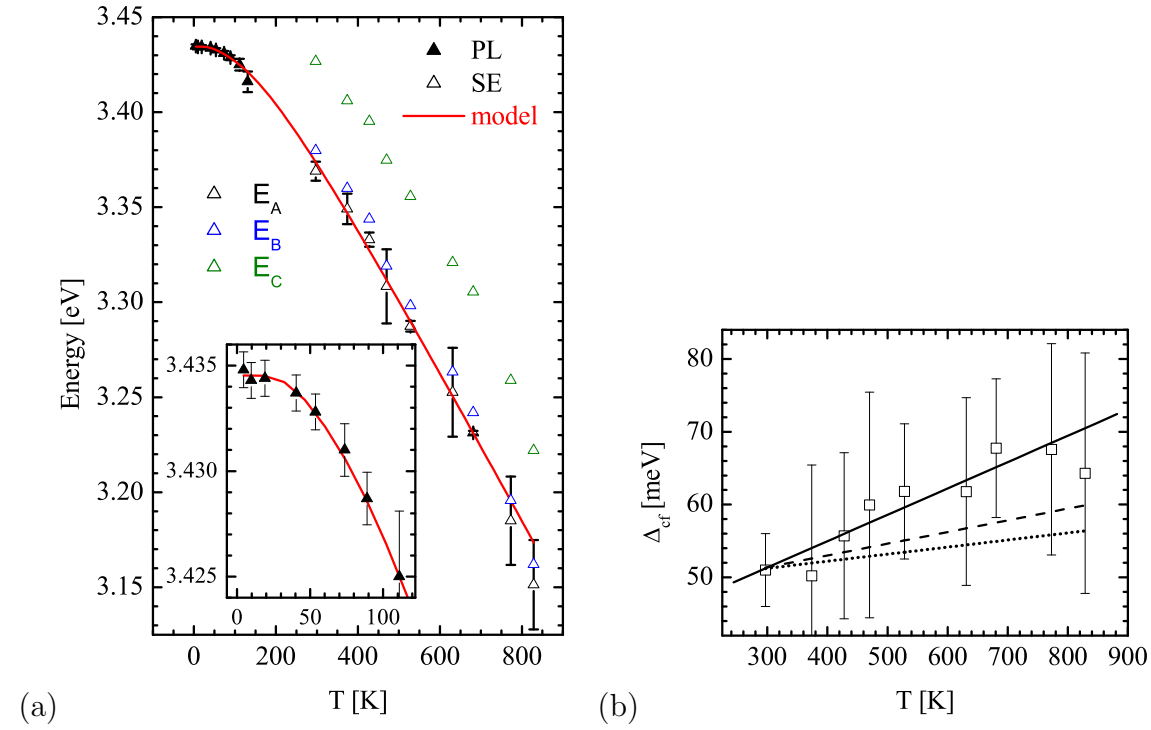

Figure 7.22: (a) Bandgap transition energies E_A, E_B, and E_C (best-fit model dielectric function parameters) obtained from ellipsometry data analysis (experimental - symbols: ellipsometry and photoluminescence; best-fit model calculations - lines, two-oscillator model) versus temperature. The inset enlarges the low- temperature region. (b) Crystal-field splitting energy Δ_{cf} obtained from the bandgap transition energies E_A, E_B, and E_C (symbols, solid line: linear fit). The dashed and dotted line represents Δ_{cf} calculated using deformation potentials given in the literature.

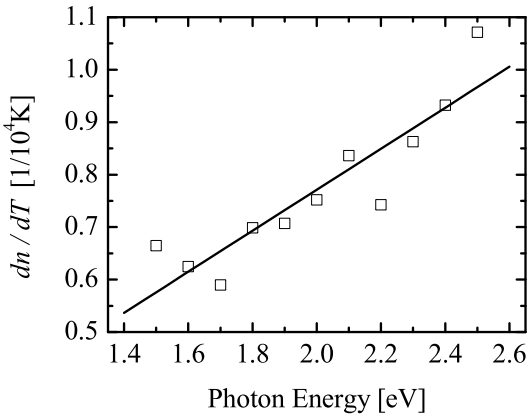

Figure 7.23: Temperature dependence of the ZnO refractive index versus photon energy for polarization perpendicular to the wurtzite-structure c-axis.

strong contributions due to optical phonons at elevated temperatures, whereas acoustic phonons dominate the electron-phonon coupling at low temperatures. Figure 7.23 shows the temperature dependence dn/dT of the ZnO below-bandgap refractive index n for polarization perpendicular to the c-axis as a function of photon energy. The values for the room-temperature refractive index are given e.g. in [1].

This work was supported by the Bundesministerium für Bildung und Forschung within the Wachstumskern INNOCIS (FK 03WKI09). The authors acknowledge valuable discussions with R. Pässler.

[1] R. Schmidt et al., Appl. Phys. Lett. **82**, 2260 (2003).

7.18 *I-V-T* Measurements on ZnO Schottky Diodes

H. von Wenckstern, G. Biehne, H. Hochmuth, M. Lorenz, M. Grundmann

Pd was evaporated on epitaxial ZnO thin films grown by pulsed laser deposition to obtain Schottky contacts. Such Schottky diodes were investigated by temperature dependent current voltage (I-V) measurements. The current density of a typical diode at room temperature at $-3\,\mathrm{V}$ is $-2 \times 10^{-5}\,\mathrm{A/cm^2}$ at $-5\,\mathrm{V}$ it is $-4 \times 10^{-5}\,\mathrm{A/cm^2}$. Considering thermionic emission as the dominating current transport process across the Schottky barrier, we determined the effective barrier height $\Phi_{\mathrm{B,eff}}$ and the ideality factor η to be 0.76 eV and 1.46, respectively. These parameters define currently the state of the art for ZnO Schottky diodes realized on epitaxial thin films. I-V measurements were performed for temperatures ranging from 200 to 300 K. The Richardson plot, i.e. $\ln(j_d/T^2)$ vs. $1/T$, from which $\Phi_{\mathrm{B,eff}}$ at 0 K and the Richardson constant can be determined is, however, curved. Therefore, we analyzed the temperature dependence of $\Phi_{\mathrm{B,eff}}$ by taking lateral fluctuations of $\Phi_{\mathrm{B,eff}}$ into account. We follow Werner *et al.* [1] and modelled these fluctuations by a Gaussian distribution with standard deviation σ around a mean barrier height $\Phi_{\mathrm{B,m}}$. The relation between the mean barrier height and the effective barrier height is $\Phi_{\mathrm{B,eff}} = \Phi_{\mathrm{B,m}}(U = 0\,V) - \sigma^2/(2kT)$. By fitting the experimental data depicted in Fig. 7.24a, we were able to determine the mean barrier height to be 1.10 eV and the standard deviation $\sigma = 0.13\,\mathrm{eV}$ for the first time for Pd Schottky contacts on ZnO [2]. Capacitance voltage measurements on a similar diode gave a value of $\Phi_{\mathrm{B,m}} = 1.08\,\mathrm{eV}$ and are in good agreement with the value determined obtained from the temperature

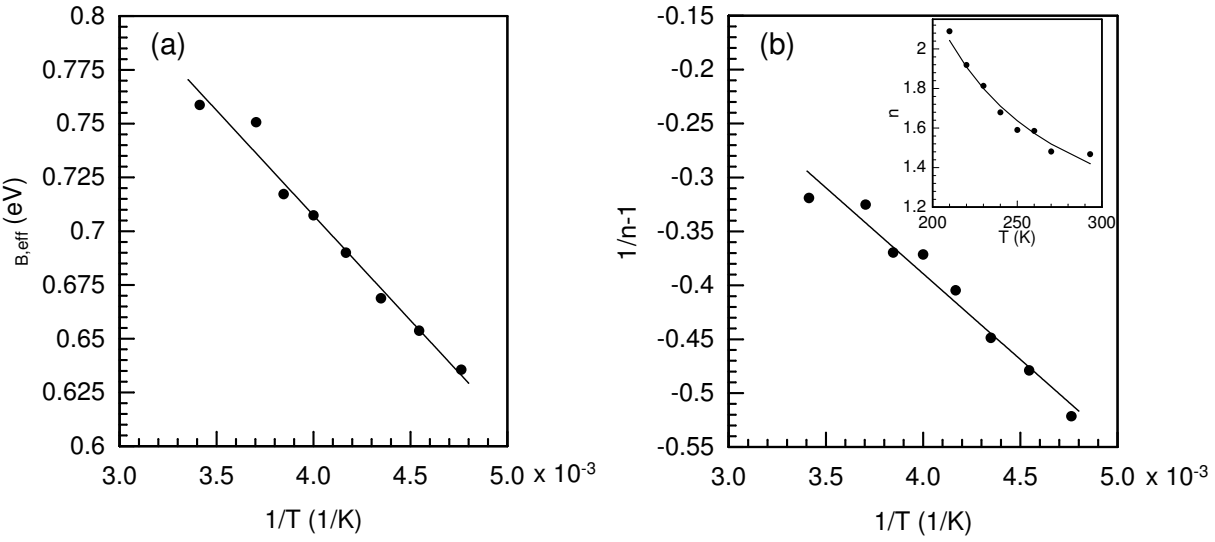

Figure 7.24: (a) Effective barrier height versus reciprocal temperature and corresponding fit (see text) and (b) η versus reciprocal temperature and corresponding fit.

dependence of the I-V characteristics. We note that the model of [1] also allows to model the temperature dependence of the ideality factor $\eta^{-1} = 1 - \rho_2 + e\rho_3/(2kT)$. The coefficients ρ_2 and ρ_3 are a measure of the voltage dependence of $\Phi_{\mathrm{B,m}}$ and σ, respectively, and are determined from the fit shown in Fig. 7.24b. The values obtained are $\rho_2 = -0.25$ and $\rho_3 = -0.028\,\mathrm{V}$.

This work is supported by the DFG within SPP 1136 (Gr 1011/10-1).

[1] J.H. Werner and H.H. Güttler, J. Appl. Phys. **69**, 1522 (1991).
[2] H. v. Wenckstern, G. Biehne, H. Hochmuth, M. Lorenz, and M. Grundmann, Appl. Phys. Lett. (2005), *in press*.

7.19 Deep Donor Levels in ZnO

H. von Wenckstern, S. Weinhold, G. Biehne, R. Pickenhain, M. Grundmann

The concentration N_d, the thermal activation energy $E_\mathrm{c} - E_\mathrm{d}$, and the capture cross-section σ of deep donor-like defect levels were determined in nominally undoped n-type ZnO. Schottky diodes were realized on ZnO single crystals (Type A) and on epitaxial ZnO thin films grown by pulsed laser deposition (Type B). The diodes were characterized by deep level transient spectroscopy (DLTS) measurements and thermal admittance spectroscopy (TAS) for temperatures between 4 K and 325 K. For the diode of Type A TAS and DLTS measurements revealed the existence of a level labelled E1 lying about 110 meV below the conduction band minimum. Furthermore, the existence of the levels labelled E3 and E4 having activation energies of 300 and 540 meV [1] was confirmed by DLTS measurements. The levels E1 and E3 are present in the diode of Type B (PLD film). Again, the level E1 could be detected by DLTS and TAS. The parameters obtained are summarized in Tab. 7.1 for both type of samples [2]. The emission rates determined from DLTS and TAS are shown in an Arrhenius plot in Fig. 7.25. The origin and microscopic nature of these defects are so far not known.

This work is supported by the DFG within SPP 1136.

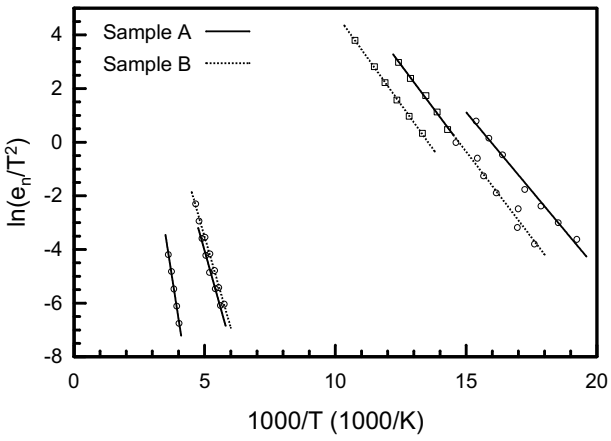

Figure 7.25: Arrhenius plot of defects determined with TAS (*squares*) or DLTS (*circles*) of Samples A and B and corresponding fits (*lines*).

Table 7.1: Parameters of deep donor levels in ZnO.

Sample	Exp.	Defect	N_d (10^{15} cm^{-3})	$E_c - E_d$ (meV)	σ (10^{-14} cm^2)
	TAS	E1	1.5 ± 0.2	110 ± 20	21 ± 5
A	DLTS	E1	1.4 ± 0.2	100 ± 20	12 ± 5
	DLTS	E3	0.22 ± 0.04	300 ± 30	0.062 ± 0.007
	DLTS	E4	0.18 ± 0.04	540 ± 40	10 ± 7
	TAS	E1	1.3 ± 0.5	120 ± 20	15 ± 5
B	DLTS	E1	1.4 ± 0.2	110 ± 20	9.3 ± 2
	DLTS	E3	6.2 ± 0.7	290 ± 30	0.062 ± 0.007

[1] F.D. Auret, S.A. Goodman, M.J. Legodi, W.E. Meyer, and D.C. Look, Appl. Phys. Lett. **80**, 1340 (2002).
[2] H. v. Wenckstern, S. Weinhold, G. Biehne, R. Pickenhain, H. Hochmuth, and M. Grundmann, Adv. Sol. Stat. Phys. (2005), in press.

7.20 Growth of Semi-Insulating ZnO

H. von Wenckstern, M. Lorenz, M. Grundmann, H. Schmid*, W. Mader*
*Institut für Anorganische Chemie, Universität Bonn

ZnO is a naturally n-type semiconductor. The realization of high quality p-type ZnO is necessary for commercial application of ZnO as, e.g., diodes. The growth of p-type ZnO remains a challenge due to strong self compensation effects and the low solubility of appropriate acceptors. As a first step we have demonstrated the growth of semi-insulating ZnO by pulsed laser deposition (PLD) on sapphire using two different approaches. The dominant donor in PLD thin films grown on sapphire is Al which diffuses during growth into the ZnO layer. In the first approach we reduced the incorporation of Al by using low growth temperatures and compensated the remaining donors by acceptors. It is based on the co-doping method [1] and relies on the higher incorporation of group V acceptors in the presence of a group III donor. We have used ZnO targets containing 0.5 ppm Ga_2O_3 and introduced N_2O via a radio frequency plasma source to supply the group III and group V elements. For optimal conditions, semi-insulating thin films were obtained. In the second approach, we reduced the indiffusion of Al by buffer layer engineering. An about 10 nm thick MgO buffer layer prevents the incorporation of Al in the ZnO thin film strongly. This is confirmed by secondary neutral mass spectroscopy, an analysis of a ZnO layer grown directly on sapphire and a ZnO layer grown on a MgO buffer layer is depicted in Fig. 7.26a. The Al signal of a MgO-buffered ZnO layer falls at the MgO/ZnO interface below the detection limit of the setup. The free electron concentration at room temperature of such films is as low as 10^{14} cm^{-3}. Figure 7.26b shows a bright field high resolution transmission electron microscopy (HRTEM) image. The interface is smooth and abrupt. With that we have demonstrated two possibilities of obtaining semi-insulating ZnO. The latter is a good starting point for acceptor doping of ZnO.

This work is supported by the DFG within the SPP 1136.

[1] T. Yamamoto and H. Katayama-Yoshida, Jpn. J. Appl. Phys. **38**, L166 (1999).

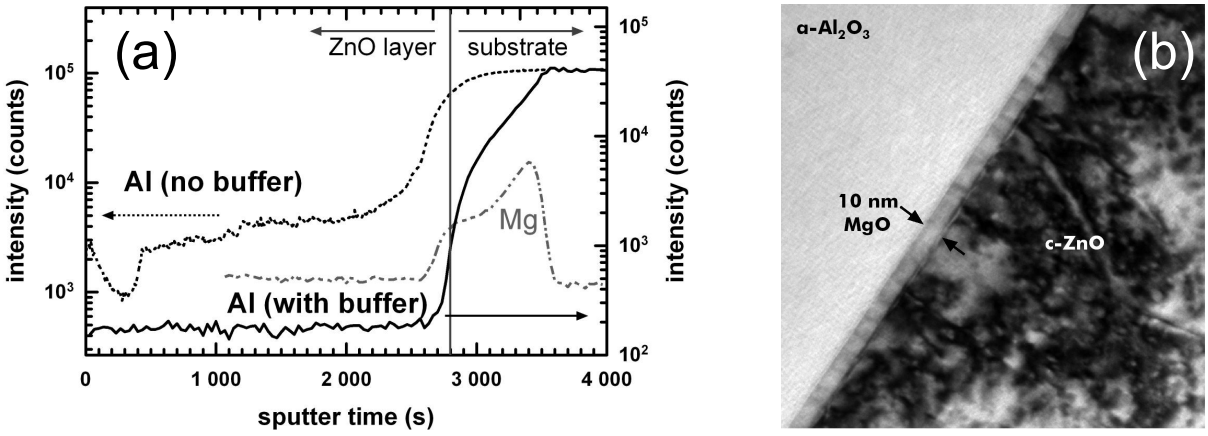

Figure 7.26: (a) Al diffusion profile of ZnO layers grown with (solid line) or without (dashed line) MgO buffer layer and (b) bright field HRTEM image of the Al_2O_3/MgO/ZnO interfaces.

7.21 Specific Peptide Cluster Adhesion on Semiconductor Surfaces

K. Goede, M. Grundmann, M. Bachmann*, W. Janke*

*Institut for Theoretical Physics

One of today's physics major challenges is bridging the gap between inorganic matter, i.e. the prime working field of previous physics, and living matter which until recently was mostly looked upon by biologists and chemists. However, merging these two research fields may promote both a better understanding of the world that surrounds us and an unimagined range of applications from 'smart' protheses or quick organics detection and coated, functionalised surfaces to true nanoscale opto-electronics and data processing in single molecules. However, given the nanometer size of organic building blocks and their necessary number for a single device, the true potential of such hybrid organic-anorganic nanostructures will remain under-utilised until there are appropriate self-assembly techniques. In this regard, using DNA or amino-acid based molecules like peptides or proteins is one of the most promising approaches. In nature, recognition and assembly capabilities driven by amino acids or base pairs govern the replication of all living structures. We have devoted ourselves to the fundamentally new field of applying these self-assembly principles to peptide clusters on surfaces of classic, anorganic semiconductors.

We enjoy a fruitful cooperation with Prof. A. Beck-Sickinger of the Biochemistry Institute of Universität Leipzig where the peptides have been synthesised. By taking AFM micrographs and subsequently analysing them, we have quantitatively shown that on the one hand the adhesion rate (the percentage of surface covered by peptide clusters) of a specially selected 12-mer peptide on nine different semiconductor surfaces ranges from 25 % to 0 % under the same standard conditions (Fig. 7.27). We partly ascribe this specificity to the interplay between polar amino-acid side chains and the surface atoms with their respective electronegativity. The different adhesion rates are qualitatively explainable by considering these values for the substrate elements under investigation. On the other hand, different peptides adhere rather different to equal surfaces. This is visualised in Fig. 7.28 for four different sequences. Both the existence of certain amino acids, in our case notably those with basic side chains, and the arrangement of given amino acids

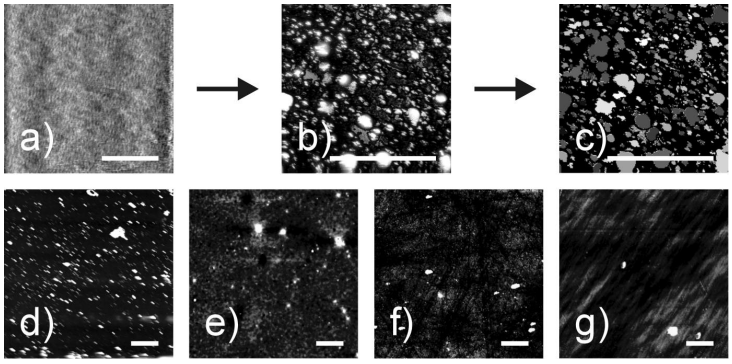

Figure 7.27: Exemplary AFM micrographs of peptide-covered semiconductor surfaces. Peptide sequence was alanine(A)-glutamine(Q)-asparagine(N)-proline(P)-serine(S)-aspartate(D)-N-N-threonine(T)-histidine(H)-T-H. Scale bars 1 µm each. (a) Peptide-free GaAs(100) surface. (b) Peptide-covered GaAs(100) surface. (c) Visualisation of the subsequent grain analysis on the (b) image. (d) - (g) Peptide-covered (100) surfaces of GaP (d), InP (e), Ge (f) and Si (g). From [1].

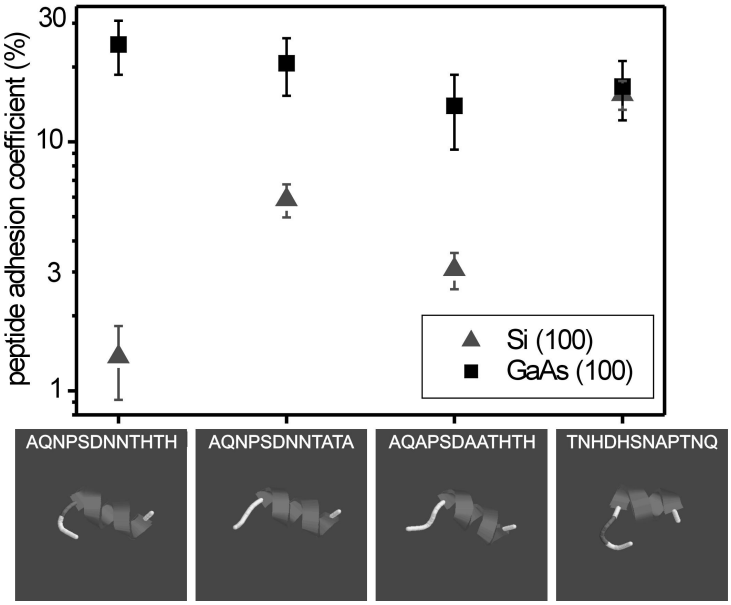

Figure 7.28: Experimentally observed adhesion coefficient and schematic representation of the simulated vacuum conformation for four different peptides on (100) surfaces of GaAs and Si. Far left peptide has the original sequence; centre left peptide has polar amino acid H exchanged for nonpolar A; centre right peptide has polar amino acid N exchanged for nonpolar A; far right peptide has a random permutated sequence of the original peptide. Partly from [1].

within the peptide seem to have crucial influence on the adhesion properties [1]. Our current research focus lies on clarifying how the chemical composition of the peptide and its spatial conformation microscopically determine adhesion properties. In pursuing this goal, we want to employ also theoretical simulations of the peptide convolution and phase transitions. A first result of this cooperation is shown at the bottom of Fig. 7.28 where the simulated vacuum conformation of each experimentally investigated peptide is shown.

This work has been supported by start-up funds of the Universität Leipzig.

[1] K. Goede, P. Busch, and M. Grundmann, Binding specificity of a peptide on semiconductor surfaces, Nano Lett. 2004, 4 (11), 2115-2120.

7.22 MOVPE Growth of $B_xGa_{1-x}P$ Alloys on (001) GaP and GaAs Substrates

V. Gottschalch*, G. Leibiger*, J. Bauer*, G. Benndorf, G. Wagner†, D. Hirsch‡, J. Kovac◇

*Institut für Anorganische Chemie, Universität Leipzig

†Institut für Mineralogie und Kristallographie, Universität Leipzig

‡Leibniz-Institut für Oberflächenmodifizierung Leipzig

◇Slovak Technical University, Department of Microelectronics, Bratislava, Slovakia

Only a few data are available on the boron incorporation in $A^{III}B^{V}$ compounds. BP and the ternary and quaternary alloys (BGa)N, (BGa)As, (BGaIn)As, and (BAlGa)As have been grown with metal-organic vapour-phase epitaxy (MOVPE). We have studied the boron incorporation in GaP to investigate their optoelectronic properties for potential application in optoelectronic devices.

We have grown $B_xGa_{1-x}P$-layers on (001) GaP and GaAs substrates using the precursors triethylboron, trimethylgallium and phosphine in a commercial low pressure MOVPE reactor (AIX 200) in dependence on different growth parameters such as growth temperature and V/III ratio.

The pseudomorphic growth behaviour and the mole fractions of boron ($0 \leq x \leq 0.04$) were determined with high-resolution X-ray diffraction (Fig. 7.29). Additionally, SIMS measurements have been carried out in order to determine the boron concentration.Raman investigations at room temperature show BP-like optical phonons which develop from the localized vibration modes due to B_{Ga} isoelectronic substitution. The direct interband critical-point transitions E_0^{direct} and E_1 of $B_xGa_{1-x}P$-alloys were determined using spectroscopic ellipsometry (Fig. 7.30). In addition to the SE-investigations we performed PL-measurements at $T = 2\,\text{K}$. We assigned the dominant peaks to donator-acceptor-pair transitions.

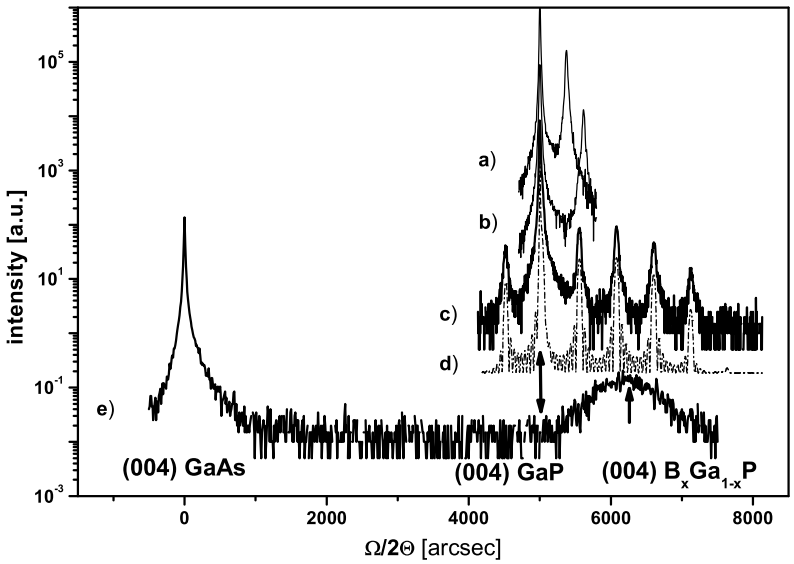

Figure 7.29: Double-crystal X-ray diffraction (DCXRD) pattern of various (BGa)P-structures (004 reflection): a,b) single layers of $B_xGa_{1-x}P$ on (001) GaP substrate with $x = 0.009$ and 0.014, c) MQW-structure of $B_{0.03}Ga_{0.97}P$ and GaP, d) simulation of c, e) 300 nm thick $B_{0.03}Ga_{0.97}P$ layers on (001) GaAs.

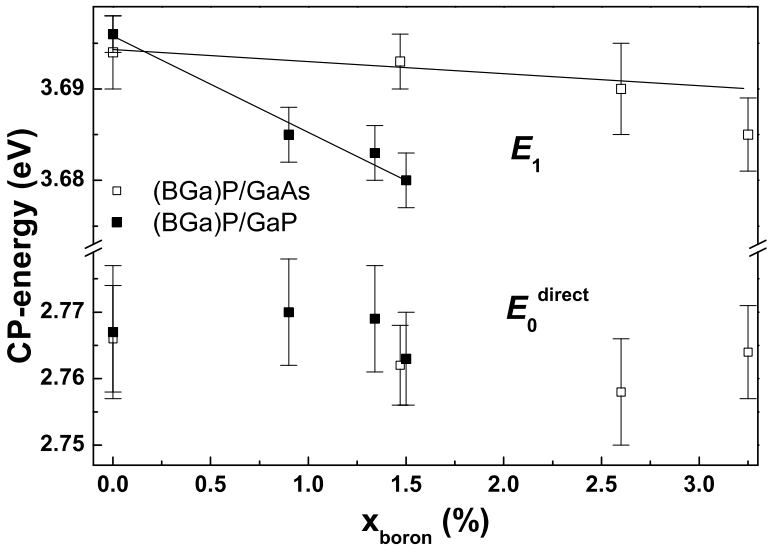

Figure 7.30: Dependence of the E_0^{direct} and E_1 CP-transition energies of $B_xGa_{1-x}P$ on the boron incorporation.

7.23 Properties of (InGa)As/GaAs QW (1.2 µm) Facet-Coated Edge-Emitting Diode Lasers

T. Gühne*, V. Gottschalch*, G. Leibiger*, H. Herrnberger*, J. Kovac†, J. Kovac jr.‡, R. Schmidt-Grund, B. Rheinländer

*Institut für Anorganische Chemie, Universität Leipzig
†Slovak Technical University, Faculty of Microelectronics, Bratislava, Slovakia
‡International Laser Center, Bratislava, Slovakia

Dielectric layers, for instance of silicon and silicon-oxide, can be used for coatings of laser devices. We study the influence of these materials as mirrors and low reflection coatings on the light power output of $\lambda \sim 1.2\,\mu$m laser diodes.

All laser structures have been grown by MOVPE. The active region consists of a double quantum-well structure of (InGa)As with a thickness of 8 nm, that is embedded in GaAs. As gladding layers $Al_{0.35}Ga_{0.65}As$ is used. All runs have been carried out at low pressure. The quantum wells with high indium content of 37 % were grown at 550°C . We worked with oxid stripe laser bars. By PECVD the facets of these bars have been coated. These experiments were carried out with Pasmalab80 at 250°C . A 5 1/2-Bragg mirror of silicon and siliconoxide was deposited. This material combination has a high refractive index difference of $\Delta n \sim 2.04$ at 1550 nm. That means a deposition of mirrors of 99.5 % reflectivity is possible. Due to this coating, nearly the entire light power is emitted through the front facet. Furthermore, the reflectivity of this facet can be lowered by a SiO_x-coating. A significantly higher power output at the front facet can be achieved as shown in Fig. 7.31. Varying the thickness of the antireflection coating, the differential quantum efficiency is changed. Figure 7.32 shows that the maximum is achieved for 200 nm SiO_x. We also investigated the influence on the mode spectra. Lasers with antireflection coating show nearly twice the side mode suppression compared with uncoated lasers. As it can be seen from Fig. 7.33 the narrow peak width of lasers with Bragg mirror is a result of higher light output.

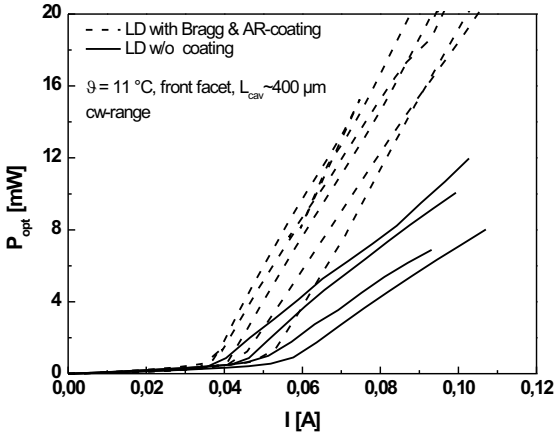

Figure 7.31: CW-power output vs. current for coated and uncoated lasers.

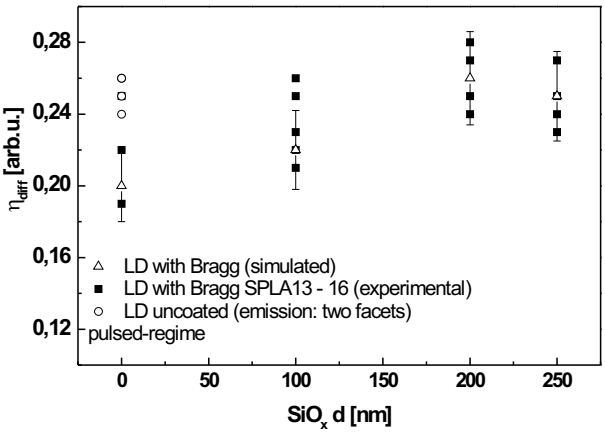

Figure 7.32: Differential quantum efficiency η_{diff} vs. SiO_x thickness on front facet.

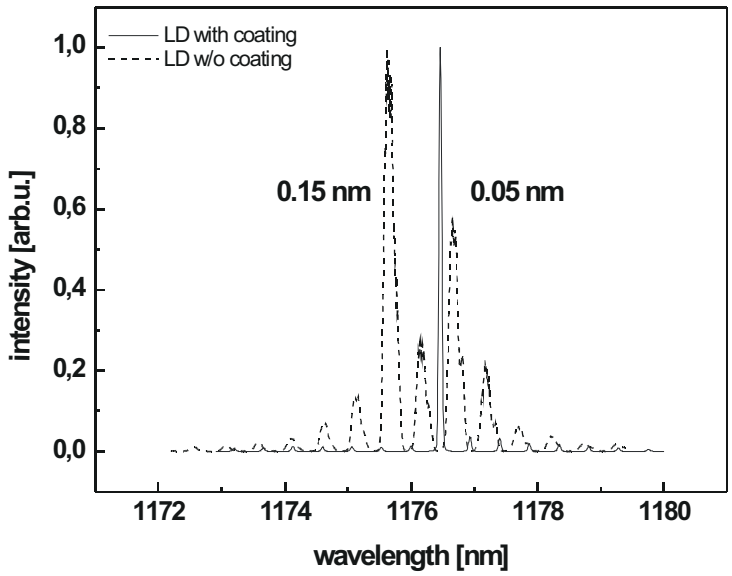

Figure 7.33: Mode spectra of lasers without coating and with Bragg mirror and antireflection coating

7.24 Funding

Investigation of inter-sublevel transitions in self-organized quantum dots; development of novel infrared detectors and lasers
Prof. Dr. Marius Grundmann
DFG Gr 1011/7-3

Transferability of the codoping concept to ternary ZnO:(Cd,Mg)
Prof. Dr. Marius Grundmann, Dr. H. Schmidt
DFG Gr 1011/10-2 im DFG-Schwerpunktprogramm 1136
“Substitutionseffekte in ionischen Festkörpern”

Self-assembled Semiconductor Nanostructures for New Devices in Photonics and Electronics (SANDiE)
Coordinator: Universität Leipzig, Prof. Dr. M. Grundmann
Sixth Framework Programme, European Network of Excellence, Contract NMP4-CT-2004-500101

III-V-Semiconductor Nano-Heterostructures for Advanced Opto-Electronic Devices
Prof. Dr. Bernd Rheinländer
BMBF: Bilaterale Zusammenarbeit BRD-Slowakei: SVK 01/001

New gallium phosphide grown by vertical gradient freeze method for light emitting diodes
Prof. Dr. Bernd Rheinländer
(VGF GaP - LED's) No. IST - 2001-32793
EU-FP5-Projekt und BMBF: Bilaterale Zusammenarbeit BRD-Slowakei: SVK 01/001

Intraband and interband carrier transitions in type I and type II nanostructures with quantum dots, quantum dot molecules and impurities
Prof. Dr. Marius Grundmann
INTAS 01-0615

One-dimensional heterostructures and nano-forests
Prof. Dr. Marius Grundmann, Dr. Michael Lorenz
DFG Gr 1011/11-1
within DFG Forschergruppe FOR 522
Architecture of nano- and microdimensional building blocks

Lateral optical confinement of microresonators
Prof. Dr. Bernd Rheinländer, Dr. V. Gottschalch
DFG Rh 28/4-1
within DFG Forschergruppe FOR 522
Architecture of nano- and microdimensional building blocks

Interface-related properties of oxide quantum wells
Prof. Dr. Marius Grundmann, Dr. V. Gottschalch
DFG Gr 1011/14-1
within DFG Forschergruppe FOR 404
Oxidic interfaces

Interface-induced electro-optical properties of oxide semiconductor-ferroelectric layered structures
Dr. Mathias Schubert, Dr. Michael Lorenz
within DFG Forschergruppe FOR 404
Oxidic interfaces

Magnetoelectronics of ferromagnetic traps in TCO and of single spin traps in quantum dots
Dr. Heidemarie Schmidt
BMBF FKZ 03N8708
im BMBF-Nachwuchswettbewerb "Nanotechnologie"

Semiconductor oxides for UV optoelectronics, surface acoustics and spintronics Prof. Dr. Marius Grundmann, Dr. Michael Lorenz
SOXESS European Network on ZnO (Thematic Network), Fifth Framework Programme, Competitive and sustainable growth, Contract G5RT-CT-2002-05075

7.25 Organizational Duties

Marius Grundmann

- Vertrauensdozent der Studienstiftung des deutschen Volkes
- Direktor des Institut für Experimentelle Physik II
- Coordinator of the European Network of Excellence on 'Self-Assembled semiconductor Nanostructures for new Devices in photonics and Electronics' (SANDiE, www.sandie.org)
- Sprecher der DFG Forschergruppe 'Architektur von nano- und mikrodimensionalen Strukturelementen' (FOR 522, http://www.uni-leipzig.de/~for522/)
- Sprecher der Fächerübergreifenden Arbeitsgemeinschaft Halbleiterforschung Leipzig (FAHL, http://www.uni-leipzig.de/~fahl/)
- Mitglied des Beirat Ionenstrahlzentrum, FZR, Rossendorf
- Organizer of Conference TCO2004, Leipzig
- Member of Program Committee IQEC-2005, Japan
- Berufungskommission Nachfolge Michel, Vorsitzender
- Project Reviewer: Deutsche Forschungsgemeinschaft (DFG), Alexander-von-Humboldt Stiftung (AvH), Schweizerischer Nationalfonds zur Förderung der wissenschaftlichen Forschung (FNSNF), Fonds zur Förderung der Wissenschaften (FWF)
- Referee: Appl. Phys. Lett., Phys. Rev. B., Phys. Rev. Lett., Electr. Lett., Physica E, phys. stat. sol., J. Appl. Phys., IEEE

Michael Lorenz

- Project Reviewer: United States - Israel Binational Science Foundation (BSF)
- Referee: Applied Physics Letters, IEEE Transactions Applied Superconductivity, J. American Chemical Society, J. Physics D Applied Physics, Thin Solid Films, J. Crystal Growth, Materials Letters, Applied Surface Science.

7.26 External Cooperations

Academic

A. F. Ioffe-Institut, St. Petersburg
Prof. Dr. Zh. I. Alferov, Dr. V. M. Ustinov, Dr. G. Cirlin

Forschungszentrum Karlsruhe, Institut für Materialforschung III
Dr. H. Heidinger, Dr. J. Halbritter

Leibnitz-Institut für Oberflächenmodifizierung e. V., Leipzig
Prof. Dr. B. Rauschenbach, Dr. E. Schubert

Universität Leipzig, Fakultät für Biowissenschaften, Pharmazie und Psychologie
Prof. Dr. A. Beck-Sickinger

Universität Leipzig, Fakultät für Chemie und Mineralogie
Dr. V. Gottschalch, Prof. Dr. K. Bente

Universität Halle-Wittenberg
Prof. Dr. I. Mertig

Max-Planck-Institut für Mikrostrukturphysik, Halle/Saale
Dr. O. Breitenstein, Dr. D. Hesse, Dr. A. Ernst

St. Petersburg State Technical University
Prof. Dr. L. Vorob'jew, Dr. V. Shalygin

Slovak University of Technology, Bratislava, Slovak
Prof. Dr. J. Kovàc, Dr. F. Uherek

Oak Ridge National Laboratory, Condensed Matter Science Division, TN, U.S.A.
Dr. Hans M. Christen

Technische Universität Berlin
Prof. Dr. D. Bimberg, Dr. A. Hoffmann

Universidade de Aveiro, Portugal
Prof. Dr. N. Sobolev

Kinki University, Dept. of Electronics Systems and Information Engeneering, Japan
Dr. M. Kusunoki

Paul Scherer Institut, Villingen
Prof. Dr. H. Sigg

Université Paris-Sud
Prof. Dr. F. Julien

Chinese Academy of Sciences, Institute of Physics, Beijing
Prof. Dr. Yusheng He

Universität Gießen
Prof. Dr. B. Meyer, Dr. D. Hofmann, Prof. Dr. J. Janek

Universität Magdeburg
Prof. Dr. A. Krost, Dr. A. Dadgar

Universität Bonn
Prof. Dr. W. Mader

Universität Hannover
Prof. Dr. M. Binnewies

Industry

Solarion GmbH, Leipzig
Dr. Gerd Lippold, Dr. Alexander Braun

El-Mul Technologies, Yavne, Israel
Dr. Armin Schön

7.27 Publications

Journals

Thomas Nobis, Evgeni M. Kaidashev, Andreas Rahm, Michael Lorenz, Marius Grundmann
Whispering gallery modes in nano-sized dielectric resonators with hexagonal cross section
Phys. Rev. Lett. 93, 103903 (2004)

Thomas Nobis, Evgeni M. Kaidashev, Andreas Rahm, Michael Lorenz, Jörg Lenzner,, Marius Grundmann
Optical Resonances Of Single Zinc Oxide Microcrystals
Proc. Int. Conf. on the Physics of Semiconductors (ICPS-27), Flagstaff, AZ, USA, 2004, eds. J. Menéndez, C. G. Van de Walle, American Institute of Physics

R. Schmidt-Grund, D. Fritsch, M. Schubert, B. Rheinländer, H. Schmidt, H. Hochmut, M. Lorenz, C. M. Herzinger, M. Grundmann
Band-to-band transitions and optical properties of $Mg_xZn_{1-x}O$ ($0 \leq x \leq 1$) films
Proc. Int. Conf. on the Physics of Semiconductors (ICPS-27), Flagstaff, AZ, USA, 2004, eds. J. Menéndez, C. G. Van de Walle, American Institute of Physics

H.Schmidt, M.Diaconu, E.Guzman, H.Hochmuth, M.Lorenz , G.Benndorf, A.Setzer, P.Esquinazi, H.v.Wenckstern, D.Spemann, A.Pöppl, R.Böttcher, M.Grundmann
N-conducting, ferromagnetic Mn-doped ZnO thin films on sapphire substrates
Proc. Int. Conf. on the Physics of Semiconductors (ICPS-27), Flagstaff, AZ, USA, 2004, eds. J. Menéndez, C. G. Van de Walle, American Institute of Physics

Andreas Rahm, Thomas Nobis, Evgeni M. Kaidashev, Michael Lorenz, Gerald Wagner, Jörg Lenzner, Marius Grundmann
High-pressure Pulsed Laser Deposition and Structural Characterization of Zinc Oxide Nanowires
Proc. Int. Conf. on the Physics of Semiconductors (ICPS-27), Flagstaff, AZ, USA, 2004, eds. J. Menéndez, C. G. Van de Walle, American Institute of Physics

H. v. Wenckstern, S. Weinhold, G. Biehne, R. Pickenhain, E. M. Kaidashev, M. Lorenz, and M. Grundmann
Static and transient capacitance spectroscopy on ZnO
Proc. Int. Conf. on the Physics of Semiconductors (ICPS-27), Flagstaff, AZ, USA, 2004, eds. J. Menéndez, C. G. Van de Walle, American Institute of Physics

C. Bundesmann, M. Schubert, D. Spemann, A. Rahm, H. Hochmuth, M. Lorenz, and M. Grundmann
Infrared dielectric function and phonon modes of Mg-rich cubic $Mg_xZn_{1-x}O$ ($x > 0.67$) thin films on sapphire [0001]
Appl. Phys. Lett. 85, 905 (2004)

Thomas Nobis, Evgeni M. Kaidashev, Andreas Rahm, Michael Lorenz, Jörg Lenzner, Marius Grundmann
Spatially inhomogeneous impurity distribution in ZnO micropillars
Nano Lett. 4, 797 (2004)

D. Spemann, M. Lorenz, T. Butz, K. Otte
Ion beam analysis of CuInSe2 solar cells deposited on polyimide foil
Anal. Bioanal. Chem. 379, 622-627 (2004)

D. Spemann, E. M. Kaidashev, M. Lorenz, J. Vogt, T. Butz
Ion beam analysis of epitaxial (Mg, Cd)$_x$Zn$_{1-x}$O and ZnO:(Li, Al, Ga, Sb) thin films grown on c-plane sapphire
Nucl. Instr. Meth. B 219-220, 891-896 (2004)

C. Bundesmann, N. Ashkenov, M. Schubert, A. Rahm, H. v. Wenckstern, E. M. Kaidashev, M. Lorenz, and M. Grundmann
Infrared dielectric functions and crystal orientation of a-plane ZnO thin films on r-plane sapphire determined by generalized ellipsometry
Thin Solid Films 455-456, 161-166 (2004)

R. Schmidt-Grund, M. Schubert, B. Rheinländer, D. Fritsch, H. Schmidt, E. M. Kaidashev, M. Lorenz, C. M. Herzinger, and M. Grundmann
UV-VUV Spectroscopic ellipsometry of ternary Mg$_x$Zn$_{1-x}$O ($x < 0.53$) thin films
Thin Solid Films 455-456, 500-504 (2004)

M. Lorenz, J. Lenzner, E.M. Kaidashev, H. Hochmuth, M. Grundmann
Cathodoluminescence of selected single ZnO nanowires on sapphire
Annalen der Physik 13 No. 1-2 (2004) 39-42.

E. Guzman, H. Hochmuth, M. Lorenz, H. von Wenckstern, A. Rahm, E. M. Kaidashev, M. Ziese, A. Setzer, P. Esquinazi, A. Pöppl, D. Spemann, R. Pickenhain, H. Schmidt, M. Grundmann
Pulsed Laser Deposition of Fe- and Fe, Cu-doped ZnO thin films
Annalen der Physik 13 No. 1-2 (2004) 57-58.

M. Lorenz, H. Hochmuth, R. Schmidt-Grund, E.M. Kaidashev, M. Grundmann
Advances of pulsed laser deposition of ZnO thin films
Annalen der Physik 13 No. 1-2 (2004) 59-60.

M. Schubert, N. Ashkenov, T. Hofmann, M. Lorenz, H. Hochmuth, H. von Wenckstern, M. Grundmann, G. Wagner
Electro-optical properties of ZnO-BaTiO$_3$-ZnO heterostructures grown by pulsed laser deposition
Annalen der Physik 13, No. 1-2 (2004) 61-62

H. von Wenckstern, E. M. Kaidashev, M. Lorenz, H. Hochmuth, G. Biehne, J. Lenzner, V. Gottschalch, R. Pickenhain, M. Grundmann
Lateral homogeneity of Schottky contacts on n-type ZnO
Appl. Phys. Lett. 84 No. 1, 79 (2004)

M. P. Seah, S. J. Spencer, F. Bensebaa, I. Vickridge, H. Danzebrink, M. Krumrey, T. Gross, U. Beck, W. Oesterle, E. Wendler, B. Rheinländer, Y. Azuma, I. Kojima, N. Suzuki, M. Suzuki, S. Tanuma, D. W. Moon, L. Hwackjoo, H. M. Cho, C. Huayi, A. T. S. Wee, T. Osipowicz, J. S. Pan, W. A. Jordan, R. Hauert, U. Klotz, C. van der Marel, M. Verheijen, Y. Tamminga, C. Jeynes, P. Bailey, S. Biswas, U. Falke, N. Nguyen, D. Chandler-Horowitz, D. Muller, J. A. Dura
Critical review of the current status of the thickness measurement for ultrathin SiO_2 on

Si - Part V: Results of a CCQM pilot study
Surf. Interface Anal. 36 (2004) 1269 - 1303

J. Kovac, J. Kvietkova, J. Kovac,Jr., J. Chovan, S. Hardt, B. Rheinländer, V. Gottschalch, J. Jakabovic, D. Pudis
Edge Emitting Laser Including an InAs/GaAs Monolayers Active Region Embedded in an AlAs/AlGaAs Vertival Resonant Cavity
Laser Physics 14 (2004) 521-526

Karsten Goede, Peter Busch, Marius Grundmann
Binding specificity of a peptide on semiconductor surfaces
Nano Lett. 4, 2115 (2004)

C. Bundesmann, M. Schubert, N. Ashkenov, M. Grundmann, G. Lippold and J. Piltz
Combined Raman scattering, X-ray fluorescence and ellipsometry in-situ growth monitoring of $CuInSe_2$-based photoabsorber layers on polyimide substrates
Proc. Int. Conf. on the Physics of Semiconductors (ICPS-27), Flagstaff, AZ, USA, 2004

Holger v. Wenckstern, Rainer Pickenhain, Swen Weinhold, Michael Ziese, Pablo Esquinazi, Marius Grundmann
Electrical properties of Ni/GaAs and Au/GaAs Schottky contacts in high magnetic fields
Proc. Int. Conf. on the Physics of Semiconductors (ICPS-27), Flagstaff, AZ, USA, 2004

D. Fritsch, H. Schmidt, M. Grundmann
Band dispersion relations of zinc-blende and wurtzite InN
Phys. Rev. B 69, 165204 (2004)

V. Gottschalch, G. Leibiger, G. Benndorf, H. Herrnberger, D. Spemann
Intrinsic carbon doping of (AlGa)As for (InGa)As laser structures ($\lambda \sim 1.17\,\mu$m)
J. Cryst. Growth 272 (2004) 642-649

M. Lorenz, E.M. Kaidashev, A. Rahm, T. Nobis, J. Lenzner, G. Wagner, D. Spemann, H. Hochmuth, M. Grundmann
$Mg_xZn_{1-x}O$ ($0 \leq x < 0.2$) nanowire arrays on sapphire grown by high-pressure pulsed-laser deposition
Appl. Phys. Lett. 86, 143113 (2005)

in press

N. Ashkenov, M. Schubert, E. Twerdowski, B. N. Mbenkum, H. Hochmut, M. Lorenz, H. v. Wenckstern, W. Grill, and M. Grundmann
Asymmetric ferroelectric polarization loops and offsets in Pt-$BaTiO_3$ ZnO-Pt thin film capacitor structures
Thin Solid Films, in press

A. Rahm, G.W. Yang, M. Lorenz, T. Nobis, J. Lenzner, G. Wagner, M. Grundmann
Two-dimensional ZnO:Al nanosheets and nanowalls obtained by Al2O3-assisted thermal evaporation
Thin Solid Films, in press

M. Lorenz, H. Hochmuth, J. Lenzner, T. Nobis, G. Zimmermann, M. Diaconu, H. Schmidt, H. von Wenckstern, M. Grundmann
Room-temperature luminescence of n-type ZnO thin films grown by pulsed laser deposition in N_2, N_2O, and O_2 background gas
Thin Solid Films, in press

M. Diaconu, H. Schmidt, H. Hochmuth, M. Lorenz, G. Benndorf, J. Lenzner, D. Spemann, A. Setzer, K.-W. Nielsen, P. Esquinazi, M. Grundmann
UV optical properties of ferromagnetic Mn-doped ZnO thin films grown by PLD
Thin Solid Films, in press

M. Grundmann
Quantum devices of reduced dimensionality
in Encyclopedia of Condensed Matter Physics, F. Bassani, J. Liedl, P. Wyder, eds., (Elsevier, Kidlington, 2005), in press

T. Nobis, E.M. Kaidashev, A. Rahm, M. Lorenz, M. Grundmann
Optical properties of single ZnO nanocolumns and nanoneedles
Proc. of the NATO Advanced Research Workshop 'ZnO as a material for micro- and optoelectronic applications', H. Nickel, E. Terukov, eds. (Kluwer, 2005), in press

7.28 Graduations

Diploma

Anke Carstens
Spektroskopische Ellipsometrie an kubischem $Mg_xZn_{1-x}O$
3.11.2004

Wolfram Czakai
Photolumineszenz an Zinkoxid
25.2.2004

Claudia Krahmer
Metallorganische Gasphasenepitaxie von AIII-BV-Dünnschichtsolarzellen: Einsatz neuartiger Absorbermaterialien
26.7.2004

Gregor Zimmermann
Rastersondenmikroskopie an Zinkoxid-Dünnschichten und -Nanostrukturen
8/2004

M.Sc.

Chegnui Bekeny
Metal contacts on n-type ZnO
7/2004

Kanneh Wadinga Fomba
Surface Analysis of ZnO Thin Films for Formation of Schottky contacts
10/2004

Marc Schillgalies
Photoreflectance spectroscopy on ZnO based structures
8/2004

7.29 Guests

Prof. Dr. Guowei W. Yang
State Key Laboratory of Optoelectronic Materials and Technologies,
School of Physics and Engineering, Zhongshan University, Guangzhou, P.R. China
01.04.2004 – 30.06.2004

Dr. Evgeni M. Kaidashev
Rostov-on-Don State University, Russia
01.08.2004 – 30.09.2004

8

Solid State Optics and Acoustics

8.1 Development of a Miniaturized Advanced Diagnostic Technology Demonstrator 'DIAMOND' - Technology Study Phase 2

W. Grill, M. Löffler, J. Jahny, O. Lenkeit, R. Wannemacher

A miniaturized universal scanning microscope ('space microscope') is being developed for potential operation on board of the International Space Station ISS, which allows diagnostics of samples by means of optical scanning microscopy, partly combined with spectral resolution, as well as by means of acoustic microscopy with vector contrast. Foreseen microscopic techniques are confocal optical microscopy in reflection, scanning microscopy in transmission, as well as spectrally resolved fluorescence and Raman microscopy. Acoustic microscopy permits spatially resolved determination of micromechanical sample properties.

This work is supported by European Space Organization ESA/ESTEC

8.2 Ultrasound Diagnostics of Directional Solidification

W. Grill, R. Wannemacher, S. Knauth, J. Jahny, O. Lenkeit

An ultrasonic measuring device based on guided waves has been developed in order to determine the growth rate of alloys, in particular of opaque metallic alloys. Experimental tests show that a high resolution is achievable in the determination of the position of the solid-liquid interface, down to 0.01 mm. The ultrasonic technique is therefore an appropriate tool for the measurement of the solidification velocity for stable as well as unstable solidification processes. The aim consists in the investigation of the impact of process parameters on the resulting material properties. Controlled non-stationary growth presently appears to become a main research object for the next future, in particular in the context of industrial applications. The measurement of the solidification velocity by ultrasound is a diagnostic tool for directional solidification experiments. It was developed in the framework of the Technological Research Programme of the European Space Organization. An ultrasound pulse launched from the cold end of the sample and being reflected from the

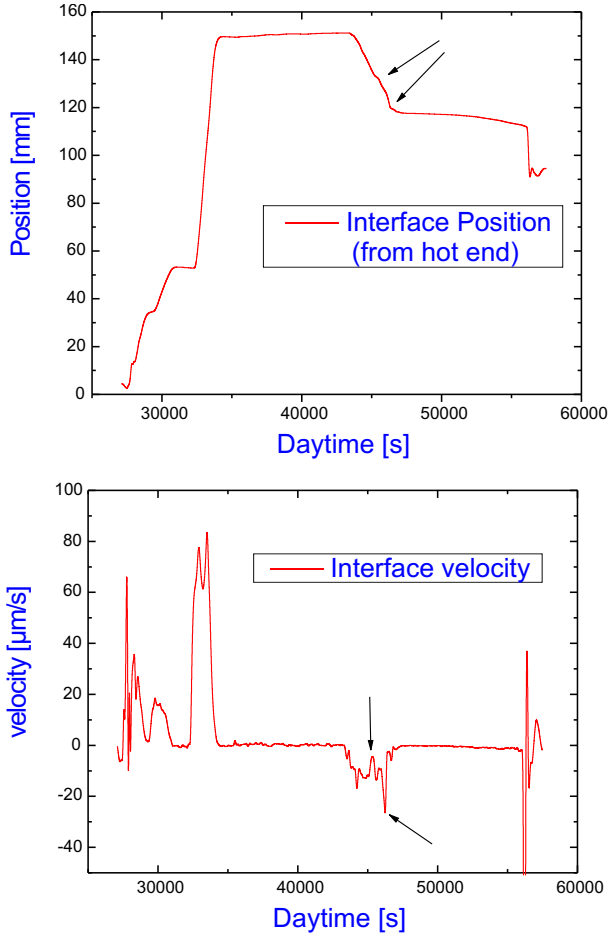

Figure 8.1: Time-of-flight analysis of melting and directional solidification of an Aluminium alloy cylinder. Arrows indicate distortions, possibly by bubble formation or adherence

phase boundary of solidification allows to determine the position of the solid-liquid interface. Given the speed of sound in the sample the position of the phase boundary can be determined as a function of time and, hence, the solidification velocity via precise measurement of the propagation time by means of an autocorrelation technique.

Funded by European Space Organization ESA/ESTEC

8.3 Development and Verification of the Applicability of Ultrasonic Methods

W. Grill, Z. Kojro

Possible applications associated with the company Schott GLAS of the ultrasound techniques developed and published by our group are investigated. Techniques, sensors, and measurement devices are being developed. The work is conducted in cooperation with Schott GLAS. New techniques were developed and tested.

Funded by Schott GLAS Mainz

8.4 Development and Verification of the Applicability of Ultrasonic Methods

W. Grill, Z. Kojro

Based on techniques developed and published by us dedicated ultrasonic techniques, sensors, and devices are being developed for use at the company PFW Technologies GmbH. The work is conducted in cooperation with PFW Technologies GmbH. The developed techniques are a spin-off of the projects of our group financed by the European Spcae Organization (ESA).

Funded by PFW Technologies GmbH

8.5 Support in the Development of Ultrasound Based Sensors

W. Grill, Z. Kojro

Based on techniques developed and published by us dedicated ultrasonic sensors and devices are being developed for use at the company Ashland, Drew Marine Division. The work is conducted in cooperation with Ashland, Drew Marine Division. The developed techniques are a spin-off of the projects of our group financed by the European Spcae Organization (ESA).

Funded by PFW Technologies GmbH

8.6 Fourier Inversion of Acoustic Wave Fields in Anisotropic Solids

M. Pluta, A.G. Every, W. Grill, T.J. Kim, E. Twerdowski

This ongoing work [1, 2] is concerned with the analysis of acoustic wave fields encountered in phase-sensitive acoustic microscopy (PSAM) applied to elastically anisotropic solids.We show that the fast Fourier transform technique provides a computationally efficient method of calculating two-dimensional amplitude and phase images of these fields. More importantly, we demonstrate how this technique, applied to complex wave field data, can be used to treat inverse problems such as source reconstruction, image quality assessment, and the determination of elastic constants. Monochromatic and also more general time-dependent excitations, such as tone bursts and short pulses, are treated, and the resulting wave fields described. The evolution of these wave fields with increasing frequency is discussed, and emerging infinite frequency features, such as the ray surface and phonon focusing caustics, are identified. We show how phonon caustics,at finite frequency, unfold into characteristic diffraction patterns. Then, as the frequency is lowered further, the fringes progressively broaden and merge, until ultimately only the broadest vestiges of the original focusing pattern can be discerned. Time gating and limiting the wave vector domain over which the requisite Fourier integrals are done, is used to isolate the diffraction patterns of elementary caustic structures such as cusps and folds. Calculations are reported for GaAs and Si, which are in good agreement with experiment.A number

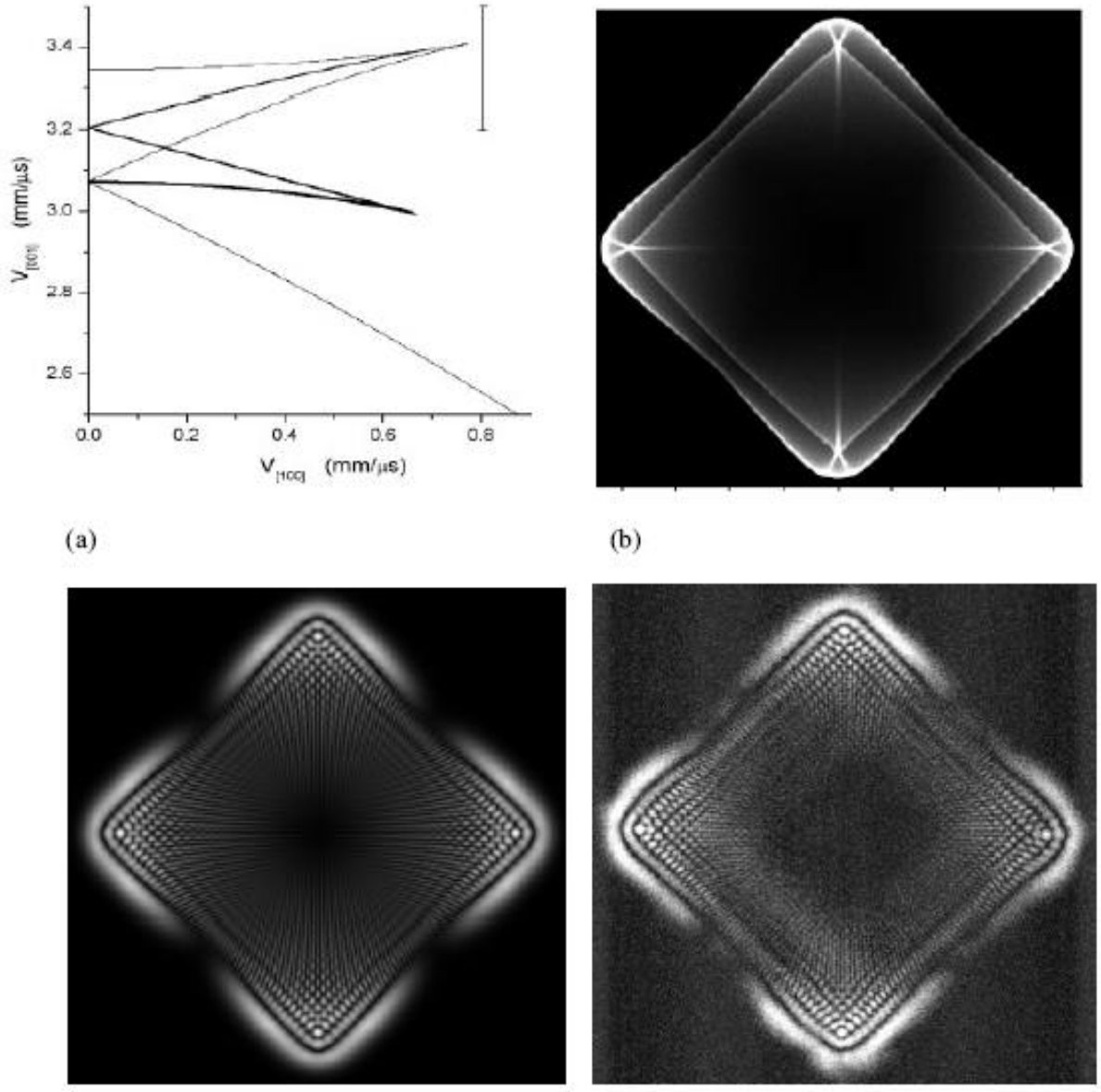

Figure 8.2: (a) (010) Section of the cuspidal region of the wave surface of GaAs, showing the velocity gate used in capturing the accompanying images. (b) Calculated phonon focusing pattern. (c) Calculated amplitude diffraction image for h = 4.8 mm and f = 362 MHz, and (d) corresponding measured image.

of numerical simulations are presented that are in good agreement with measured data from the literature.

[1] M. Pluta, A.G. Every, W. Grill, Inversion of acoustic diffraction fields in anisotropic solids Ultrasonics **42**, 243–248 (2004)

[2] A.G. Every, M. Pluta, W. Grill, K.U. Würz, Progression from ballistic phonon focusing to internal diffraction of ultrasound in crystals, phys. stat. sol. c **1**, 2951–2954 (2004)

8.7 Phase-Sensitive Acoustic Imaging and Micro-Metrology of Polymer Blend Thin Films

W. Ngwa, A. Kamanyi, R. Wannemacher, W. Grill, T. Kundu

The three-dimensional images obtained by scanning acoustic microscopy with vector contrast (PSAM), contain significant qualitative and quantitative information that is not easily obtainable by other methods. We employ this technique to examine homopolymer and polymer blend thin films. The complex V(z) functions derived from the images, and the results obtained by image processing and meticulous analysis are employed to render the morphology, composition and micro-mechanical properties of the polymer films. In addition, ways by which the information inherent in the phase images can be extracted are examined. This is highly desirable, as the phase images contain very useful additional information [1].

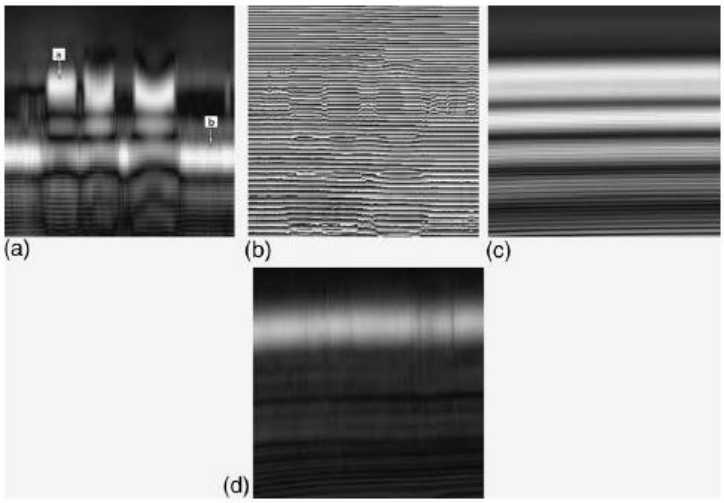

Figure 8.3: $(140 \times 32\,\mu\mathrm{m}^2)$ $y-z$ images of 583 nm PS film spun-cast on glass: (a) amplitude, (b) corresponding $y-z$ phase image, (c) glass substrate, (d) PS halfspace.

Tessellations arise quite naturally in numerous applications. In some situations, e.g. in cell biology, physics, or geography, one may wish to describe observed structures using models of tessellations. One way of generating them is to start with a set of discrete points in space, which are permitted to expand coetaneously in circular disks at the same rate. The disks are not allowed to overlap, so they must deform, and one finally gets polygons. Voronoi tessellations have been observed for dewetting thin film polymer bilayers. Earlier on, such structures were chronicled as a stage of dewetting in homopolymer films prior to the formation of droplets. Here we report the observation of such tessellations for unannealed polymer blend thin films. An exegesis of the phase separation process accounting for this observation is proposed [2].

[1] W. Ngwa, R. Wannemacher, W. Grill, Phase-sensitive acoustic microscopy of polymer thin films, Ultrasonics **42**, 983-987 (2004)
[2] W. Ngwa, R. Wannemacher, W. Grill, A. Serghei, F. Kremer, T. Kundu, Voronoi Tessellations in Thin Polymer Blend Film, Macromolecules **37**, 1691-1692 (2004)

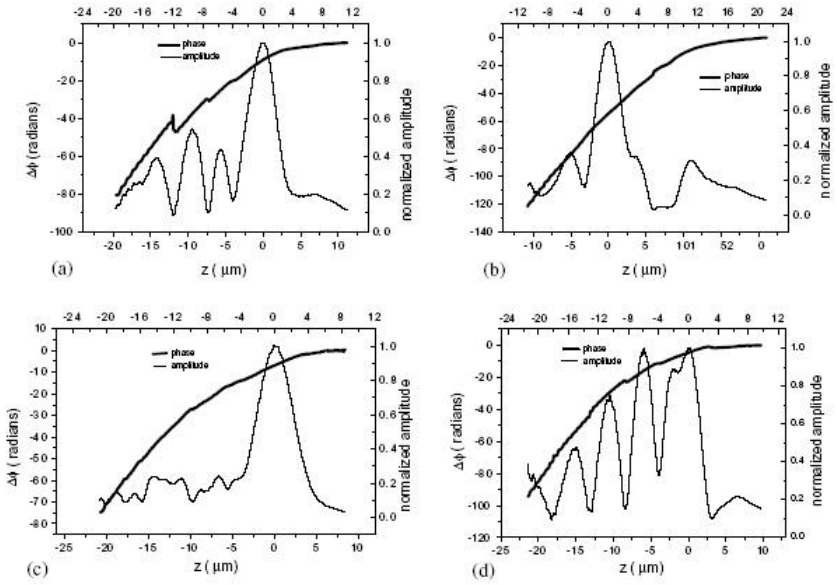

Figure 8.4: Complex V(z) curves of (a) spot 'a' of Fig. 8.5a, (b) spot 'b' of Fig. 8.5a, (c) PS half-space, (d) glass substrate. The graphs show the dependencies of the differential phase and amplitude signals obtained by PSAM, on the position of the sample along the acoustic lens axis. The substrate is glass; coupling fluid water; and the frequency is 1.2 GHz.

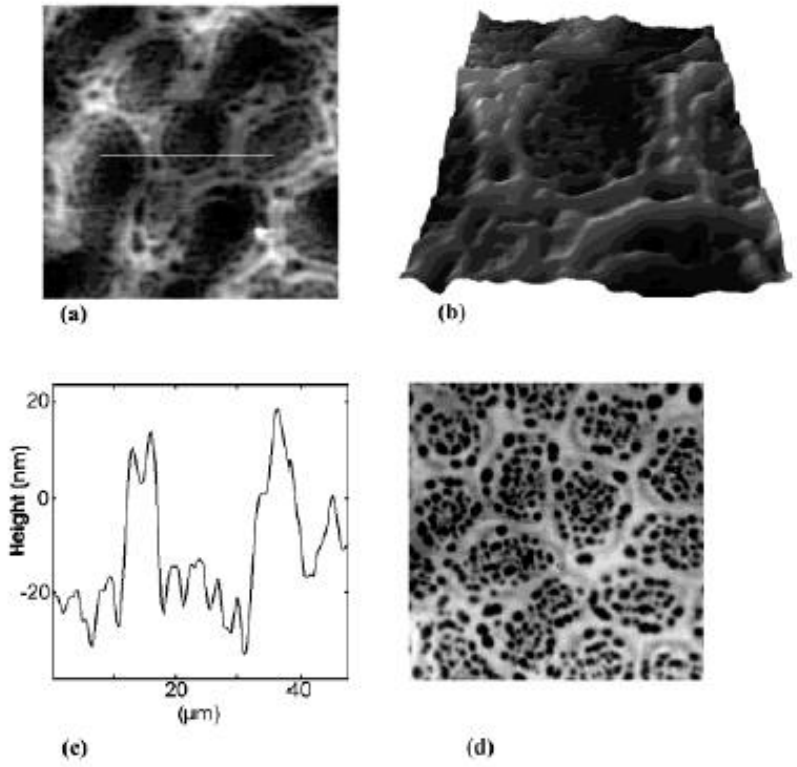

Figure 8.5: (a) ($82 \times 82\,\mu m^2$) AFM image of an unannealed 165 nm thick PS/PMMA blend film on a silicon substrate. A Voronoi tessellation pattern is clearly visible. (b) Perspective view of single cell from (a). (c) Line profile from region marked with a line in (a). (d) ($100 \times 100\,\mu m^2$) PSAM maximum amplitude image showing tessellations of the unannealed blend film. The darker regions correspond to PS and bright regions to PMMA.

8.8 Applications of Phase-Sensitive Acoustic Microscopy in Biology

C. Laforsch, W. Ngwa, W. Grill, R. Tollrian

Inducible defenses are common strategies for coping with the selective force of predation in heterogeneous environments. In recent years the conspicuous and often dramatic morphological plasticity of several waterflea species of the genus Daphnia have been found to be inducible defenses activated by chemical cues released by predators. However, the exact defensive mechanisms remained mysterious. Because even some minute morphological alterations proved to be protective against predatory invertebrates, it has been suggested that the visible morphological changes are only the tip of the iceberg of the entire protective mechanisms. Here we applied a method of ultrasonic microscopy with vector contrast at 1.2 GHz to probe hidden morphological defenses. We found that induction with predator kairomones increases the stability of the carapace in two Daphnia species up to 350 %. This morphological plasticity provides a major advantage for the induced morphs during predation because predatory invertebrates need to crush or puncture the carapace of their prey to consume them. Our ultrastructural analyses revealed that the internal architecture of the carapace ensures maximal rigidity with minimal material investment. Our

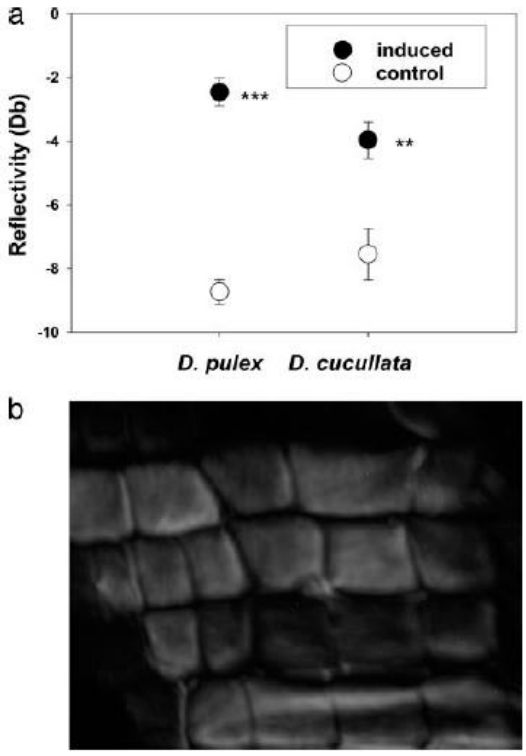

Figure 8.6: Acoustic microscopy. (a) Mean reflectivity (measurement of the strength of a material) of the carapace of D. cucullata and D. pulex. Plastic responses of both Daphnia species were induced by water-soluble chemicals released by the predacious phantom-midge larvae. Asterisks indicate signifi- cant differences to the control (***, $P < 0.001$; **, $P < 0.01$). (b) A 1.2 GHz phase-sensitive acoustic microscopy amplitude image of the carapace of D. pulex ($140 \times 150\,\mu m^2$).

results uncover hidden morphological plasticity and suggest a reconsideration of former classifi- cation systems in defended and undefended genotypes in Daphnia and possibly in other prey organisms as well. [1].

[1] Christian Laforsch, Wilfred Ngwa, Wolfgang Grill, Ralph Tollrian, An acoustic microscopy technique reveals hidden morphological defenses in Daphnia, Proc. Nat. Acad. Sci. **101**, 15911-15914 (2004)

8.9 Photonic Molecules Doped with Semiconductor Nanocrystals

B. Möller, U. Woggon, M.V. Artemyev, R. Wannemacher

We report on coherent cavity field coupling in linear chains and arrays of exactly size-matched spherical microcavities doped with CdSe quantum dots. The spatial distribution and the dominant polarization type of both the weakly and strongly coupled cavity resonances are studied spectrally and spatially resolved in various coupled resonator geometries. Both experiment and theory show strong photon mode coupling with pronounced mode splitting as well as weak coupling with no significant loss in Q-factor depending on the emitter position and orientation. [1].

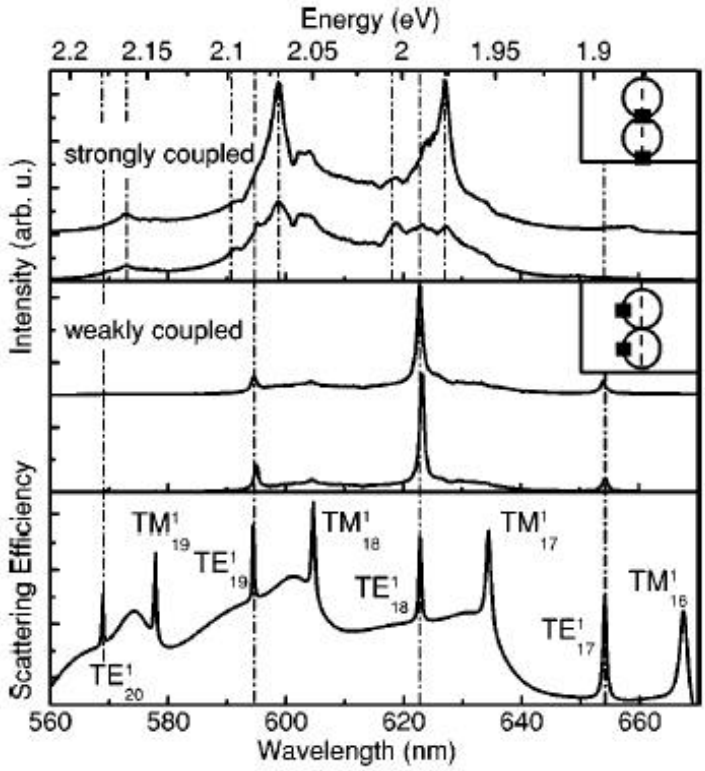

Figure 8.7: Emission spectra taken in TE-sensitive detection at characteristic bisphere points. Upper panel: redshifted, bonding resonances measured at the intersection point (uppermost curve) and weaker, antibonding modes taken at the edge position; middle panel: spectra of the spectrally unshifted bisphere modes taken at detection points apart from the bisphere axis; lower panel: Mie-scattering spectrum for a single polystyrene sphere.

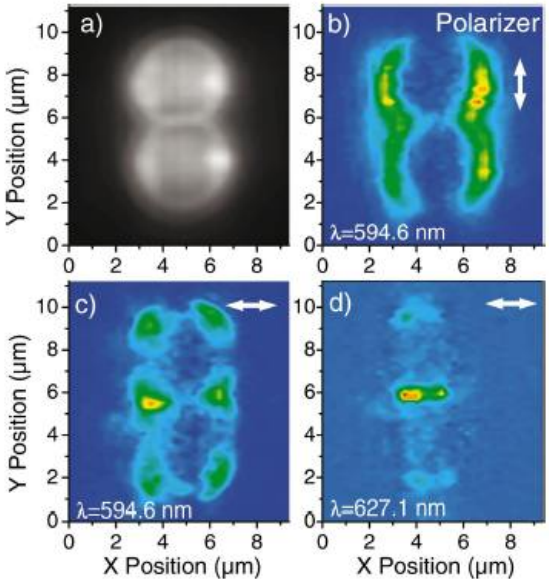

Figure 8.8: Polarization-sensitive intensity maps of a bisphere photonic molecule for a weakly coupled TE_{19}-type resonance (b) and (c) and a strongly coupled bonding TE_{18}-type resonance (d) (note the stronger intensity in the bisphere center compared to that at the poles indicating the bonding type of the mode). The orientation of the polarizer is given by arrows. In (a) the spectrally integrated, unpolarized emission is shown. For the spectral positions see Fig. 8.7.

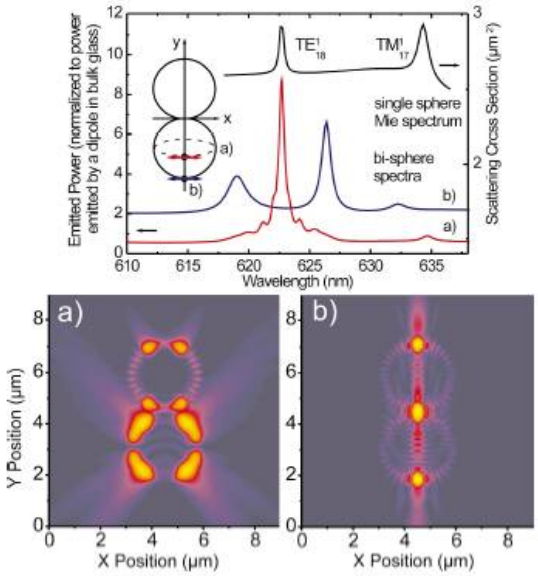

Figure 8.9: Calculated emission spectrum and electric field intensity distributions $|E|^2$ excited by a dipole oscillating in x direction and (a) located in the lower sphere 1.2 mm from the center at the equator and (b) at the pole on the bisphere axis (see scheme in the inset). The upper panel shows the spectra, the lower panel the $|E|^2$-distribution in the xy plane in a logarithmic color-coded scale of 40 dB. Spectrum (b) has an offset of +1.5 for clarity.

[1] B. Möller, M.V. Artemyev, U. Woggon, R. Wannemacher, Photonic molecules doped with semiconductor nanocrystals, Phys. Rev. B **70**, 115323 (2004)

8.10 Anti-Site Incorporation of Mn in $Zn_{1-x}Mn_xSe$ Mixed Crystals

T. Hofmann, T. Chavdarov, M. Wiedenmann, K. Argawal*, B. Daniel*, M. Hetterich*, M. Schubert

*Institut für Angewandte Physik and CFN, Universität Karlsruhe

Recently, diluted magnetic semiconductors (DMS) like $Zn_{1-x}Mn_xSe$ have been demonstrated as possible candidates for spin aligners in spin-based opto-electronic devices [1]. However, information regarding the influence of the Mn concentration on several fundamental material parameters is still poor. Magnetooptic generalized ellipsometric measurements are employed in order to investigate the phonon and free-charge-carrier properties of $Zn_{1-x}Mn_xSe$ as a function of composition and doping concentration. We observe an "intermediate-mode" behavior for the optical phonon modes in $Zn_{1-x}Mn_xSe$ in the composition range $0 \leq x \leq 0.28$. In addition to the known ZnSe-like and MnSe-like phonon resonances a weak mode is found below the MnSe-like phonon band. We conclude from linear chain calculations that this mode is due to an impurity phonon resonance caused by Mn incorporation on the Se-sublattice sites. A distinct reduction of the effective electron mass in ZnSe is observed upon Mn-incorporation [$m^*_{\mathrm{ZnSe}} = 0.130 \pm 0.005\, m_e$; $m^*_{\mathrm{Zn_{0.9}Mn_{0.1}Se}} = 0.103 \pm 0.005\, m_e$]. Additionally, the dopability decreases drastically with increasing Mn concentration likely due to the unintentional Mn co-doping caused by the Mn incorporation on the Se-sublattice sites as suggested by the phonon mode properties.

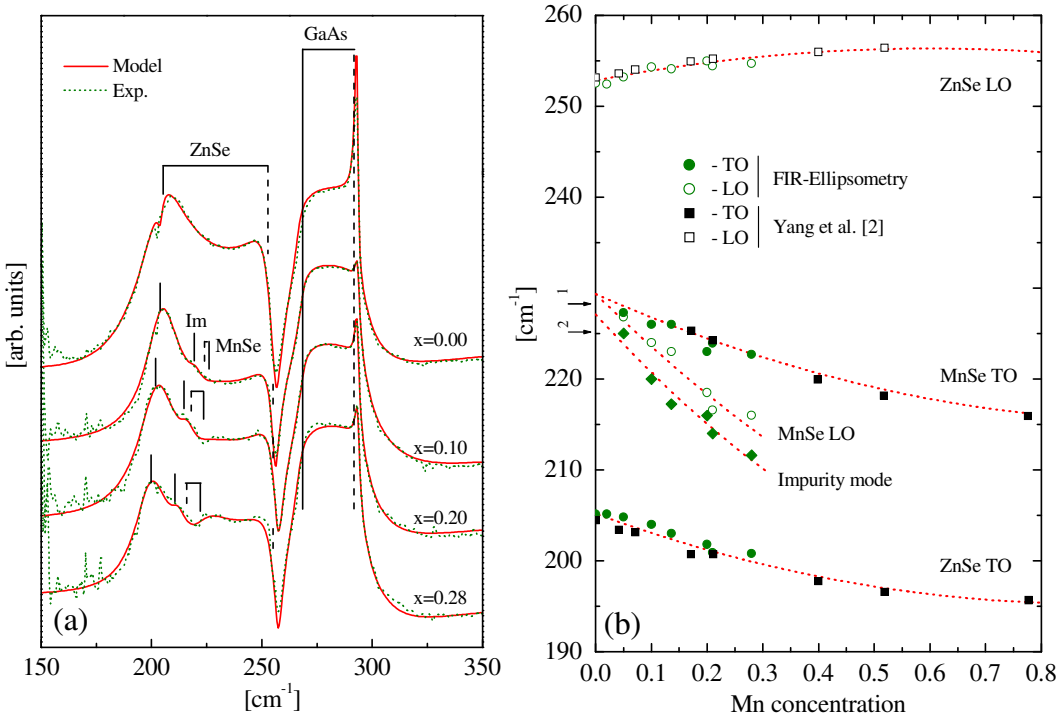

Figure 8.10: (a) Experimental (dotted lines) and best-fit calculation (solid lines) ellipsometry data at $\Phi_a = 70°$. The impurity mode caused by anti-site incorporation of Mn is indicated by Im. (b) Concentration dependence of the phonon modes in $Zn_{1-x}Mn_xSe$. The calculated impurity mode frequencies for Mn on Zn- and Se-lattice sites $\omega_1 = 228\,\mathrm{cm}^{-1}$ and $\omega_2 = 225\,\mathrm{cm}^{-1}$, respectively are indicated by horizontal arrows.

[1] R. Fiederling et al. Nature (London) **402**, 787 (1999)
[2] T.R. Yang et al. Phys. Rev. B **60**, 16058 (1999)

8.11 Raman Study of $Mg_xZn_{1-x}O$ Micro-Structures

C. Bundesmann, U. Teschner, M. Schubert

Upon the determination of the phonon mode properties of hexagonal $Mg_xZn_{1-x}O$ thin films [1, 2], it is now possible to study $Mg_xZn_{1-x}O$ microstructures or $Mg_xZn_{1-x}O$-based heterostructures. Figure 8.11 depicts a microscopic image of a $Mg_xZn_{1-x}O$-microstructure grown by PLD on sapphire. By comparing the spectra recorded at the $Mg_xZn_{1-x}O$-rod (see Fig. 8.12) with the corresponding spectra of a bare sapphire substrate (not shown here), typical $Mg_xZn_{1-x}O$-related phonon modes can be identified: the multi-phonon structure (MP), the A_1(TO) mode, E_1(TO) mode, and the $E_2^{(2)}$ mode as labelled in Fig. 8.12.

Because the $Mg_xZn_{1-x}O$-modes appear only in certain scattering configurations, for instance, the $A_1(TO)$-mode is only in the $x(yy)x'$ and $x(zz)x'$ scattering configuration present, it can be concluded that the rods are single-crystalline with the c-axis parallel to the axis of the rod. Furthermore, from the wave numbers of the phonon modes the Mg mole fraction can be estimated to be $x = 0.20(0.05)$.

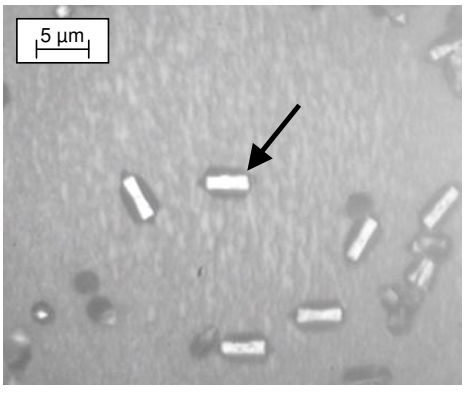

Figure 8.11: Microscope image of $Mg_xZn_{1-x}O$-rods on c-plane sapphire. The Raman spectra in figure 8.12 are recorded for the rod marked by the arrow.

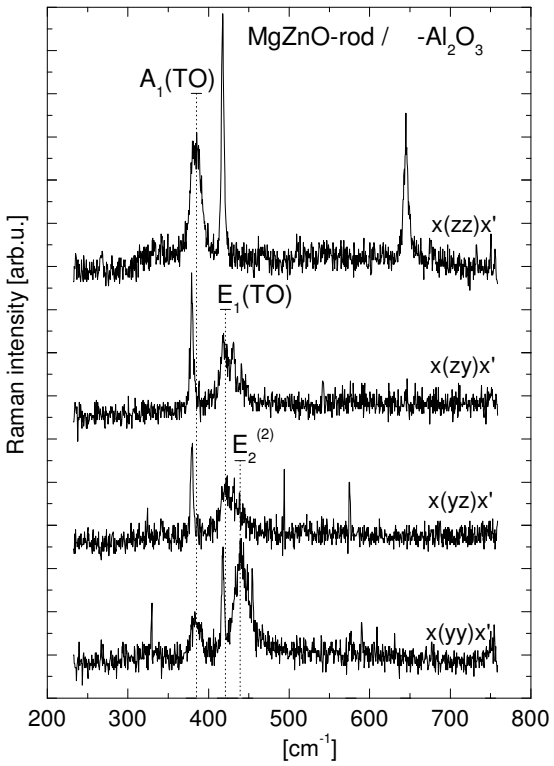

Figure 8.12: Polarized micro-Raman spectra of a $Mg_xZn_{1-x}O$-rod on sapphire. Spectra are shifted for clarity. MgZnO phonon modes are marked by vertical dotted lines. Unlabelled modes are due to the substrate.

[1] C. Bundesmann *et al.*, Appl. Phys. Lett. 81, 2376 (2002); Appl. Phys. Lett. 85, 905 (2004); Thin Solid Films 455-456, 161 - 166 (2004)
[2] R. Schmidt *et al.*, Proceedings of the 27th International Conference on Semiconductor Physics, Flagstaff, 2004.

8.12 Exchange Polarization Coupling in Wurtzite-Perovskite Oxide Interfaces: ZnO-$BaTiO_3$ Heterostructures

N. Ashkenov, H. v. Wenckstern, H. Hochmuth, M. Lorenz, M. Grundmann, M. Schubert

Coupling between the fixed ionic interface charge in wurtzite structure semiconductors and the switchable interface charge in ferroelectric semiconductors gives rise to polarization exchange coupling phenomena. Structural, electrical, and electro-optical properties of ZnO/BTO and ZnO/BTO/ZnO heterostructures, grown by pulsed laser deposition on c-Al_2O_3 and (001)Si were reported recently [1–3]. Temperature-dependent electric polarisation, current-voltage, and capacitance-voltage studies revealed the interplay between the spontaneous wurtzite and the switchable ferroelectric polarization. Figure 8.13 depicts a switchable rectifying current-voltage characteristics, which is assigned to the wurtzite-polarization biased switching of the ferroelectric domains, and which control the current through the hetersotructure interfaces. A memory-shaped capacitance is obtained by capacitance-voltage (C-V) measurements on Pt/ZnO/BTO/ZnO/Pt/Si heterostructures (Fig. 8.14).

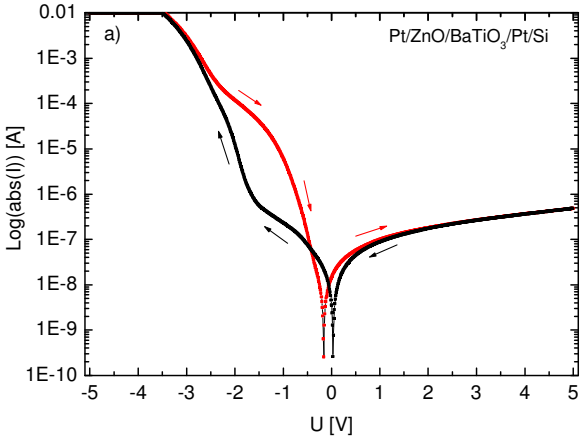

Figure 8.13: Current-Voltage characteristics of a Pt/ZnO/$BaTiO_3$/Pt/Si heterostructure grown by Pulsed Laser deposition.

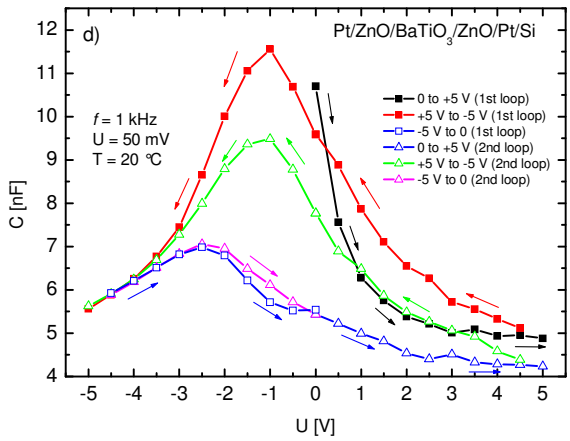

Figure 8.14: Capacitance-Voltage characteristics of a Pt/ZnO/$BaTiO_3$/ZnO/Pt/Si heterostructure.

[1] M. Schubert et al. Ann. Phys. 13, 61 (2004).
[2] B. Mbenkum et al. Appl. Phys. Lett. 86. 091904 (2005).
[3] N. Ashkenov et al. Thin Solid Films xx, (2004), xxx-xxx.(in press)

8.13 Ellipsometric Study of the Structural and Optical Properties of ITO Thin Films

M. Saenger, T. Hofmann, M. Schubert

Spectroscopic Ellipsometry in the range from 0.73 to 3.35 eV has been used to study the optical and structural properties of Tin-doped In_2O_3 (ITO) transparent thin films prepared by magnetron sputtering on glass substrate. It is known [1] that ITO exhibits a graded microstructure which widely depends on the deposition conditions which causes the optical as well as the electrical properties to vary. A Grading-Model using Drude and Cauchy terms has been found capable to reproduce accurately the ellipsometric experimental data (Figs. 8.15, 8.16).

This description of the system showed a very good consistency with data obtained from Transmission measurements. Furthermore the resistivity of the film obtained from the model is in good concordance with literature values [2] for ITO around the 2×10^{-4} Ohm cm.

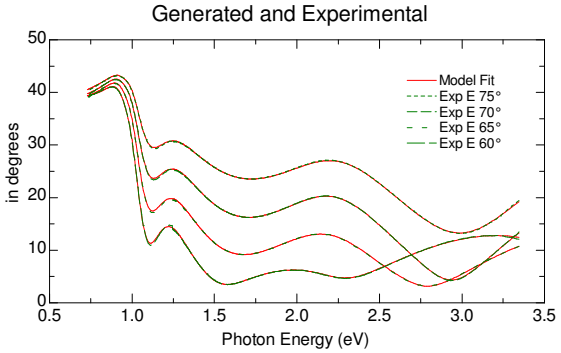

Figure 8.15: Experimental and generated ellipsometric data are practically the same.

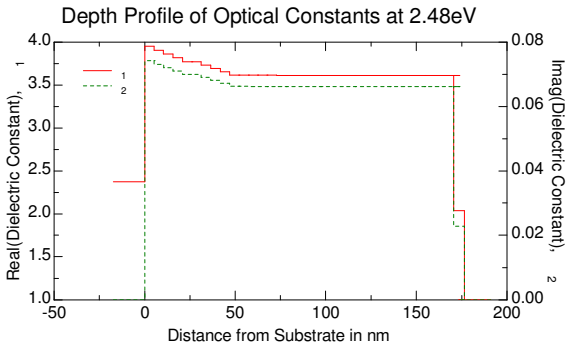

Figure 8.16: Depth Profile of the dielectric function at 2.48 eV in dependence of the film depth.

[1] R.A. Synowicki, Thin Solid Films 313-314 (1998) 394-397.
[2] S. Seki, *et. al*, Surface and Coat. Tech. 169-170 (2003) 525-527.

8.14 Sub-Wavelength Diffraction from 3D-Silicon Nanostructures

M. Schubert, B. Gallas*, J. Lafait*, J. Rivory*, E. Schubert†

* Université Pierre et Marie Curie, Laboratoire d'Optique des Solides, Paris, France
† Institut für Oberflächenmodifizierung Leipzig e.V.

Three-dimensional artificial nano-architectures are becoming available from progressed deposition techniques, such as by glancing angle ion beam deposition. Spirals, screws, rods, and 3D- wire gratings with three-fold or four-fold base made froom nano-crystalline Si are depicted in Fig. 8.17, for example. Many of their new physical properties are yet to be explored. Spectrally resolved stray light intensity measurements as a function

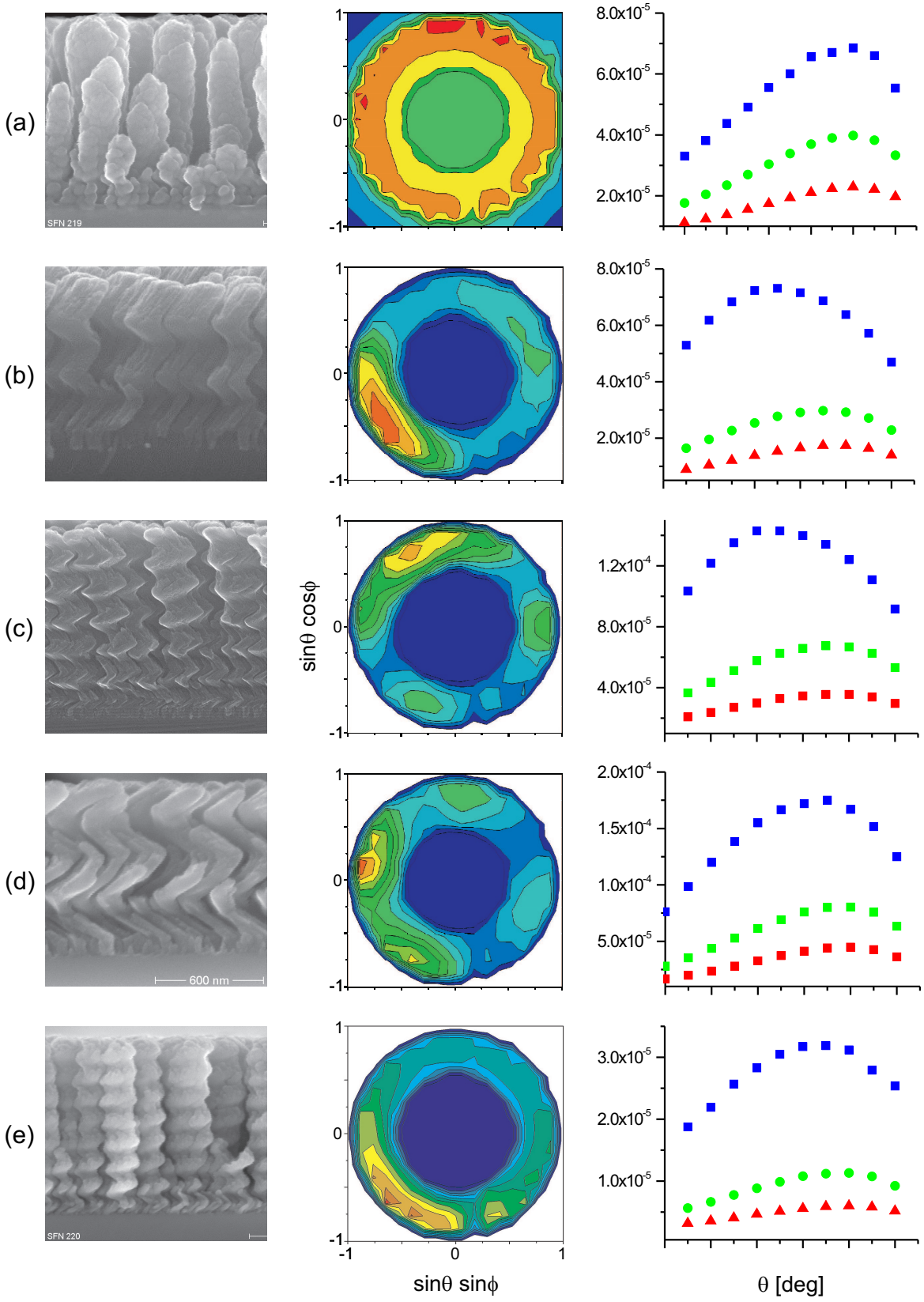

Figure 8.17: Left panel: Scanning electron micrographs from silicon nanostructures grown by glancing angle deposition, middle panel: integral scatter intensity as a function of polar (φ) and azimuthal (θ) observation angle (Illumination is from the top), and right panel: Color-resolved scatter intensity from Si-rods (a), Si-chevrons (zig-zag's) (b), Si-spirals with three-fold base (c), four-fold base (d), and Si-helices (d).

of the observation angle reveal interesting diffraction phenomena. The structures with dimensions well below the illuminating light source, but yet above the limit for effective medium considerations, cause distinct spatial light scattering with puzzling color and intensity variation. Thereby, spatial filters for white light decomposition, image capturing, or optical security elements may be envisioned. A full electromagnetic calculation of the optical diffraction characteristics for the 3D nano-structures establishes a challenging task.

8.15 Funding

Development of a Miniaturized Advanced Diagnostic Technology Demonstrator 'DIAMOND' - Technology Study Phase 2
European Space Organization ESA/ESTEC

Ultrasound Diagnostics of Directional Solidification
European Space Organization ESA/ESTEC

Development and verification of the applicability of ultrasonic methods
Schott GLAS Mainz

Development and verification of the applicability of ultrasonic methods
PFW Technologies GmbH

Support in the Development of Ultrasound Based Sensors
Ashland, Drew Marine Division

Generalized far-infrared ellipsometry of magnetooptic free-carrier-effects in III-V semiconductor layer structures
Deutsche Forschungsgemeinschaft (German National Science Foundation)
SCHUH 1338/3-1 (M. Schubert)

Interface-induced electro-optic properties of oxide semiconductor - ferroelectrica heterostructures
Deutsche Forschungsgemeinschaft, in Forschergruppe 404 "Oxidische Grenzflächen" (German National Science Foundation)
SCHUH 1338/4-1,2 (M. Schubert, together with M. Lorenz, HLP)

in-situ Analytik des Wachstums flexibler Solarzellen auf $CuInSe_2$-Basis
Solarion GmbH, Leipzig, Germany (SME)
(M. Schubert)

Parallel in-line design for optical PVD process control
von Ardenne Anlagenbau GmbH, Dresden, Germany (SME)
(M. Schubert)

Functional optical thin films II
Flabeg GmbH Co. KG, Furth im Wald, Germany (SME)
(M. Schubert)

Electrical and optical properties of transparent conductive oxides
von Ardenne Anlagenbau GmbH, Dresden, Germany (SME)
(M. Schubert)

Development of Raman tools for industrial in-line applications
Chamber of Industry and Commerce of the City Leipzig and University Leipzig, Leipzig, Germany
(M. Schubert)

Industrial in-situ Raman scattering tool
Solarion GmbH, Leipzig, Germany (SME)
(M. Schubert)

Optical measurement tools for automation of PVD deposition systems
Roth und Rau AG, Hohenstein-Ernstthal, Germany (SME)
(M. Schubert)

8.16 Organizational Duties

Wolfgang Grill

- Adjunct Professor and Member of the Graduate School, The University of Georgia, Athens, GA, USA
- Project Reviewer: Deutsche Forschungsgemeinschaft, Alexander von Humboldt Foundation

Reinhold Wannemacher

- Referee: Nature Materials, Opt. Lett., Opt. Express, J. Lumin.

Mathias Schubert

- Topical Editor (Polarization and Thin Films) Journal Optical Society of America A
- Organization board member of the Deutsche Arbeitskreis Ellipsometrie
- Referee: Applied Optics, Applied Physics Letters, European Physical Journal B (condensed matter), IEEE Transactions on Nanotechnology, Journal of Applied Physics, Journal of Materials Research, Journal of Optics A: Pure and Applied Optics, Journal of The Electrochemical Society, Journal of the Optical Society of America A, Journal of Physics D: Applied Physics, Journal of Vacuum Science and Technology, Langmuir, Materials Science and Engineering B, Measurement Science and Technology, Optics Communications, Optics Express, Optics Letters, physica status solidi, Physical Review B, Physical Review Letters, Physics Letters A, Review of Scientific Instruments, Surface and Interface Analysis, Thin Solid Films
- Project Reviewer: National Science Foundation (USA)

8.17 External Cooperations

Academic

University of the Witwatersrand, Johannesburg, South Africa
Prof. Dr. A. Every

Wroclaw Institute of Technology, Wroclaw, Poland
Dr. M. Pluta

University of Arizona, Tucson, Arizona, USA
Prof. Dr. T. Kundu

University of Central Florida, Orlando, Forida, USA
Prof. Dr. W. Luo

Universität Frankfurt
Prof. Dr. J. Bereiter-Hahn

Universität Dortmund
Prof. Dr. U. Woggon

University Linköping, Sweden
Prof. Dr. H. Arwin, Prof. Dr. O. Inganäs, Prof. Dr. B. Monemar, Dr. V. Darakchieva

UCLA, USA
Prof. Dr. W. Dollase

ISAS Berlin, Germany
PD Dr. N. Esser

MPI Halle, Germany
PD Dr. D. Hesse

Université Pierre et Marie Curie, Paris, France
Prof. Dr. J. Rivory, Dr. B. Gallas

BESSY II Berlin, Germany
Dr. U. Schade

University of Nebraska-Lincoln, USA
Prof. Dr. J. A. Woollam

Institut für Oberflächenmodifizierung Leipzig e.V., Germany
H. Neumann, Dr. E. Schubert

International Organizations

European Space Organization ESA/ESTEC

Industry

PfW Technologies GmbH

Schott GLAS Mainz

Ashland, Drew Marine Division

Dr. Gerd Birkelbach (self-owned Engineering Company)

Fraunhofer FEP Dresden, Germany
Dr. Liebig

J.A. Woollam Co. Inc., Lincoln, USA
Dr. C.M. Herzinger

FHR Anlagenbau Ottendorf-Okrilla, Germany
W. Häntsch

Flabeg GmbH, Furth im Wald, Germany
Dr. T. Höing

von Ardenne Anlagenbau GmbH Dresden, Germany
M. Kammer, Dr. M. List

Solarion GmbH Leipzig, Germany
Dr. G. Lippold, Dr. C. Otte

Alanod Aluminium-Veredlung GmbH Co. KG, Ennepetal, Germany
Dr. D. Peros

OSRAM Opto Semiconductors GmbH Regensburg, Germany
Dr. K. Streubel,Dr. I. Pietzonka

L.O.T.-Oriel GmbH, Darmstadt, Germany
Dr. T. Wagner

Roth und Rau AG, Hohenstein-Ernstthal, Germany
Dr. D. Roth

8.18 Publications

Journals

M. Pluta, A.G. Every, W. Grill
Inversion of acoustic diffraction fields in anisotropic solids
Ultrasonics **42**, 243-248 (2004)

A.G. Every, M. Pluta, W. Grill, K.U. Würz
Progression from ballistic phonon focusing to internal diffraction of ultrasound in crystals
phys. stat. sol. c **1**, 2951-2954 (2004)

W. Ngwa, R. Wannemacher, W. Grill
Phase-sensitive acoustic microscopy of polymer thin films
Ultrasonics **42**, 983-987 (2004)

W. Ngwa, S. Knauth, C. Laforsch, W. Grill
Precision measurement of acoustic reflectivity for a scanning acoustic microscope that measures amplitude and phase: Applicability in biology
Proc. IEEE **5394**, 233 (2004)

W. Ngwa, R. Wannemacher, W. Grill, A. Serghei, F. Kremer, T. Kundu
Voronoi Tessellations in Thin Polymer Blend Film
Macromolecules **37**, 1691-1692 (2004)

Christian Laforsch, Wilfred Ngwa, Wolfgang Grill, Ralph Tollrian
An acoustic microscopy technique reveals hidden morphological defenses in Daphnia
Proc. Nat. Acad. Sci. **101**, 15911-15914 (2004)

B. Möller, M.V. Artemyev, U. Woggon, R. Wannemacher
Photonic molecules doped with semiconductor nanocrystals
Phys. Rev. B **70**, 115323 (2004)

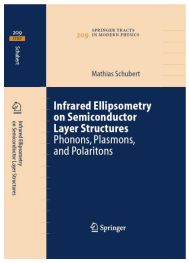

M. Schubert
Infrared Ellipsometry on Semiconductor Layer Structures: Phonons, Plasmons and Polaritons
Springer Tracts in Modern Physics, Vol 209 (Springer, Heidelberg, 2004) ISBN 3-540-23249-4

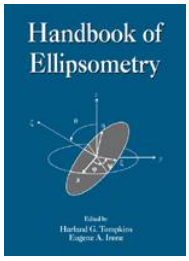

M. Schubert
Theory and Application of Generalized Ellipsometry
In Handbook of Ellipsometry edited by G.E. Irene and H.G. Tompkins (Springer, Heidelberg, 2004) ISBN: 3-540-22293-6

N. Ashkenov, M. Schubert, E. Twerdowski, B.N. Mbenkum, H. Hochmuth, M. Lorenz, H. v. Wenkstern, M. Grundmann
Asymmetric ferroelectric polarization loops and offsets in Pt-BaTiO3-ZnO-Pt thin film capacitor structures
Thin Solid Films XXX, XXXX (2005)

V. Darakchieva, E. Valcheva, P.P. Paskov, M. Schubert, T. Paskova, B. Monemar, H. Amano, and I. Akasaki
Phonon mode behavior of wurtzite AlN/GaN superlattices
Phys. Rev. B XX, XXXX (2005)

B.N. Mbenkum, N. Ashkenov, M. Schubert, M. Lorenz, H. Hochmuth, D. Michel, M. Grundmann
Temperature-dependent dielectric and electro-optic properties of ZnO-$BaTiO_3$-ZnO heterostructures grown by pulsed laser deposition
Appl. Phys. Lett. 86, 091904 (2005)

V. Darakchieva, T. Paskova, P.P. Paskov, B. Monemar, N. Ashkenov, M. Schubert
Structural characteristics and lattice parameters of HVPE-GaN free-standing quasi-substrates
J. Appl. Phys. 97 013517 (2005

M. Schubert, T. Hofmann, J. Sik
Long-wavelength interface modes in semiconductor layer structures
Phys. Rev. B 71 035324 (2005)

V. Darakchieva, P. Paskov, E. Valcheva, T. Paskova, M. Schubert, C. Bundesmann, H. Lu, W.J. Schaff, B. Monemar
Infrared Ellipsometry and Raman Studies of hexagonal InN films: correlation between strain and vibrational properties
Superlattices and Microstructures 36, 573 - 580 (2004)

T. Hofmann, M. Schubert, C. von Middendorff, G. Leibiger, V. Gottschalch, C.M. Herzinger, A. Lindsay and E. O Reily
The inertial-mass scale for free-charge-carriers in semiconductor heterostructures
Proceedings of the 27th International Conference on Semiconductor Physics, Flagstaff, 2004

C. Bundesmann, M. Schubert, N. Ashkenov, M. Grundmann, G. Lippold, and J. Piltz
Combined Raman scattering, X-ray fluorescence and ellipsometry in-situ growth monitoring of $CuInSe_2$-based photoabsorber layers on polyimide substrates
Proceedings of the 27th International Conference on Semiconductor Physics, Flagstaff, 2004

R. Schmidt-Grund, D. Fritsch, M. Schubert, B. Rheinländer, H. Schmidt, H. Hochmuth, M. Lorenz, C.M. Herzinger, and M. Grundmann
Band-to-band transitions and optical properties of $Mg_xZn_{1-x}O$ ($0 \leq x \leq 1$) films
Proceedings of the 27th International Conference on Semiconductor Physics, Flagstaff, 2004

A. Kasic, D. Gogova, H. Larsson, C. Hemmingsson, I. Ivanov, B. Momenar, C. Bundesmann, M. Schubert
Micro-Raman scattering profiles studies on HVPE-grown free-standing GaN
phys. stat. sol. (a) 201 2773 - 2775 (2004)

C. Bundesmann, M. Schubert, A. Rahm, D. Spemann, H. Hochmuth, M. Lorenz, M. Grundmann
Infrared dielectric function and phonon modes of Mg-rich cubic MgZnO thin films on sapphire
Appl. Phys. Lett. 85, 905 (2004)

V. Darakchieva, J. Birch, M. Schubert, A. Kasic, S. Tungasmita, T. Paskova, B. Monemar
Strain related structural and vibrational properties of thin epitaxial AlN layers
Phys. Rev. B 70, 045511 (2004)

J. Kvietkova, B. Daniel, M. Hetterich, M. Schubert, D. Spemann, D. Litvinov, D. Gerthsen
Near-band-gap dielectric function of $Zn_{1-x}Mn_xSe$ thin films determined by spectroscopic ellipsometry
Phys. Rev. B 70, 045316 (2004)

V. Darakchieva, P.P. Paskov, E. Valcheva, T. Paskova, B. Monemar, M. Schubert, H. Lu, W.J. Schaff
Deformation potentials of the E_1(TO) and E_2 modes of InN
Appl. Phys. Lett. 84, 3636 (2004)
Nils-Krister Persson, M. Schubert, O. Inganäs
Optical modelling of a layered photovoltaic device with a polyfluorene-copolymer as the active layer
Solar Energy Materials and Solar Cells 83, 169 - 186 (2004)

J. Kvietkova, B. Daniel, M. Hetterich, M. Schubert, D. Spemann, P. Pfundstein, and D. Gerthsen
Optical properties of $Zn_{1-x}Mn_xSe$ epilayers determined by spectroscopic ellipsometry
Thin Solid Films 455-456, 228 - 230 (2004)

O.P.A. Lindquist, M. Schubert, H. Arwin, K. Järrendahl
Infrared to vacuum ultraviolet optical properties of 3C, 4H and 6H silicon carbide measured by spectroscopic ellipsometry
Thin Solid Films 455-456, 235 - 238 (2004)

L.M. Karlsson, M. Schubert, N. Ashkenov, H. Arwin
Protein adsorption in porous silicon gradients monitored by spatially-resolved spectroscopic ellipsometry
Thin Solid Films 455-456, 726 - 730 (2004)

G. Leibiger, V. Gottschalch, N. Razek, M. Schubert
Hydrogen implantation in InGaNAs studied by spectroscopic ellipsometry
Thin Solid Films 455-456, 231 - 234 (2004)

R. Schmidt-Grund, M. Schubert, B. Rheinländer, D. Fritsch, H. Schmidt, E.M. Kaidashev, M. Lorenz, C.M. Herzinger, M. Grundmann
UV-VUV spectroscopic ellipsometry of ternary $Mg_xZn_{1-x}O$ ($0 < x < 0.53$) thin films
Thin Solid Films 455-456, 500 - 504 (2004)

T. Hofmann, M. Schubert, V. Gottschalch
Far-infrared dielectric function and phonon modes of spontaneously ordered $(Al_xGa_{1-x})_{0.52}In_{0.48}P$
Thin Solid Films 455-456, 601 - 604 (2004)

M. Schubert, T. Hofmann, C.M. Herzinger, W. Dollase
Generalized ellipsometry for orthorhombic absorbing materials: Dielectric functions, phonon modes and band-to-band transitions of Sb_2S_3
Thin Solid Films 455-456, 619 - 623 (2004)

C. Bundesmann, N. Ashkenov, M. Schubert, A. Rahm, H. v. Wenckstern, E.M. Kaidashev, M. Lorenz, M. Grundmann
Infrared dielectric functions and crystal orientation of a-plane ZnO thin films on r-plane sapphire determined by generalized ellipsometry
Thin Solid Films 455-456, 161 - 166 (2004)

M. Schubert, C. Bundesmann, G. Jakopic, H. Maresch, H. Arwin, N.-C. Persson, F. Zhang, O. Inganäs
Infrared ellipsometry characterization of conducting thin organic films
Thin Solid Films 455-456, 295 - 300 (2004)

M. Schubert, T. Hofmann, C.M. Herzinger
Far-infrared magnetooptic generalized ellipsometry: Determination of free-charge-carrier parameters in semiconductor thin film structures
Thin Solid Films 455-456, 563 - 570 (2004)

D. Gogova, A. Kasic, H. Larsson, B. Pécz, R. Yakimova, B. Magnusson, B. Monemar, F. Tuomisto, K. Saarinen, C.R. Miskys, M. Stutzmann, C. Bundesmann, M. Schubert
Optical and structural characteristics of virtually unstrained bulk-like GaN
Jpn. J. Appl. Phys. 43, 1264 - 1268 (2004)

M. Schubert, C. Bundesmann, H. v. Weckstern, G. Jakopic, A. Haase, N.-K. Persson, F. Zhang, H. Arwin, O. Inganäs
Carrier redistribution in organic/inorganic (PEDOT/PSS - Si) heterojunction
Appl. Phys. Lett. 84, 1311 - 1313 (2004)

V. Darakchieva, P.P. Paskov, M. Schubert, E. Valcheva, T. Paskova, H. Arwin, B. Monemar, H. Amano, I. Akasaki
Strain evolution and phonons in AlN/GaN superlattices
Mat. Res. Soc. Symp. 798, Y5.60 (2004)

M. Schubert, N. Ashkenov, T. Hofmann, H. Hochmuth, M. Lorenz, M. Grundmann, G. Wagner
Electro-optical properties of ZnO-$BaTiO_3$-ZnO heterostructures grown by pulsed laser deposition
Ann. Phys. 13, 61 - 62 (2004)

M. Schubert, C. Bundesmann, G. Jakopic, H. Maresch, H. Arwin
Infrared dielectric function and vibrational modes of pentacene thin films
Appl. Phys. Lett. 84, 200 - 202 (2004)

8.19 Graduations

PhD

Dipl.-Phys. Martin Schubert
3D-Ultraschallmikroskopie
Neue Möglichkeiten der akustischen konfokalen Mikroskopie mit Amplituden- und Phasenkontrast

Dipl.-Phys. Tino Hofmann
Far-infrared Ellipsometry on AIII-BV Semiconductor Heterostructures

Dipl.-Phys.

Claas von Middendorff
Magnetooptische Ellipsometrie an freien Ladungsträgern in Halbleiterschichtstrukturen

M.Sc.

Albert Kamanyi, B.Sc.
Combinatory Phase-Sensitive Acoustic and Confocal Scanning Microscopy

Beri N. Mbenkum, B.Sc.
Temperature Dependent Electro-Optic and Dielectric Properties of a Novel Wurtzite-Perovskite Heterostructure Grown by Pulsed Laser Deposition

B.Sc.

Shouwei Dong
Stress Detection in Bolts by Ultrasound

8.20 Guests

Prof. Tribikram Kundu, Humboldt Prize Winner
1 month

Dr. Mietek Pluta
Technical University of Wroclaw, Poland
1 month

8.21 Awards

Best Paper Award at SPIE's 9^{th} Annual International Symposium on NDE for Health Monitoring and Diagnostics, San Diego, USA, March 14^{th}-18^{th}, 2004
Presentation:
W. Ngwa, W. Grill, T. Kundu
Bio-soft matter imaging and micro-metrology by phase-sensitive ultrasonic microscopy

9

Superconductivity and Magnetism

9.1 Introduction

Research into the basic properties of ferromagnetic and superconducting materials has a long-standing tradition. The present focus of the Division of Superconductivity and Magnetism is on two branches of contemporary magnetism: (1) magnetic and transport phenomena in carbon-based materials and (2) oxide spin-electronics.

After the discovery of ferromagnetism in proton-irradiated graphite in the year 2003 (see P. Esquinazi *et al.*, Phys. Rev. Lett. **91**, 227201 (2003)) through an intensive cooperation between our group and the Division of Nuclear Solid State Physics, we have continued studying the effects on the magnetism of amorphous carbon and fullerene films produced by irradiation. We were able to produce magnetic microstructures on pure graphite surfaces. This research is extended to other carbon-based structures. To study a magnetic proximity effect in graphite, we have performed magnetization as well as magnetotransport measurements on magnetite/graphite/disordered carbon films. The study of the transport properties of graphite has been extended to the magnetothermal properties, especially the thermal conductivity and the Nernst effect.

In the field of oxide spin-electronics research is focused on the study of magnetotransport processes at interfaces. Future aims of this project are the study of magnetic oxide nanocontacts and the fabrication of spin-transistors.

P. Esquinazi

9.2 Ferromagnetism and Transport Properties of Carbon Structures

9.2.1 Quantitative determination of the magnetization of proton irradiated spots in graphite with magnetic force microscopy

K.-H. Han, P. Esquinazi

Using the point probe approximation of magnetic force microscopy (MFM) and measurements of the MFM signal as a function of the tip-to-sample distance, we have determined quantitatively the magnetization of proton irradiated spots in highly oriented pyrolytic

graphite. Although with a large error due to uncertainties in certain parameters, the order of magnitude of the magnetization is in the same range as those from soft magnetic materials, i.e. of the order of 10^6 A/m. For details see J. Applied Physics **96**, 1581-1584 (2004).

9.2.2 Ferromagnetic Structures in Graphite and Amorphous Carbon Films Produced by High Energy Proton Irradiation

R. Höhne, P. Esquinazi, K.-H. Han, D. Spemann*, A. Setzer, U. Schaufuß, V. Riede†, T. Butz*, P. Streubel†, R. Hesse†

* Nuclear Solid State Physics Group

† Wilhelm-Ostwald Institute for Physical and Theoretical Chemistry

In this study ferro- (or ferri-)magnetic structures were created both in highly oriented pyrolitic graphite and in amorphous carbon films by proton irradiation. For this purpose spots of diameters of the order of 1 μm and 0.8 mm were irradiated with ion doses ranging from 0.05 nC/μm^2 to 75 nC/μm^2 using a 2.25 MeV proton beam. Measurements performed with magnetic force microscopy and a superconducting quantum interferometer device (SQUID) reveal that the magnetic ordering is stable at room temperature. Raman measurements and X-ray photoelectron spectroscopy were also used for sample characterization before and after the irradiation. Our results reveal induced ferromagnetism by proton irradiation in pure carbon. For more details see Proceedings of the 16. International Conference of Soft Magnetic Materials (ISBN 3-514-00711-X) edited by D. Raabe, 185 (2004).

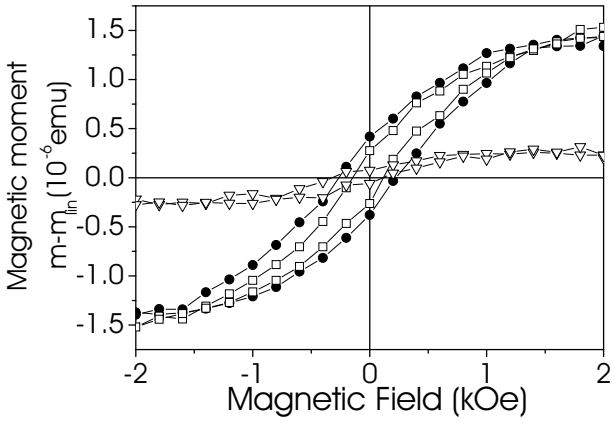

Figure 9.1: The magnetic moment (in units of 10^{-6} emu = 10^{-9} Am^2) of the carbon film after subtraction of the linear diamagnetic part as a function of magnetic field by cycling the field between +2 kOe and –2 kOe for the amorphous film before proton irradiation ($\bigtriangledown$, 8 spots with 0.8 mm diameter and 150 μC total charge each) at T = 300 K and after irradiation ($\bullet, \square$) at T = 5 K and T = 300 K, respectively.

9.2.3 Magnetothermal Transport of Oriented Graphite at Low Temperatures

K. Ulrich, P. Esquinazi

We have studied the magnetic field dependence of the thermal conductivity $\kappa(T, B)$ of highly oriented pyrolytic graphite samples at temperatures $0.2\,\mathrm{K} \leq T < 10\,\mathrm{K}$ and fields $0\mathrm{T} \leq B \leq 9\,\mathrm{T}$. The samples show clear deviations from the Wiedemann-Franz law with a kink behaviour at fields $B \sim 0.1\,\mathrm{T}$ near the metal-insulator transition observed in electrical resistivity measurements. We further show that the oscillations in the thermal conductivity at the quantum limit $B > 1\,\mathrm{T}$, which are correlated with the Landau quantization observed in Hall measurements, increase in amplitude with temperature following a $\sim T^3$ law at $T > 0.2\,\mathrm{K}$ and show a maximum at $T \sim 6\,\mathrm{K}$, suggesting that they are phonon-mediated. For details see J. Low Temp. Phys. **137**, 217-231 (2004).

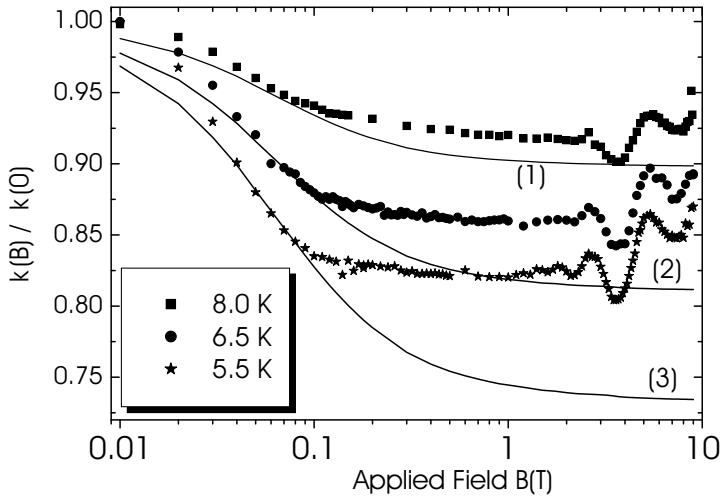

Figure 9.2: Normalized thermal conductivity as a function of applied field at different constant temperatures of a Union Carbide HOPG sample. The continuous lines (1) to (3) are calculated using the Wiedemann-Franz (WF) law (assuming that the phonon conductivity does not depend on magnetic field) and the measured in-plane electrical resistivity at 8.0 K, 6.5 K and 5.5 K, respectively. The measurements for this sample show a clear kink at a field of $B \sim 0.1\,\mathrm{T}$, which is near the field at which the Metal-Insulator Transition occurs. At this field a clear deviation from the WF expected behaviour is clearly seen.

9.3 Microstructure and Magnetic Properties of Magnetite Thin Films Produced by PLD

A. Bollero, M. Ziese, R. Höhne, H.-C. Semmelhack, A. Setzer, P. Esquinazi

The pulsed laser deposition technique has been used to produce magnetite (Fe_3O_4) films with thickness ranging from 26 to 320 nm grown on $MgAl_2O_4$ (001) and MgO (001) substrates. Microstructural characterization of the films has revealed enlarged grains with increasing thickness, i.e. deposition time. Magnetization hysteresis loops have been measured at different temperatures in the range 25 – 300 K for various samples. The evolution

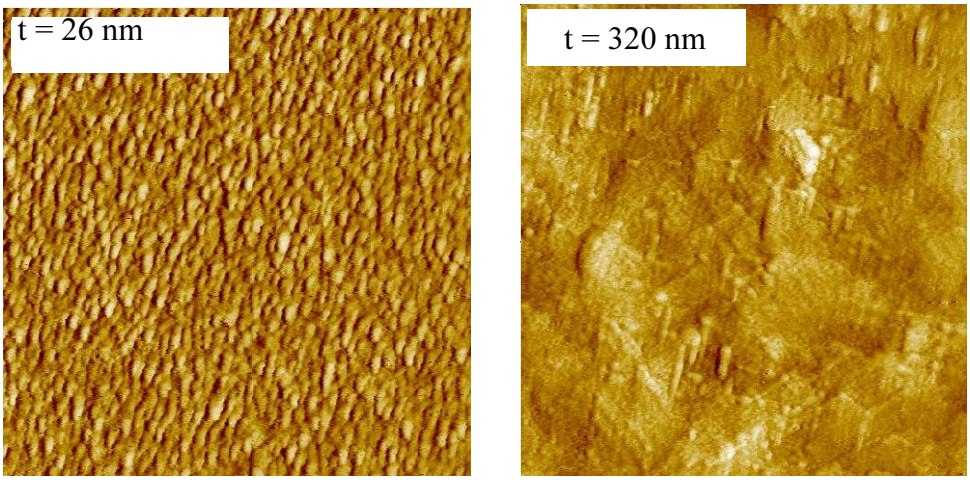

Figure 9.3: STM images of a 26 and a 320 nm thick magnetite film on $MgAl_2O_4$.

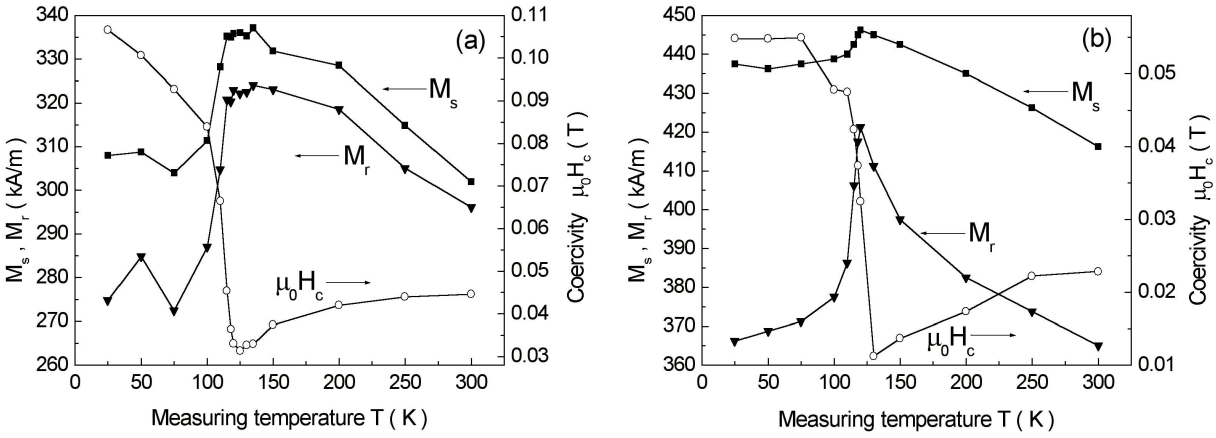

Figure 9.4: Dependence of the magnetic properties on temperature for (a) 26 nm and (b) 320 nm thick Fe_3O_4 films grown on $MgAl_2O_4$ (001) substrates.

of the remanence and the coercivity with temperature shows significant differences depending on film thickness. This can be understood in terms of the effect of the interfacial strain as well as the influence of the deposition time on the grain sizes and the variation in the density of antiphase boundaries. All films studied exhibit a minimum of the coercivity at about 130 K, the temperature at which the magnetocrystalline anisotropy constant K_1 vanishes for bulk material.

9.4 Magnetoresistance in Bi-Crystal Fe_3O_4 Thin Films

A. Bollero, M. Ziese, P. Esquinazi, K. Dörr*, I. Mönch*

*Institute for Metallic Materials, IFW Dresden

An epitaxial magnetite film has been deposited by pulsed laser deposition on a bi-crystal MgO substrate with a tilt angle of 24°. Magnetoresistance measurements on patterned stripes (width = 20 μm) across the bi-crystal grain boundary have not revealed a distin-

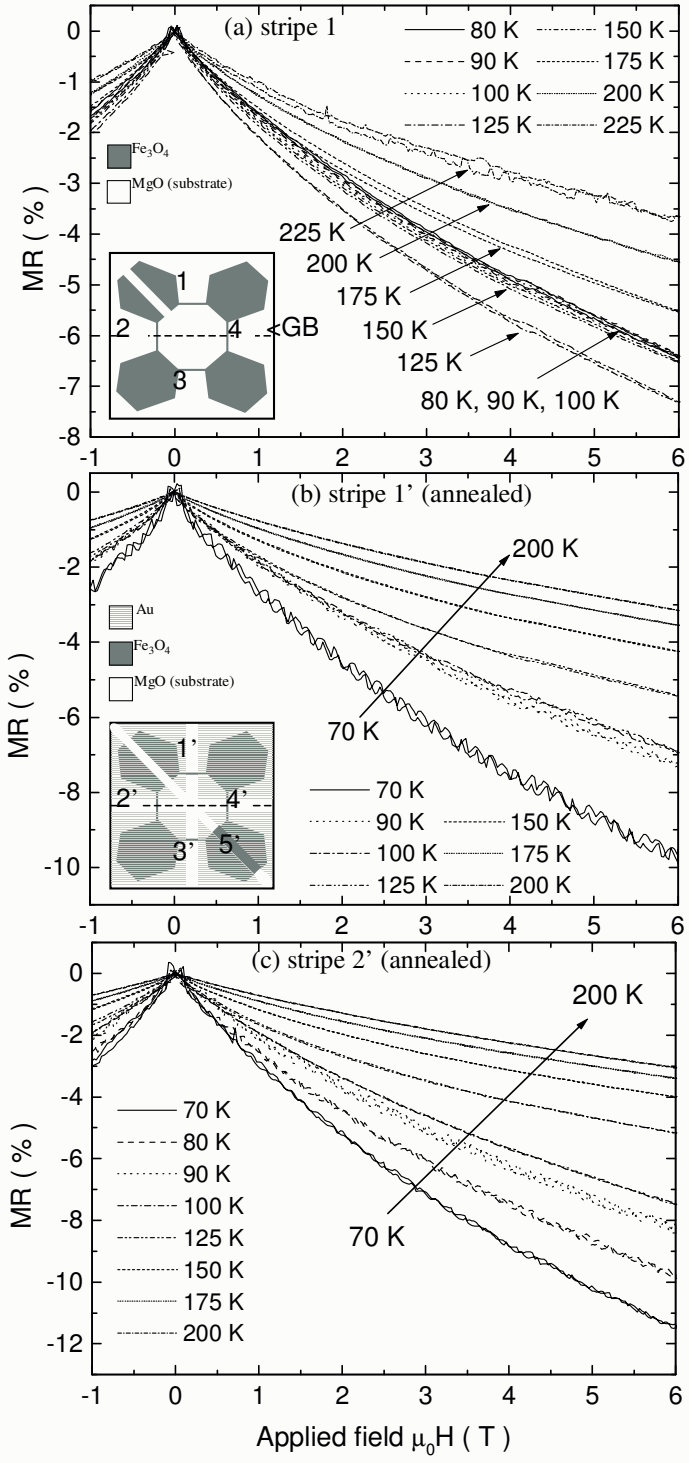

Figure 9.5: Magnetoresistance for: (a) stripe 1; (b) stripe 1' (after annealing); (c) stripe 2' (after annealing). The insets show the sample geometry.

guishable grain boundary contribution in the as-deposited film. Post-annealing of the film has a strong influence on the relaxation degree of the film and on the density of antiphase boundaries. Magnetotransport measurements of the micrometer patterned annealed film show significantly enlarged high-field magnetoresistance values at low temperatures.

9.5 Structural, Magnetic and Magnetotransport Properties of $La_{0.67}Sr_{0.33}MnO_3$ Powder Compacts

M. Ziese, A. Bollero, I. Panagiotopoulos*, N. Moutis†

* Department of Materials Science and Engineering, University of Ioannina, Greece
† Institute of Materials Science, NCSR "Demokritos", Athens, Greece

The structural, magnetic and magnetotransport properties of a series of $La_{2/3}Sr_{1/3}MnO_3$ powder samples with different grain sizes produced by high energy ball milling were studied. The magnetoconductivity shows a typical low field contribution superimposed on a linear high field dependence. In grain sizes of several microns the field value H_P at which the conductivity is minimized is substantially larger than the coercive field H_C indicating that the process of interfacial spin alignment which governs the magnetoconductive response is decoupled from that in the bulk of the grain which defines the magnetization hysteresis. In intensively milled samples, having grain sizes approaching the single domain size, the values of H_P and H_C converge and the low field magnetoconductivity scales with $(1/3)(M/M_S)^2$, M_S being the saturation magnetization.

The magnetoconductance was calculated in a model based on inelastic tunnelling via Mn sites situated in the tunneling barrier. This model satisfactorily accounts for the strong decrease of the low field magnetoconductance as a function of temperature due to spin depolarization in the inelastic tunnelling processes.

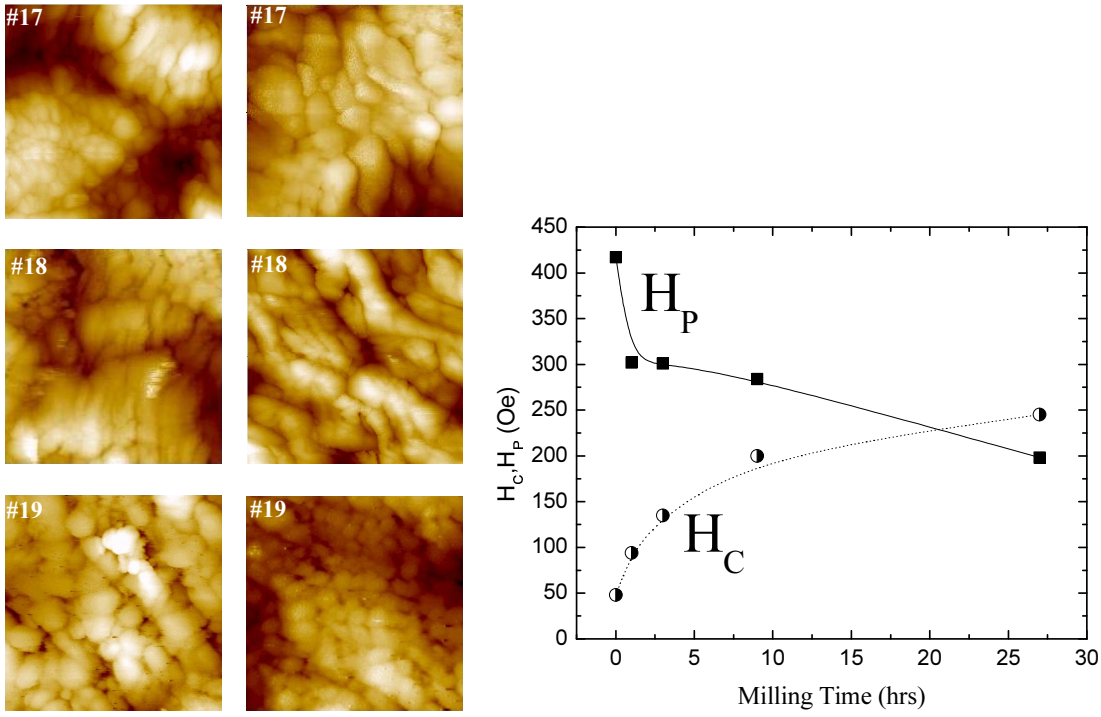

Figure 9.6: (Left) STM images of samples #17 (milling time 3 h), #18 (9 h) and #19 (27 h). Scan area was $250\times250\,nm^2$. (Right) Coercivity H_C of the magnetic hysteresis loop and field value H_P at the minimum of the magnetoconductance curve as a function of milling time.

9.6 Studies of Flux Creep in $YBa_2Cu_3O_7$ Rings Using AC-Susceptibility

K. Schindler, M. Ziese, P. Esquinazi, H. Hochmuth*, M. Lorenz*, K. Zimmer†, E.H. Brandt‡

*Semiconductor Physics Group

†Institute for Surface Modification, Leipzig

‡Max-Planck-Institut für Metallforschung, Stuttgart

The critical current density and flux-creep activation energy of $YBa_2C_3O_7$ rings were determined from ac-susceptibility measurements. A novel approach was developed theoretically and experimentally to derive the flux-creep exponent from higher susceptibility harmonics. An alternative method using a scaling approach yielded similar sample-to-sample variations, but qualitatively different values for the flux-creep exponent. This might be related to the limits of validity of the logarithmic approximation to the flux-line activation energy that is commonly used in calculations.

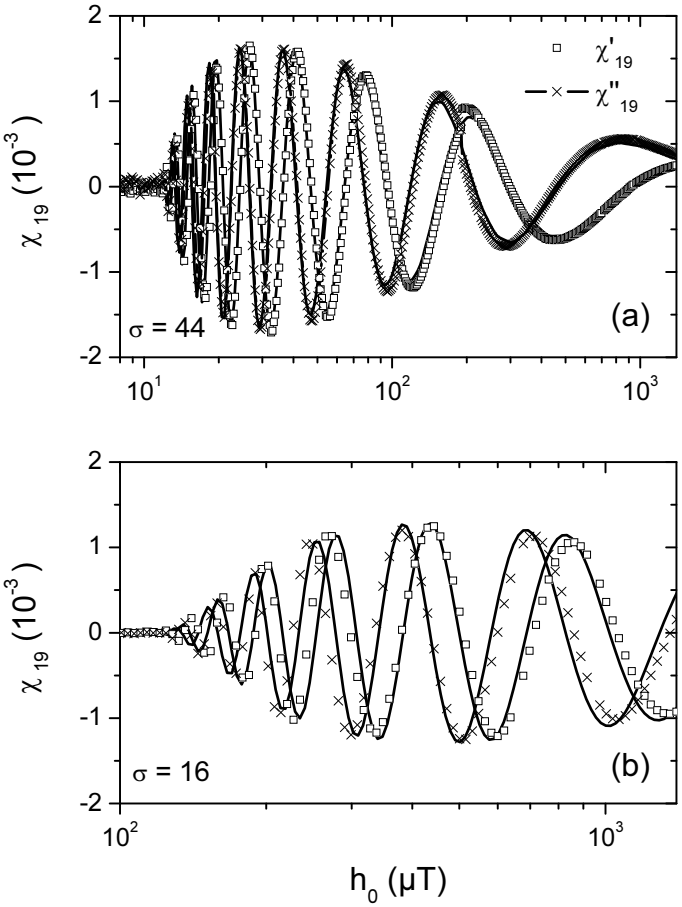

Figure 9.7: Measured in- and out-of-phase component of the 19th harmonic susceptibility of (a) ring 01 (diameter 1 mm, width 55 µm, thickness 260 nm) at 79.4 K and (b) ring 03 (diameter 1 mm, width 102 µm, thickness 260 nm) at 83.7 K. The solid lines were calculated numerically including the effects of flux creep on the ac-susceptibility. σ indicates the non-linearity of the current voltage characteristics with $V \propto I^{\sigma+1}$.

9.7 Funding

Wechselspiel zwischen Supraleitung und Magnetismus in Graphit und in ungeordneten Metallen
Prof. P. Esquinazi
DFG ES 86/6-3

The origin of carbon-based magnetism and the role of hydrogen
Prof. P. Esquinazi
DFG ES 86/11-1

Magnetotransport in Oxide Thin Film Systems
Prof. P. Esquinazi
Dr. M. Ziese
DFG Es 86/7-4
within Forschergruppe FOR 404 "Oxidic interfaces"

Oxidische Heterostrukturen für die Spin-Elektronik
Dr. M. Ziese
DAAD D/03/43168

9.8 Organizational Duties

Pablo Esquinazi

- Project Reviewer: Deutsche Forschungsgemeinschaft (DFG), National Science Foundation (USA), German-Israeli Foundation
- Referee: Phys. Rev. Lett, Phys. Rev. B., Physica C, Phys. Lett. A, phys. stat. sol., J. Low Temp. Phys., Carbon, J. Chem. Phys., Eur. J. Phys. B, J. Magn. Magn. Mater.

Roland Höhne

- Referee: phys. stat. sol., Thin Solid Films

Michael Ziese

- Project Reviewer: BSF (United States-Israel Binational Science Foundation)
- Referee: Phys. Rev. Lett., Phys. Rev. B., J. Phys. D: Appl. Phys., phys. stat. sol., J. Magn. Magn. Mater., Eur. J. Phys. B, Thin Solid Films

9.9 External Cooperations

Academic

State University of Campinas, Campinas, Brazil
Prof. Dr. Yakov Kopelevich

Umea University, Sweden
Dr. Tatiana Makarova

Universidad Autónoma de Madrid, Spain
Prof. Dr. Miguel Angel Ramos

Universidad Autónoma de Madrid, Spain
Prof. Dr. Sebastian Vieira

Institute for Metal Physics of National Academy of Sciences of Ukraine, Kiev, Ukraine
Prof. Dr. V. M. Pan

Institut für Oberflächenmodifizierung e.V., Leipzig
Dr. Klaus Zimmer

Universität Leipzig, Fakultät für Chemie und Mineralogie
Prof. R. Szargan

University of the Negev, Beer Sheva, Israel
Dr. Evgeny Rozenberg

Trinity College Dublin
Prof. Dr. J. M. D. Coey

IFW-Dresden, Germany
Dr. Kathrin Dörr

University of Ioannina, Greece
Dr. Ioannis Panagiotopoulos

National Center of Scientific Research "Demokritos", Greece
Dr. Nikos Moutis

Max-Planck-Institut für Metallforschung
Dr. E. H. Brandt

9.10 Publications

Journals

P. Esquinazi
Kann auch Kohlenstoff magnetisch sein?
Physik unserer Zeit **35**, 59 (2004).

P. Esquinazi, R. Höhne, K.-H. Han, A. Setzer, D. Spemann and T. Butz
Magnetic carbon: Explicit evidence of ferromagnetism induced by proton irradiation
Carbon **42**, 1213 (2004).

P. Esquinazi, M.A. Ramos and R. König
Acoustic Properties of Amorphous Solids at Very Low Temperatures: The Quest for Interacting Tunneling States
J. Low Temp. Phys. **135**, 27 (2004).

K.-H. Han, D. Spemann, P. Esquinazi, R. Höhne, V. Riede and T. Butz
Magnetic signals of proton irradiated spots created on highly oriented pyrolytic graphite surface
J. Magn. Magn. Mater. **272-276**, 1190 (2004).

K.-H. Han and P. Esquinazi
Quantitative determination of the magnetization of proton irradiated spots in graphite with magnetic force microscopy
J. Applied Physics **96**, 1581-1584 (2004).

R. Höhne, M. Ziese and P. Esquinazi
Searching for a magnetic proximity effect in magnetite-carbon structures
Carbon **42**, 3109 (2004).

R. Höhne, K.-H. Han, P. Esquinazi, A. Setzer, H.-C. Semmelhack, D. Spemann and T. Butz
Magnetism of pure, disordered carbon films prepared by pulsed laser deposition
J. Magn. Magn. Mater. **272-276**, e839 (2004).

U. Köhler, M. Ziese, A. Bollero, R. Höhne and P. Esquinazi
On the road to an all-oxide spin-transistor: study of magnetotransport properties of magnetite/Nb:STO interfaces
J. Magn. Magn. Mater. **272-276**, e1437 (2004).

R. Ocaña and P. Esquinazi
Quasiparticles in the mixed state of Y-123 crystals: what do we learn from thermal magnetoconductivity tensor results?
Physica C **408-410**, 716 (2004).

A.V. Pan and P. Esquinazi
Decoupling transition of two coherent vortex arrays within the surface superconductivity state
Phys. Rev. B **70**, 184510 (2004).

D. Spemann, K.-H. Han, P. Esquinazi, R. Höhne and T. Butz
Ferromagnetic microstructures in highly oriented pyrolytic graphite created by high energy proton irradiation
Nuclear Instruments and Methods in Physics Research B **219-220**, 886 (2004).

K. Ulrich and P. Esquinazi
Magnetothermal Transport of Oriented Graphite at Low Temperatures
J. Low Temp. Phys. **137**, 217 (2004).

M. Ziese
Two-parameter scaling of the Hall effect in manganites
phys. stat. sol. (b) **241**, R19 (2004).

M. Ziese, R. Höhne, H.-C. Semmelhack, K.-H. Han, P. Esquinazi and K. Zimmer
Magnetic and magnetotransport properties of magnetite films with step edges
J. Magn. Magn. Mater. **279**, 331 (2004).

E. Guzman, H. Hochmuth, M. Lorenz, H. von Wenckstern, A. Rahm, E.M. Kaidashev, M. Ziese, A. Setzer, P. Esquinazi, A. Pöppl, D. Spemann, R. Pickenhain, H. Schmidt and M. Grundmann
Pulsed laser deposition of Fe- and Fe, Cu-doped ZnO thin films
Annalen der Physik **13**, 57 (2004).

S.A. Krasnikov, A.S. Vinogradov, K.-H. Hallmeier, R. Höhne, M. Ziese, P. Esquinazi, T. Chassé and R. Szargan
Oxidation effects in epitaxial Fe_2O_3 layers on MgO and $MgAl_2O_4$ substrates studied by X-ray absorption, fluorescence and photoemission
Materials Science and Engineering B **109**, 207 (2004).

D.A. Luzhbin, A.V. Pan, V.A. Komashko, V.S. Flis, V.M. Pan, S.X. Dou and P. Esquinazi
Origin of paramagnetic magentization in field-cooled $YBa_2Cu_3O_{7-\delta}$ films
Phys. Rev. B **69**, 024506 (2004).

E. Rozenberg, V. Markovich, Ya. Yuzhelevskii, G. Gorodetsky and M. Ziese
Mesoscopic magnetotransport in thin $La_{0.7}Ca_{0.3}MnO_3$ / $SrTiO_3$ films
J. Appl. Phys. **95**, 7103 (2004).

R. Höhne, P. Esquinazi, K.-H. Han, D. Spemann, A. Setzer, U. Schaufuß, V. Riede, T. Butz, P. Streubel and R. Hesse
Ferromagnetic Structures in Graphite and Amorphous Carbon Films Produced by High Energy Proton Irradiation
Soft Magnetic Materials **16**, edited by D. Raabe, 185 (2004).

A.I. Shames, E. Rozenberg, G. Gorodetsky, and M. Ziese, EMR study of thin $La_{0.7}Ca_{0.3}MnO_3$ films epitaxially grown on $SrTiO_3$
in Nanostructured Magnetic Materials and Their Applications
edited by B. Aktas, L. Tagirov and F. Mikailov
Kluwer Academic Publishers, Netherlands, (2004) 205-212.

in press

M. Ziese, A. Bollero, I. Panagiotopoulos and N. Moutis
Grain-boundary magnetoconductance and inelastic tunnelling
Phys. Rev. B.

I. Panagiotopoulos, N. Moutis, M. Ziese and A. Bollero
Magnetoconductunce and Hysteresis in milled $La_{0.77}Sr_{0.33}MnO_3$ powder compacts
J. Magn. Magn. Mater.

M. Ziese, U. Köhler, A. Bollero, R. Höhne and P. Esquinazi
Schottky-barrier and spin-polarization at the Fe_3O_4-Nb:$SrTiO_3$ interface
Phys. Rev. B.

M Ziese
Study of the micromagnetic structure of a $La_{0.7}Sr_{0.3}MnO_3$ film
J. Magn. Magn. Mater.

M. Ziese, U. Köhler, R. Höhne, A. Bollero and P. Esquinazi
Schottky barrier formation at the Fe_3O_4/Nb:$SrTiO_3$ interface
J. Magn. Magn. Mater.

A. Bollero, M. Ziese, P. Esquinazi, K. Dörr and I. Mönch
Magnetoresistance in bi-crystal Fe_3O_4 thin films
J. Magn. Magn. Mater.

M. Ziese, R. Höhne, A. Bollero, H.-C. Semmelhack, P. Esquinazi and K. Zimmer
Magnetic domain structure dependence of the exchange-bias field in exchange-coupled ferrimagnetic bilayers
Eur. J. Physics B.

K. Schindler, M. Ziese, P. Esquinazi, H. Hochmuth, M. Lorenz, K. Zimmer and E.H. Brandt
A novel method for the determination of the flux-creep exponent from higher harmonic ac-susceptibility measurements
Physica C **417**, 141 (2005).

A. Bollero, M. Ziese, R. Höhne, H.-C. Semmelhack, U. Köhler, A. Setzer and P. Esquinazi
Influence of thickness on microstructural and magnetic properties in Fe_3O_4 thin films produced by PLD
J. Magn. Magn. Mater. **285**, 279 (2005).

Invited Talks

Magnetic Carbon
P. Esquinazi
February 2004, Osaka University, Osaka, Japan

February 2004, Transport properties of Graphite: An overview of the experimental evidence
P. Esquinazi
Osaka University, Osaka, Japan

Induced Magnetic Ordering by Ion Irradiation in Carbon-based Samples
P. Esquinazi
14. 07. 2004, Keynote lecture, Carbon 2004, Brown University, Providence, USA

Quantum Hall Effect in Highly Oriented Pyrolytic Graphite
P. Esquinazi
13. 07. 2004, Carbon 2004, Brown University, Providence, USA

Magnetism in Carbon Structures
P. Esquinazi
10. 09. 2004, Tutorial talk at the Joint European Magnetic Symposia, Dresden

Orden Magnetico en carbon, el ferromagnetico del siglo XXI
P. Esquinazi
24. 09. 2004, Facultad de Ciencias, Universidad de Chile, Santiago

Magnetismo en estructuras de carbono
P. Esquinazi
01. 10. 2004, Facultad de Ciencias Fisicas y Matematicas, Universidad de Chile, Santiago

Magnetische Ordnung in Kohlenstoff
P. Esquinazi
6. 10. 2004, FAHL Academy on Magnetic Semiconductors, Wörlitz

Spin-Electronics in magnetic oxides and carbon: results, bottlenecks and challenges
M. Ziese
February 2004, University of Osaka, Japan.

Spin-dependent Transport Properties of Magnetic Oxides
M. Ziese
7. June 2004, University of Kent, Canterbury, United Kingdom.

Extrinsic Magnetoresistance Phenomena in Magnetic Oxides
M. Ziese
2. Juli 2004, Universität zu Köln

Spin-dependent Transport
M. Ziese
6. August 2004, University of Sheffield, Sheffield, United Kingdom

Spin-abhängige Transporteigenschaften in magnetischen Oxiden
M. Ziese
6. October 2004, FAHL Academy on Magnetic Semiconductors, Wörlitz

9.11 Graduations

PhD

Dipl. Phys. Heiko Kempa
Der Metall-Isolator-Übergang in hochorientiertem pyrolytischem Graphit

Roberto Ocaña
Thermal Conductivity Tensor in $YBa_2Cu_3O_{7-x}$

Diploma

Uwe Schaufuß
Herstellung von amorphen Kohlenstoffschichten mittels PLD und Charakterisierung mit Widerstandsmessungen

Konstantin Ulrich
Thermomagnetische Transporteigenschaften von Graphit bei tiefen Temperaturen

Kristian Schindler
Untersuchungen zum Nernst-Effekt von hochorientiertem pyrolytischem Graphit

M.Sc.

Andreas Glaser
Noise Measurements on Magnetite

9.12 Guests

Prof. Dr. Yakov Kopelevich
Mercator Visiting Professorship
State University of Campinas, Campinas, Brazil
01. 02. 2004 – 31. 07. 2004

Dimitrii Medvedev
University of Minsk, Belorussia
02. 07. 2004 – 24. 09. 2004

Supasit Appiwattanapong
University of Bangkok, Thailand
30. 09. 2004 – 30. 12. 2004

Dr. Ioannis Panagiotopoulos
University of Ioannina, Greece
20. 06. 2004 – 27. 06. 2004

Dr. Nikos Moutis
National Center of Scientific Research "Demokritos", Greece
20. 06. 2004 – 27. 06. 2004

Prof. Dr. Alexander Gerber
Tel Aviv University, Israel
02. 09. 2004 – 05. 09. 2004

Dr. Evgeny Rozenberg
Beer Sheva University, Israel
11. 09. 2004 – 13. 09. 2004

III

Institute for Theoretical Physics

10

Introduction

The aim of the research at the Institute for Theoretical Physics (ITP) is to explore the theoretical and mathematical fundamentals of physics. The key areas of research are the theory of elementary particles and the theory of condensed matter, which fruitfully interact with each other. Fundamental problems of the structure of space, time and matter (from the smallest conceivable unit of length up to cosmic dimensions) are examined and practical problems of complex physical systems with mesoscopic dimensions are tackled.

The institute consists of the following research groups:

- **Quantum Field Theory (QFT)** –fundamental problems of mathematical physics, general structure of gauge theories, primary and effective interactions of elementary particles.
- **Particle Physics Group (TET)** –quantum field theory of elementary particles, supersymmetrical theories, quantum chromodynamics, lattice gauge theory.
- **Theory of Condensed Matter (TKM)** –noise-induced phenomena, structure formation in liquid crystals, non-linear dynamics in biological models, immune system, strongly coupled electron systems.
- **Computer-Oriented Quantum Field Theory (CQT)** –computer simulations of phase transitions and critical phenomena, physics of soft matter and disordered systems, quantum magnets.
- **Molecule Dynamics/Computer Simulation (MDC)** –computer simulations of molecules at interfaces, computations of structural data, studies of thermodynamic parameters and transport coefficients.
- **Statistical Physics (STP)** –interacting many-particle systems, statistical and quantum-field theoretical methods.

In the respective chapters,for each group a short overview of the research profile is followed by extended abstracts describing their most relevant current projects. Added is a subsection devoted to the Graduate Studies Programme "Quantum Field Theory", which plays an important integrating rôle not only within the ITP, but also for the scientific interaction with the Department of Mathematics and Computer Sciences and the Max-Planck Institute for Mathematics in the Sciences (MIS). In addition the research groups of the ITP take part in many of the interdisciplinary research projects of the Centre for

Theoretical Sciences (NTZ) which is part of the Centre of Advanced Studies (ZHS) of the University of Leipzig. The publications of members of the ITP of the year 2004 and organizational activities of ITP members are also listed at the level of each group.

K. Sibold
March 2005

11

Quantum Field Theory

11.1 Local Approach to Vacuum Polarization

D. Vassilevich

The heat kernel approach provides the opportunity to investigate locally properties of models in quantum field theory which are due to global properties of the underlying manifold. The investigation focused on the Dirac operator on a manifold with local boundary conditions. The boundary contributions to the chial anomly have been calculated in two and in four dimensions [1]. Furthermore the asymptotics of the Laplace operator has been investigated on a noncommutative torus. The coefficients are integral invariants and can be expressed in terms of polynomials with Moyal product [2]. Eventually the spectrum of the quantum fluctuation had been investigated in the noncommutative case. It turned out that the noncommutativity of space-time tends to create an infinite number of bound states [3]. We have also extended our analysis of the heat kernel to curved noncommuative manifolds and calculated leading terms in the heat kernel expansion and a noncommutative Polyakov action in two dimension [4]. In [5] a canonical method was suggested which allows to define the notion of first-class constraints and to find explicitely the gauge transformations in space-time noncommuative theories. We analysed [6] quantum field theory on non-smooth backgrounds and found an analytic expression for the Casimir energy densities in the large-mass expansion. The paper [7] reviews various boundary value problems which appear in the context of quantum field theory.

[1] V.N. Marachevsky and D.V. Vassilevich, Nucl. Phys. B **677** (2004) 535.
[2] D.V. Vassilevich, Lett. Math. Phys. **67** (2004) 185.
[3] D.V. Vassilevich and A. Yurov, Phys. Rev. D **69** (2004) 105006.
[4] D.V. Vassilevich, hep-th/0406163; to appear in Nucl. Phys. B
[5] D.V. Vassilevich, hep-th/0502120; to appear in Theor. Math. Phys.
[6] M. Bordag and D.V. Vassilevich, Phys. Rev. D **70** (2004) 045003.
[7] D.V. Vassilevich, Contemp. Math. **366** (2005) 3

11.2 Higher Order Correlation Corrections to Color Ferromagnetic Vacuum State at Finite Temperature

M. Bordag, A. Strelchenko

Topic of the investigation is the stability of the ground state of QCD with temperature and color magnetic magnetic background field by means of the calculation fo the polarization tensor of the gluon field. Special attention was payed to the spontaneous creation of a color magnetic field. Within the work on his PhD-thesis A. Strelchenko calculated the polarization tensor for color neutral gluons at high temperature and investigated its contribution to the effective action. By M. Bordag and V. Skalozub the investigation of the polarization tensor for the color charged gluons was started. Different gauge fixing conditions have been considered and the general structure of the polarization tensor had been clarified.

[1] V.V. Skalozub and A.V. Strelchenko, Eur. Phys. J. C **40** (2005) 121 [arXiv:hep-ph/0408030].

11.3 Spectral Zeta Functions and Heat Kernel Technique in Quantum Field Theory with Nonstandard Boundary Condition

M. Bordag

Spectral zeta function and heat kernel are the most important instruments for the investigation of the ultraviolettproerties of vacuum energy. For a number of boundary condition, for instnce if the leading ymbol of the differential operator is not simple or if the ellipticity of the operator is lost, there is so far no general pprocedure to btain the coefficinets. In this project we try to adopt the method of integral equattion for these prolems. For the case of a dielectric body with differeent speeds of light on both sides a system of integral equations was derived and a special case was investigated in detail.

[1] I.G. Pirozhenko, V.V. Nesterenko and M. Bordag, arXiv:hep-th/0409289, to appear in JMP

11.4 Quantization of Electrodynamics with Boundary Conditions

M. Bordag

The quantization of electrodynamics with boundary conditions was reconsidered. It was shown that the conductor boundary conditions do not provide a unique realisation. Especially, it was shown that there exists a realization where the normal component of the electric field on the boundary does not obey any condition. Measurable consequences had been found in the Casimir-Polder force which appears reduced by about 13 % in that case.

[1] M. Bordag, Phys. Rev. D **70** (2004) 085010.

11.5 Casimir Effect and Real Media

M. Bordag, B. Geyer

The vacuum of quantum fields shows a response to changes in external conditions with measurable consequences. The investigation of the electromagnetic vacuum in the presence of real media is of actual interest in view of current experiments as well as nanoscopic electro-mechanical devices [1]. In recent experiments using atomic force microscopy the Casimir effect had been measured with high accuracy. This required a detailed investigation of the influence of real experimental structures on the corresponding force.

Using the surface impedance approach the Lifschitz formula for the free energy and the Casimir force between real metals was derived in perfect agreement with thermodynamics; thereby a longstanding controversy had been resolved [2]. The result was applied to a configuration of two parallel plates of gold; the dependence on the temperature has been determined. That approach was criticized in Ref. [3] to be in contradiction to fluctuation-dissipation theorem which we showed to be not the case [4]. Furthermore, an alternative method proposed in [3] could be proven to be in contradiction with Nernst heat theorem [4]. In fact, our approach was shown to be in agreement with both thermodynamics and experimental data.

[1] M. Bordag, U. Mohideen, V.M. Mostepanenko, Phys. Rept. **353** (2001) 1.
[2] B. Geyer, G.L. Klimchitskaya, V.M. Mostepanenko, Phys. Rev. A **67** (2003) 062102.
[3] V.B. Svetovoy, Phys. Rev. **A 70** (2004) 016101.
[4] B. Geyer, G.L. Klimchitskaya, and V.M. Mostepanenko, Phys. Rev. **A 70** (2004) 016102.

11.6 Quantum Field Theory of Light-Cone Dominated Hadronic Processes

B. Geyer, J. Eilers

Light-cone dominated, polarized hadronic processes at large momentum transfer factorize into process-dependent hard scattering amplitudes and process-independent non-perturbative generalized parton distribution (GPD). Growing experimental accuracy requires the entanglement of various twist as well as (target) mass contributions and radiative corrections. Their quantum field theoretic prescription is based on the nonlocal light-cone expansion [1] and the decomposition of the *nonlocal, tensor-valued* QCD operators into operators with well-defined geometric twist developed previously [2].

Continuing these studies the following results were obtained and applied to generic hadronic processes:

• A general, constructive procedure of determining the (infinite) spin resp. twist decomposition of non-local off-cone tensor operators of any rank and arbitrary symmetry type, in any space-time dimension d, has been given and implemented in a `Java` programme [3].

• The off-cone twist decomposition of non-local vector operators has been used in order to determine the power corrections (in x-space) of QCD operators which are essential for the GPDs [4].

• For the virtual (non-forward) Compton scattering at twist-2 the target mass dependence of their GPDs has been rigorously determined [5]. Thereby, in case of antisymmetric and symmetric tensor part a Wandzura-Wilczek and a (target mass corrected) Callan-Gross representation, respectively, has been derived which has the same functional form as for the forward scattering. Together with some new relations it has been shown that only three independent structure functions determine these matrix elements completely.
• The foregoing results have been generalized as operator relations by studying the twist-2 Compton operator [6]. From the Wandzura-Wilczek and Callan-Gross operator relations one could obtain corresponding relations for any matrix elements of the Compton operator, including arbitrary additional final state particles as well as concerning diffractive scattering.

[1] S.A. Anikin, O.I. Zavialov, Ann. Phys. **116** (1978) 135; D. Müller, D. Robaschik, B. Geyer, F.-M. Dittes, J. Hořejši, Fort. Phys. **42** (1994) 101.
[2] B. Geyer, M. Lazar and D. Robaschik, Nucl. Phys. **B 559**, 339 (1999); **B 618**, (2001) 99; B. Geyer and M. Lazar, Nucl. Phys. **B 581** (2000) 341, Phys. Rev. **D 63** (2001) 094003; J. Eilers and B. Geyer, Phys. Lett. **B 546** (2002) 78.
[3] J. Eilers, *The decomposition of local and non-local operators with respect to irreducible representations of the orthogonal group and some of its applications in Quantum Chromodynamics*, Thesis, Leipzig 2004.
[4] J. Eilers, B. Geyer, and M. Lazar, Phys. Rev. **D 69** (2004) 034015.
[5] B. Geyer, D. Robaschik, and J. Eilers, Nucl. Phys. **B 704** (2005) 279.
[6] B. Geyer and D. Robaschik, Phys. Rev. **D 71** (2005) 054018.

11.7 Quantum Symmetries of General Gauge Theories

B. Geyer

General gauge theories are characterized by local symmetries whose generators, in contrast to the well-known Yang-Mills theories, not necessarily obey a Lie algebra structure. Their gauge algebra may be open, i.e., closed only modulo equations of motion, and, in addition, may be reducible (up to any finite order of reducibility) requiring for the introduction of various extra ghost and auxiliary fields. Nevertheless, the quantum symmetries of such theories [including higher dimensional and $N-$extended super Yang-Mills theories (SYM), (super) string theories and topological field theories (TQFT)] are governed by (extended) BRST operations resp. master equations.

Two different routes of research have been considered:

Lagrangian quantization of general gauge theories:
The well-known Batalin-Vilkovisky (BV) quantization using a master equation in terms of fields and antifields (sources) previously was extended to the (modified) triplectic quantization [1]. This approach has been studied further. Thereby, we obtained the following results:
• The study of modified triplectic quantization in general coordinates, which formerly was restricted to bosonic basis manifolds [2], has been extended to the case when the basic manifold consists of fields with both even and odd Grassmann parity [3]. Thereby, the

necessity of introducing Fedosov supermanifolds appeared. In addition, for this approach a superfield formulation was given [4]. Furthermore, the whole space of the (anti)fields of the triplectic formalism has been equipped with an even symplectic structure and its geometric meaning has been clarified. Also its connection with closed two-forms arising from the superfield approach has been studied [5].

• Basic properties of Fedosov supermanifolds, i.e. even (odd) supermanifolds endowed with a connection respecting a given symplectic structure, have been extensively studied. Especially, it was shown that their Ricci curvature in the even resp. odd case vanishes resp. (in general) does not vanish [6]. These manifolds have been studied further in terms of normal coordinates [7]. We derived an infinite system of equations for the affine extensions of the Christoffel symbols, proved a relation between the first order affine extension of Christoffel symbols and symplectic curvature tensor, and derived a relation between the second order affine extension of the symplectic structure and symplectic curvature tensor. These results have been reviewed in [8].

• An iterative reduction procedure to the canonical form has been presented for the Euler-Lagrange equations of a general gauge theory - including theories with higher derivatives [9]. That procedure reveals the constraints in the Lagrangian formulation of singular systems and allows to find the gauge identities between the Euler-Lagrange equations. The influence of external fields has been discussed.

[1] I.A. Batalin, R. Marnelius, Phys. Lett. **B 350** (1995) 44; Nucl. Phys. B **465**, 521 (1996); I.A. Batalin, R. Marnelius, A.M. Semikhatov, Nucl. Phys. B **446** (1995) 249; B. Geyer, D.M. Gitman, P.M. Lavrov, Mod. Phys. Lett. A **14** (1999) 661; Theor. Math. Phys. **123** (2000) 813.
[2] B. Geyer, P.M. Lavrov, A.P. Nersessian, Phys. Lett. **B 512** (2001) 211; Int. J. Mod. Phys. A **17** (2002) 349.
[3] B. Geyer and P.M. Lavrov, Int. J. Mod. Phys. A **19** (2004) 1639.
[4] B. Geyer, D.M. Gitman, P.M. Lavrov, P.Yu. Moshin, Int. J. Mod. Phys. A **19** (2004) 737.
[5] B. Geyer, P.M. Lavrov and A. Nersessian, hep-th/0406201.
[6] B. Geyer and P.M. Lavrov, Int. J. Mod. Phys. A **19** (2004) 3195.
[7] B. Geyer and P.M. Lavrov, hep-th/0406206, subm. Int. J. Mod. Phys. A
[8] B. Geyer and P.M. Lavrov, *Basic properties of Fedosov supermanifolds*, Vestnik Tomsk State Pedagogical University, Special Issue devoted to 70th Anniversary of Physical and Mathematical Department, hep-th/0406236.
[9] B. Geyer, D.M. Gitman, and I.V. Tyutin, Proc. "QFT Under the Influence of External Conditions", Rinton Press 2004, p. 276.

Cohomological gauge theories:

Topological quantum field theories are the simplest QFT's with the defining property that their Green functions are independent of the local Riemannian structure of the underlying manifold. An interesting class of cohomological gauge theories are those with special holonomy group $\mathcal{H} \in SO(D)$ in $D > 4$ dimensions being invariant under metric variations respecting $\mathcal{H}$.

• From Minkowskian $10D$ super Yang-Mills theory, by dimensional reduction and continuous Weyl-rotation, an $8D$ Euclidean, cohomological $Spin(7)$-invariant action $S^{N_T=1}_{\rm cohom}$ has been derived. By reduction to $7D$ the cohomological G_2-invariant action $S^{N_T=2}_{\rm cohom}$ with global $SU(2)$ symmetry has been obtained. Compatibility of chirality with generalized

self-duality and octonionic algebra was shown [10]. In fact, the G_2–invariant theory may obtained via ordinary dimensional reduction. Moreover, the G_2-invariant theory may be regarded as $7D$ analogue of $N_T = 2$, $3D$ super–BF theory (with matter), just as the $Spin(7)$–invariant theory may be regarded as $8D$ analogue of $N_T = 1$, $4D$ Donaldson–Witten theory (with matter hypermultiplet).

• We showed that the $Spin(7)$–invariant theory $S^{N_T=1}_{\rm cohom}$, which relies on the existence of the Cayley invariant, has a cohomological extension which relies on the existence of the $8D$ analogue of the Pontryagin invariant. Using the $8D$ quartic analogue of the chiral primary operator and of the Pontryagin invariant the topological observables have been constructed [11]. This extension, which in flat space is uniquely determined by the shift and vector SUSY, can be related to one–loop string–corrected counterterms.

• The construction of a $N_T = 3$ cohomological gauge theory on the hyper–Kähler eight–fold, whose group theoretical description was given by Blau and Thompson [12], has been performed explicitly [13]. Starting with the $SO(8)$-invariant action of Euclidean $N = 2$, $D = 8$ SYM in flat space and reducing the symmetry to $Sp(4) \otimes Sp(2)$ the corresponding generalized instanton equations have been derived. Then, we formulated this theory on the hyper–Kähler eight–fold, i.e, for the particular case when the curvature of the $Sp(2)$ spin connections vanishes.

[10] D. Mülsch, B. Geyer, Int. J. Geom. Meth. Mod. Phys. **1** (2004) 185.
[11] D. Mülsch, B. Geyer, Nucl. Phys. B **684** (2004) 351.
[12] M. Blau and G. Thompson, Phys. Lett. B **415** (1997) 242.
[13] D. Mülsch, B. Geyer, *Euclidean super Yang-Mills theory on a quaternionic Kähler manifold*, to appear: Int. J. Geom. Meth. Mod. Phys. (2005).

11.8 Nonperturbative Aspects of 2D Gravity

D. Grumiller, D.V. Vassilevich, M. Bordag

One of the main goals of contemporary theoretical physics is a unification of gravity with quantum theory, i.e., to create a consistent theory of quantum gravity. Due to the complexity and difficulty (both conceptually and technically) of this task there exist many different ways to approach this problem, the most prominent ones being string theory and loop quantum gravity (for a recent survey discussing the status of quantum gravity cf. e.g. [1]). One way to simplify the problem technically (but encountering still essentially the same conceptual problems) is to consider lowerdimensional models. For an extensive review on dilaton gravity in two dimensions cf. [2]. The successes of the "Wiener Schule" are intimately related to a first order formulation in terms of Cartan variables and auxiliary fields, a bit in the spirit of Ashtekar's formulation of 4D gravity, but without necessarily invoking a 1+1 split.

In this way, for instance, the phenomenon of virtual black holes arising as intermediate states in S-matrix calculations can be described quantitatively without invoking ad-hoc assumptions and without encountering information loss (for a recent review cf. [3]).

Another example concerns the so-called Witten black hole [4] and its nonperturbative generalization, the exact string black hole (ESBH) [5]. Exploiting first order techniques only recently an action for the ESBH had been constructed which for the first time since

the discovery of the ESBH in 1992 allowed a thorough discussion of its mass and entropy, as well as supersymmetric extensions and quantization [6].

[1] S. Carlip, Rept. Prog. Phys. **64** (2001) 885 [gr-qc/0108040].
[2] D. Grumiller, W. Kummer, D.V. Vassilevich, Phys. Rept. **369** (2002) 327–430 [hep-th/0204253].
[3] D. Grumiller, Int. J. Mod. Phys. D **13** (2004) 1973–2002 [hep-th/0409231].
[4] E. Witten, Phys. Rev. D44 (1991) 314–324.
[5] R. Dijkgraaf, E. Verlinde, H. Verlinde, Nucl. Phys. B371 (1992) 269–314.
[6] D. Grumiller, hep-th/0501208.

11.9 Structure of the Gauge Orbit Space and Study of Gauge Theoretical Models

G. Rudolph, Sz. Charzynski, E. Fischer, N. Große, M. Schmidt

Based upon our results on the structure of the gauge orbit space [1] and on lattice gauge theories [2–4], we continued to investigate non-perturbative aspects of quantum gauge theory with special emphasis on the following items:
i) The study of the physical role of nongeneric strata in the gauge orbit space was continued. Singular Marsden-Weinstein reduction [5] of the phase space of an SU(3)-gauge theory on a spatial lattice of 1 plaquette was worked out. Based on that, aspects of the classical dynamics of the reduced system were studied. Using invariant theory, the configuration space for a lattice of 2 plaquettes was constructed [6]. The topological structure of this space was investigated by means of a cell decomposition.
ii) The study of non-perturbative aspects of gauge theories on the lattice in terms of gauge-invariant quantities ('observables') was continued. The structure of the algebra of observables for QCD and the superselection structure of its representations was completely clarified [7].
iii) Studying the structure of the observable algebra for lattice QCD in purely algebraic (representation independent) terms, we were led to investigate generalizations of ordinary superalgebras, see [8]. This is a promising field of pure mathematics, with applications in different areas of physics.
(iv) There are still close relations with Christian Fleischhack (MPI MIS Leipzig). He studied the problem of generalizing the Stone-von Neumann theorem to diffeomorphism-invariant theories, especially to loop quantum gravity. He found that, in the category of piecewise analytic paths and surfaces, under reasonable assumptions the standard representation of the corresponding Weyl algebra by multiplication and translation operators is the only regular representation (up to unitary equivalence) with a cyclic diffeomorphism-invariant vector [9].

[1] G. Rudolph, M. Schmidt, I.P. Volobuev, J. Math. Phys. Anal. Geom. **5** (2002) 201–241; J. Geom. Phys. **42** (2002) 106-138; J. Phys. A: Math. Gen. **35** (2002) R1–R50.
[2] J. Kijowski, G. Rudolph, A. Thielmann, Commun. Math. Phys. **188** (1997) 535–564.
[3] J. Kijowski, G. Rudolph and C. Śliwa, Annales H. Poincaré **4** (2003) 1137.
[4] J. Kijowski, G. Rudolph, J. Math. Phys. **43** (2002) 1796.
[5] R. Sjamaar, E. Lerman, Ann. Math. (2), **134** (1991) 375.

[6] S. Charzyński, J. Kijowski, G. Rudolph, M. Schmidt: On the Stratified Classical Configuration Space of Lattice QCD, J. Geom. Phys., in print, hep-th/0409297.
[7] J. Kijowski, G. Rudolph, Charge Superselection Sectors for QCD on the Lattice, J. Math. Phys., in print, hep-th/0404155.
[8] P. Jarvis and G. Rudolph, J. Phys. A, **36**, No. 20 (2003) 5531; On the Structure of the Observable Algebra of QCD on the Lattice, hep-th/0412143.
[9] Ch. Fleischhack, Commun. Math. Phys. 249 (2004) 331–352; Math. Nachr. 263–264 (2004) 83–102.

11.10 Noncommutative Geometry

G. Rudolph, R. Matthes*, P. Hajac*, W. Szymanski†
*Warsaw
†Newcastle

First, the study of quantum principal bundles was continued. The examples of generalized locally trivial Hopf bundle have been further analyzed. One has two nonisomorphic quantum principal bundles living over two different quantum two-spheres. One of these two-spheres is topologically the generic Podleś sphere, the other one results from a gluing of two quantum discs with an extra twist (mirror-type quantum sphere). Meanwhile, several independent proofs of the non-isomorphy of the C^*-algebras of these quantum two-spheres have been found. A publication concerning these matters is under preparation. The total spaces of the bundles coincide and are hybrids of the 3-sphere of the locally trivial bundle and the 3-sphere of Matsumoto [5]. Many of the results known for the locally trivial quantum Hopf bundle (in particular Chern numbers) are true also for these generalizations. The total space can be viewed as a quantum analogue of a Heegaard splitting of the 3-sphere. Its topological properties (in particular K-theory) have been investigated in collaboration with P. Baum [1]. There it is shown that on the C^*-level this quantum 3-sphere is a gluing of two quantum solid tori (whose C^*-algebras are crossed products of the Toeplitz algebra by an action of the integers), and that its K-groups (being computed by means of the Pimsner-Voiculescu and Mayer-Vietoris sequences) coincide with those of the classical 3-sphere.

As a new project, the investigation of topological invariants (K-theory) of observable algebras has been started. This concerns observable algebras determined by Kijowski and Rudolph [3] for several models of gauge field theory. The hope is to identify superselection sectors of quantum field theory as invariants of K-theory and to relate them to other notions of noncommutative geometry.

In collaboration with H.-D. Doebner [2], differential calculi corresponding to spectral triples on a discrete lattice have been analyzed, much in the spirit of [4].

[1] P. Baum, P.M. Hajac, R. Matthes, W. Szymański, math.KT/0409537, to appear in K-Theory
[2] H.-D. Doebner, R. Matthes, On a spectral triple related to discrete quantum mechanics, in: H.-D. Doebner and V.K. Dobrev (eds.), Proc. V. Int. Workshop on Lie Theory and its Applications in Physics, Varna 2003, World Scientific, Singapore 2004, 353-363

[3] J. Kijowski, G. Rudolph, A. Thielmann, Commun. Math. Phys. **188** (1997) 535–564. J. Kijowski, G. Rudolph, J. Math. Phys. **43** (2002) 1796; Charge Superselection Sectors for QCD on the Lattice, J. Math. Phys., in print, hep-th/0404155.
[4] R. Matthes, O. Richter and G. Rudolph, J. Geom. Phys. **46**, 48 (2003); Banach Center Publications **61** (2003) 125–147.
[5] K. Matsumoto, Japan J. Math. **17** (1991) 333–356.

11.11 One-Particle Properties of Quasiparticles in the Half-Filled Landau Level

W. Weller

Using field theoretical methods, two-dimensional electron systems in strong magnetic fields were studied. The investigations were concentrated on the half-filled lowest Landau level.

The theory for the half-filled lowest Landau level of Halperin *et al.* [1] transforms from the electrons to Chern–Simons Fermions by eliminating the external magnetic field. The theory leads to an infrared divergent energy. It was shown [2] that this is due to missing diagrams and to the fact that in [1] the ordering of the operators in the path integral was changed. The correct formulation yields a three-particle interaction. For this interaction, a path integral representation was developed [2] with correct ordering of the operators. The energy was computed by evaluating the path integral in various approximations. The calculated energies are convergent and agree well with numerical simulations. The idea of the Singwi-Sjölander approach to the 3d Coulomb problem was extended to the Chern-Simons theory [3] with even better results for the energies. An approximation scheme was developed conserving the particle number and the constraints.

For the numerical evaluation of the analytical field theory we use the Luttinger–Ward variational principle for the thermodynamic potential. Because this is the first numerical application of that principle, the method was tested on the simpler two–dimensional Coulomb system.

From the analytical theory the effective mass of the Composite Fermions was calculated in good agreement with the experimental results.

[1] B.I. Halperin, P.A. Lee, N. Read, Phys. Rev. B **47** (1993) 7312.
[2] W. Weller, J. Dietel, Th. Koschny, W. Apel in R. Casalbuoni et al. (eds.), 6th Int. Conf. on Path Integrals, World Scientific, Singapore 1999, p. 466.
[3] J. Dietel, W. Weller, Phys. Rev. B **64** (2001) 195307.

11.12 Funding

Graduiertenkolleg Quantenfeldtheorie: Mathematische Struktur und Anwendungen in der Elementarteilchen- und Festkörperphysik
Spokesman: B. Geyer
DFG GRK 52/4-04

Lokale Methoden zur Berechnung der Vakuumpolarisation
M. Bordag
DFG Bo 1112/12-1

Higher order correlation corrections to color ferromagnetic vacuum state at finite temperature
M. Bordag, D. Vassilevich
DFG 436 UKR 17/19/03 and GK QFT

Spectral Zeta Functions and Heat Kernel Technique in Quantum Field Theory with Non-standard Boundary Condition
M. Bordag, D. Vassilevich
Heisenberg-Landau programme

Casimir force between real boundaries
B. Geyer
SMWK Az.: 4-7531.50-04-0361-03/1

Differential geometry on Fedosov supermanifolds and Lagrangian extended BRST quantization
B. Geyer
DFG 436 RUS 17/15/04

Nonperturbative aspects of 2D dilaton gravity
D. Grumiller
Erwin-Schrödinger Stipendium granted by the Austrian Science Foundation (FWF), project J2330-N08

Untersuchungen zur physikalischen Bedeutung der Stratifizierung des Eichorbitraumes
G. Rudolph
DFG RU 692/3-1

One-particle properties of quasiparticles in the half-filled Landau level
W. Weller
DFG-Schwerpunktprogramm "Quanten-Hall-Systeme", WE 480/3-3

11.13 Organizational Duties

Michael Bordag

- Referee: J. Phys. A, Phys. Rev., J. Math. Phys., Phys.Lett.
- Head of International Organizing Committee for the 'Workshop on Quantum Field Theory under the influence of external conditions', to be held Sept. 2005 in Barcelona

Christian Fleischhack

- Spokesman Arbeitsgruppe Wissenschaftspolitik der Jungen Akademie
- Member of the election committee for the Studienstiftung des deutschen Volkes
- Co-organizer of the planned British-German meeting "Frontiers of Science"
- Corrector for the Mathematics Olympiad
- Referee: J. Math. Phys.

Bodo Geyer

- Spokesman of the Graduiertenkolleg Quantenfeldtheorie: Mathematische Struktur und Anwendungen in Elementarteilchen- und Festkörperphysik
- Member of electing board Latin America-South of DAAD
- Vertrauensdozent of the Gesellschaft Dt. Naturforscher und Ärzte
- Referee: DFG, DAAD, Humboldt Foundation

Daniel Grumiller

- Referee: Class. Quant. Grav., Int. J. Mod. Phys. D, Mod. Phys. Lett. A
- Member of Editorial Board of FAKT webpage (Fachausschuss Kern- und Teilchenphysik of the Austrian Physical Society) `http://www.teilchen.at`

Gerd Rudolph

- Referee: Rep. Math. Phys., J. Phys. A, J. Geom. Phys., Class. Quant. Grav., J. Math. Phys.

Armin Uhlmann

- Board member: Rep. Math. Phys., Open Systems and Information Dynamics

Dmitri V. Vassilevich

- Referee: Class. Quant. Grav., J. Phys. A, Nucl. Phys. B, Mod. Phys. Lett. A, J. High Energy Phys., Nuovo Cimento B, London Math. Soc., Foundations of Physics, J. Math. Phys.
- Program Committee, Fock School on Advances in Physics (St.Petersburg)

Wolfgang Weller

- Board member: Physikalische Blätter

11.14 External Cooperations

Academic

Max-Planck Institute for Mathematics in the Sciences, Leipzig
Dr. Markus Lazar

Max-Planck Institute for Mathematics in the Sciences, Leipzig
Dr. Ch. Fleischhack

DESY-Institute of High Energy Physics, Zeuthen
Dr. Johannes Blümlein

Institute of Theoretical Physics, Brandenburg Technical University, Cottbus
Prof. Dr. Dieter Robaschik

Physikalisch-Technische Bundesanstalt
PD Dr. habil. W. Apel, Mayank P. Agnihotri

Technical University, Wien
Dr. Herbert Balasin, Dr. Luzi Bergamin, Dr. Christian Böhmer, Prof. Wolfgang Kummer, Daniel Mayerhofer

Polish Academy of Sciences, Center for Theoretical Physics, Warsaw
Prof. J. Kijowski

Polish Academy of Sciences, Mathematics Institute and University of Warsaw
Prof. P. Hajac, Dr. R. Matthes

Instytut Fizyki Teoretycznej, University of Warsaw
Prof. J. Lewandowski

Université des Sciences et Technologies de Lille
Prof. J. Huebschmann

Massachusets Institute for Technology (MIT)
Dr. Alfredo Iorio, Prof. Roman Jackiw, Dr. Carlos Nuñez

State University of New York at Stony Brook
Prof. P. van Nieuwenhuizen

University of Oregon
Prof. P.B. Gilkey

Center for Gravitation Physics and Geometry, Penn State University
Prof. A. Ashtekar, Dr. H. Sahlmann

St. Petersburg University
Prof. Yu.V. Novozhilov, Dr. V. Marachevsky

Dept. of Physics, North-West Polytechnical University St. Petersburg
Prof. Dr. Galina L. Klimchitskaya

Skobeltsyn Institute of Nuclear Physics, Lomonosov Moscow State University
Dr. I.P. Volobuev

Noncommercial Partnership "Scientific Instruments" of Ministry of Industry, Sciences and Technologies, Moscow,
Prof. Dr. Vladimir M. Mostepanenko

Department of Mathematical Physics, Pedagogical University Tomsk
Prof. Dr. Petr M. Lavrov

National University, Dnepropetrovsk
Prof. V. Skalozub

Dept. of Theoretical Physics, Yerevan State University,
Prof. Dr. Armen Nersessian

Universidad de Zacatecas
Prof. Dharam Ahluwalia-Khalilova

Institute of Nuclear Physics, University of São Paulo
Prof. Dr. Dmitry M. Gitman
Dr. P.Yu. Moshin (on absence of Pedagogical University Tomsk)

University of Newcastle
Prof. W. Szymanski

University of Tasmania, Hobart
Prof. P. Jarvis

11.15 Publications

Journals and Books

H. Balasin and D. Grumiller
The ultrarelativistic limit of 2d dilaton gravity and its energy momentum tensor
Class. Quant. Grav. **21** (2004) 2859–2872.

L. Bergamin, D. Grumiller and W. Kummer
Quantization of 2d dilaton supergravity with matter
JHEP **05** (2004) 060.

L. Bergamin, D. Grumiller, A. Iorio and C. Nuñez
Chemistry of Chern-Simons supergravity: Reduction to a BPS kink, oxidation to M-theory and thermodynamical aspects
JHEP **11** (2004) 021.

M. Bordag and D.V. Vassilevich
Nonsmooth backgrounds in quantum field theory
Phys. Rev. D **70** (2004) 045003.

M. Bordag
Reconsidering the quantization of electrodynamics with boundary conditions and some measurable consequences
Phys. Rev. D **70** (2004) 085010.

H.-D. Doebner, R. Matthes
On a spectral triple related to discrete quantum mechanics
in: H.-D. Doebner and V.K. Dobrev (eds.), Proc. V. Int. Workshop on Lie Theory and its Applications in Physics, Varna 2003, World Scientific, Singapore 2004, 353-363.

J. Eilers, B. Geyer, and M. Lazar
Complete twist decomposition for nonlocal QCD vector operators in x-space
Phys. Rev. D **69** (2004) 034015.

Ch. Fleischhack
Proof of a Conjecture by Lewandowski and Thiemann
Commun. Math. Phys. **249** (2004) 331–352.

Ch. Fleischhack
Parallel Transports in Webs
Math. Nachr. **263–264** (2004) 83–102

B. Geyer, D.M. Gitman, P. Lavrov and P.Yu. Moshin
Superfield Extended BRST Quantization in General Coordinates
Int. J. Mod. Phys. A **19** (2004) 737 - 749.

B. Geyer, D.M. Gitman, and I.V. Tyutin
Reduction of Euler-Lagrange equations in general gauge theories with external fields
Proc. "Quantum Field Theory Under the Influence of External Conditions", Oklahoma, Sept. 2003; Ed.K.A. Milton, Rinton Press 2004, p. 276 - 281.

B. Geyer, G.L. Klimchitskaja, and V.M. Mostepanenko
Reply to "Comment on Surface-impedance approach solves the problems with the thermal Casismir force between real metals"
Phys. Rev. A **70** (2004) 016102.

B. Geyer and P. Lavrov
Modified triplectic quantization in general coordinates
Int. J. Mod. Phys. A **19** (2004) 1639 - 1654.

B. Geyer and P.M. Lavrov
Fedosov supermanifolds: Basic properties and the difference in even and odd cases
Int. J. Mod. Phys. A **19** (2004) 3195 - 3207.

D. Grumiller Long time black hole evaporation with bounded Hawking flux
JCAP **05** (2004) 005.

D. Grumiller
Virtual black holes and the S-matrix
Int. J. Mod. Phys. D **13** (2004) 1973–2002.

D. Grumiller and D. Mayerhofer On static solutions in 2d dilaton gravity with scalar matter
Class. Quant. Grav. **21** (2004) 5893–5914.

D. Mülsch and B. Geyer
G(2)-invariant 7D Euclidean Super Yang-Mills Theory as a Higher Dimensional Analogue of the 3D Super BF Theory
Int. J. Geom. Meth. Mod. Phys. **1** (2004) 185 - 200.

D. Mülsch and B. Geyer
Cohomological extension of Spin(7) invariant super Yang-Mills Theory in eight dimensions
Nucl. Phys. B **684** (2004) 351 - 368.

in press

P. Baum, P.M. Hajac, R. Matthes, W. Szymański
K-Theory, math.KT/0409537.

L. Bergamin, D. Grumiller, W. Kummer and D.V. Vassilevich
lassical and quantum integrability of 2D dilaton gravities in Euclidean space
Class. Quant. Grav., hep-th/0412007

S. Charzyński, J. Kijowski, G. Rudolph, M. Schmidt
On the Stratified Classical Configuration Space of Lattice QCD
J. Geom. Phys., hep-th/0409297

B. Geyer and P.M. Lavrov
Basic properties of Fedosov supermanifolds
to appear: Vestnik of Tomsk State Pedagogical University, Special Issue devoted to 70th Anniversary of Physical and Mathematical Department.

B. Geyer and P.M. Lavrov
Fedosov supermanifolds II. Normal coordinates
Int. J. Mod. Phys. A, hep-th/0406206.

J. Kijowski, G. Rudolph
Charge Superselection Sectors for QCD on the Lattice
J. Math. Phys., hep-th/0404155

J. Kijowski, G. Rudolph
The Observable Algebra of Lattice QCD
Rep. Math. Phys.

D. Mülsch and B. Geyer
An abelian cohomological gauge theory
Proc. Xth Int. Marcel Grossmann Conf., Rio de Janeiro, July 2003, World Scientific Publishers, Singapore, 2005.

I.G. Pirozhenko, V.V. Nesterenko and M. Bordag
Integral equations for heat kernel in compound media
hep-th/0409289

D.V. Vassilevich
Spectral problems from quantum field theory
Contemp. Math., math-ph/0403052.

D.V. Vassilevich
Constraints, gauge symmetries, and noncommutative gravity in two dimensions
Theor. Math. Phys., hep-th/0502120

D.V. Vassilevich
Quantum noncommutative gravity in two dimensions
Nucl. Phys. B, hep-th/0406163

Conference contributions

Cohomological gauge theories of Hodge-type (T)
B. Geyer and D. Mülsch
67. Physikertagung (DPG), Ulm, March 14–18, 2004

New results on cohomological gauge theories (inv. T)
B. Geyer and D. Mülsch
Sixth International Alexander Friedman Seminar, Cargèse (France)
June 28–July 07, 2004

Twist-2 Compton operator and its hidden structure: Wandzura-Wilczek, Callan-Gross and other relations
B. Geyer and D. Robaschik
Int. Conf. “Light-Cone 2004”, Amsterdam, August 16–20, 2004

2D type 0A/0B as dilaton gravity in 2D (P)
D. Grumiller
GR17, Dublin, July 2004.

On the end point of black hole evaporation (P)
D. Grumiller
GR17, Dublin, July 2004.

BPS-Kink and more solutions of the Chern-Simons (Super)Gravity Term (T)
D. Grumiller
First Vienna Central European Seminar on Particle Physics and Quantum Field Theory "Advances in Quantum Field Theory", November 2004.

The Observable Algebra of Lattice QCD (invT)
G. Rudolph
36th Symposium for Mathematical Physics, Torun, June 2004

On the Structure of the Observable Algebra of Lattice QCD (invT)
G. Rudolph
Workshop on Mathematical Physics and Lie Theory, Coolangatta, December 2004,

Introduction to 2D gravity (inv. T)
D. Vassilevich
Advanced Summer School on Modern Mathematical Physics, Dubna, July 4–18, 2004

Noncommutative gravity in two dimensions
D. Vassilevich
International Fock School on Advances in Physics, St.Petersburg, November 22–28, 2004

Luttinger-Ward Variational Principle–Test for the 2d Coulomb System (P)
M.P. Agnihotri, W. Apel, W. Weller
Quantum Hall Systems, Hamburg, September 22–24, 2004

11.16 Graduations

PhD

Igor Drozdow
Vacuum energy of quantum fields in classical background configurations

Jörg Eilers
The decomposition of local and non-local operators with respect to irreducible representations of the orthogonal group and some of its applications in Quantum Chromodynamics

Diploma

Elisabeth Fischer
Singular Marsden-Weinstein reduction in lattice gauge theory

Oliver Witzel
Heavy Meson Distribution Amplitudes of Definite Geometric vs. Dynamic Twist

11.17 Guests

Dr. Luzi Bergamin
TU Vienna
June 28–July 3, 2004

Dr. Christian Böhmer
TU Vienna
May 17-22, 2004

Dr. C. Fleischhack
Max-Planck Institute for Mathematics in the Sciences, Leipzig
Guest lecturer in the summer term 2004

Prof. P. Hajac
Polish Academy of Sciences, Mathematics Institute and University of Warsaw
April 4–18, 2004

Dr. Alfredo Iorio
MIT
June 6-12, 2004

Prof. P. Jarvis
University of Tasmania, Hobart
June 1–30, 2004

Prof. J. Kijowski
Center for Theoretical Physics, Polish Academy of Sciences, Warsaw
September 1–30, 2004

Prof. Dr. G.L. Klimchitskaya
Dept. of Physics, North-West Polytechnical University St. Petersburg
and
Prof. Dr. P. Lavrov
Dept. Mathematical Physics, Tomsk State Pegagog. University
April 1 - June 29, 2004

Dr. R. Matthes
Polish Academy of Sciences, Mathematics Institute and University of Warsaw
Guest lecturer in the summer term 2004

Prof. Dr. V.M. Mostepanenko
Noncommercial Partnership "Scientific Instruments" of Ministry of Industry, Sciences and Technologies, Moscow
January 20 - February 19, 2004

Prof. Dr. A. Nersessian
Dept. Theor. Phys., Yerevan State University
April 10 - May 20, 2004

Prof. Dr. D. Robaschik
Fakultät 1, Brandenburg Technical University, Cottbus
February 22 - March 13, 2004

12

Theory of Elementary Particles

12.1 Introduction

The Particle Physics Group performs basic research in the quantum field theoretic description of elementary particles and in phenomenology. Topics of current interest are conformal symmetry and its breaking in the context of supersymmetric theories, the formulation of models which realize noncommutative geometry, renormalization problems, electroweak matter at finite temperature, the lattice formulation of gauge theories, the derivation of Regge behaviour of scattering amplitudes from Quantum Chromodynamics and the related study of integrable models with and without supersymmetry. Perturbative and non-perturbative methods are applied to answer the respective questions. In perturbation theory the work is essentially analytic using computers only as a helpful tool. Lattice Monte Carlo calculations as one important non-perturbative approach however are based on computers as an indispensable instrument. Correspondingly the respective working groups are organized: in analytical work usually very few people collaborate, in the lattice community rather big collaborations are the rule. Our group is involved in many cooperations on the national and international level (DESY, Munich; France, Russia, Armenia, USA, Japan). Since elementary particles are very tiny (of the order of 10^{-15} m) and for the study of their interactions large accelerators producing enormously high energy are needed, it is clear that results in this direction of research do not have applications in daily life immediately. To clarify the structure of matter is first of all an aim in its own and is not pursued for other reasons. But particle theory has nevertheless a very noticeable impact on many other branches of physics by its power of providing new methodological insight. Similarly for the student specializing in this field the main benefit is her/his training in analysing complex situations and in applying tools which are appropriate for the respective problem. As a rule there will be no standard procedures which have to be learned and then followed, but the student has to develop her/his own skill according to the need that arises. This may be a mathematical topic or a tool in computer application. Jobs which plainly continue these studies are to be found at universities and research institutes only. But the basic knowledge which one acquires in pursuing such a subject opens the way to many fields where analytical thinking is to be combined with application of advanced mathematics. Nowadays this seems to be the case in banks, insurance companies and consulting business.

12.2 High-Energy Asymptotics and Integrable Quantum Systems

R. Kirschner

The aim of this project is to develop methods for treating the Regge and Bjorken limits in gauge theories like QCD. We rely on the idea of the high-energy effective action [1] which we have shown in recent years to be a useful tool for analyzing the asymptotics of scattering amplitudes. In the Regge case the action describes the scattering by the exchange of reggeized quarks and gluons. The reggeon and parton interactions exhibit remarkable symmetry properties and can be related to integrable quantum systems.

In 2004 we have analyzed the Bjorken asymptotics of supersymmetric Yang-Mills theory. We have constructed superconformal operators describing the one-loop parton interactions or the renormalization of composite light-ray operators [2]. The study relies on the effective action method developed for the Bjorken asymptotics of QCD [3] and extends the results of that paper.

Our work contributed to the study of conformal symmetry and integrability properties of composite operator renormalization performed in quite a number of papers in last two years e.g. [4, 5], motivated by questions of application in Quantum Chromodynamics and also of the relations between gauge and string theories.

Two dimensional intergrable theories in application to high energy scattering, Dr. R. Kirschner. Support of the visit of D.R. Karakhanyan by Graduate College (DFG)

[1] L.N. Lipatov, Nucl. Phys. B365(1991)614; R. Kirschner, L.N. Lipatov and L. Szymanowski, Nucl. Phys. B452(1994)579; Phys. Rev. D51(1995)838; L.N. Lipatov, Nucl. Phys. B452(1995)369; R. Kirschner and L. Szymanowski, Phys. Rev. D52(1995)2333; Phys. Lett. B419 (1998) 348; Phys. Rev. D58(1998) 014004.
[2] R. Kirschner, JHEP 0407 (2004) 064, [arXiv:hep-th/0404060].
[3] S.E. Derkachov and R. Kirschner, Phys. Rev. D **64** (2001) 074013, [arXiv:hep-ph/0101174].
[4] A.V. Kotikov, L.N. Lipatov, A.I. Onishchenko and V.N. Velizhanin, Phys. Lett. B **595** (2004) 521, [arXiv:hep-th/0404092].
[5] A.V. Belitsky, S.E. Derkachov, G.P. Korchemsky and A.N. Manashov, Nucl. Phys. B **708** (2005) 115, [arXiv:hep-th/0409120].

12.3 Quantized Equations of Motion in Non-Commutative Theories

P. Heslop, K. Sibold

Space and time will, at extremely short distances, require new notions in both mathematical description and physical content. A simple physical argument for this is based on the uncertainty principle which says that black holes can be formed thus leading to a horizon and other consequences when precision in time is high enough. As a modest step into this direction one may understand the introduction of Moyal products in otherwise

rather conventional flat space-time quantum field theory. They arise when the coordinates are being considered as Hermitian operators which satisfy simple, but non-trivial commutation relations.

Quantum field theories based on interactions which contain the Moyal star product suffer however, in the general case when time does not commute with space, from several diseases: quantum equation of motions contain unusual terms, conserved currents can not be defined and the residual spacetime symmetry is not maintained. All these problems have the same origin: time ordering does not commute with taking the star product. Here we show that these difficulties can be circumvented by a new definition of time ordering: namely with respect to a light-cone variable. In particular the original spacetime symmetries $SO(1,1) \times SO(2)$ and translation invariance turn out to be respected. Unitarity is guaranteed as well.

Thinking of extensions of our results one can indeed have the hope that gauge theories exist as well for generic θ since global symmetry currents will exist due to the simple form of the quantum equations of motion. Hence the examples which are known to exist for vanishing θ_e should all be generalisable to generic θ. In the actual formulation of gauge fixing and BRS invariance the expertise collected in light cone quantization should be helpful. For higher orders analogously one should at least be able to construct what can be constructed for restricted θ. Since with the time ordering the integrals truly change one should also have a fresh look at the ultraviolet/infrared connection. If the above mentioned symmetry can be maintained it is clear from kinematical arguments that this problem is avoided since the limit of vanishing momenta seems to exist.

[1] S. Doplicher, K. Fredenhagen, and J.E. Roberts, "Space-time quantization induced by classical gravity," *Phys. Lett.* **B331** (1994) 39–44; "The Quantum structure of spacetime at the Planck scale and quantum fields," Commun. Math. Phys. **172** (1995) 187 [arXiv:hep-th/0303037].
[2] Y. Liao and K. Sibold, "Time-ordered perturbation theory on noncommutative spacetime: Basic rules," *Eur. Phys. J.* **C25** (2002) 469–477,
[3] Y. Liao and K. Sibold, "Time-ordered perturbation theory on noncommutative spacetime. II. Unitarity," *Eur. Phys. J.* **C25** (2002) 479–486,

12.4 Superconformal Theories in Six Dimensions

P. Heslop

One exciting product of string theory is the hint of the existence of a maximally supersymmetric quantum theory in six space-time dimensions. This theory has been conjectured to give a non-perturbative description of the unique maximally supersymmetric quantum field theory in four dimensions: $N = 4$ super Yang-Mills. The six dimensional theory, compactified on a torus should give $N = 4$ super Yang-Mills, with the shape of the torus being related to the coupling constant of the Yang-Mills theory. This latter theory has huge theoretical and pedagogical interest: one studies this theory as a stepping stone for learning more about more complicated but phenomenologically more interesting gauge theories such as QCD or GUTs and such a non-perturbative description would be fantastic. This proposal is however very difficult to check as the six dimesnional theory is

unknown, and indeed is not believed to be describable as a local field theory - the way we are used to describing theories in physics.

There are however a couple of possibilities for examining this proposal: firstly one can use the large amount of symmetry of the six dimensional theory. It has (2,0) superconformal symmetry and it is possible to analyse correlation functions using this symmetry. In particular four point functions give information about operators occuring in the operator product expansion. In [1] a complete conformal partial wave expansion of the four-point function of four energy momentum multiplets was performed.

The other possibility for studying the theory comes from the remarkable AdS/CFT corespondence [2] which in this context suggests that this theory is equivalent to the a priori completely inequivalent supergravity theory in eleven dimensions on an anti de Sitter space-time background. From this correspondence one obtains a putative four-point function of four energy momentum tensors [3] which can then be analysed to give information about operators in the OPE of two energy momentum tensors. This analyis was performed in [1].

It would be interesting to extend these results to consider four-point functions of more general operators. It would also be extremely interesting to examine the compactification on a torus discussed above and see what could be said about four-point functions in N=4 super Yang-Mills non-perturbatively.

[1] P.J. Heslop, JHEP **0407** (2004) 056 [arXiv:hep-th/0405245].
[2] J.M. Maldacena, Adv. Theor. Math. Phys. **2** (1998) 231 [Int. J. Theor. Phys. **38** (1999) 1113];
[3] G. Arutyunov and E. Sokatchev, Nucl. Phys. B **635**, 3 (2002) [arXiv:hep-th/0201145].

12.5 H/A Higgs Mixing in CP-Noninvariant Supersymmetric Theories

Y. Liao

For large masses, the two heavy neutral Higgs bosons are nearly degenerate in many 2-Higgs doublet models, and particularly in supersymmetric models. In such a scenario the mixing between the states can be very large if the theory is CP-noninvariant. We have analyzed such scenarios in a general quantum mechanical language that provides us with a clear and transparent understanding of the phenomena in the general 2-Higgs doublet model. Moreover, the effects are illustrated in the Minimal Supersymmetric Standard Model extended by CP violating interactions. Higgs formation in $\gamma\gamma$ collisions proves particularly interesting for observing such effects. However, exciting experimental effects are also predicted in such scenarios for $t\bar{t}$ final state analyses in decays of the heavy Higgs bosons at LHC and in the e^+e^- mode of linear colliders.

[1] S.Y. Choi, J. Kalinowski, Y. Liao, P.M. Zerwas, arXiv: hep-ph/0407347, Eur. Phys. J. C, to appear (2005).

12.6 On Evaluation of Nonplanar Diagrams in Noncommutative Field Theory

Y. Liao

This is a technical work about how to evaluate loop integrals appearing in one loop nonplanar (NP) diagrams in noncommutative (NC) field theory [1]. The conventional wisdom [2] says that, barring the ultraviolet/infrared (UV/IR) mixing problem, NP diagrams whose planar counterparts are UV divergent are rendered finite by NC phases that couple the loop momentum to the external ones p through an NC momentum $\rho^\mu = \theta^{\mu\nu}p_\nu$. We show that this is generally not the case. We find that subtleties arise already in the simpler case of Euclidean spacetime. The situation is even worse in Minkowski spacetime due to its indefinite metric. We compare different prescriptions that may be used to evaluate loop integrals in ordinary theory. They are equivalent in the sense that they always yield identical results. However, in NC theory there is no a priori reason that these prescriptions, except for the defining one that is built in the Feynman propagator, are physically justified even when they seem mathematically meaningful. Employing them can lead to ambiguous results, which are also different from those obtained according to the defining prescription. For ρ^20, the NC phase can worsen the UV property of loop integrals instead of always improving it in high dimensions. We explain how this surprising phenomenon comes about from the indefinite metric. This lends a strong support to the point of view that the naive approach is not well-founded when time does not commute with space. For $\rho^2 < 0$, the NC phase improves the UV property and softens the quadratic UV divergence in ordinary theory to a bounded but indefinite UV oscillation. We employ a cut-off method to quantify the new UV non-regular terms. For ρ^20, these terms are generally complex and thus also harm unitarity in addition to those found previously. As the new terms for both cases are not available in the Lagrangian and in addition can be non-Hermitian when time does not commute with space, our result casts doubts on previous demonstrations of one loop renormalizability based exclusively upon analysis of planar diagrams, especially in theories with quadratic divergences.

[1] Y. Liao, arXiv: hep-th/0408047, Nucl. Phys. B, to appear (2005).
[2] See for example, S. Minwalla, M.V. Raamsdonk and N. Seiberg, JHEP 02 (2000) 020; J. Gomis, T. Mehen, Nucl. Phys. B591 (2000) 265.

12.7 Generalised Parton Distributions from Lattice QCD with $N_f = 2$ Flavours

M. Göckeler

Parton distributions of the nucleon describe the logitudinal momentum distribution of quarks and gluons. Generalised parton distributions (GPDs) contain information about the interplay of longitudinal momentum and transverse coordinate space, as well as spin and orbital angular momentum degrees of freedom. (For a review see [1].) GPDs are generalised in the sense that they are defined in terms of nucleon matrix elements of light-cone operators with *non-vanishing* momentum transfer Δ. They depend on $t = \Delta^2$ and on the two momentum fractions x and ξ. For $\Delta = 0$ they reproduce the ordinary

parton distributions, e.g., the unpolarised GPD H_q becomes the quark distribution $q(x)$ for flavour q: $H_q(x, \xi = 0, t = 0) = q(x)$ for $x0$. For purely transverse momentum transfer $\Delta = \Delta_\perp$ (and thus $\xi = 0$) M. Burkardt [2] has shown that

$$q(x, \vec{b}_\perp) = \int \frac{\mathrm{d}^2\Delta_\perp}{(2\pi)^2}\, \mathrm{e}^{\mathrm{i}\vec{b}_\perp\cdot\vec{\Delta}_\perp} H_q(x, 0, -\vec{\Delta}_\perp^2) \tag{12.1}$$

can be interpreted as the probability density for a quark with longitudinal momentum fraction x and transverse position $\vec{b}_\perp$. For large x, one expects $q(x, \vec{b}_\perp)$ (being defined with the transverse centre of mass as reference point) to become very narrow.

Moments (with respect to x) of GPDs can be represented in terms of generalised form factors $A^q_{n0}(t), \ldots$, which also appear in the form factor decomposition of non-forward nucleon matrix elements of local operators – the same operators that determine the moments of ordinary parton distributions. Since such matrix elements can be calculated on the lattice, it is possible to extract moments of GPDs from lattice QCD simulations [3]. Within the QCDSF-UKQCD collaboration we are pursuing such investigations using $N_f = 2$ flavours of non-perturbatively $O(a)$-improved Wilson fermions [4]. Some results for

$$A^q_{n0}(t) = \int_{-1}^{1} \mathrm{d}x\, x^{n-1} H_q(x, 0, t) \tag{12.2}$$

$(n = 1, 2, 3)$ in the flavour non-singlet case are shown in Fig. 12.1. As n increases, $A^{u-d}_{n0}(t)$ flattens, which means that H_q (as a function of t) becomes wider as x grows. From (12.1) we can then read off that q as a function of $\vec{b}_\perp$ becomes narrower as x approaches 1, in accordance with our expectations.

Once the form factors $A^q_{n0}(t)$ are sufficiently well known, one could compute $H_q(x, 0, t)$ from (12.2) via an inverse Mellin transform and then use (12.1) to determine the distribution $q(x, \vec{b}_\perp)$. In this way one would arrive at a three-dimensional picture of the internal structure of the nucleon! While it is unlikely that such a programme can be performed on

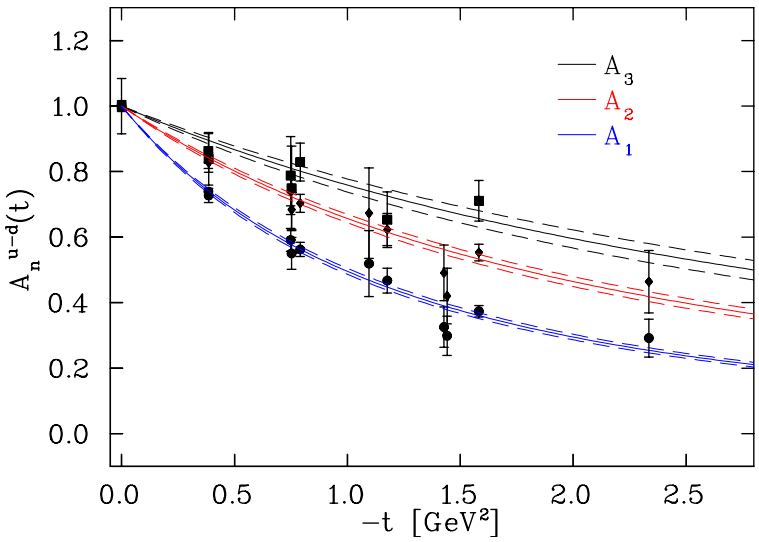

Figure 12.1: Generalised form factors A^{u-d}_{10}, A^{u-d}_{20}, A^{u-d}_{30} together with dipole fits. All form factors have been normalised to unity at $t = 0$. Simulation parameters: $\beta = 5.4$, $\kappa = 0.1350$, lattice size $24^3 \times 48$.

the basis of lattice data alone, it is to be expected that lattice QCD results will play an important role in these attempts by constraining possible ansätze, fixing model parameters etc. It is therefore an exciting task to extract as much information on GPDs from the lattice as possible.

This project has been supported in part by the DFG (Forschergruppe Gitter-Hadronen-Phänomenologie), by the EU Integrated Infrastructure Initiative Hadron Physics, and by the Helmholtz Association.

The numerical calculations have been performed on the Hitachi SR8000 at LRZ (Munich), on the Cray T3E at EPCC (Edinburgh) under PPARC grant PPA/G/S/1998/00777, and on the APEmille at NIC/DESY (Zeuthen).

[1] M. Diehl, Phys. Rept. **388** (2003) 41.
[2] M. Burkardt, Int. J. Mod. Phys. A **18** (2003) 173.
[3] M. Göckeler, R. Horsley, D. Pleiter, P.E.L. Rakow, A. Schäfer, G. Schierholz and W. Schroers, Phys. Rev. Lett. **92** (2004) 042002; Ph. Hägler, J. Negele, D.B. Renner, W. Schroers, T. Lippert and K. Schilling, Phys. Rev. D **68** (2003) 034505.
[4] M. Göckeler, Ph. Hägler, R. Horsley, D. Pleiter, P.E.L. Rakow, A. Schäfer, G. Schierholz and J.M. Zanotti, arXiv:hep-lat/0410023; arXiv:hep-lat/0501029.

12.8 3D Abelian Higgs Model with Singly and Doubly-Charged Matter Fields

A. Schiller

In this project we continue to study properties of coupled gauge-Higgs models in three dimensions using Monte Carlo methods.

Unfreezing the radial degree of freedom, we study the three-dimensional Abelian Higgs model with compact gauge field and fundamentally charged matter [1]. For small quartic Higgs self coupling and finite gauge coupling the model possesses a first order transition from the confined/symmetric phase to the deconfined/Higgs phase separated at some hopping parameter κ_c. Latent heat and surface tension are obtained in the first order regime. At larger quartic coupling the first order transition ceases to exist, and the behavior becomes similar to that known from the London limit. These observations are complemented by a study of the photon propagator in Landau gauge in the two different regimes. The problems afflicting the gauge fixing procedure are carefully investigated. We propose an improved gauge fixing algorithm which uses a finite subgroup in a preselection/preconditioning stage. The computational gain in the expensive confinement region is a speed-up factor around 10. In Landau gauge the 3D photon propagator in momentum spcae is given by $D_{\mu\nu}(\vec{p}) = (\delta_{\mu\nu} - p_\mu p_\nu/p^2)\ D(p^2)$. The form factor $D(p^2)$ has been fitted by

$$D(p^2) = \frac{Z\, m^{2\alpha}}{\beta\,[p^{2(1+\alpha)} + m^{2(1+\alpha)}]} + C\,, \tag{12.3}$$

where the fitting parameters Z denote the renormalization of the photon wavefunction, α the anomalous dimension and m the photon mass. In Fig. 12.2 we demonstrate how

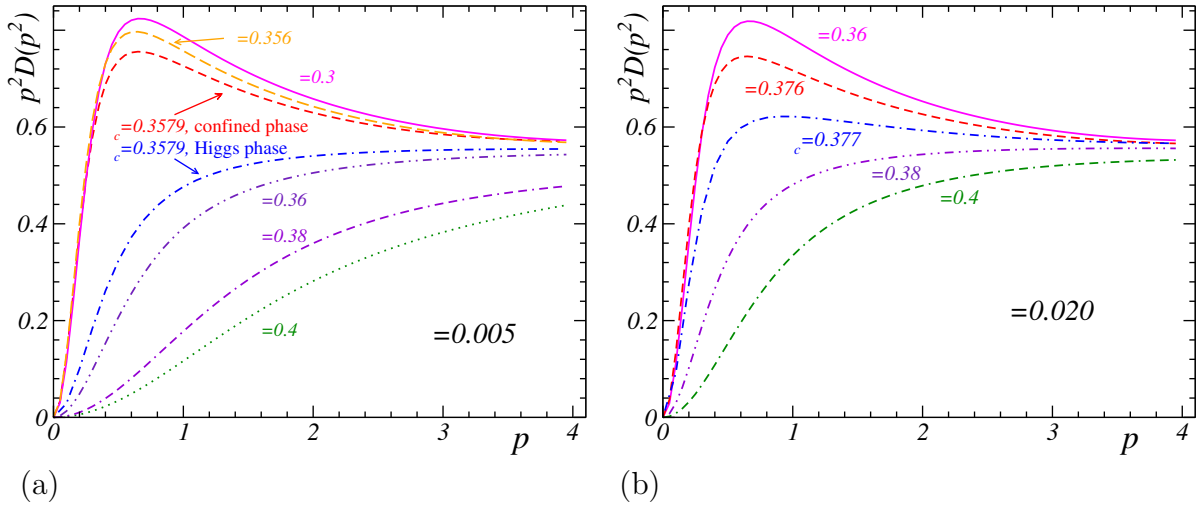

Figure 12.2: Momentum dependence of the fitted photon propagator form factor $D(p^2)$ multiplied by p^2 for different κ's near criticality for the first order (a) and continuous transition (b) regime.

the momentum dependence of the propagator changes when crossing the first order or continuous transition (varying the hopping parameter κ).

The propagator in momentum space has a non-zero α in the confined phase whereas it vanishes in the Higgs phase. As far as the gauge boson propagator is concerned, we find that the radially active Higgs field provides qualitatively no new effect compared to the radially frozen Higgs field studied before.

The properties of topological defects in the lattice compact Abelian Higgs Model with charge Q=2 matter field are studied in [2]. We find that monopoles and antimonopoles form chain-like structures which are dense in the confinement/symmetric phase. In Figure 12.3 we visualize a typical monopole/vortex configuration observed in our numerical

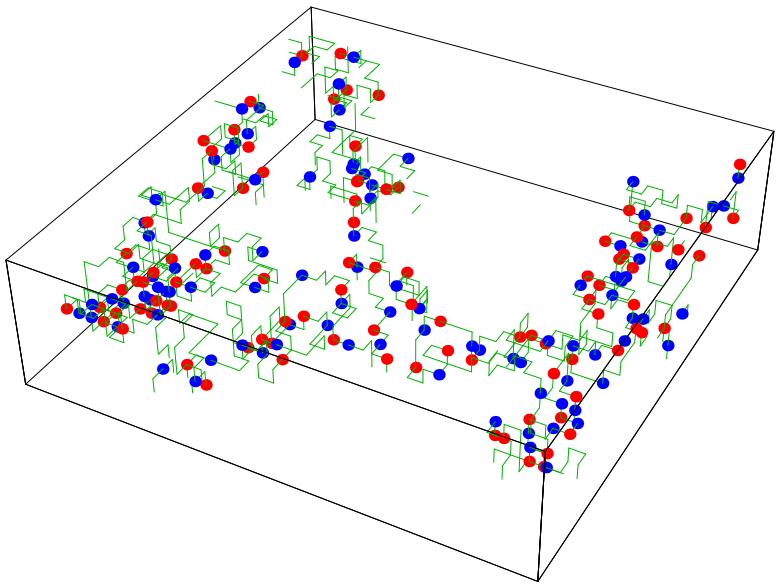

Figure 12.3: Example of a monopole/vortex configuration in the confinement phase (at $\kappa = 1.275$); monopoles are shown by circles, vortices by lines.

simulations. In this phase the mentioned structure explains both the confinement of singly-charged and the breaking of strings spanned between doubly-charged test particles. In the confinement phase the monopole chains are percolating as in Figure 12.3 (so that the monopoles are relevant to infrared physics similarly to the monopoles in QCD) whereas in the Higgs phase the monopole chains are relatively short. This observation helps to understand how the non-diagonal gluons, once taken into consideration in the Abelian projection of gluodynamics, could reproduce in this framework the string breaking for adjoint charges.

The project is supported by grants RFBR 01-02-17456, DFG 436 RUS 113/73910, RFBR-DFG 03-02-04016, JSPS S04045 and MK-4019.2004.2 and by DFG through the DFG-Forschergruppe "Lattice Hadron Phenomenology" (FOR 465).

[1] M.N. Chernodub, R. Feldmann, E.-M. Ilgenfritz and A. Schiller, Phys. Rev. D **70** (2004) 074501 [arXiv:hep-lat/0405005].
[2] M.N. Chernodub, R. Feldmann, E.-M. Ilgenfritz and A. Schiller, Phys. Lett. B **605** (2005) 161 [arXiv:hep-lat/0406015].

12.9 Lattice Pertubation Theory and Renormalisation

A. Schiller (QCDSF-collaboration)

In this project we continue the calculation of one-loop renormalisation factors in lattice perturbation theory necessary to relate lattice to continuum matrix elements of operators related to the structure of the nucleon. Typical diagrams to be taken into account are shown in Fig. 12.4.

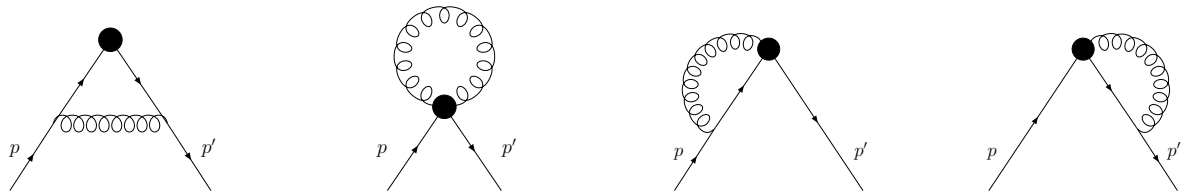

Figure 12.4: One-loop lattice diagrams for amputed Green functions. The dots denote the operator insertions with covariant derivatives.

In Ref. [1] we have computed lattice renormalisation constants of local bilinear quark operators for overlap fermions and improved gauge actions. Among the actions we consider are the Symanzik, Lüscher-Weisz, Iwasaki and DBW2 gauge actions. The results are given for a variety of ρ parameters. We show how to apply mean field (tadpole) improvement to overlap fermions. The question, what is a good gauge action, is discussed from the perturbative point of view. Finally, we show analytically that the gauge dependent part of the self-energy and the amputated Green functions are independent of the lattice fermion representation, using either Wilson or overlap fermions.

Monte Carlo results for the nucleon's axial charge g_A and the first moment $\langle x \rangle$ of the unpolarized parton distribution function from a simulation of quenched overlap fermions are given in [2], partly using the calculated renormalisation factors.

In a further work [3, 4] we have calculated the non-forward quark matrix elements of operators with two covariant derivatives needed for the renormalisation of the second moment of generalised parton distributions in one-loop lattice perturbation theory using Wilson fermions (see also Göckeler, Sect. 12.7). For some representations of the hypercubic group commonly used in simulations we determine the sets of all possible mixing operators. For those representations the one-loop mixing matrices of renormalisation factors are found. Due to non-vanishing contributions of operators with external ordinary derivatives the number of contributing operators increases compared to forward matrix elements.

This work is supported by the European Community's Human Potential Program under contract HPRN-CT-2000-00145 Hadrons/Lattice QCD and by DFG under contract FOR 465 (Forschergruppe Gitter-Hadronen-Phänomenologie).

The numerical calculations were performed at the HLRN (IBM pSeries 690) and at NIC Jülich (IBM pSeries 690). We thank these institutions for their support.

[1] R. Horsley, H. Perlt, P.E.L. Rakow, G. Schierholz and A. Schiller [QCDSF Collaboration], Nucl. Phys. B **693** (2004) 3 [arXiv:hep-lat/0404007].
[2] M. Gürtler *et al.*, arXiv:hep-lat/0409164.
[3] M. Göckeler, R. Horsley, H. Perlt, P.E.L. Rakow, A. Schäfer, G. Schierholz and A. Schiller, Nucl. Phys. Proc. Suppl. 140 (2005) 722 [arXiv:hep-lat/0409025].
[4] M. Göckeler, R. Horsley, H. Perlt, P.E.L. Rakow, A. Schäfer, G. Schierholz and A. Schiller, arXiv:hep-lat/0410009.

12.10 Organizational Duties

Roland Kirschner

- Referee: Eur. Physics Journal C, Phys. Rev. D, Progr. Part. Nucl. Phys.
- Member of a finding commission for a faculty position

Klaus Sibold

- Vice dean of the faculty "Physics and earth sciences"
- Director of the ITP
- Member of the "Forschungskommission" of the university
- Member of the "Gerätekommission" of the university
- Member of the "Graduiertenkolleg: Quantenfeldtheorie"
- Associated member of the Graduiertenkolleg: Analysis, Geometrie und die Naturwissenschaften"
- Coorganizer of the "Mitteldeutsche Physik-Combo" (joint graduate lecture courses with universities Jena and Halle)
- Member of the "Beirat" of the Fachverband "Mathematische und Theoretische Grundlagen der Physik" (German Physical Society)

Yi Liao

- Referee: Eur. Phys. J. C

Arwed Schiller

- Referee: Phys. Rev. D

12.11 External Cooperations

Academic

Prof. L.N. Lipatov
St. Petersburg, Nuclear Physics Institute

Dr. S.E. Derkachov St. Petersburg, University and Technology Institute

Prof. Ara Sedrakyan
Yerevan Physics Institute, Theory Dept.

Dr. Lech Szymanowski
Soltan Institut of Nucl. Studies, Warsaw

Prof. J. Bartels
Universität Hamburg, Institut für Theoretische Physik/DESY

Prof. A. Schäfer, Prof. V. Braun
Universität Regensburg, Institut für Theoretische Physik

Prof. B. Pire
Ecole Polytechnique, Paris-Palaiseau

S.Y. Choi
Chonbuk National University

J. Kalinowski
Warsaw University

P.M. Zerwas
DESY, Hamburg

Ph. Hägler
Vrije Universiteit Amsterdam

R. Horsley
University of Edinburgh

D. Pleiter and J.M. Zanotti
John von Neumann–Institut für Computing NIC, Zeuthen

P.E.L. Rakow
University of Liverpool

G. Schierholz
John von Neumann–Institut für Computing NIC, Zeuthen, and DESY, Hamburg

M.N. Chernodub
Kanazawa U., Inst. Theor. Phys. & Moscow, ITEP)

E.-M. Ilgenfritz
Humboldt Universität, Berlin

M. Gürtler, T. Streuer
NIC, Zeuthen & DESY Zeuthen

V. Linke
Freie Universität, Berlin

H. Perlt
Universität Regensburg

12.12 Publications

Journals

R. Kirschner,
Parton interaction in super Yang Mills theory,
JHEP **0407** (2004) 064, [arXiv:hep-th/0404060].

A. Ivanov and R. Kirschner,
Diffractive large transferred momentum photoproduction of vector mesons,
Eur. Phys. J. C **36** (2004) 43, [arXiv:hep-ph/0311077].

S. Derkachov, D. Karakhanyan and R. Kirschner,
Universal R operator with Jordanian deformation of conformal symmetry,
Nucl. Phys. B **681** (2004) 295, [arXiv:nlin.si/0310019].

P.J. Heslop and P.S. Howe,
"Aspects of N = 4 SYM,"
JHEP **0401** (2004) 058.

P.J. Heslop,
"Aspects of superconformal field theories in six dimensions,"
JHEP **0407**, 056 (2004) [arXiv:hep-th/0405245].

Y. Liao, K. Sibold,
On double gauging of $U(1)$ symmetry on noncommutative space,
Phys. Lett. B586, 420 (2004).

Y. Liao,
Note on CKM matrix renormalization,
Phys. Rev. D69, 016001 (2004).

M. Göckeler, R. Horsley, D. Pleiter, P.E.L. Rakow, A. Schäfer, G. Schierholz and W. Schroers [QCDSF Collaboration],
"Generalized parton distributions from lattice QCD,"
Phys. Rev. Lett. **92** (2004) 042002 [arXiv:hep-ph/0304249].

T. Bakeyev, M. Göckeler, R. Horsley, D. Pleiter, P.E.L. Rakow, G. Schierholz and H. Stüben [QCDSF-UKQCD Collaboration],
"Non-perturbative renormalisation and improvement of the local vector current for quenched and unquenched Wilson fermions,"
Phys. Lett. B **580** (2004) 197 [arXiv:hep-lat/0305014].

C. Gattringer *et al.* [BGR Collaboration],
"Quenched spectroscopy with fixed-point and chirally improved fermions,"
Nucl. Phys. B **677** (2004) 3 [arXiv:hep-lat/0307013].

A. Ali Khan *et al.* [QCDSF-UKQCD Collaboration],
"The nucleon mass in N(f) = 2 lattice QCD: Finite size effects from chiral perturbation theory,"
Nucl. Phys. B **689** (2004) 175 [arXiv:hep-lat/0312030].

M. Göckeler, R. Horsley, W. Kurzinger, D. Pleiter, P.E.L. Rakow and G. Schierholz [QCDSF Collaboration],
"Vacuum polarisation and hadronic contribution to muon g-2 from lattice QCD,"
Nucl. Phys. B **688** (2004) 135 [arXiv:hep-lat/0312032].

C. Gattringer, M. Göckeler, P. Huber and C.B. Lang,
"Renormalization of bilinear quark operators for the chirally improved lattice Dirac operator,"
Nucl. Phys. B **694** (2004) 170 [arXiv:hep-lat/0404006].

M.N. Chernodub, E.-M. Ilgenfritz and A. Schiller,
"The photon propagator in compact QED(2+1): The effect of wrapping Dirac strings,"
Phys. Rev. D **69** (2004) 094502 [arXiv:hep-lat/0311033].

R. Horsley, H. Perlt, P.E.L. Rakow, G. Schierholz and A. Schiller [QCDSF Collaboration],
"One-loop renormalisation of quark bilinears for overlap fermions with improved gauge actions,"
Nucl. Phys. B **693** (2004) 3 [arXiv:hep-lat/0404007].

M.N. Chernodub, R. Feldmann, E.-M. Ilgenfritz and A. Schiller,
"Phase structure and gauge boson propagator in the radially active 3D compact Abelian Higgs model,"
Phys. Rev. D **70** (2004) 074501 [arXiv:hep-lat/0405005].

in press

S.Y. Choi, J. Kalinowski, Y. Liao, P.M. Zerwas,
H/A Higgs mixing in CP-noninvariant supersymmetric theories,
Eur. Phys. J. C in press [arXiv: hep-ph/0407347].

Y. Liao,
On evaluation of nonplanar diagrams in noncommutative field theories,
Nucl. Phys. B in press [arXiv: hep-th/0408047].

Conference contributions

P.J. Heslop,
"Superconformal field theories in analytic superspace,"
arXiv:hep-th/0403144. Proceedings of International Seminar on Supersymmetries and Quantum Symmetries SQS 03, Dubna, Russia, 24-29 Jul 2003, Eds. E. Ivanov, A. Pashnev.

A. Ali Khan *et al.*,
"Accelerating Hasenbusch's acceleration of hybrid Monte Carlo,"
Nucl. Phys. Proc. Suppl. **129** (2004) 853 [arXiv:hep-lat/0309078].

A. Ali Khan *et al.* [QCDSF Collaboration],
"Chiral perturbation theory and finite size effects on the nucleon mass in unquenched QCD,"
Nucl. Phys. Proc. Suppl. **129** (2004) 176 [arXiv:hep-lat/0309133].

M. Göckeler, R. Horsley, W. Kurzinger, D. Pleiter, P.E.L. Rakow and G. Schierholz,
"Vacuum polarisation and the muon g-2 in lattice QCD,"
Nucl. Phys. Proc. Suppl. **129** (2004) 293 [arXiv:hep-lat/0310027].

T. Bakeyev *et al.* [QCDSF-UKQCD Collaboration],
"Structure functions and form factors close to the chiral limit from lattice QCD,"
Nucl. Phys. Proc. Suppl. **128** (2004) 82 [arXiv:hep-lat/0311017].

M. Göckeler *et al.* [QCSSF Collaboration],
"Structure of the nucleon,"
Nucl. Phys. Proc. Suppl. **128** (2004) 203 [arXiv:hep-ph/0312104].

M. Göckeler *et al.* [QCDSF Collaboration],
"Nucleon structure from lattice QCD,"
Nucl. Phys. Proc. Suppl. **135** (2004) 156.

C. Carimalo, A. Schiller and V.G. Serbo,
"A new method for calculating jet-like QED processes,"
Nucl. Phys. Proc. Suppl. **126** (2004) 360 [arXiv:hep-ph/0305293].

D. Galletly *et al.* [QCDSF-UKQCD Collaboration],
"Quark spectra and light hadron phenomenology from overlap fermions with improved gauge field action,"
Nucl. Phys. Proc. Suppl. **129** (2004) 453 [arXiv:hep-lat/0310028].

13

Theory of Condensed Matter

13.1 Introduction

The topics of research in the Theory of Condensed Matter group are stochasticity and disorder as well as structure formation in soft condensed matter and solids, models of complex biological systems, strongly correlated electron systems, and superconducting materials. Investigations using modern analytic methods and computer applications complement and stimulate each other. Research is performed in cooperation with mathematicians as well as with theoretical and experimental physicists, biologists and researchers in medicine. There are well established collaborations with research groups in France, Germany, Italy, Russia, Switzerland, UK, and USA.

Noise induced phenomena. Analogies to phase transitions, e.g. the critical behaviour and universality classes, are studied in coupled arrays of stochastically driven nonlinear systems; the continuum limit is carefully considered. Analogies to self-organized criticality are investigated in stochastic nonlinear systems with time delay.

Mathematical modeling of the immune system. Using methods of nonlinear dynamics and statistical physics, we study the architecture and the random evolution of the idiotypic network of the B-cell subsystem and describe the regulation of balance of Th1/Th2-cell subsystems, its relation to allergy and the hyposensitization therapy (Cooperation with the Institute for Clinical Immunology and Transfusion Medicine).

Strongly correlated electron systems. The unconventional magnetic properties of transition metal oxides, such as the mixed-valency manganites, are investigated on the basis of correlation models including anisotropic Heisenberg-type exchange interactions. Using Green's function techniques the effects of magnetic short-range order at arbitrary temperatures are studied in comparison with experiments.

Superconductors. Conventional and high-temperature superconductivity are studied within a gauge field theory by drawing parallels between an Abelian Higgs-like model in the isotropic case and a time-dependent Lawrence-Doniach model for layered high-T_c cuprates. The aim is the microscopic derivation of an effective action to describe the dynamics of the superconducting condensate at zero temperature in the presence of electromagnetism.

13.2 Nonlinear Dynamics and Statistical Physics of the Immune System

U. Behn, H. Schmidtchen, R. Vogel

The immune system is a hierarchically organized natural adaptive system built by a macroscopic number of constituents which shows a very complex behaviour on several scales of temporal, spatial, and functional organization. It is thus naturally a subject of modeling with methods of statistical physics and nonlinear dynamics, for recent reviews see, e.g., [1–3]. We investigate models describing the architecture of the idiotypic network formed by the subsystem of B-lymphocytes and the regulation of the Th1-Th2 balance of the T-lymphocyte subsystem.

B-cells express on their surface receptors (antibodies) of a given specificity (idiotype). Crosslinking these receptors by complementary structures (antigen or antibodies) stimulates the lymphocyte to proliferate. Thus even without antigen there is a large functional network of interacting lymphocytes, the idiotypic network. The idiotypes are caricatured by bitstrings. The dynamics of the idiotypic network is driven by the influx of new idiotypes randomly produced in the bone marrow and by the population dynamics of the lymphocytes themself. Modelling this dynamics by simple cellular automata rules [4] we describe the architecture of the idiotypic network as the highly organized product of a random temporal evolution.

T-helper lymphocytes have subtypes which differ in their spectrum of secreted cytokines. These cytokines have autocrine effects on the own subtype and cross-suppressive effects on the other subtype and regulate further the type of immunoglobulines secreted by B-lymphocytes. The balance of Th1- and Th2-cells is perturbed in several diseases. For example, in allergy the response to allergen is Th2-dominated. A widespread and successful therapy consists in the injection of increasing doses of allergen following empirically justified protocols of administration. We give an explanation of this therapy studying the nonlinear dynamics of a nonautonomous system of few variables which describes the Th1/Th2 populations in the sense of a mean field theory [5, 6]. Indeed, the system is driven by proper injections of allergen towards new attractors, where the response is Th1-dominated as for healthy individuals. The bifurcation behaviour of the nonautonomous system is closer investigated. This investigation is performed in collaboration with Prof. G. Metzner (Institute of Clinical Immunology).

[1] A.S. Perelson and G. Weisbuch, Rev. Mod. Phys. **69** 1219 (1997).
[2] U. Behn, F. Celada, and P.E. Seiden, in: *Frontiers of Life*, Vol. II, Part Two: *The Immunological System*, eds. A. Lanzavecchia, B. Malissen and R. Sitia, (Academic Press, London, 2001), p. 611.
[3] U. Behn, M. Brede, and J. Richter, in: Function and regulation of cellular systems: Experiments and Models, A. Deutsch, J. Howard, M. Falcke, W. Zimmermann (Eds.), Birkhäuser, Basel (2004), 399-410.
[4] M. Brede and U. Behn, Phys. Rev. E **64**, 011908 (2001), ibid. **67**, 031920 (2003).
[5] J. Richter, G. Metzner and U. Behn, J. Theor. Med. **4**, 119 (2002).
[6] J. Richter, U. Behn, and G. Metzner, in: Clinical Immunology and Allergy in Medicine, Proc. 21st EAACI Congress 2002, Naples, G. Marone (Ed.), JGC Editions, Naples (2003), 257-262.

13.3 Noise Induced Phenomena in Nonlinear Systems

U. Behn, M. Krieger-Hauwede, A. Traulsen, F. Senf

We describe non-equilibrium phase transitions [1] in arrays of spatially coupled dynamical systems with different nonlinearities driven by multiplicative Gaussian white noise. Those systems show close analogies to phase transitions in equilibrium. We have determined the phase diagram, the order of the transitions, and the critical behaviour for both global coupling and nearest neighbour coupling on simple cubic lattices comparing analytical results and numerical simulations [2, 3]. For global coupling we give an analytical result for the critical exponent of the order parameter which exhibits a transition from an universal value (depending on the order of the saturation term) to a non-universal behaviour with increasing ratio of noise strength and magnitude of the spatial coupling. The critical exponent of the order parameter as a function of the strength of the spatial coupling has been calculated, universality classes have been determined, and the influence of additive noise was shown [4]. Current analytic investigations concentrate on the approach of the system to the stationary state.

Spatially coupled stochastically driven systems are considered in the continuum limit which leads to stochastic partial differential equations. We show that it is preferable to use spatiotemporal colored noise in order to avoid unphysical divergencies in this limit, new analytical results for a number of models are given [5]. A generalization of the Ornstein-Uhlenbeck process in $1 + 1$ dimensions was proposed [6].

For a class of stochastically driven nonlinear systems with delayed time argument we investigated the persistence problem and determined the probability density of first passage times. For systems spontaneously evolving to a marginally stable state the density is a power law over several decades. Analogies to the phenomenon of self-organized criticality in spatially extended systems are closer investigated.

[1] C. Van den Broeck, J.M.R. Parrondo and R. Toral, Phys. Rev. Lett. **73**, 3395 (1994); J. Garcia-Ojalvo, J.M. Sancho, *Noise in Spatially Extended Systems*, (Springer, New York, 1999).
[2] R. Müller, K. Lippert, A. Kühnel and U. Behn, Phys. Rev. E **56**, 2658 (1997).
[3] T. Birner, K. Lippert, R. Müller, A. Kühnel and U. Behn, Phys. Rev. E **65**, 046110 (2002).
[4] J. Przybilla, *Kritisches Verhalten in global gekoppelten rauschgetriebenen nichtlinearen Systemen*, Diploma thesis, University of Leipzig (2002); J. Przybilla, U. Behn, in preparation.
[5] A. Traulsen, *Coupled stochastically driven systems in the continuum limit*, Diploma thesis, University of Leipzig (2002); A. Traulsen, U. Behn, in preparation.
[6] A. Traulsen, K. Lippert, U. Behn, Phys. Rev. E **69**, 026116 (2004).

13.4 Spin Correlations in Anisotropic Quantum Magnets

D. Ihle, I. Junger, J. Richter*

*Universität Magdeburg

In the theory of magnetism [1] the interplay of quantum and thermal fluctuations and the effects of spin and spatial anisotropies are of basic interest. For example, in $LaMnO_3$, being a spin $S = 2$ parent compound of the colossal magnetoresistance manganites [2], neutron-scattering experiments [3] yield evidence for a pronounced ferromagnetic short-range order (SRO) in the paramagnetic phase and for a single-ion easy-axis spin anisotropy. Moreover, the study of low-dimensional quantum ferromagnets, also in a magnetic field, was motivated by the progress in the synthesis of new materials. To provide a good description of SRO at arbitrary temperatures, the standard spin-wave approaches cannot be adopted.

In this project low-dimensional anisotropic quantum spin models were considered, and a second-order Green's-function theory along the lines indicated in Refs. [4] and [5] was developed. Moreover, exact finite-lattice diagonalizations (ED) were performed. For the one- and two-dimensional $S = 1/2$ Heisenberg ferromagnet in a magnetic field [6], the thermodynamic properties (magnetization, magnetic susceptibility, specific heat) at arbitrary temperatures and fields were calculated in good agreement with ED and Monte-Carlo data [7]. In addition, in the one-dimensional case, exact calculations by the Bethe-ansatz method for the quantum transfer matrix were performed, and at very low fields two maxima in the temperature dependence of the specific heat were found. For $S \geq 1$ ferromagnetic Heisenberg chains with uniaxial single-ion anisotropy, the spin-wave spectra and thermodynamics were investigated. For sufficient large anisotropies, the existence of two maxima in the temperature dependence of the specific heat was shown. A good agreement of the theoretical specific heat with experiments on some Ni complexes was found, and predictions for the magnetic susceptibilities and spin-wave spectra of those compounds were made.

The project was supported by the DFG through the graduate college "Quantum Field Theory".

[1] *Quantum magnetism, Lecture Notes in Physics*, Vol. **645**, edited by U. Schollwöck, J. Richter, D.J.J. Farnell, and R.F. Bishop (Springer, Berlin, 2004).
[2] A.P. Ramirez, J. Phys.: Condens. Matter **9**, 817 (1997). E.L. Nagaev, Phys. Rep. **346**, 387 (2001).
[3] F. Moussa *et al.*, Phys. Rev. B **54**, 15149 (1996). K. Hirota, N. Kaneko, A. Nishizawa and Y. Endoh, J. Phys. Soc. Jpn. **65**, 3736 (1996).
[4] S. Winterfeldt and D. Ihle, Phys. Rev. B **56**, 5535 (1997); **59**, 6010(1999).
[5] D. Ihle, C. Schindelin and H. Fehske, Phys. Rev. B **64**, 054419 (2001).
[6] I. Junger, D. Ihle, J. Richter, and A. Klümper, Phys. Rev. B **70**, 104419 (2004).
[7] P. Henelius, A.W. Sandvik, C. Timm and S.M. Girvin, Phys. Rev. B **61**, 364 (2000).

13.5 Magnetic Systems with Frustration

J. Richter*, D. Schmalfuß*, D. Ihle

* Universität Magdeburg

In low-dimensional frustrated quantum spin systems [1], such as the spin-half Heisenberg antiferromagnet on the two-dimensional (2D) kagomé lattice [2], the interplay of quantum and frustration effects causes interesting physics. Thereby, the influence of the dimensionality on the stability of the spin-liquid phase and the finite-temperature properties are of particular interest. To describe the magnetic short-range order at arbitrary temperatures, especially in the spin-liquid phase, one has to go beyond the usual spin-wave approaches [3]. Previously, it was shown that frustration effects in the two-dimensional Heisenberg model with antiferromagnetic nearest- and next-nearest-neighbor couplings (J_1-J_2 model) may be described successfully by a spin-rotation-invariant Green's-function theory [4, 5]. The role of the interplane coupling in the stabilization of long-range order in non-frustrated systems was also well described by this theory [6].

In this project, the second-order Green's-function approach of Refs. [4] to [6] was extended to a theory for frustrated spin lattices with basis [7]. In the kagomé antiferromagnet the influence of the interplane coupling on the spin correlation functions and the thermodynamic properties was investigated. As the main result, the spin-liquid phase was found to be stable with respect to the interplane coupling. To shed more light into the suppression of long-range order by frustration, the ferromagnet on the stacked kagomé lattice, where quantum fluctuations and frustration effects occur at non-zero temperatures only, was considered in comparison with the ferromagnet on the stacked square lattice having an equal coordination number. The thermodynamical properties (e.g., magnetization, specific heat, magnetic susceptibility) were calculated, where the Curie temperature was found to be smaller for the kagomé lattice.

The work is supported by the DFG through the projects RI 615/12-1 and IH 13/7-1.

[1] *Quantum magnetism, Lecture Notes in Physics*, Vol. **645**, edited by U. Schollwöck, J. Richter, D.J.J. Farnell, and R.F. Bishop (Springer, Berlin, 2004).
[2] J. Schulenburg, A. Honecker, J. Schnack, J. Richter and H.J. Schmidt, Phys. Rev. Lett. **88**, 167207 (2002).
[3] A.B. Harris *et al.*, Phys. Rev. B **64**, 024436 (2001).
[4] L. Siurakshina, D. Ihle and R. Hayn, Phys. Rev. B **64**, 104406 (2001).
[5] S. Winterfeldt and D. Ihle, Phys. Rev. B **56**, 5535 (1997); **59**, 6010 (1999).
[6] D. Ihle, C. Schindelin and H. Fehske, Phys. Rev. B **64**, 054419 (2001).
[7] D. Schmalfuß, J. Richter, and D. Ihle, Phys. Rev. B **70**, 184412 (2004).

13.6 Superconductivity and Relativity

W. Kolley

The conventional London equations of superconductivity are not covariant. Lorentz invariance at superconductivity is needed [1–3], e.g., to treat internal electric and magnetic fields on the same footing. The electrodynamics and magnetohydrodynamics of charged superfluids can be described within the Abelian Higgs model. The Klein-Gordon-type

equation of motion for the superconducting condensate at zero temperature is decomposed into the continuity equation and a relativistic Hamilton-Jacobi-Bohm-type equation.

The mathematical structure of the present U(1) gauge theory is expressed in exterior differential forms (see, e.g., [4, 5]), where the exterior derivative applied twice to any differential form gives zero (Poincaré's lemma). When applied to the potential 1-form, the resulting 1-2-3 relation yields the homogeneous Maxwell equations. A 2-3-4 relation implies the conservation of the supercurrent. It is shown that the Hodge-dual vector-valued 3-form of the total energy-momentum is closed in the Higgs model of superconductivity. Such a formal structure occurs also in general relativity [6].

The topological identity that the boundary of a boundary is zero can be taken as a fundamental principle [6]; its local consequences are equivalent to Poincaré's lemma. Thus a tautology dominates the laws of superconductivity on a macroscopic level, a realization of the concept of austerity [6] in field theories.

[1] J. Govaerts, J. Phys. A **34**, 8955 (2001).
[2] J.E. Hirsch, Phys. Rev. B **69**, 214515 (2004).
[3] W. Kolley, Mod. Phys. Lett. B **13**, 89 (1999).
[4] F.W. Hehl and Yu.N. Obukhov, *Foundations of Classical Electrodynamics* (Birkhäuser, Boston, 2003).
[5] Y. Itin, J. Phys. A **36**, 8867 (2003).
[6] A. Kheyfets, Found. Phys. **16**, 483 (1986); A. Kheyfets and J.A. Wheeler, Int. J. Theor. Phys. **25**, 573 (1986); A. Kheyfets and W.A. Miller, J. Math. Phys. **32**, 3168 (1991).

13.7 Funding

Rotationsinvariante Greenfunktionsmethode für Quantenspingitter
Prof. Dr. J. Richter (Magdeburg), Prof. Dr. D. Ihle
DFG RI 615/12-1, IH13/7-1

13.8 Organizational Duties

Ulrich Behn

- Journal referee: Physical Review Letters, Physical Review E, Journal of Physics A, Journal of Theoretical Biology, Advances in Complex Systems
- Reviewer: Deutsche Studienstiftung, Deutscher Akademischer Austauschdienst, Leopoldina-Stiftung, University of Cambridge, ETH Zürich, California Institute of Technology
- Vertrauensdozent für die Nobelpreisträgertagungen in Lindau

Dieter Ihle

- Journal reeferee: Physical Review B, phys. stat. sol. (b)

Winfried Kolley

- Member of the Promotionsauschuß of the Faculty

Adolf Kühnel

- Member of the Executive Commitee of the *International Center for Scientific Co-operation* with residence in Tübingen

13.9 External Cooperations

Academic

Prof. Dr. Gerhard Metzner
Institut für Klinische Immunologie, Universität Leipzig

Prof. Dr. Franco Celada
Department of Oncology, Biology and Genetics, University of Genoa

Prof. Dr. Valentin Zagrebnov
Centre de Physique Theorique, CNRS, Marseille

Prof. Dr. Slava Priezzhev
Bogolyubov Laboratory of Theoretical Physics, JINR, Dubna

Prof. Dr. Hirokazu Fujisaka
Department of Applied Analysis and Complex Dynamical Systems, Kyoto University

Prof. Dr. Ralf Stannarius
Institut für Experimentelle Physik, Otto-von-Guericke-Universität Magdeburg

Dr. Angela Stevens
Max Planck Institute for Mathematics in Science, Leipzig

Dr. Jan Richter
Cyprus Institute of Neurology and Genetics, Nicosia

Dr. Markus Brede
Center for Complex Systems Science, CSIRO, Canberra

Prof. Dr. Holger Fehske
Institut für Physik, Ernst-Moritz-Arndt-Universität Greifswald

Prof. Dr. Johannes Richter
Institut für Theoretische Physik, Otto-von-Guericke-Universität Magdeburg

Prof. Dr. Nikolai M. Plakida
Bogolyubov Laboratory of Theoretical Physics, JINR, Dubna

Prof. Dr. Peter Wachter
Laboratorium für Festkörperphysik, ETH Zürich

13.10 Publications

U. Behn, M. Brede, J. Richter,
Nonlinear dynamics and statistical physics of models for the immune system,
in: Function and regulation of cellular systems: Experiments and Models, A. Deutsch, J. Howard, M. Falcke, W. Zimmermann (Eds.), Birkhäuser, Basel (2004), 399-410

A. Traulsen, K. Lippert, U. Behn,
Generation of spatiotemporal correlated noise in 1+1 dimensions,
Phys. Rev. E **69**, 026116 (2004)

I. Junger, D. Ihle, J. Richter, A. Klümper,
Green-function theory of the Heisenberg ferromagnet in a magnetic field,
Phys. Rev. B **70**, 104419-1/8 (2004)

D. Schmalfuß, J. Richter, D. Ihle,
Absence of long-range order in a spin-half Heisenberg antiferromagnet on the stacked kagomé lattice,
Phys. Rev. B **70**, 184412-1/7 (2004)

Talks and posters

U. Behn
Randomly evolving idiotypic networks,
Theorie-Kolloquium, Institut für Theoretische Physik, Universität zu Köln, 23.7.04

U. Behn
Architecture of randomly evolving idiotypic networks (inv. T),
Joint COPIRA/NTZ Workshop on Application of Networks, Institut für Theoretische Physik, Universität Leipzig, 24.11.04

U. Behn, A. Traulsen, K. Lippert
Generation of spatiotemporal correlated noise in 1+1 dimensions (T),
CompPhys04, 5th NTZ Workshop on Computational Physics, Universität Leipzig, 26.11.04

D. Ihle
Magnetite – an old but modern material: Polaronic short-range order and geometrical frustration effects on the Verwey transition and charge transport,
Seminar, Lehrstuhl Theoretische Physik II, Universität Greifswald, 10.5.04
Seminar, MPI für Physik Komplexer Systeme, Dresden, 6.6.04
Seminar, Bogoljubov Laboratory of Theoretical Physics, Dubna, 16.6.04
Seminar, Institut für Theoretische Physik, TU Dresden, 26.6.04
Seminar, Institut für Theoretische Physik, Universität Magdeburg, 25.11.04

13.11 Graduations

PhD

Thomas John
Experimentelle und theoretische Untersuchungen zur stochastisch getriebenen Elektrokonvektion in nematischen Flüssigkristallen

13.12 Guests

Prof. Dr. Joe Pulé
Department of Mathematical Physics, University College Dublin
1.7.-31.7.2004

14

Computational Quantum Field Theory

14.1 Introduction

The Computational Physics Group performs basic research into classical and quantum statistical physics with special emphasis on phase transitions and critical phenomena. In the centre of interest are currently spin glasses, diluted magnets and other physical systems with quenched, random disorder, a geometrical approach to the statistical physics of topological defects with applications to superconductors and superfluids, biologically motivated problems (e.g., protein folding and semiflexible polymers), fluctuating geometries with applications to quantum gravity (e.g., dynamical triangulations) and soft condensed matter physics (e.g., membranes and interfaces). Supported by a Development Host grant of the European Commission, currently also research into the physics of anisotropic quantum magnets is established.

The methodology is a combination of analytical and numerical techniques. The numerical tools are currently mainly Monte Carlo computer simulations and high-temperature series expansions. The computational approach to theoretical physics is expected to gain more and more importance with the future advances of computer technology, and will probably become the third basis of physics besides experiment and analytical theory. Already now it can help to bridge the gap between experiments and the often necessarily approximate calculations of analytical work. To achieve the desired high efficiency of the numerical studies we develop new algorithms, and to guarantee the flexibility required by basic research all computer codes are implemented by ourselves. The technical tools are Fortran, C, and C++ programs running under Unix or Linux operating systems and computer algebra using Maple or Mathematica. The software is developed and tested at the Institute on a cluster of PCs and workstations, where also most of the numerical analyses are performed. Large-scale simulations requiring vast amounts of computer time are carried out at the Institute on a recently installed Beowulf cluster with 40 Athlon MP1800+ CPUs and a brandnew Opteron cluster with 18 processors of 64-bit architecture, at the parallel computers of the University computing center, and upon grant application at the national supercomputing centres in Jülich and München on IBM and Hitachi parallel supercomputers. This combination of various platforms gives good training opportunities for the students and offers promising job perspectives in many different fields for their future career.

The research is embedded in a wide net of national and international collaborations funded by network grants of the European Commission, the European Science Foundation (ESF) and the German-Israel-Foundation (GIF), and by a binational research grant with scientists in Sweden. Close contacts and collaborations are also established with research groups in Armenia, Austria, China, France, Great Britain, Israel, Italy, Poland, Russia, Spain, Taiwan, Turkey, Ukraine, and the United States.

W. Janke

14.2 Monte Carlo Studies of Spin Glasses

B. A. Berg*, A. Billoire†, E. Bittner, W. Janke, A. Nußbaumer, D. B. Saakian‡

*Florida State University, Tallahassee, USA
†CEA/Saclay, Gif-sur-Yvette, France
‡Yerevan Physics Institute, Yerevan, Armenia

Spin glasses are examples for the important class of materials with random, competing interactions [1]. This introduces so-called "frustration", since no unique spin configuration is favoured by all interactions, and consequently leads to a rugged free energy landscape with many minima separated by barriers. To cope with the problems of standard Monte Carlo simulations to overcome those barriers, we developed a multi-overlap Monte Carlo algorithm [2] which can be optimally tailored for the sampling of rare-events [3]. Employing this technique we first studied for the three-dimensional (3D) short-range Edwards-Anderson Ising (EAI) $\pm J$ model the scaling behaviour of the barrier heights [4] and the tails of the overlap-parameter distribution [5]. Recently we improved our methodology by combining it with parallel tempering and N-fold way ideas [6]. First tests with the new algorithm indicate [7] that it will enable us to push the studies of the spin-glass phase further towards the physically more interesting low-temperature regime. Currently we are extending our investigations also to the Sherrington-Kirkpatrick (SK) mean-field and random orthogonal models where particular focus is placed on studies of inherent structures and inhomogeneities in dynamical response functions. Since very large computing times of the order of several years are required, we have adapted our computer codes to the special architecture of the recently installed supercomputer JUMP at ZAM/NIC Jülich.

In a second, more analytically oriented subproject we consider the diluted generalized random-energy model (DGREM). This formulation provides an approximation to the ground-state energy of spin glasses whose exact computation belongs to the class of expensive NP problems of combinatoric optimization (the computation time grows exponentially with the size of the system). Besides applications to the 3D EAI model, we developed a generalization to q-state Potts spin glasses whose accuracy was tested against numerically determined ground-state energies for the two-dimensional models with $q = 3$ and 4 [8].

[1] K. H. Fischer and J. A. Hertz, *Spin Glasses* (Cambridge University Press, 1991).
[2] B. A. Berg and W. Janke, Phys. Rev. Lett. **80**, 4771 (1998).
[3] W. Janke, in: *Computer Simulations of Surfaces and Interfaces*, NATO Science Series, II. Mathematics, Physics and Chemistry – Vol. **114**, edited by B. Dünweg, D. P. Landau and A. I. Milchev (Kluwer, Dordrecht, 2003), p. 137.

[4] B. A. Berg, A. Billoire and W. Janke, Phys. Rev. B **61**, 12143 (2000); Physica A **321**, 49 (2003).
[5] B. A. Berg, A. Billoire and W. Janke, Phys. Rev. E **65**, 045102(R) (2002); *ibid.* **66**, 046122 (2002).
[6] A. Nußbaumer, E. Bittner and W. Janke, to be published.
[7] A. Nußbaumer, Diploma Thesis, University of Leipzig (2003).
[8] E. Bittner, W. Janke and D. B. Saakian, Phys. Rev. E **67**, 016105 (2003).

14.3 Monte Carlo Studies of Diluted Magnets

B. Berche*, P.-E. Berche†, C. Chatelain*, W. Janke

*Université Nancy, France
†Université Rouen, France

The influence of quenched, random disorder on phase transitions has been the subject of exciting experimental, analytical and numerical studies over many years. Generically one expects that under certain conditions quenched disorder modifies the critical behaviour at a second-order transition (Harris criterion) and can soften a first-order transition to become second order (Imry-Wortis effect) [1]. In two dimensions these effects are fairly well understood [2]. In three dimensions (3D), numerical studies have mainly focused on the site-diluted Ising model [3], where good agreement with field theoretical predictions was obtained. For the case of a first-order transition in the pure model, large-scale simulations have only been performed for the 3-state Potts model with site-dilution [4].

In this project we have performed intensive Monte Carlo studies of the 3D Ising and 4-state Potts models with *bond*-dilution. The phase diagrams of the diluted models, starting from the pure model limit down to the neighbourhood of the percolation threshold, were found in very good agreement with the single-bond effective-medium approximation and our parallel high-temperature series expansions for the same models. For the estimation of critical exponents in the Ising case [5, 6], we first performed finite-size scaling analyses at three different dilutions to check the stability of the disorder fixed point. We observe strong cross-over effects between the pure, disorder and percolation fixed points, leading to effective critical exponents apparently dependent on the dilution. In addition also the temperature behaviour of physical quantities was studied in order to characterize the disorder fixed point more accurately. This allowed us to determine critical amplitude ratios which are usually more sensitive to the universality class than critical exponents. Moreover, non-self-averaging properties at the disorder fixed point were found in good agreement with approximate analytical predictions. Overall our numerical results provide strong evidence for universality of bond and site dilution in the 3D Ising model. Similar simulations of the 3D bond-diluted 4-state Potts model [7] yield clear evidence for disorder induced softening to a second-order transition above a (tricritical) disorder strength. Here also the role of rare-event contributions was studied in great detail.

[1] A. B. Harris, J. Phys. C **7**, 1671 (1974); Y. Imry and M. Wortis, Phys. Rev. B **19**, 3580 (1979).
[2] B. Berche and C. Chatelain, in: *Order, Disorder, and Criticality*, edited by Yu. Holovatch (World Scientific, Singapore, 2004), p. 147 [cond-mat/0207421].

[3] S. Wiseman and E. Domany, Phys. Rev. Lett. **81**, 22 (1998); Phys. Rev. E **58**, 2938 (1998); H. G. Ballesteros, L. A. Fernández, V. Martín-Mayor, A. Muñoz Sudupe, G. Parisi and J. J. Ruiz-Lorenzo, Phys. Rev. B **58**, 2740 (1998).
[4] H. G. Ballesteros, L. A. Fernández, V. Martín-Mayor, A. Muñoz Sudupe, G. Parisi and J. J. Ruiz-Lorenzo, Phys. Rev. B **61**, 3215 (2000).
[5] P.-E. Berche, C. Chatelain, B. Berche and W. Janke, Eur. Phys. J. B **38**, 463 (2004).
[6] B. Berche, P.-E. Berche, C. Chatelain and W. Janke, Condens. Matter Phys. **8**, 47 (2005).
[7] C. Chatelain, B. Berche, W. Janke and P.-E. Berche, cond-mat/0501115.

14.4 High-Temperature Series Expansions for Spin Glasses and Disordered Magnets

M. Hellmund*, W. Janke

*Fakultät für Mathematik und Informatik

Systematic series expansions for statistical models defined on a lattice are a well-known alternative to large-scale numerical simulations for the study of phase transitions and critical phenomena [1]. For quenched disordered systems the extension of this method [2] requires especially adapted graph theoretical and algebraic algorithms. In this project we developed a computer package based on the "star-graph" method [3] which allows the generation of high-temperature series expansions for the free energy and susceptibility. We consider the class of disordered q-state Potts models on d-dimensional hypercubic lattices $\mathbb{Z}^d$ with bimodal probability distributions of quenched couplings parametrized by $P(J_{ij}) = p\delta(J_{ij}-J_0)+(1-p)\delta(J_{ij}-RJ_0)$, which includes spin glasses, diluted ferromagnets, random-bond models and transitions between them. The limiting case $p = 1$ describes

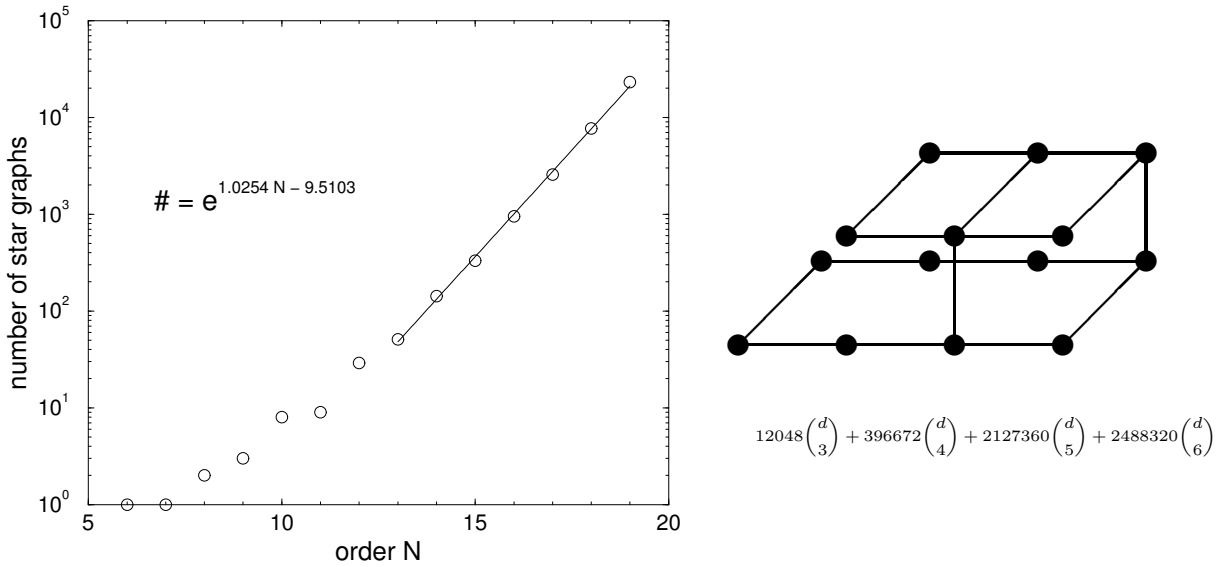

Figure 14.1: Left: Growth behaviour of the number of star graphs of order N that can be embedded in hypercubic lattices $\mathbb{Z}^d$. Right: A star graph of order 17 and its (weak) embedding number, carrying the dependence on the dimension (up to $d = 6$).

the pure ferromagnetic ($J_0 > 0$) models. Even though the method is highly optimized for the problem at hand, it is extremely demanding since the number of contributing graphs grows exponentially with the order of the series and all intermediate calculations have to be performed by means of symbolic computer algebra, which we implemented ourselves in C++ since the available standard software products such as `Mathematica` or `Maple` are too slow and require too much memory. In the analysis we focused up to now mainly on the bond-diluted Ising model ($q = 2$) for which we used our computer package to generate high-temperature series up to order 21 in $d = 3$ dimensions [4, 5] and up to order 19 in $d = 4, 5$ [5]. Applying various analysis tools we determined the phase diagrams in the temperature-dilution plane and estimated the critical exponent γ, parametrizing the singularity of the susceptibility at criticality, $\chi \sim (T - T_c)^{-\gamma}$. Depending on the dimension, our results can be compared with field-theoretic predictions and estimates from our Monte Carlo simulations performed in another project. For the 4-state Potts model in $d = 3$ dimensions [6], which in the pure case exhibits a first-order phase transition, we observed the expected softening by quenched disorder and estimated the critical exponent of the induced second-order transition.

Further new results were also obtained for the bond-percolation problem in various dimensions d, which is contained in the general formulation as the $q \to 1$ limit [7].

[1] C. Domb and M. S. Green, eds, *Phase Transitions and Critical Phenomena*, Vol. 3 (Academic Press, New York, 1974).
[2] R. R. P. Singh and S. Chakravarty, Phys. Rev. B **36**, 546 (1987).
[3] M. Hellmund and W. Janke, Condens. Matter Phys. **8**, 59 (2005).
[4] M. Hellmund and W. Janke, Comp. Phys. Comm. **147**, 435 (2002).
[5] M. Hellmund and W. Janke, Leipzig preprint (2005), to be published.
[6] M. Hellmund and W. Janke, Nucl Phys. B (Proc. Suppl.) **106/107**, 923 (2002); Phys. Rev. E **67**, 026118 (2003).
[7] M. Hellmund and W. Janke, Leipzig preprint (2005), to be published.

14.5 Droplet/Strip and Evaporation/Condensation Transitions

E. Bittner, W. Janke, A. Nußbaumer

The free energy of the three-dimensional Edwards-Anderson Ising spin-glass model exhibits in the low-temperature phase a rugged multi-valley structure. Consequently standard canonical Monte Carlo simulations are severely hampered by an exponential slowing down with increasing system size. This led to the application of multicanonical simulations, e.g. for the overlap parameter, which are designed by means of auxiliary weight factors to smooth out the energy landscape and thus to lead to uniform probability distributions. Given such a flat distribution, a much faster random walk behaviour in the corresponding observable is naively expected. In the actual simulations, however, one still observes jumps in the time series which can be attributed to so-called "hidden barriers". Building up on early analytical considerations of Leung and Zia [1], in a recent numerical work Neuhaus and Hager [2] were able to identify such barriers in the magnetisation M of the much simpler two-dimensional Ising model. They observed a geometrically induced

first-order phase transition from a droplet to a strip domain and showed that even a perfect multimagnetic simulation operating with the optimal weights still needs an exponential time to overcome the associated free energy barrier. To obtain more qualitative insights, we determined directly the anisotropy of a configuration during the transition by measuring its structure function. Simulating different system sizes with Kawasaki dynamics ($M = \text{const.}$), the scaling of the anisotropy leads to a value for the barrier height in good agreement with the theoretical prediction. By generalising these considerations to the case of the three-dimensional Ising model, new transitions could be identified analytically and verified numerically. Also the various crystal shapes emerging during the transition could be visualised.

Another first-order like transition can be identified when the first large droplet forms out of the fluctuations around the equilibrium magnetization. Invoking the equivalent lattice-gas picture, Biskup *et al.* [3] recently studied the behaviour of d-dimensional finite-volume liquid-vapour systems at a fixed excess δN of particles above the ambient gas density. Identifiying a dimensionless parameter $\Delta(\delta N)$ and a universal constant $\Delta_{\mathrm{c}}(d)$, they were able to show that for $\Delta < \Delta_c$ a droplet of the dense phase occurs, while for $\Delta > \Delta_c$ the excess is absorbed in the background. The fraction λ_Δ of excess particles forming the droplet is given explicitly. To verify these results, we have simulated the spin-1/2 Ising model on a square lattice at constant magnetisation equivalent to a fixed particle excess. We measured the largest minority droplet, corresponding to the liquid phase, at various system sizes ($L = 40 \ldots 640$). Using analytic values for the spontaneous magnetisation m_0, the susceptibility χ and interfacial free energy τ_{W} for the infinite system, we were able to determine λ_Δ in very good agreement with the theoretical prediction. In order to test the universal aspects of this evaporation/condensation transition, the measurements were repeated for next-nearest neighbour interactions and on a triangular lattice, giving similarly good results.

[1] K. Leung and R. Zia, J. Phys. A **23**, 4593 (1990).
[2] T. Neuhaus and J. Hager, Stat. Phys. **113**, 47 (2003).
[3] M. Biskup, L. Chayes and R. Kotecký, Europhys. Lett. **60**, 21 (2002).

14.6 Harris-Luck Criterion and Potts Models on Random Graphs

W. Janke, G. Kähler, M. Weigel*

*University of Waterloo, Canada

The Harris criterion judges the relevance of uncorrelated, quenched disorder for altering the universal properties of physical systems close to a continuous phase transition [1]. For this situation, as e.g., in the paradigmatic case of a quenched random-bond or bond diluted model, a change of universal properties is expected for models with a positive specific heat exponent α, i.e., the relevance threshold is given by $\alpha_c = 0$. For the physically more realistic case of spatially correlated disorder degrees of freedom, Harris' scaling argument can be generalised, yielding a shifted relevance threshold $-\infty < \alpha_c \leq 1$ known as Luck criterion [2]. The value of α_c depends on the quality and strength of the spatial disorder correlations as expressed in a so-called geometrical fluctuation or *wandering exponent*.

We consider the effect of a different, topologically defined type of disorder, namely the result of *connectivity disorder* produced by placing spin models on *random graphs*. As it turns out, the Harris-Luck argument can be generalised to this situation, leading to a criterion again involving a suitably defined wandering exponent of the underlying random graph ensemble. Using a carefully tailored series of finite-size scaling analyses, we precisely determine the wandering exponents of the two-dimensional ensembles of Poissonian Voronoï-Delaunay random lattices as well as the quantum gravity graphs of the dynamical triangulations model, thus arriving at explicit predictions for the relevance threshold α_c for these lattices [3]. As a result, for Poissonian Voronoï-Delaunay random graphs the Harris criterion $\alpha_c = 0$ should stay in effect, whereas for the dynamical triangulations the threshold is shifted to a negative value, $\alpha_c \approx -2$. The latter result is in perfect agreement with Monte Carlo simulations of the q-states Potts model [4] as well as an available exact solution of the percolation limit $q \to 1$ [5]. For the Voronoï-Delaunay triangulations, the Ising case $q = 2$ with $\alpha = 0$ is marginal and a change of universal properties cannot normally be expected. The $q = 3$ Potts model with $\alpha = 1/3$, on the other hand, should be shifted to a new universality class. Following up on a first exploratory study for small graphs [6], we performed high-precision cluster-update Monte Carlo simulations for rather large lattices of up to 80 000 triangles to investigate this model. Astonishingly, however, the (exactly known) critical exponents of the square-lattice $q = 3$ Potts model are reproduced to high precision [7]. To clarify this situation, we recently studied a generalised model introducing a distance dependence of the interactions [8].

[1] A. B. Harris, J. Phys. C **7**, 1671 (1974).
[2] A. Weinrib and B. I. Halperin, Phys. Rev. B **27**, 413 (1983); J. M. Luck, Europhys. Lett. **24**, 359 (1993).
[3] W. Janke and M. Weigel, Phys. Rev. B **69**, 144208 (2004).
[4] W. Janke and D. A. Johnston, Nucl. Phys. B **578**, 681 (2000).
[5] V. A. Kazakov, Mod. Phys. Lett. A **4**, 1691 (1989).
[6] F. W. S. Lima, U. M. S. Costa, M. P. Almeida and J. S. Andrade, Eur. Phys. J. B **17**, 111 (2000).
[7] W. Janke and M. Weigel, Acta Phys. Polon. B **34**, 4891 (2003).
[8] G. Kähler, Diploma Thesis, University of Leipzig (2004).

14.7 The F Model on Quantum Gravity Graphs

W. Janke, M. Weigel*

*University of Waterloo, Canada

As an alternative to various other approaches towards a theory of quantum gravity, the *dynamical triangulations* method has proved to be a successful discrete Euclidean formulation in two dimensions (2D). There, the integration over all metric tensors as the dynamic variables is performed by a summation over all possible gluings of equilateral triangles to form a closed surface of a given (usually planar) topology. The powerful methods of matrix integrals and generating functions allow for an exact solution of the pure 2D gravity model. Furthermore, matrix models can be formulated for spin models coupled to random graphs and some of them could be solved analytically. More generally,

the "dressing" of the weights of $c < 1$ conformal matter coupled to 2D quantum gravity is predicted by the KPZ/DDK formula [1], in agreement with all known exact solutions.

One of the most general models in statistical mechanics is Baxter's 8-vertex model [2]. Thus its behaviour on coupling it to dynamical *quadrangulations*, i.e., surfaces built from simplicial squares, is of general interest. Although a solution of special slices of this model could recently be achieved [3], the general model could not yet be solved. Heading for computer simulations, one first has to ensure the correct handling of the (quite unorthodox) geometry of four-valent graphs or quadrangulations in the dual language. While simulations of three-valent graphs have already been extensively done, the code for ϕ^4 graphs had to be newly developed and tested [4]. Due to the fractal structure of the graphs being described as a self-similar tree of "baby universes", this local dynamics suffers from critical slowing down. To alleviate the situation, we adapted a non-local update algorithm known as "minBU surgery" [5].

Combining the developed techniques, we simulated the F model, a symmetric case of the 8-vertex model, coupled to planar random ϕ^4 graphs. On regular [6] as well as random lattices [7], this model is expected to exhibit a Kosterlitz-Thouless transition to an antiferroelectrically ordered state [2, 3]. The numerical analysis of this model turned out to be exceptionally difficult due to the combined effect of the highly fractal structure of the graphs and the presence of strong logarithmic corrections. Still, a scaling analysis of the staggered polarizability yields results [7] in agreement with the predictions of Ref. [3] as far as the order of the transition and the location of the transition point are concerned.

[1] V. Knizhnik, A. Polyakov and A. Zamolodchikov, Mod. Phys. Lett. A **3**, 819 (1988); F. David, Mod. Phys. Lett. A **3**, 1651 (1988); J. Distler and H. Kawai, Nucl. Phys. B **321**, 509 (1989).
[2] R. Baxter, *Exactly Solved Models in Statistical Mechanics* (Academic Press, London, 1982).
[3] V. A. Kazakov and P. Zinn-Justin, Nucl. Phys. B **546**, 647 (1999); I. Kostov, Nucl. Phys. B **575**, 513 (2000); P. Zinn-Justin, Europhys. Lett. **50**, 15 (2000).
[4] M. Weigel and W. Janke, Nucl. Phys. B (Proc. Suppl.) **106–107**, 986 (2002); M. Weigel, Ph.D. Thesis, University of Leipzig (2002).
[5] J. Ambjørn *et al.*, Phys. Lett. B **325**, 337 (1994).
[6] M. Weigel and W. Janke, cond-mat/0501222, submitted to J. Phys. A.
[7] M. Weigel and W. Janke, hep-lat/0409028, submitted to Nucl. Phys. B.

14.8 Crystal Shapes and Sequence Dependence of Polymer and Heteropolymer Ground States

M. Bachmann, W. Janke, A. Kallias, R. Schiemann*, T. Vogel

*ETH Zürich, Switzerland

It has not been clarified yet whether polymers and proteins form crystallline or amorphous global energy minimum conformations. Proteins are generally expected to possess a stable geometric structure which is strongly connected with its biological function, or at least a small number of metastable states being important for dynamical processes (a well-known example is the synthase of ATP). The study of this problem is interesting

from different perspectives. First, the kinetics of the folding process through possibly well-defined folding channels in the free-energy landscape will strongly be influenced by the kind of transition towards the ground-state conformation. Second, from a purely pragmatic point of view, many complex analyses of polymer folding can only be performed by considering much simpler lattice models which are widely used for qualitative studies. If there would be, in fact, a relation between ground-state structures and crystal shapes, then lattice model studies could also give selective quantitative answers.

We have applied minimization algorithms to effective, coarse-grained lattice and off-lattice polymer and heteropolymer models in two and three dimensions. For the simple case of a pure Lennard-Jones polymer in two dimensions we could show the expected crystallization on a triangular lattice quite clearly. In three dimensions, the identification of the crystal shape, if any, is much more complicated, since surface effects affect the shape of the lowest-energy conformations more strongly. There are, however, some indications that the core could take face-centered cubic (fcc) or hexagonal closely packed (hcp) structures.

In a separate but related study we have investigated the thermodynamics of conformational transitions of lattice heteropolymers. We analysed short peptides, consisting only of two different types of amino acid classes (hydrophobic and polar), with up to 19 monomers extensively by exactly enumerating all possible sequences and conformations [1–3]. We identified all so-called designing sequences whose ground state is nondegenerate. One of the main results is that the ground-state conformations of heteropolymers with these sequences are not necessarily maximally compact, i.e., the radius of gyration of these structures is not the smallest possible. This is a consequence of the formation of a hydrophobic core, surrounded by a shell of polar monomers. Interestingly, many lattice heteropolymers experience two conformational transitions: the random-coil–globule collapse and the formation of the hydrophobic core. This was confirmed in our simulations of selected, much longer heteropolymers with up to 103 monomers [4], where we applied our recently developed multicanonical chain-growth algorithm [5].

[1] R. Schiemann, M. Bachmann and W. Janke, Comp. Phys. Comm. **166**, 8 (2005).
[2] R. Schiemann, M. Bachmann and W. Janke, J. Chem. Phys. **122**, 114705 (2005) [q-bio/0405009].
[3] T. Vogel, Diploma Thesis, University of Leipzig (2004).
[4] M. Bachmann and W. Janke, J. Chem. Phys. **120**, 6779 (2004).
[5] M. Bachmann and W. Janke, Phys. Rev. Lett. **91**, 208105 (2003).

14.9 Folding Channels in Coarse-Grained and All-Atom Peptide Models

H. Arkın*, M. Bachmann, W. Janke, A. Kallias, J. Schluttig, S. Schnabel

*Hacettepe University, Ankara, Turkey

Notwithstanding enormous computational capacities, simulations of realistic protein models are still highly nontrivial and, with respect to studies of their folding dynamics, currently impossible. The reason is that the folding of a protein takes milliseconds to seconds, while the time scale of present molecular dynamics simulations is orders of magnitude

smaller. As an alternative, Monte Carlo simulations are used to study the kinetics of folding transitions, although the dynamics of Markov chains, Monte Carlo methods are based upon, has no relation to Newtonian equations of motion. Therefore, kinetic studies by means of Monte Carlo methods are restricted to statements on ensemble properties, e.g., conformational phases. But, in fact, conformational transitions, where cooperative rearrangements of monomers happen, *could be* the key to understand folding kinetics even on this statistical level. Since more than a decade it has been known that some (short) proteins with less than 100 residues are two-state folder, i.e., the ensemble is dominated either by random conformations or by conformations which are structurally similar to the folded state. In this case the free energy is directly related with the Kramers rate and therefore, implicitly, with the dynamics of the folding process. Since these systems are too large to be simulated as all-atom models, however, the importance of so-called Gō models has drastically increased in the past years. The "energy" of an arbitrary conformation is determined by its structural deviation from the global energy minimum conformation (which is a priori unknown and enters into the model as experimental input). These models are, however, rather unsatisfying from the physical point of view as no natural forces appear in the model.

We investigate the main aspects of these general problems from different perspectives. One of the projects is the ongoing study of the 13-residue C-peptide of Ribonuclease A which has the nice property to only form an α-helix. Therefore it is a good example for studying two-state folding. We use a generalized-ensemble (multicanonical) method to perform the simulation and to study fluctuations of a helical order parameter to determine the characteristic folding transition and a structural order parameter to reconstruct the folding path. Another focus of our study is the comparison of simple coarse-grained (but physical) heteropolymer models and their Gō analogue. This is done by means of the replica exchange (parallel tempering) Monte Carlo method and molecular dynamics, where we are mostly interested in comparisons of dynamic components of the conformational transitions in these models. It is also important to understand how to modify coarse-grained models in order to make them capable to yield results being quantitatively competitive. Concerning two-state folding, for example, it is interesting to know how bending and torsion of successive covalent bonds influence the folding transition and to what extent these forces are responsible for the occurrence of intermediary states that slow down the folding dynamics [1, 2].

[1] M. Bachmann and W. Janke, to appear in Comp. Phys. Comm. (in print).
[2] H. Arkın, M. Bachmann and W. Janke, Phys. Rev. E **71**, 031906 (2005).

14.10 Substrate Specificity of Peptide Adsorption

M. Bachmann, K. Goede*, M. Grundmann*, W. Janke

* Institute for Experimental PhysicsII

From recent experiments of the adsorption of short peptides at semiconductor substrates it is known that different surface properties (materials such as Si or GaAs, crystal orientation, etc.) as well as different amino acid sequences strongly influence the binding of these peptides at the substrate [1, 2]. This specificity will be of essential importance for future sensory devices and pattern recognition at the nanometer scale. The reasons for this

binding specificity are far from being clear, and it is a big challenge from the experimental and theoretical point of view to understand the basic principles of substrate–peptide cooperativity. The experimental equipment has reached such a high resolution that it allows a precise identification of single molecule shapes at the substrate, and the available computational capacities and sophisticated algorithms necessary for probing appropriate models will make it possible to come closer to a solution of this problem in the near future.

In order to reduce the complexity of the problem to a minimum, we study a heteropolymer with given sequence of only two types of monomers: hydrophobic (H) and polar (P). Another simplification is the restriction of the conformational space to self-avoiding walks in a cavity. The heteropolymer is modeled by the hydrophobic–polar (HP) model [3], which has become very popular for studies of the sequence and conformational space of lattice heteropolymers [4]. We use the simplest form, where only the hydrophobic force acts and the number of nearest-neighbour contacts between H monomers being nonadjacent along the chain is related to the energy of the heteropolymer. The interaction with the substrate is modeled in a like manner: The energy of the heteropolymer is reduced by the number of next-neighbor contacts between the substrate and those monomers that experience the attractive force of the substrate. For all other monomers the influence of the substrate is only entropic. In order to study the specificity of surface–binding, we investigate three attractive substrate models. In the first variant, all monomers, independent of their hydrophobic or polar character, are equally attracted by the substrate and the energy of the system is proportional to the total number of monomer–surface contacts. In the second and third model, the substrate is either hydrophobic or polar, i.e., only the hydrophobic or polar monomers in the heteropolymer sequence are attracted by the substrate, respectively.

For studying these systems, we have redesigned the multicanonical chain-growth algorithm [5] to sample the space of monomer–substrate and monomer–monomer contacts within a single simulation. This contact density method has already proven to be very efficient for a nongrafted homopolymer in solution near an adsorbing surface [6].

[1] S. R. Whaley, D. S. English, E. L. Hu, P. F. Barbara and A. M. Belcher, Nature **405**, 665 (2000).
[2] K. Goede, P. Busch and M. Grundmann, Nano Lett. **4**, 2115 (2004).
[3] K. F. Lau and K. A. Dill, Macromolecules **22**, 3986 (1989).
[4] R. Schiemann, M. Bachmann and W. Janke, J. Chem. Phys. **122**, 114705 (2005).
[5] M. Bachmann and W. Janke, Phys. Rev. Lett. **91**, 208105 (2003).
[6] M. Bachmann and W. Janke, cond-mat/0502138, submitted to Phys. Rev. Lett.

14.11 End-To-End Distribution of Stiff Polymers

B. Hamprecht*, W. Janke, H. Kleinert*

*FU Berlin

In this project we consider so-called Porod-Kratky wormlike chains which model stiff polymers [1]. By mapping the statistical physics problem onto an equivalent path-integral representation of quantum mechanics, it is possible to derive via the associated Schrödinger

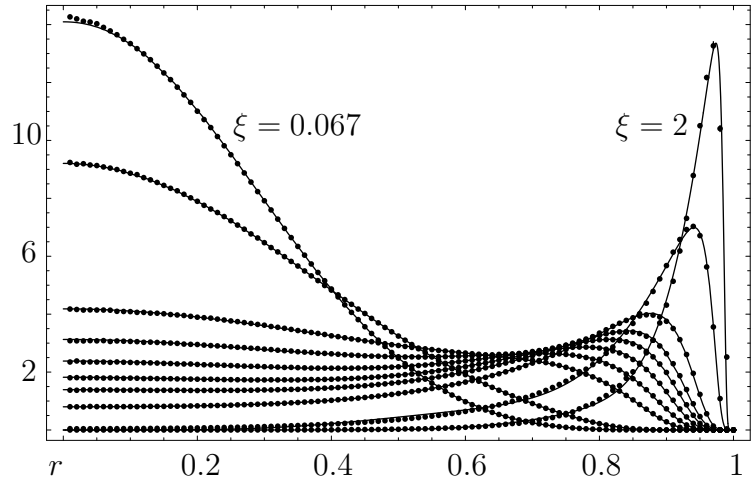

Figure 14.2: Comparison of analytical results (lines) and Monte Carlo data (dots) for the radial end-to-end distribution density of two-dimensional stiff polymers with persistence length ξ.

equation recursion relations for all even moments of the end-to-end distribution function [2]. By means of the algebraic computer software `Mathematica` these equations have been solved exactly to very high order in two and three dimensions.

The knowledge of these moments allows a very precise parametrization of the distribution function with uniform accuracy for all persistence lengths ξ of the polymer. This is a great advantage over earlier methods which could only be applied in limiting cases. We tested the accuracy of our analytical parametrization method by comparing it with extensive Monte Carlo simulations, see Fig. 14.2. With both methods we observed the interesting dip structure at intermediate values of the persistence length if one plots the radial distribution density for the two-dimensional system. Analogous analyses of the three-dimensional system are still in progress.

[1] H. Yamakawa, *Modern Theory of Polymer Solution* (Harper and Row, New York, 1971); *Helical Wormlike Chains in Polymer Solution* (Springer, Berlin, 1997).
[2] B. Hamprecht and H. Kleinert, cond-mat/0305226.
[3] B. Hamprecht, W. Janke and H. Kleinert, Phys. Lett. A **330**, 254 (2004).

14.12 Geometrical Approach to Phase Transitions

W. Janke, A. M. J. Schakel

This project aims at a geometrical description for a variety of phase transitions, ranging from thermal transitions in spin models over Bose-Einstein condensation in dilute gases to the deconfinement transition in gauge theories. Since many exact results are known in two dimensions, 2D models form the main focus of the present research. Using Monte Carlo simulations, the fractal structure of the spin configurations of the 2D Ising model was investigated [1], whose thermal critical behaviour can be equivalently described as percolation of suitably defined clusters of spins. The fractal dimension of these so-called Fortuin-Kasteleyn clusters, which encode the entire critical behaviour, and that of their boundaries have been determined numerically by applying standard finite-size scaling

to observables such as the percolation probability and the average cluster size. The obtained results are in excellent agreement with theoretical predictions and partly provide significant improvements in precision over existing numerical estimates [2].

Also the naive "geometrical" spin clusters encode critical behaviour, namely that of the diluted model. Within this project, recently a one-to-one map between the two cluster types could be established. By numerically determining the fractal structure of the geometrical clusters and that of their boundaries, this map was verified to high precision [1]. Based on numerical results on the high-temperature representation of the 2D Ising model [3], a generalization of the famous de Gennes result, that connects the critical behaviour of the O(N) model in the limit $N \to 0$ to the configurational entropy of a polymer chain in a good solvent, to arbitrary $-2 \leq N \leq 2$ was given [4]. The high-temperature representation can be visualized by graphs on the lattice. In the high-temperature phase, where they have a finite line tension, large graphs are exponentially suppressed. Upon approaching the critical temperature, the line tension vanishes and the graphs proliferate. Their fractal structure was shown to encode the entire critical behaviour, so that a purely geometrical description of the phase transition in the O(N) model was obtained.

When including vacancies, it is generally believed that the O(N) model gives in addition to critical behaviour rise to also tricritical behaviour. By gradually increasing the activity of the vacancies, the continuous O(N) phase transition is eventually driven first order at a tricritical point. In the context of polymers ($N \to 0$), the latter obtains by lowering the temperature to the so-called Θ point where the increasingly important van der Waals attraction between monomers causes the polymer chain to collapse. Up to now, relatively little is known about the tricritical behaviour for $N \neq 0$. By arguing that the fractal dimensions of the high-temperature graphs close to the tricritical point are in one-to-one correspondence with those at the critical point, exact, albeit non-rigorous, predictions could be made for the tricritical exponent η and, through scaling relations, for the ratios β/ν and γ/ν [4].

[1] W. Janke and A. M. J. Schakel, Nucl. Phys. B [FS] **700**, 385 (2004).
[2] J. Asikainen, A. Aharony, B. B. Mandelbrot, E. M. Rauch and J.-P. Hovi, Eur. Phys. J. B **34**, 479 (2003); S. Fortunato, Phys. Rev. B **66**, 054107 (2002).
[3] W. Janke and A. M. J. Schakel, Phys. Rev. E **71**, 036703 (2005).
[4] W. Janke and A. M. J. Schakel, cond-mat/0502062, submitted to Phys. Rev. Lett.

14.13 Vortex-Line Percolation in a Three-Dimensional Complex Ginzburg-Landau Model

E. Bittner, W. Janke, A. Krinner, A. M. J. Schakel, A. Schiller*, S. Wenzel

*TET group

The superfluid phase transition can be described either by a directional XY model or by an O(2) symmetric scalar field theory, whose Hamiltonian is commonly expressed with a complex field $\psi(\vec{r}) = |\psi(\vec{r})|e^{i\phi(\vec{r})}$ in the Ginzburg-Landau form. Therefore the model can also be represented by the partition function of an equivalent theory in which the spin configurations are replaced by configurations of closed lines. The loops of this equivalent

theory can be identified with the vortex lines of the original theory, therefore they might play an important role in determining the properties of the phase transition. A seemingly natural approach to study the vortex degrees of freedom is to associate with every spin configuration generated in a lattice Monte Carlo simulation a number of vortex loops. The hope is then that the transition could be identified with a non-zero probability of finding vortex loops that extend through the whole system [1], a phenomenon which is usually called percolation.

Percolational studies of spin clusters in the Ising model showed that one has to handle this approach carefully. It only works, if one uses a proper stochastic definition of clusters [2–5]. The Fortuin-Kasteleyn (FK) clusters of spins can be obtained from the geometrical spin clusters, which consist of nearest neighbor sites with their spin variables in the same state, by laying bonds with a certain probability between the nearest neighbors. The resulting FK clusters are in general smaller than the geometrical ones and also more loosely connected. For the different cluster types one may find different percolation thresholds and critical exponents.

The work of this project concentrates on the three-dimensional complex Ginzburg-Landau model, which belongs to the O(2) universality class. Two experimentally important cases are studied: The pure complex Ginzburg-Landau model [6–8], relevant for the universal properties of the λ-transition in liquid helium, and its extension with a minimal coupling to an external compact U(1) gauge field (Abelian Higgs model) [9, 10], relevant for the universal aspects of superconductors and also for elementary particle physics and cosmology. In the latter case, a first-order phase transition line ending at a critical point was found in the Higgs coupling – "hopping parameter" ($\lambda - \kappa$) plane for small λ at a fixed gauge coupling (β) which, similar to the liquid-gas phase diagram, separates the Higgs and "confinement" phase. Based on our data for the magnetic monopole density and other quantities we present arguments that this phase boundary continues for larger λ as a so-called Kertész line [10], across which no phase transition in a strict thermodynamic sense takes place, but percolation observables do exhibit singular behaviour. This picture is completely analogous to the scenario proposed by Kertész for the liquid-gas phase diagram.

In three-dimensional, globally O(2) symmetric theories the percolating objects are vortex lines forming closed networks. One of the main questions we want to address is: Is there a similar clue in the case of vortex networks as for spin clusters, or do they display different features? Therefore we connect the obtained vortex-line elements to closed loops, which are geometrically defined objects. When a branching point, where $n \geq 2$ junctions are encountered, is reached, a decision on how to continue has to be made. This step involves a certain ambiguity. We want to investigate the influence of the probability of treating such a branching point as a knot, see Fig. 14.3.

In discussing the phase transition of the Ginzburg-Landau theory, we study a geometrically defined vortex-loop network as well as the magnetic properties of the system in the vicinity of the critical point. Using high-precision Monte Carlo techniques we consider an alternative formulation of the geometrical excitations in relation to the global O(2) symmetry breaking, and check if both of them exhibit the same critical behaviour leading to the same critical exponents and therefore to a consistent description of the phase transition. Different percolation observables are taken into account and compared with each other.

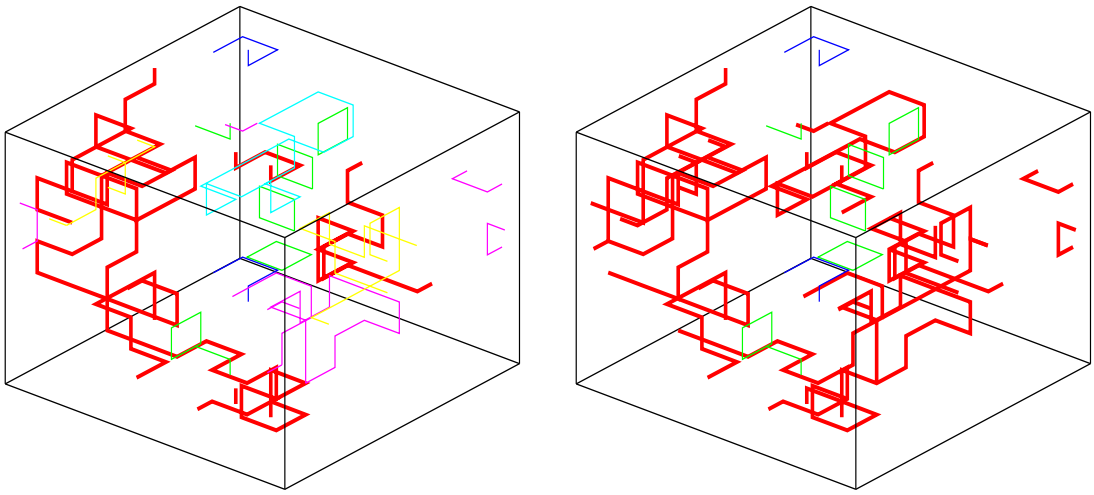

Figure 14.3: Left: Vortex-loop network generated at the thermodynamic critical point for lattice size $L = 8$ and probability $c = 0.4$ to treat a branching point as a knot. Right: Vortex-loop network generated treating *all* branching points as knots for the same spin configuration as in the left plot.

[1] K. Kajantie, M. Laine, T. Neuhaus, A. Rajanie and K. Rummukainen, Phys. Lett. B **482**, 114 (2000).
[2] P. W. Kasteleyn and C. M. Fortuin, J. Phys. Soc. of Japan **26** (Suppl.), 11 (1969); C. M. Fortuin and P. W. Kasteleyn, Physica **57**, 536 (1972); C. M. Fortuin, Physica **58**, 393 (1972), *ibid.* **59**, 545 (1972).
[3] A. Coniglio and W. Klein, J. Phys. A **13**, 2775 (1980).
[4] S. Fortunato, J. Phys. A **36**, 4269 (2003).
[5] W. Janke and A. M. J. Schakel, Nucl. Phys. B **700**, 385 (2004).
[6] A. Krinner, Diploma Thesis, University of Leipzig (2004).
[7] E. Bittner and W. Janke, Phys. Rev. B **71**, 024512 (2005).
[8] E. Bittner, A. Krinner and W. Janke, Leipzig preprint (2005), to be published.
[9] S. Wenzel, Master Thesis, University of Leipzig (2003).
[10] S. Wenzel, E. Bittner, W. Janke, A. M. J. Schakel and A. Schiller, cond-mat/0503599, submitted to Phys. Rev. Lett.

14.14 Information Geometry and Phase Transitions

W. Janke, D. A. Johnston*, R. Kenna†, R. P. K. C. Malmini‡

*Heriot-Watt University, Edinburgh, Scotland
†Coventry University, England
‡University of Sri Jayewardenepura, Sri Lanka

Motivated by ideas in parametric statistics [1], various authors have recently discussed the advantages of taking a geometrical perspective on statistical mechanics [2]. The "distance" between two probability distributions in parametric statistics can be measured using a geodesic distance which is calculated from the Fisher information matrix for the system. To this end the manifold $\mathcal{M}$ of parameters is endowed with a natural Riemannian metric, the Fisher-Rao metric [1]. For the example of a spin model in a magnetic field

h, $\mathcal{M}$ is a two-dimensional manifold parametrised by $(\theta^1, \theta^2) = (\beta, h)$, where $\beta = 1/k_B T$ is the inverse temperature. The components of the Fisher-Rao metric take the simple form $G_{ij} = \partial_i \partial_j f$ in this case, where f is the reduced free energy per site and $\partial_i = \partial/\partial\theta^i$. A natural object to consider in any geometrical approach is the scalar or Gaussian curvature $\mathcal{R}$ which in various two-parameter calculable models has been found to diverge at the phase transition point β_c according to the scaling relation $\mathcal{R} \sim |\beta - \beta_c|^{\alpha-2}$, where α is the usual specific heat critical exponent. For spin models the necessity of calculating in non-zero field has limited analytic consideration to 1D, mean-field and Bethe lattice Ising models [3].

In this project we used the exact solution in field of the Ising model on an ensemble of fluctuating planar random graphs (where $\alpha = -1,\ \beta = 1/2,\ \gamma = 2$) [4] to evaluate the scaling behaviour of the scalar curvature explicitly, and find $\mathcal{R} \sim |\beta - \beta_c|^{-2}$ [5]. The apparent discrepancy with the general scaling postulate is traced back to the effect of a *negative* α [5]. As anticipated, the same effect is found in exact calculations for the *three*-dimensional spherical model [6, 7], which was solved (in field) in the classic Berlin and Kac paper [8] and shares the same critical exponents as the Ising model on *two*-dimensional planar random graphs. We mainly concentrated on the 3D case, but also discussed other dimensions [6, 7], in particular the mean-field like behaviour which sets in at $D = 4$. Similar considerations have been used to explain a possible critical behaviour in families of solutions for black holes which we also briefly discuss [7].

[1] R. A. Fisher, Phil. Trans. R. Soc. Lond., Ser. A **222**, 309 (1922); C. R. Rao, Bull. Calcutta Math. Soc. **37**, 81 (1945).
[2] G. Ruppeiner, Rev. Mod. Phys. **67**, 605 (1995); D. Brody and N. Rivier, Phys. Rev. E **51**, 1006 (1995); D. Brody and L. Hughston, Proc. Roy. Soc. London A **455**, 1683 (1999).
[3] B. P. Dolan, D. A. Johnston and R. Kenna, J. Phys. A **35**, 9025 (2002).
[4] D. V. Boulatov and V. A. Kazakov, Phys. Lett. B **186**, 379 (1987).
[5] W. Janke, D. A. Johnston and R. P. K. C. Malmini, Phys. Rev. E **66**, 056119 (2002).
[6] W. Janke, D. A. Johnston and R. Kenna, Phys. Rev. E **67**, 046106 (2003); Physica **A336**, 181 (2004).
[7] D. A. Johnston, W. Janke and R. Kenna, Acta Physica Polonica B **34**, 4923 (2003).
[8] T. Berlin and M. Kac, Phys. Rev. **86**, 821 (1952).

14.15 Ageing Phenomena in Ferromagnets

W. Janke, D. A. Johnston*, E. Lorenz, R. Megaides

*Heriot-Watt University, Edinburgh, Scotland

When a ferromagnet is suddenly quenched from the disordered into the ordered phase at a temperature below the Curie point, its temporal relaxation exhibits ageing phenomena similar to the behaviour of glasses and spin glasses. For ferromagnets this effect could recently be described in quite some detail with the help of dynamical symmetry arguments [1]. While the assumptions underlying these theoretical considerations are very plausible, their validity is not proven and it is hence important to test the predictions by means of alternative methods such as Monte Carlo simulations. Recent studies of the Ising model in two and three dimensions showed indeed good agreement [2]. Still, to ensure the

general applicability of the theoretical framework, typical representative models of other universality classes should be investigated. In this project we therefore perform a Monte Carlo study of the two-dimensional 3-state Potts model and determine two-time correlators as well as the thermoremanent response function. In order to achieve the necessary accuracy, one has to prepare many independent random start configurations and monitors for each copy its stochastic time evolution after the quench into the low-temperature phase. The final results are obtained by averaging over the copies. Also for this model our preliminary results [3] show good agreement with the analytical predictions.

Quite similar phenomena can be observed in the so-called gonihedric lattice spin model which was orginally constructed as a discretized string (or, equivalently, self-avoiding surface) model [4]. Generically it consists of nearest-neighbour, next-nearest neighbour and plaquette interactions with fine-tuned coupling constants. In its original formulation the spins are taken to be of Ising type, i.e., $s = \pm 1$. It was soon recognized that this type of model exhibits a very intricate temporal relaxation behaviour in Monte Carlo simulations reminiscent of ageing phenomena in structural glasses. The analogy is, in fact, closer to (off-lattice) structural than to (lattice) spin glasses since *no* quenched disorder is involved in gonihedric models. The gonihedric model is hence a rare example for lattice models *without* quenched disorder that display ageing phenomena, and from this point of view it has attracted considerable interest also in the statistical physics community. After reproducing the quite intricate relaxation behaviour for the Ising case [5] and refining some of the measurement prescriptions with further input from our experiences with the properties of glasses and spin glasses, we also performed first exploratory computer experiments with suitable generalizations to Potts and O(n) symmetric spin models with $n \geq 2$, in particular the O(2) or XY model [6].

[1] M. Henkel, Nucl. Phys. B **641**, 405 (2002).
[2] M. Henkel and M. Pleimling, Phys. Rev. E **68**, 065101(R) (2003); M. Henkel, A. Picone and M. Pleimling, Europhys. Lett. **68**, 191 (2004).
[3] E. Lorenz, Diploma Thesis, University of Leipzig (in preparation).
[4] G. K. Savvidy and K. G. Savvidy, Phys. Lett. B **337**, 333 (1994).
[5] P. Dimopoulos, D. Espriu, E. Jané and A. Prats, Phys. Rev. E **66**, 056112 (2002).
[6] R. Megaides, Master Thesis, University of Leipzig (2004).

14.16 Critical Amplitude Ratios in the Baxter-Wu Model

W. Janke, L. N. Shchur*

*Landau Institute, Chernogolovka, Russia

At a second-order phase transition not only critical exponents but also certain amplitude ratios are universal, i.e., do not depend on the details of the considered statistical system. A typical example is provided by the scaling relation for the magnetic suceptibility χ which in the vicinity of the critical temperature T_c behaves according to $\chi \sim \Gamma_{\pm}|T/T_c - 1|^{-\gamma}$, where γ is a critical exponent and Γ_+ and Γ_- denote the critical amplitudes in the high- and low-temperature phase, respectively. The ratio Γ_+/Γ_- is then such a universal amplitude ratio, whose value could recently be predicted analytically for the two-dimensional

q-state Potts model with $q = 2$, 3 and 4 states [1, 2]. While for $q = 2$ and 3 this prediction could subsequently be confirmed with numerical techniques (Monte Carlo simulations and high-temperature series expansions) [3], the situation for $q = 4$ remained controversial. The resason for the disagreement lies probably in relatively strong logarithmic corrections of the leading scaling behaviour [4]. In order to test this conjecture, we considered the two-dimensional Baxter-Wu model [5] (a model with three-spin interaction on a triangular lattice) which is known from its exact solution to belong to the $q = 4$ universality class, but does *not* exhibit logarithmic corrections. By employing a special cluster-update algorithm [6] we have performed extensive Monte Carlo simulations of this model which are currently analysed.

[1] G. Delfino and J. L. Cardy, Nucl. Phys. B [FS] **519**, 551 (1998).
[2] G. Delfino, G. T. Barkema and J. L. Cardy, Nucl. Phys. B **565**, 521 (2000).
[3] L. N. Shchur, P. Butera and B. Berche, Nucl. Phys. B **620**, 579 (2002).
[4] J. Salas and A. D. Sokal, J. Stat. Phys. **88**, 567 (1997).
[5] R. J. Baxter and F. Y. Wu, Phys. Rev. Lett. **31**, 1294 (1973); Aust. J. Phys. **27**, 357 (1974).
[6] M. A. Novotny and H. G. Evertz, in: *Computer Simulation Studies in Condensed Matter Physics*, Vol. VI, edited by D. P. Landau, K. K. Mon and H.-B. Schüttler (Springer, Berlin, 1993), p. 188.

14.17 Quantum Monte Carlo Studies of Spin-Wave Superconductivity

R. Bischof, L. Bogacz, P. R. Crompton, W. Janke, Z. X. Xu*, H. P. Ying*, B. Zheng*, S. Wenzel

*Zhejiang Institute of Modern Physics, Zhejiang University, Hangzhou, P.R. China

The Valence Bond Solid picture of spin-wave superconductivity developed following Haldane's conjecture [1] gives a precise framework for determining the critical properties of a variety of quasi-one dimensional ferromagnetic spin applications exploiting low-temperature superconductivity phenomena currently being fabricated for use in the computing and recording industries. We investigate valence bond state quantum phase transitions by means of the continuous time Quantum Monte Carlo loop cluster algorithm [2]. The algorithm has allowed for numerical investigation in regimes previously limited by algorithmic development, and also of the analytic conjecture itself (recently generalised for our inhomogeneous-spin cases of interest [3]) with now indications of novel quantum interference effects [4]. The proposal of Haldane was essentially for single-spin chains but the numerical testing of the ideas has subsequently pushed forward the boundaries of potential quantum interference solutions [5, 6]. Making for a closing mapping into experimental systems through the inclusion of higher spin representations and off-diagonal Hamiltonian contributions such as spin-ladder models, treatable via numerical study [7].

Specifically, we are determining the critical exponents that govern the scaling of numerical results to allow both for a closer experimental mapping and to further investigate the range of applicability of the central algorithmic technique [8]. An investigation of the short-time dynamics exponents of this method further establishes the credibility of

this approach for the novel states we would intend to investigate [9, 10]. Providing also a means to further develop both improved estimators for the superconducting gap states by means of new cross-correlated statistical measures, and to also gain a deeper understanding of the effect of applying and removing magnetic fields to these systems and magnetic impurities.

[1] F. D. M. Haldane, Phys. Rev. Lett. **61**, 8 (1988).
[2] B. B. Beard and U.-J. Wiese, Phys. Rev. Lett. **77**, 5130 (1996).
[3] K. Takano, Phys. Rev. B **61**, 13 (2000).
[4] P. Zhang, Z. X. Xu, H. P. Ying and J. H. Dai, to appear in Mod. Phys. Lett. A (2005).
[5] Z. Xu, J. Dai, H. Ying and B. Zheng, Phys. Rev. B **67**, 214426 (2003).
[6] P. R. Crompton, W. Janke, Z. X. Xu and H. P. Ying, Nucl. Phys. B (Proc. Suppl.) **140**, 817 (2005).
[7] S. Todo, M. Matsumoto, C. Yasuda and H. Takayama, Phys. Rev. B **64**, 224412 (2001); M. Nakamura and S. Todo, Phys. Rev. Lett. **89**, 077204 (2002).
[8] R. Bischof, P. R. Crompton and W. Janke, Leipzig preprint (in preparation).
[9] W. Janke and R. Villanova, Phys. Rev. B **66**, 134208 (2002).
[10] H. P. Ying and K. Harada, Phys. Rev. E **62**, 1 (2000).

14.18 Funding

Discrete Random Geometries: From Solid State Physics to Quantum Gravity
W. Janke
EU-Network "EUROGRID"
Grant No. HPRN-CT-1999-000161

Hochtemperaturreihen für Random-Bond-Modelle und Spingläser
W. Janke
Deutsche Forschungsgemeinschaft (DFG)
Grant No. JA 483/17-3

Dynamik und Statik von Spingläsern
W. Janke
Deutsche Forschungsgemeinschaft (DFG)
Grant No. JA483/22-1

Investigation of Thermodynamic Properties of Lattice and Off-Lattice Models for Proteins and Polymers
M. Bachmann and W. Janke
Deutsche Forschungsgemeinschaft (DFG)
Grant No. JA483/24-1/2

Two-Dimensional Magnetic Systems with Anisotropy
W. Janke
EU Marie Curie Development Host Fellowship
Grant No. IHP-HPMD-CT-2001-00108

Quantenfeldtheorie: Mathematische Struktur und Anwendungen in der Elementarteilchen- und Festkörperphysik
Dozenten der Theoretischen Physik und Mathematik (Sprecher B. Geyer)
Deutsche Forschungsgemeinschaft (DFG)
Graduiertenkolleg, Grant No. 52

Numerical Simulations of Biologically Motivated Problems in Statistical Physics
H. Arkın and W. Janke
Deutsche Forschungsgemeinschaft (DFG) and TÜBITAK
Grant No. 446TÜR112/14/04

Universal Critical Amplitude Rations in the Baxter-Wu Model
L. N. Shchur and W. Janke
Deutsche Forschungsgemeinschaft (DFG)
Grant No. 436RUS17/122/03

Numerical Approaches to Protein Folding
A. Irbäck and W. Janke
DAAD-STINT Collaborative Research Grant with the University of Lund, Sweden
Grant No. D/05/26016

Statistical Physics of Random Structures with Applications to Life and Material Sciences
W. Janke
German-Israel-Foundation (GIF)
Grant No. I-653-181.14/1999

Challenges in Molecular Simulations: Bridging the Length and Time-Scale Gap
W. Janke
ESF Programme "SIMU"

Statistical Physics of Glassy and Non-Equilibrium Systems
W. Janke
ESF Programme "SPHINX"

Multi-Overlap Simulationen von Spingläsern
W. Janke
NIC Jülich (computer time grant for T3E)
Grant No. hmz09

Ungeordnete Ferromagnete
W. Janke
NIC Jülich (computer time grant for T3E)
Grant No. hlz06

Disordered Ferromagnets
W. Janke
LRZ Munich (computer time grant for Hitachi)
Grant No. h0611

Monte Carlo Simulationen der Statik und Dynamik von Spingläsern
E. Bittner and W. Janke
NIC Jülich (computer time grant for "JUMP")
Grant No. hlz10

Protein and Polymer Models
M. Bachmann and W. Janke
NIC Jülich (computer time grant for "JUMP")
Grant No. hlz11

14.19 Organizational Duties

Michael Bachmann

- Co-organizer of the Workshop *LEILAT04 – 14. Workshop on Lattice Field Theory*, ITP, Universität Leipzig, 3–5 June 2004 (with W. Janke, A. Schiller, E. Bittner)
- Scientific Secretary of the Workshop *CompPhys04 – 5. NTZ-Workshop on Computational Physics*, ITP, Universität Leipzig, 25–26 November 2004

Elmar Bittner

- Co-organizer of the Workshop *LEILAT04 – 14. Workshop on Lattice Field Theory*, ITP, Universität Leipzig, 3–5 June 2004 (with W. Janke, A. Schiller, M. Bachmann)
- Scientific Secretary of the Workshop *CompPhys04 – 5. NTZ-Workshop on Computational Physics*, ITP, Universität Leipzig, 25–26 November 2004

Leszek Bogacz

- Scientific Secretary of the Workshop *ANet04 – Joint COPIRA/NTZ-Workshop Networks and Their Applications*, ITP, Universität Leipzig, 24–25 November 2004

Wolfhard Janke

- Director of the Naturwissenschaftlich-Theoretisches Zentrum (NTZ) at the Zentrum für Höhere Studien (ZHS), Universität Leipzig
- Organizer of the Workshop *LEILAT04 – 14. Workshop on Lattice Field Theory*, ITP, Universität Leipzig, 3–5 June 2004 (with A. Schiller, E. Bittner, M. Bachmann)
- Organizer of the Workshop *ANet04 – Joint COPIRA/NTZ-Workshop Networks and Their Applications*, ITP, Universität Leipzig, 24–25 November 2004 (with Z. Burda (Krakow))
- Organizer of the Workshop *CompPhys04 – 5. NTZ-Workshop on Computational Physics*, ITP, Universität Leipzig, 25–26 November 2004
- Permanent Member of International Advisory Board, *Conference of the Middle European Cooperation in Statistical Physics (MECO)*
- Member of Advisory Committee, *TIRLAT05 – 15. Workshop on Lattice Field Theory*, Tirana, Albania (2005)
- Referee: Physical Review Letters, Physical Review B, Physical Review E, Europhysics Letters, Physics Letters A, Physics Letters B, The European Physical Journal B, Physica A, Journal of Physics A, Computer Physics Communications, JSTAT, New Journal of Physics

14.20 External Cooperations

Academic

EU-Network "EUROGRID" – *Discrete Random Geometries: From Solid State Physics to Quantum Gravity* with 11 teams throughout Europe

GIF-Network *Statistical Physics of Random Structures with Applications to Life and Material Sciences* with Joan Adler (Technion, Haifa), Amnon Aharony (Tel Aviv Univ.), Eytan Domany (Weizmann Inst., Rehovot), Kurt Binder (Mainz), Peter Grassberger (Jülich and Wuppertal), Thomas Nattermann (Köln) and Dietrich Stauffer (Köln)

Dept. of Physics, Florida State University, Tallahassee, USA
Prof. Dr. Bernd A. Berg

CEA/Saclay, Service de Physique Théorique, France
Dr. Alain Billoire

Laboratoire de Physique des Matériaux (UMR CNRS No 7556), Université Henri Poincaré, Nancy, France
Prof. Dr. Bertrand Berche, Dr. Christophe Chatelain

Groupe de Physique des Matériaux (UMR CNRS No 6634), Université de Rouen, France
Dr. Pierre-Emmanuel Berche

School of Mathematical and Computer Sciences, Heriot-Watt University, Edinburgh, Scotland
Prof. Dr. Desmond A. Johnston

School of Mathematical and Information Sciences, Coventry University, England
Dr. Ralph Kenna

Dept. of Physics, Hacettepe University, Ankara, Turkey
Dr. Handan Arkın

Complex Systems Division, Department of Theoretical Physics, Lund University, Lund, Sweden
Prof. Dr. Anders Irbäck

NIC, Forschungszentrum Jülich
Prof. Dr. Peter Grassberger, Dr. Hsiao-Ping Hsu

Atominstitut, TU Wien, Austria
Prof. Dr. Harald Markum, Dr. Rainer Pullirsch

Dept. of Physics, University of Wales Swansea, Swansea, Wales
Dr. Simon Hands

Service de Physique Théorique, CEA/DSM/SPhT Saclay, France
Dr. Gernot Akemann

Inst. für Theoretische Physik, FU Berlin
Prof. Dr. Bodo Hamprecht, Prof. Dr. Hagen Kleinert

IAC-1, Universität Stuttgart
Priv.-Doz. Dr. Rudolf Hilfer

Inst. für Theoretische Physik, Universität Bielefeld
Priv.-Doz. Dr. Thomas Neuhaus

Institute of Physics, Jagellonian University, Kraków, Poland
Prof. Dr. Zdzisław Burda

Landau Institute for Theoretical Physics, Chernogolovka, Russia
Prof. Dr. Lev N. Shchur

Yerevan Physics Institute, Yerevan, Armenia
Prof. Dr. David B. Saakian

University of Sri Jayewardenepura, Sri Lanka
Dr. Ranasinghe P. K. C. Malmini

Department of Physics, Sri Venkateswara College, University of Delhi, New Delhi, India
Dr. Bibudhananda Biswal

Department of Mechanical Engineering and Intelligent Systems, Tokyo University of Electro-communications, Chofu, Tokyo, Japan
Prof. Dr. Hans-Georg Mattutis

Zhejiang Institute of Modern Physics, Zhejiang University, Hangzhou, P.R. China
Prof. Dr. He-Ping Ying, Prof. Dr. Bo Zheng

14.21 Publications

Journals

Bachmann, M.; Janke, W.
Thermodynamics of Lattice Heteropolymers
J. Chem. Phys. **120** (2004) 6779–6791

Berche, P.-E.; Chatelain, C.; Berche, B.; Janke, W.
Bond Dilution in the 3D Ising Model: A Monte Carlo Study
Eur. Phys. J. **B38** (2004) 463–474

Bittner, E.; Hands, S.; Markum, H.; Pullirsch, R.
Quantum Chaos in Supersymmetric QCD at Finite Density
Proceedings of the Workshop on *Finite Density QCD*, Nara, Japan, July 10–12, 2003, Prog. Theor. Phys. Suppl. **153** (2004) 295–300

Blythe, R.A.; Janke, W.; Johnston, D.A.; Kenna, R.
The Grand-Canonical Asymmetric Exclusion Process and the One-Transit Walk
J. Stat. Mech.: Theor. Exp. (2004) P06001-1–10

Blythe, R.A.; Janke, W.; Johnston, D.A.; Kenna, R.
Dyck Paths, Motzkin Paths and Traffic Jams
J. Stat. Mech.: Theor. Exp. (2004) P10007-1–22

Hamprecht, B.; Janke, W.; Kleinert, H.
End-to-End Distribution Function of Two-Dimensional Stiff Polymers for all Persistence Lengths
Phys. Lett. **A330** (2004) 254–259

Janke, W.; Berche, P.-E.; Chatelain, C.; Berche, B.
Quenched Disorder Distributions in Three-Dimensional Diluted Ferromagnets
In: Landau, D.P.; Lewis, S.P.; Schüttler, H.-B. (Eds.): *Computer Simulation Studies in Condensed-Matter Physics XVI*
Berlin, Springer, 2004; pp. 89–94

Janke, W.; Johnston, D.A.; Kenna, R.
Phase Transition Strength through Densities of General Distributions of Zeroes
Nucl. Phys. **B682** (2004) 618–634

Janke, W.; Johnston, D.A.; Kenna, R.
Information Geometry and Phase Transitions
Physica **A336** (2004) 181–186

Janke, W.; Schakel, A.M.J.
Geometrical vs. Fortuin-Kasteleyn Clusters in the Two-Dimensional q-State Potts Model
Nucl. Phys. **B700** (2004) 385–406

Janke, W.; Weigel, M.
The Harris-Luck Criterion for Random Lattices
Phys. Rev. **B69** (2004) 144208-1–12

Janke, W.; Weigel, M.
Monte Carlo Studies of Connectivity Disorder
In: Wagner, S.; Hanke, W.; Bode, A.; Durst, F. (Eds.): *High Performance Computing in Science and Engineering, Munich 2004*, transactions of the *Second Joint HLRB and KONWIHR Result and Reviewing Workshop*
Berlin, Springer, 2004; pp. 363–374

Journals January–March 2005

Akemann, G; Bittner E.; Lombardo, M.-P.; Markum, H.; Pullirsch R.
Density Profiles of Small Dirac Operator Eigenvalues for Two Color QCD at Nonzero Chemical Potential Compared to Matrix Models
Nucl. Phys. **B** (Proc. Suppl.) **140** (2005) 568–570

Bittner, E.; Janke, W.
Nature of Phase Transitions in a Generalized Complex $|\psi|^4$ Model
Phys. Rev. **B71** (2005) 024512-1–11

Crompton, P.R.; Janke, W.; Xu, Z.X.; Ying, H.P.
Finite-Size Scaling, Fisher Zeroes and N=4 Super Yang-Mills
Nucl. Phys. **B** (Proc. Suppl.) **140** (2005) 817–819

Schiemann, R.; Bachmann, M.; Janke, W.
Exact Enumeration for Three-Dimensional Lattice Proteins
Comp. Phys. Comm. **166** (2005) 8–16

Bachmann, M.; Arkın, H.; Janke, W.
Multicanonical Study of Coarse-Grained Off-Lattice Models for Protein Folding
Phys. Rev. **E71** (2005) 031906-1–11

Berche, B.; Berche, P.-E.; Chatelain, C.; Janke, W.
Random Ising Model in Three Dimensions: Theory, Experiment and Simulation – a Difficult Coexistence
Condens. Matter Phys. **8** (2005) 47–58

Hellmund, M.; Janke, W.
High-temperature Series Expansions for Random Potts Models
Condens. Matter Phys. **8** (2005) 59–74

Janke, W.; Schakel, A.M.J.
Fractal Structure of Spin Clusters and Domain Walls in 2D Ising Model
Phys. Rev. **E71** (2005) 036703-1–8

Schiemann, R.; Bachmann, M.; Janke, W.
Exact Sequence Analysis for Three-Dimensional HP Lattice Proteins
J. Chem. Phys. **122** (2005) 114705-1–10

In press

Bachmann, M.; Janke, W.
Conformational Transitions of Heteropolymers
Leipzig preprint (August 2004), to appear in Proceedings *CCP2004*, Genoa, Italy, 1 – 4 September, 2004 (in press)

Hilfer, R.; Biswal, B.; Mattutis, H.-G.; Janke, W.
Multicanonical Simulations of the Tails of the Order-Parameter Distribution of the 2D Ising Model
Stuttgart/New Delhi/Tokyo/Leipzig preprint (August 2004), e-print cond-mat/0502408, to appear in Proceedings *CCP2004*, Genoa, Italy, 1 – 4 September, 2004 (in press)

Janke, W.; Johnston, D.A.; Kenna, R.
Phase Transition Strength from General Distributions of Zeroes
Leipzig/Edinburgh/Coventry preprint (August 2004), to appear in Proceedings *CCP2004*, Genoa, Italy, 1 – 4 September, 2004 (in press)

Janke, W.; Schakel, A.M.J.
Geometrical Phase Transitions
Leipzig preprint (August 2004), e-print cond-mat/0409267, to appear in Proceedings *CCP2004*, Genoa, Italy, 1 – 4 September, 2004 (in press)

Talks and Posters

Michael Bachmann
Statistical Properties of Off-Lattice Heteropolymers
(with Janke, W.; Arkın, H.) Winter School on Computational Soft Matter, Bonn, February 29 – March 6 (P)

Michael Bachmann
Thermodynamics of Off-Lattice Heteropolymers
DPG-Frühjahrstagung Regensburg, March 8–12 (T)

Michael Bachmann
Off-Lattice Heteropolymers
Seminar on Complex Systems, John von Neumann Institut für Computing (NIC), Forschungszentrum Jülich, March 16–20 (T)

Michael Bachmann
Multicanonical Study of Effective Off-Lattice Models for Heteropolymers
(with Janke, W.; Arkın, H.) 29th Conference of the Middle European Cooperation in Statistical Physics (MECO29), Bratislava, Slovakia, March 28 – April 1 (P)

Michael Bachmann
Thermodynamics of Heteropolymers
Statistical Physics Workshop, Technische Universität Wien, Austria, April 1–3 (T)

Michael Bachmann
Conformational Transitions of Heteropolymers
Theorie-Seminar, Hahn-Meitner-Institut, Berlin, April 29 (T)

Michael Bachmann
Thermodynamics of Simple Heteropolymer Models
Theorie-Seminar, Max-Planck-Institut für Kolloid- und Grenzflächenforschung, Golm, May 10 (T)

Michael Bachmann
Statistical Properties of Off-Lattice Heteropolymers
(with Janke, W.; Arkın, H.) 3rd Day of Biotechnology, Leipzig, May 19 (P)

Michael Bachmann
Conformational Transitions of Lattice Heteropolymers
14th Workshop on Lattice Field Theory (LEILAT04), Leipzig, June 3–5 (T)

Michael Bachmann
Conformational Transitions of Heteropolymers
Conference on Computational Physics (CCP04), Genoa, Italy, September 1–4 (T)

Michael Bachmann
Multicanonical Simulations of Heteropolymers
(with Janke, W.; Arkın, H.) Conference on Computational Physics (CCP04), Genoa, Italy, September 1–4 (P)

Elmar Bittner
Phase Diagram of the Generalized Complex $|\psi|^4$ Model
DPG-Frühjahrstagung, Arbeitskreis Festkörperphysik, Universität Regensburg, March 8–12 (T)

Elmar Bittner
Phase Diagram of the Generalized Ginzburg-Landau Model
(with Janke, W.) 4th EUROGRID Conference on Random Geometry: Theory and Applications, Les Houches, France, March 22–26 (T)

Elmar Bittner
Generalized Complex $|\psi|^4$ Model in Two and Three Dimensions
(with Janke, W.) 29th Conference of the Middle European Cooperation in Statistical Physics (MECO29), Bratislava, Slovakia, March 28–April 1 (P)

Elmar Bittner
Phase Diagram of a Generalized $|\psi|^4$ Model in Two and Three Dimensions
14th Workshop on Lattice Field Theory (LEILAT04), Leipzig, June 3–5 (T)

Elmar Bittner
Vortex Line Percolation in a Complex ψ^4 Model
(with Krinner, A.; Janke, W.)
Conference on Computational Physics (CCP04), Genoa, Italy, September 1–4 (P)

Leszek Bogacz
Dirac Operator Coupled to 2D Lorentzian Quantum Gravity
4th EUROGRID Conference on Random Geometry: Theory and Applications, Les Houches, France, March 22–26 (P)

Peter Crompton
Quantum Phase Transitions and the Nonlinear Sigma Model
14th Workshop on Lattice Field Theory (LEILAT04), Leipzig, June 3–5 (T)

Peter Crompton
Partition Function Zeroes of Quantum Phase Transitions
Conference on Exotic Order and Criticality in Quantum Matter, KITP, Santa Barbara, USA, June 7–11 (P)

Peter Crompton
Finite Size Scaling, Fisher Zeroes, and $\mathcal{N}$=4 Super Yang-Mills
The XXII International Symposium on Lattice Field Theory (Lattice 2004), Fermi National Accelerator Laboratory, Batavia, USA, June 21–26 (T)

Peter Crompton
A Fisher Zeroes Analysis of Valence Bond Solid Transitions in Quantum Spin Chains
Conference on Computational Physics (CCP 2004), Genoa, Italy, September 1–4 (T)(P)

Peter Crompton
Valence Bond Solid Transitions in Inhomogeneous Spin Chains
WE-Heraeus-Seminar on Quantum Phase Transitions, Physikzentrum, Bad Honnef, 11–14 October (P)

Peter Crompton
A Fisher Zeroes Analysis of the Continuous-time Quantum Monte Carlo Method
International Workshop Hangzhou 2004 on Simulational Physics, Zhejiang University, Hangzhou, China, November 5–7 (T)

Peter Crompton
Nonequilibrium Quantum Dynamics
5th NTZ-Workshop on Computational Physics (CompPhys04), Leipzig, December 25–26 (T)

Wolfhard Janke
Thermodynamics of Lattice Proteins using Multicanonical Chain Growth
Theoretisch-Physikalisches Kolloquium, Freie Universität Berlin, January 5 (T)

Wolfhard Janke
Monte Carlo Simulations of Complex Physical Systems
Physics Colloquium, Zhejiang University, Hangzhou, China, February 27 (T)

Wolfhard Janke
"Optimal Paths" Through Computer Simulations
Physics Seminar, Zhejiang University, Hangzhou, China, February 28 (T)

Wolfhard Janke
Monte Carlo Study of the Bond-Diluted 3D Ising Model
(with Berche, P.-E.; Chatelain, C.; Berche, B.) DPG-Frühjahrstagung, Arbeitskreis Festkörperphysik, Universität Regensburg, March 8–12 (P)

Wolfhard Janke
Multicanonical Chain Growth Method for Folding Lattice Proteins
Workshop on Markov Chain Monte Carlo, Institute for Mathematical Sciences, National University of Singapore, Singapore, March 1–28 (inv. T)

Wolfhard Janke
Multicanonical Chain Growth Simulations of Lattice Protein Folding
4th EUROGRID Conference on Random Geometry: Theory and Applications, Les Houches, France, March 22–26 (T)

Wolfhard Janke
Monte Carlo Simulations of 3D Bond-Diluted Potts Models
29th Conference of the Middle European Cooperation in Statistical Physics (MECO29), Bratislava, Slovakia, March 28 – April 1 (T)

Wolfhard Janke
Relevance of Quenched Disorder
Statistical Physics Workshop, Technische Universität Wien, Austria, April 1–3 (T)

Wolfhard Janke
Multicanonical Chain Growth Method for Folding Lattice Proteins
Physikalisches Kolloquium, Universität Erlangen-Nürnberg, April 26 (T)

Wolfhard Janke
Folding Lattice Proteins
Atelier Nancy, Université Henri Poincaré, Nancy, France, May 26–28 (inv. T)

Wolfhard Janke
Multicanonical Simulations of the Tails of the Order-Parameter Distribution of the 2D Ising Model
Conference on Computational Physics (CCP2004), Genoa, Italy, September 1–4 (T)

Wolfhard Janke
Moments of Stiff Polymer Chains
Mathematica-Aktionstag, Universität Leipzig, October 29 (T)

Wolfhard Janke
Folding Lattice Proteins: Multicanonical Chain Growth and Exact Enumerations
Statistik-Seminar, Universität Göttingen, November 10 (T)

Axel Krinner
Vortex-Loop Percolation in XY and Ginzburg-Landau Model
DPG-Frühjahrstagung, Arbeitskreis Festkörperphysik, Universität Regensburg, March 8–12 (T)

Andreas Nußbaumer
Equilibrium Crystal Shapes in Three Dimensions
DPG-Frühjahrstagung, Arbeitskreis Festkörperphysik, Universität Regensburg, March 8–12 (T)

Andreas Nußbaumer
Ising Droplets in Action
(with Bittner, E.; Janke, W.) 29th Conference of the Middle European Cooperation in Statistical Physics (MECO29), Bratislava, Slovakia, March 28 – April 1 (P)

Andreas Nußbaumer
Ising Droplets in Action
Statistical Physics Workshop, Technische Universität Wien, Austria, April 1–3 (T)

Andreas Nußbaumer
Ising Droplets in Action
14th Workshop on Lattice Field Theory (LEILAT04), Leipzig, June 3–5 (T)

Andreas Nußbaumer
Equilibrium Crystal Shapes in Three Dimension
(with Bittner, E.; Janke, W.) Conference on Computational Physics (CCP04), Genoa, Italy, September 1–4 (P)

Andreas Nußbaumer
Wulff Shapes of Ising Droplets
Mathematica-Aktionstag, Universität Leipzig, October 29 (T)

Andreas Nußbaumer
Ising Droplets in Action
(with Bittner, E.; Janke, W.) 5th NTZ-Workshop on Computational Physics (CompPhys04), Leipzig, November 25–26 (P)

Adriaan Schakel
Physics in Geometrical Potts Clusters
Seminar, March 19, 2004, Institute of Physics, Jagellonian University, Krakow, Poland, March 19 (T)

Adriaan Schakel
Geometrical Approach to Phase Transitions
8th Annual Workshop on Phase Transitions and Critical Phenomena, Lviv, Ukraine, March 23–25 (T)

Adriaan Schakel
Physics in Geometrical Potts Clusters
(with Janke, W.) 29th Conference of the Middle European Cooperation in Statistical Physics (MECO29), Bratislava, Slovakia, March 28 – April 1 (P)

Adriaan Schakel
Fractal Structure of Field Theories
14th Workshop on Lattice Field Theory (LEILAT04), Leipzig, June 3–5 (T)

Adriaan Schakel
Vortex Network Generation in Superfluid Turbulence

COSLAB Workshop on Turbulence and Vacuum Instability in Condensed Matter and Cosmology, Lammi, Finland, August 17–22 (T)

Adriaan Schakel
Loops in the 2D XY Model
Conference on Computational Physics (CCP2004), Genoa, Italy, September 1–4 (T)

Adriaan Schakel
Fractal Structure of Critical and Collapsing Loops in 2D
5th NTZ-Workshop on Computational Physics (CompPhys04), Leipzig, November 25–26 (T)

Reinhard Schiemann
Exact Sequence Analysis of HP Lattice Proteins
(with Bachmann, M.; Janke, W.) DPG-Frühjahrstagung, Arbeitskreis Festkörperphysik, Universität Regensburg, March 8–12 (P)

Thomas Vogel
HP Proteins on Generalized Lattices
(with Bachmann, M.; Janke, W.) Winter School on Computational Soft Matter, Bonn, February 29 – March 6 (P)

Thomas Vogel
Hydrophobic-Polar Lattice Heteropolymers on Generalized Lattices
(with Bachmann, M.; Janke, W.) DPG-Frühjahrstagung, Arbeitskreis Festkörperphysik, Universität Regensburg, March 8–12 (P)

Thomas Vogel
Collapse of Long Lattice Polymers
DPG-Frühjahrstagung, Arbeitskreis Festkörperphysik, Universität Regensburg, March 8–12 (T)

Thomas Vogel
HP Proteins on Generalized Lattices
(with Bachmann, M.; Janke, W.) 3rd Day of Biotechnology, Leipzig, May 19 (P)

14.22 Graduations

Diploma

Thomas Vogel
HP-Proteine auf verallgemeinerten Gittern und Homopolymerkollaps
Diploma Thesis, January 2004

Axel Krinner
Nature of Phase Transitions in a Generalized Complex Ginzburg-Landau
Diploma Thesis, March 2004

Goetz Kähler
The 3-State Potts-Model on 2-Dimensional Delaunay Random Lattices
Diploma Thesis, August 2004

M.Sc.

Rodrigo Megaides
Autocorrelation Measurements of the Gonihedric Model
Master Thesis, September 2004

14.23 Guests

Priv.-Doz. Dr. Axel Pelster
Freie Universität Berlin
NTZ-Kolloquium, January 29, 2004: *Quantum phase diagram for Bose gases*
January 29–30, 2004

Priv.-Doz. Dr. Rudolf Hilfer
ICA-1, Universität Stuttgart
NTZ-Kolloquium, February 5, 2004: *Anomalous diffusion, fractional calculus and Mittag-Leffler functions*
February 5–6, 2004

Priv.-Doz. Dr. Thomas Neuhaus
Universität Bielefeld
NTZ-Kolloquium, February 12, 2004: *Duality and scaling in 3d scalar electrodynamics*
January – February 2004

Prof. Dr. He-Ping Ying
Zhejiang University, Hangzhou, China
NTZ-Kolloquium, February 19, 2004: *Monte Carlo simulations of quantum mixed-spin chains*
February 19, 2004

Priv.-Doz. Dr. Christian Holm
MPI für Polymerforschung, Mainz
NTZ-Kolloquium, April 15, 2004: *Geladene weiche Materie: Bio – Nano – Techno*
April 14–15, 2004

Prof. Dr. Sigismund Kobe
TU Dresden
NTZ-Kolloquium, June 17, 2004: *Exact ground states of finite Ising spin glasses obtained by "branch-and-bound"*
June 17, 2004

Prof. Dr. Zdzislaw Burda
Jagellonian University, Krakow, Poland
NTZ-Kolloquium, July 8, 2004: *Statistical mechanics of random graphs*
July 7–9, 2004

Priv.-Doz. Dr. Boris Kastening
FU Berlin
NTZ-Kolloquium, July 15, 2004: *Bose-Einstein condensation temperature of a weakly interacting Bose gas*
July 15, 2004

Prof. Dr. Lev N. Shchur Landau Institute, Chernogolovka, Russia
NTZ-Kolloquium, July 22, 2004: *On the evolution of time horizons in parallel discrete event simulations*
July – August 2004

Dr. Martin Weigel
University of Waterloo, Canada
September 2004

Dr. Handan Arkin
Hacettepe University, Beytepe, Ankara, Turkey
NTZ-Kolloquium, October 14, 2004: *Generalized-ensemble simulations of peptides and proteins*
June – October 2004

Prof. Dr. Ulrich H.E. Hansmann
Michigan Technological University, Houghton, USA
NTZ-Kolloquium, November 4, 2004: *Protein folding in silico*
November 4–5, 2004

Prof. Dr. Hans-Gert Gräbe
Institut für Informatik, Universität Leizpig
NTZ-Kolloquium, November 11, 2004: *Trends und Entwicklungen in der Computeralgebra*
November 11, 2004.

Prof. Dr. Roman Kotecky
Charles University, Prague, Tschechien
TKM/NTZ-Kolloquium, November 30, 2004: *Birth of equilibrium droplet*
November 30, 2004

Priv.-Doz. Dr. Michel Pleimling
Universität Erlangen/Nürnberg
NTZ-Kolloquium, December 9, 2004: *Alterungsphänomene in Systemen fern vom Gleichgewicht*
December 9–10, 2004

Prof. Dr. Bernd A. Berg
Florida State University, Tallahassee, USA
NTZ-Kolloquium, December 16, 2004: *A tutorial lecture on Markov chain Monte Carlo simulations*
December 16–17, 2004

Prof. Dr. Lev N. Shchur
Landau Institute, Chernogolovka, Russia
October – December 2004

15

Molecular Dynamics / Computer Simulation

15.1 Introduction

Using methods of statistical physics and computer simulations we investigate classical many-particle systems interacting with interfaces. One aim of the research in our group is to built up a bridge between theoretical and experimental physics.

By means of analytical theories of statistical physics and computer simulations (Molecular dynamics, Monte Carlo procedures, percolation theories) using modern workstations and supercomputers we examine subjects for which high interest exists in basic research and industry as well. The examinations involve transport properties (diffusion of guest molecules) in zeolites and the structural and phase behaviour of complex fluids on bulk conditions and in molecular confinements. Especially we are interested to understand

- the diffusion behaviour of guest molecules in zeolites in dependence on thermodynamic parameters, steric conditions, intermolecular potentials and the concentration of the guest molecules,
- structure and phase equilibria of complex (aqueous) fluids in interfacial systems (e.g. pores, thin films, model membranes) in dependence on geometric and thermodynamic conditions
- and the migration of waste in deposits by use of percolation theories

in microscopic detail and to compare the results with experimental data. The use of a network of PC's and workstations (Unix, Linux, Windows), the preparation and application of programs (Fortran, C, C^{++}) and the interesting objects (zeolites, membranes) give excellent possibilities for future careers of undergraduates, graduate students and postdocs.

Our research is part of several national and international programs (DFG - Schwerpunktprogramm 1155, an International Research Graduate Training program (IRTG 1056), a joint research project DFG/TRF-Thailand, a joint research project DAAD/TRF-Thailand and joint research projects with UOIT Oshawa and SHARCNET, Canada) and includes a close collaboration with the Institute of Experimental Physics I (Physics of Interfaces and Biomembranes) of Leipzig University and many institutions in Germany and other countries (for details compare Sect. 15.11)

H.L. Vörtler and S. Fritzsche

15.2 Simulation and Molecular Theory of Phase Equilibria and Chemical Potentials of Aqueous Fluids in Bulk Systems and in Thin Films

H.L. Vörtler, I. Nezbeda*, M. Kettler†

* Prag, Tschechien
† Frankfurt

In this project we investigate the thermodynamics and the phase behaviour of aqueous fluids based on a hierarchic modelling of intermolecular potentials.

In order to improve the efficiency of chemical potential simulations in complex fluids we have studied and modified in 2004 recent test particle methods (monomer/dimer insertion, gradual insertion) and implemented these to dense aqueous phases By combination of these methods we were able to improve significantly the efficiency of phase equilibria simulations of strongly associating water models on both homogeneous and inhomogeneous conditions [1]. Some results are shown in the figure.

To reach a more fundamental understanding of structural properties in the critical range percolation theory is used [2].

The results have to be considered as quasi-experimental reference data for an improvement of hierarchic models of intermolecular potentials (extended primitive models

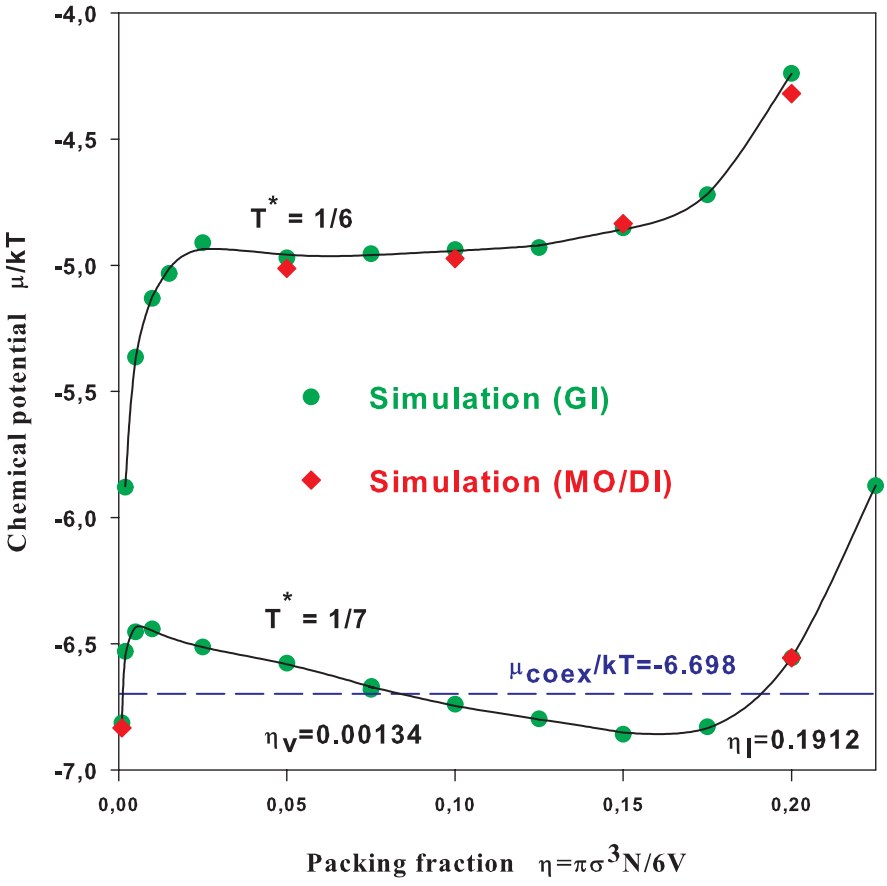

Figure 15.1: Chemical potential of EPM5 water

of water) and of thermodynamic perturbation theories which contribute to a microscopic understanding of solubility and hydration phenomena of associating fluids in molecular confinements, particularly in porous media and biomembranes.

Important results obtained in this project are summarized in the review article [3].

This work is part of an international collaboration with the group of Prof. Ivo Nezbeda, Prague.

[1] H.L. Vörtler, Talk, Efficient Simulation of Chemical Potentials, Workshop Comphys04, Leipzig, November 2004; Preprint (Mol. Phys., to be published)
[2] H.L. Vörtler, Invited lecture, Clusters and Percolation, Liquid Matter Workshop, Trest, Czech Republic, October 2004
[3] S. Fritzsche, R. Haberlandt and H.L. Vörtler, Modeling and Simulation of Structure, Thermodynamics, and Transport of Fluids in Molecular Confinements, in Molecules in Interaction With Surfaces and Interfaces, Editors: R. Haberlandt, D. Michel, A. Pöppl and R. Stannarius, Springer Verlag, Heidelberg, 2004, pp. 1-88

15.3 Cavity Distribution Functions and Phase Equilibria in Confined Fluids

H.L. Vörtler, W.R. Smith*

* Oshawa, Canada

In 2004 we have continued our studies of the molecular structure of hard-core fluids in simple molecular confinements based on a hierarchy of cavity- and background correlation functions.

We have calculated cavity pair distribution functions by means of novel MC Methods which use virtual insertions of particles and cavities. These results are used for an improvement of integral equations (closure relations of BGY-like hierarchies).

In general, the results of these studies provide basic structural information for the understanding of phase equilibria in geometrically restricted fluids on a molecular level. Of particular interest in this context is the estimation of the thermodynamic pressure in coexisting confined phases. We obtained quasi-experimental reference data of local and spreading pressures by a direct simulation of these quantities using our own new developed virtual volume variation methods.

The long-term goals of our research are contributions to a statistical-mechanical theory of phase equilibria of inhomogeneous fluids with applications to nanoporous materials and biointerfaces.

This research was supported by SHARCNET computer network (Ontario, Canada) and by research fund of University of Ontario Institute of Technology (support of research stay of H.L. Vörtler in Oshawa)

15.4 Investigation of Diffusion Mechanisms of Nonspherical Molecules in Cation Free Zeolites

S. Fritzsche, A. Schüring, R. Haberlandt

Analytical jump models for the diffusion of ethane and butene molecules adsorbed in cation free zeolites of type Linde A, chabazite and silicalite–1 have been developped basing on data resulting from Molecular Dynamics (MD) simulations. Examinations of the local free energy lead to the conclusion that the temperature dependence of the jump rates are determined by entropic barriers in some cases. The work was done in cooperation with Prof. S.M. Auerbach (Amhurst, USA) and the group of Prof. Kärger (Institute of Experimental Physics I, University Leipzig). Im 2004 two papers have been published [1, 2].

This research was supported by the DFG: SPP1155 (Grant Fr1486/2-1)

[1] A. Schüring, S. Fritzsche, R. Haberlandt, S. Vasenkov und J. Kärger, Phys. Chem. Chem. Phys., **6**, 3676 (2004)

[2] A. Schüring, S.M. Auerbach, S. Fritzsche und R. Haberlandt, Studies in Surface Sciences and Catalysis **154**, 2110 (2004)

15.5 Analytical Treatment and Computer Simulations of Anomalous Diffusion in the Transition Region Gas/Adsorbent

S. Fritzsche, S. Vasenkov, A. Schüring

While diffusion processes within zeolites have been subject of many papers already, the effects connected with the boundary between the zeolite and the gas phase are not yet sufficiently investigated. In this project such effects are analysed for normal diffusion and single–file diffusion using MD simulations, Dynamical Monte Carlo (DMC) simulations and analytical derivations. MD simulations of systems with straight channels *e.g.* AFI zeolites containing appropriate molecules of relatively simple structures like isobutane or neopentane yield a connection to real systems. It was possible to find the forecasted boundary effects in the simulation results. A publication is in preparation.

This research was supported by the DFG: SPP1155 (Grant Fr1486/2-1)

15.6 Molecular Dynamics Investigation of Structure and Dynamics of Water Adsorbed in the Zeolite Chabazite

S. Fritzsche, R. Haberlandt, S. Jost

Earlier MD simulations of water in the natural zeolite chabazite have been continued. Under normal conditions in industrial processes a partial or total hydration of zeolites,

which is usually unwanted, can hardly be avoided because natural zeolites are strongly hydrophilic. Therefore, it is of practical interest to know the behaviour of the adsorbed water in the microscopic pores. This knowledge can be used to minimize unpleasant modifications of industrial processes by the water in the zeolites. The project includes investigations of the structural properties, particularly the interplay of the polar water molecules with the cations (*e.g.* calcium) in these zeolites. The examinations of dynamical effects focus on diffusion phenomena. Die PhD thesis of Steffen Jost about these simulation was 2004 finished successfully [1]. New simulations an a paper are in preparation.

[1] S. Jost, Untersuchung struktureller und dynamischer Eigenschaften von Wasser in Zeolithen am Beispiel von Chabasit mit Hilfe von MD - Simulationen, Dissertation, Universität Leipzig, 2004

15.7 Quantum Chemical Calculations and Classical MD Simulations of Methane in Silicalite

S. Fritzsche, R. Haberlandt, S. Hannongbua, C. Bussai,

In earlier papers the diffusion of water in silicalite–1 has been investigated by means of quantum chemical calculations and MD simulations and, in cooperation with Prof. Dr. J. Kärger (Institute of Experimental Physics I, University Leipzig) of PFG–NMR measurements. In continuation of this work the quantum chemical calculations and MD simulations have now been extended to methane in silicalite–1. Comparison with earlier simulation results leads to a deeper insight in the phenomena under consideration. Two papers [1, 2] have been published in 2004.

This research was supported by the DFG: Grants FR 1486/1-1 and FR 1486/1-2 and the Thailand Research Fund, TRF

[1] C. Bussai, S. Fritzsche, R. Haberlandt und S. Hannongbua, J. Phys. Chem B, **108**, 13347, 2004
[2] C. Bussai, S. Fritzsche, R. Haberlandt and S. Hannongbua, Studies in Surface Sciences and Catalysis **154**, 2104 (2004)

15.8 How Do Guest Molecules Enter Zeolite Pores? Quantum Chemical Calculations and Classical MD Simulations

S. Fritzsche, R. Haberlandt, S. Hannongbua, T. Remsungnen, V. Kormilets, O. Saengsawang

This is a common project of the German DFG and the Thailand Research Fund. The subject of this research are quantum chemical calculations and MD simulations of the silanol groups on the surface of zeolites. Effective potentials that include rotational degrees of freedom of the silanol groups are derived. MD simulations are carried out using these potentials. One paper in J. Phys. Chem. is in press [1].

This research was supported by the DFG: Grants FR 1486/1-1 and FR 1486/1-2 and the Thailand Research Fund, TRF

[1] O. Saengsawang, T. Remsungnen, S. Fritzsche, R. Haberlandt und S. Hannongbua Structure and Energetics of Water-Silanol Binding on the Surface of Silicalite-1: Quantum Chemical Calculations, J. Phys. Chem., in print

15.9 Investigation of the Diffusion of Pentane in Silicalite-1

S. Fritzsche, A. Longsinruin, S. Hannongbua

This common project of the German DAAD and the Thailand Research Fund deals with the diffusion of . In the framework of a Royal Golden Jubilee stipend a Thai student derives effective potentials for pentane in silicalite–1. MD simulations are carried out using these potentials. The mechanism of diffusion will be investigated and peculiarities will be examined in detail. One paper [1] was published in 2004.

This research was supported by the DAAD, Grant A/01/19909 and a Royal Golden Jubilee Grant of the Thailand Research Fund, TRF

[1] A. Loisruangsin, S. Fritzsche and S. Hannongbua, Chem. Phys. Lett., **390**, 485, 2004

15.10 Organizational Duties

Horst-Ludger Vörtler

- Speaker of the MDC group

15.11 External Cooperations

Academic

University of California, Irvine
Prof. M. Wolfsberg

Charles University and Czech Acad. Sci., Prague
Prof. I. Nezbeda, Dr. M. Lisal

University of Ontario Institute of Technology, Oshawa
Prof. W.R. Smith

Universität Regensburg
Prof. H. Krienke

Chulalongkorn University, Bangkok, Thailand
Prof. Supot Hannongbua

University of Massachusetts, Amhurst, USA
Prof. S. M. Auerbach

University of Khon Khaen, Khon Khaen, Thailand
Dr. T. Remsungnen

Mahidol University, Bangkok, Thailand
Prof. T. Osotchan, Prof. T. Kerdcharoen

University of Bordeaux, Bordeaux, France
Prof. P. A. Bopp

Max-Planck-Institut für Chemie, Mainz
Dr. K. Heinzinger

University of Sassari, Sassari, Italy
Prof. G. B. Suffritti, Prof. P. Demontis

University of Athens, Greece
Prof. D. N. Theodorou

University of Kielce and Polish Academy of Sciences, Warsaw
Prof. A. S. Cukrowski

15.12 Publications

Journals

A. Schüring, S. Fritzsche, R. Haberlandt, S. Vasenkov and J. Kärger,
Phys. Chem. Chem. Phys., **6**(2004)3676

A. Schüring, S.M. Auerbach, S. Fritzsche and R. Haberlandt,
Studies in Surface Sciences and Catalysis **154** 2110(2004)2110

C. Bussai, S. Fritzsche, R. Haberlandt and S. Hannongbua,
J. Phys. Chem B, **108**(2004)13347

C. Bussai, S. Fritzsche, R. Haberlandt and S. Hannongbua,
Studies in Surface Sciences and Catalysis **154**(2004)2104

A. Loisruangsin, S. Fritzsche and S. Hannongbua,
Chem. Phys. Lett. **390**(2004)485,

S. Fritzsche, R. Haberlandt und H.L. Vörtler,
Modeling and Simulation of Structure, Thermodynamics, and Transport of Fluids in Molecular Confinements
in *Molecules in Interaction With Surfaces and Interfaces*, Editors: R. Haberlandt, D. Michel, A. Pöppl and R. Stannarius,
Springer Verlag, Heidelberg, 2004, pp. 1-88

P. Bräuer, S. Fritzsche, J. Kärger. G. Schütz und S. Vasenkov,
Diffusion in Channels and Channel Networks
in *Molecules in Interaction With Surfaces and Interfaces*, Editors: R. Haberlandt, D. Michel, A. Pöppl and R. Stannarius,
Springer Verlag, Heidelberg, 2004, pp. 89-125

in press

O. Saengsawang, T. Remsungnen, S. Fritzsche, R. Haberlandt und S. Hannongbua,
Structure and Energetics of Water-Silanol Binding on the Surface of Silicalite-1: Quantum Chemical Calculations,
J. Phys. Chem., in press

Talks and Posters

H.L. Vörtler,
Efficient Simulation of Chemical Potentials,
Talk, Workshop Comphys04, Leipzig, November 2004;
Preprint (Mol. Phys., to be published)

H.L. Vörtler,
Clusters and Percolation,
Invited lecture, Liquid Matter Workshop, Trest, Czech Republic, October 2004

15.13 Graduations

PhD

S. Jost,
Untersuchung struktureller und dynamischer Eigenschaften von Wasser in Zeolithen am Beispiel von Chabasit mit Hilfe von MD - Simulationen,
Dissertation, Universität Leipzig, 2004

15.14 Guests

Prof. Dr. Supot Hannongbua
Chulalongkorn University, Bangkok, Thailand
06.12.2004 – 20.12.2004

Dr. Tawun Remsungnen
Chulalongkorn University, Bangkok, Thailand
06.10.2004 – 20.12.2004

16

Statistical Physics

16.1 Introduction

We work on the connections of statistical mechanics to quantum field theory, on the mathematical and physical aspects of renormalization group (RG) theory and on its applications to condensed matter physics, and on quantum kinetic theory. Our methods range from mathematical proofs to computational solution of large differential equations.

One of the central topics in our current research is an RG approach to many–fermion systems, which is used to investigate the properties of the Hubbard model in the parameter range relevant for high–temperature superconductivity. The RG method applied here is an exact functional transformation of the action of the system, which leads to an infinite hierarchy of equations for the Green functions. Truncations of this hierarchy are used in applications. In a number of nontrivial cases, this truncation can be justified rigorously, so that the method lends itself to mathematical studies. These mathematical aspects are also under investigation.

Another topic we study is the long–time dynamics of large quantum systems, with a view of understanding how dissipative dynamics on the macroscopic scale arises from the microscopically reversible dynamics in interesting scaling limits.

At present, we have collaborations with ETH Zurich, the Max–Planck Institute for Solid State Research in Stuttgart, the University of British Columbia, Vancouver, the University of Munich, and Stanford University.

16.2 Renormalization Group Flows and Broken Symmetries

M. Salmhofer, C. Honerkamp, W. Metzner, O. Lauscher

The flow to strong coupling observed in many RG studies of interacting fermion systems [1, 2] indicates the occurrence of symmetry breaking. It is also a major technical problem for the attempt to give a more detailed description of the symmetry–broken phases of such models. We have developed a method to continue the fermionic renormalization group flow into phases with broken global symmetry [3]. This method does not require a Hubbard-Stratonovich decoupling of the interaction. Instead an infinitesimally small symmetry-breaking component is inserted into the initial action, as an initial condition

for the flow of the self-energy. Its flow is driven by the interaction, and at low scales it saturates at a nonzero value if there is a tendency for spontaneous symmetry breaking in the corresponding channel. For the reduced BCS model, we show how a small initial gap amplitude flows to the value given by the exact solution of the model. The method is also being applied to models with competing instabilities.

[1] C. Halboth, W. Metzner, *Phys. Rev.* **B 61** (2000) 7364; *Phys. Rev. Lett.* **85** (2000) 5162;
[2] C. Honerkamp, M. Salmhofer, N. Furukawa, T.M. Rice, *Phys. Rev.* **B 63**, 035109 (2001)
[3] M. Salmhofer, C. Honerkamp, W. Metzner, O. Lauscher, Renormalization Group Flows into Phases with Broken Symmetry Prog. Theor. Phys. 112 (2004) 943-970

16.3 Quantum Diffusion in the Anderson Model

L. Erdös, M. Salmhofer, H.-T. Yau

We consider random Schrödinger equations on Z^d for $d \geq 3$ with identically distributed random potential. Denote by λ the coupling constant and ψ_t the solution with initial data ψ_0. Suppose that the space and time variables scale as $x \sim \lambda^{-2-\kappa/2}, t \sim \lambda^{-2-\kappa}$ with small enough $\kappa > 0$. We prove that, in the limit $\lambda \to 0$, the expectation value of the Wigner distribution of ψ_t, $\mathbf{E}W_{\psi_t}(x, v)$, converges weakly to a solution of a heat equation in the space variable x for arbitrary L^2 initial data. The diffusion coefficient is uniquely determined by the kinetic energy associated to the velocity v.

The key of our method is an analysis of the phase cancellations of multiple scatterings with respect to the random potential. We prove that the amplitude of a Feynman graph (generated from taking the expectation of the absolute value of the Green function square) is smaller than its "naive size" by an extra λ factor *per non-ladder vertex*. This is the first time that the improvement over the naive estimates on the Feynman graphs grows as a power law of the small parameter with the exponent depending linearly on the number of vertices.

[1] L. Erdös, M. Salmhofer, H.-T. Yau, Quantum diffusion of the random Schrödinger evolution in the scaling limit. math-ph/0502025

16.4 Competing Ordering Tendencies in Correlated Fermions

C. Husemann, O. Lauscher, M. Salmhofer

Competing ordering tendencies occur in many of the interesting new materials, in particular in high-T_c materials near to optimal doping. The renormalization group is a powerful tool to investigate their relative strength and competition. In order to give a quantitative phase diagram and calculate correlation functions in the regime where the order parameter fields are well-developed, we study a renormalization group flow for bosons and fermions in these models. The boson fields correspond to composite fields of fermions.

As a first example, we study the interplay of ferromagnetism and superconductivity in the two–dimensional Hubbard model with hopping amplitudes t between nearest neighbours and t' between next–to–nearest neighbours, in the regime $0.3 < -t'/t < 0.5$. The study of ferromagnetism poses a number of technical challenges in RG treatments because the usual Fermi surface cutoff suppresses ferromagnetism as compared with other ordering tendencies. The temperature–flow RG, which avoids this problem, was developed in [1]. In the above–mentioned regime, it predicts a zero–temperature transition between d–wave superconductivity and ferromagnetism if the Fermi surface has van Hove singularities [1]. Our present work aims at a complete analytical understanding of this quantum phase transition.

Motivated by experiments, the general question of coexistence of ferromagnetism and superconductivity has received a lot of attention. In particular, some authors claimed that coexistence of ferromagnetism with s–wave superconductivity is possible even in simple one–band models [2].

We have done a mean–field analysis of possible coexistence [3]. No coexistence is possible, contrary to the claim in [2]. The mean-field solution found in [2] corresponds to a maximum of the free energy. Triplet superconductivity can coexist with ferromagnetism on the mean–field level.

[1] C. Honerkamp, M. Salmhofer, *Phys. Rev. Lett.* **87** (2001) 187004, *Phys. Rev.* **B 64** (2001) 184516
[2] N.I. Karchev, K.B. Blagoev, K.S. Bedell, P.B. Littlewood, Phys. Rev. Lett. 86 (2001) 846
[3] C. Husemann, diploma thesis, 2004

16.5 Effective Action in Two–Dimensional Fermion Systems

W. de Siqueira Pedra, M. Salmhofer

The method of posing counterterms in constructive field theoretic studies of two–dimensional fermion systems leads to the inversion problem which has been solved to all orders in perturbation theory [2] but not yet nonperturbatively. We introduce a new RG flow where the Fermi surface is adjusted dynamically in the flow. This allows us to give a nonperturbative construction of two–dimensional Fermi systems with a regular Fermi surface at the temperature above the critical temperature for superconductivity without using counterterms. In the proof we combine the tree expansion of [5] with the arch expansion of Iagolnitzer and Magnen (see [3]) to extract overlapping loops [1] which are crucial for the regularity properties of the selfenergy [4].

We also use these techniques to prove uniqueness of the KMS states and to determine the low–energy effective action. This action is the natural input for a study of symmetry-broken phases.

[1] J. Feldman, M. Salmhofer, E. Trubowitz, *J. Stat. Phys.* **84** (1996) 1209–1336
[2] J. Feldman, M. Salmhofer, E. Trubowitz, *Comm. Pure Appl. Math.* **53** (2000) 1350–1384
[3] M. Disertori, V. Rivasseau, *Comm. Math. Phys.* **215**, 251,291 (2000)

[4] W. Pedra, M. Salmhofer, Fermi Systems in Two Dimensions and Fermi Surface Flows, to appear in the Proceedings of the ICMP 2003 and papers to appear
[5] M. Salmhofer, C. Wieczerkowski, *J. Stat. Phys.* **99** (2000) 557–586

16.6 Funding

Max–Planck–Institut für Mathematik, Leipzig
W. Pedra

Renormierungsgruppe in Fermisystemen: Fermiflächen mit Singularitäten
M. Salmhofer
DFG Sa 1362/1-1

The International Erwin-Schrödinger Institute for Mathematical Physics, Vienna
M. Salmhofer

University of Vienna and Austrian Federal Ministery for Education, Science and Culture.
M. Salmhofer

16.7 Organizational Duties

Manfred Salmhofer

- Head of the section *Theoretische und mathematische Grundlagen der Physik* of the *Deutsche Physikalische Gesellschaft*.
- Organization of the meetings of this section at the DPG spring meeting in celebration of the 125th birthday of Albert Einstein in Ulm, March 2004.
- Member of the advisory board of the Andrejewski foundation. Organization of the Andrejewski lectures in Leipzig.
- Organization of the research program *Quantum Many–Body Theory* at the International Erwin-Schrödinger Institute (ESI) for Mathematical Physics, Vienna, September — December, 2004, including the workshops *New mathematical problems in many–body theory* (September 6–11, 2004), *Flow equation days* (October 20-22, 2004) and *Progress in mathematical many–body quantum theory.* (December 1-4, 2004)
- Journal review: Phys. Rev. Lett, Phys. Rev. B, Comm. Math. Phys., Journal of the American Mathematical Society
- Grant review: Natural Science and Engineering Research Council (NSERC), Canada

16.8 Awards

Erwin-Schrödinger Institute Senior Research Fellow (M. Salmhofer)

16.9 External Cooperations

Academic

Universität München, Mathematisches Institut
Prof. Laszlo Erdös

Stanford University, Mathematics Department
Prof. Horng–Tzer Yau

The University of British Columbia, Mathematics Department
Prof. Joel Feldman

Max-Planck-Institut für Festkörperforschung, Stuttgart
Prof. Dr. Walter Metzner, Dr. Carsten Honerkamp

ETH Zürich, Theoretische Physik
Prof. Maurice T. Rice

ETH Zürich, Mathematik
Prof. Eugene Trubowitz, Prof. Horst Knörrer

16.10 Publications

Journals

C. Landim, J. Quastel, M. Salmhofer, H.T. Yau
Superdiffusivity of asymmetric exclusion processes in dimensions one and two
Comm. Math. Phys. 244, No. 3 (2004) 455-481

L. Erdös, M. Salmhofer, H.-T. Yau
On the Quantum Boltzmann Equation
J. Stat. Phys. 116 (2004) 367-380

M. Salmhofer, C. Honerkamp, W. Metzner, O. Lauscher
Renormalization Group Flows into Phases with Broken Symmetry
Prog. Theor. Phys. 112 (2004) 943-970

Other

M. Salmhofer
Book review of *Fermionic Functional Integrals and the Renormalization Group*
by Feldman, Joel; Knörrer, Horst; Trubowitz, Eugene
Zentralblatt für Mathematik.
Expanded version published as `http://www.emis.de/misc/articles/FKT/`

Talks and Conference Contributions

M. Salmhofer
Fermionic Renormalization Group
three lectures at the winter school *Renormalization Group Methods for Interacting Electrons*, July 12th to August 6th, 2004 International Center of Condensed Matter Physics, Brasilia, DF - Brazil

M. Salmhofer
Renormalization Group and Fermi Liquid Theory
Departamento de Fisica Matematica, Instituto de Fisica, Sao Paulo, August 10, 2004

M. Salmhofer
Renormalization Group: Analysis and Applications
12 lectures in the ESI lecture series, International Erwin-Schrödinger Institute for Mathematical Physics, Vienna, September — December, 2004

M. Salmhofer
The Wilson RG: Analysis and Applications
Institut für Theoretische Physik, Universität Wien, December 7, 2004

M. Salmhofer
Many–body systems and functional integrals
Berlin–Leipzig Analysis and Stochastics Seminar, Max–Planck Institute for Mathematics in the Sciences, Leipzig December 21, 2004

O. Lauscher
Evidence for the nonperturbative renormalizability of Quantum Einstein Gravity
International Conference QMath9, September 12th-16th 2004, Giens, France

W. Pedra
Flot de renormalisation avec des surfaces de Fermi adaptatives
International Conference QMath9, September 12th-16th 2004, Giens, France

16.11 Graduations

Diploma

C. Husemann
Über die Koexistenz von Ferromagnetismus und Supraleitung auf Mean–Field–Niveau

16.12 Guests

Prof. Dr. Volker Bach
Universität Mainz
January 5–7, 2004

Prof. Dr. Jürg Fröhlich
ETH Zürich
May 24–29, 2004

Prof. Dr. Laszlo Erdös
Universität München
August 23–26, 2004

Prof. Dr. Horng–Tzer Yau
Stanford University
August 23–26, 2004

Diffusion Fundamentals I

UNIVERSITÄT LEIPZIG

Basic Principles of Theory, Experiment and Application

September 22nd - 24th, 2005
Leipzig, Germany

150 years after *Adolf Fick*'s and 100 years after *Albert Einstein*'s fundamental papers on diffusion, the world-wide community of researchers in the field of diffusion is invited to Leipzig, the place of publication of these papers, to highlight the current developments in the field.

The talks will address a broad, interdisciplinary audience rather than only the specialists in the different fields.

- One and a Half Century of Diffusion: Fick, Einstein, and some Figures before and after (*Jean Philibert,* Paris)
- From Diffusion to Anomalous Diffusion: A Century after Einstein's Brownian Motion (*Yossi Klafter,* Tel Aviv)
- How two Pairs of Magnetic Field Gradient Pulses Give Access to New Information about Molecular Dynamics (*Paul Callaghan,* Wellington)
- Solution Dynamics and Self-Organization (*William S. Price,* Sydney)
- Diffusion Measurements in Fluids by Dynamic Light Scattering (*Alfred Leipertz,* Erlangen)
- Analogies in Diffusion of Atoms, Animals, Men and Ideas (*Gero Vogl,* Wien)
- Molecular Simulation Studies of Diffusion in Zeolites and Amorphous Polymers (*Doros N. Theodorou,* Athens)
- Anomalous Transport in Complex Networks (*Shlomo Havlin,* Ramat Gan)
- Single-File Diffusion far from Equilibrium (*Gunter Schütz,* Jülich)
- Diffusion of Photons in Human Tissues (*George H. Weiss,* Bethesda)
- Molecular Motors (*Jacques Prost,* Paris)
- How Molecules Dance in Lipid Membranes (*Ilpo Vattulainen,* Helsinki)
- Biological Interpretation of Anomalous Subdiffusion (*Michael Saxton,* Davis)
- Diffusion in Nanocrystals (*Alan Chadwick,* Canterbury)
- Phenomenological Coefficients in Solid-State Diffusion (*Graeme E. Murch,* Newcastle)
- Solid-State Diffusion and NMR (*Paul Heitjans*, Hannover)
- Effects of Pore Heterogeneity on Diffusion in Nanopores (*Marc-Olivier Coppens,* Delft)
- Molecular Diffusion under Confinement (*Jörg Kärger,* Leipzig)
- Diffusion in Microporous Materials and its Technological Impact (*Douglas M. Ruthven,* Orono)

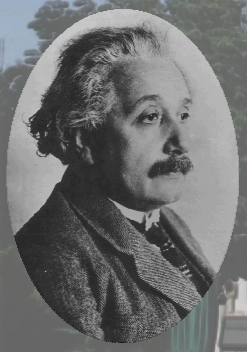

Sessions' chairmen and introduction to the posters:
Dezsö L. Beke (Debrecen)
Armin Bunde (Gießen)
Jacques Fraissard (Paris)
Heiner Kaden (Meinsberg)
Josef Käs (Leipzig)
Freek Kapteijn (Delft)
Helmut Mehrer (Münster)
Harry Pfeifer (Leipzig)

visit **www.diffusion-fundamentals.org** for complete up-to-date information

jointly organized by

Universität Leipzig

Deutsche Physikalische Gesellschaft

Sächsische Akademie der Wissenschaften zu Leipzig

DECHEMA - Gesellschaft für Chemische Technik und Biotechnologie e.V.

Deutsche Bunsen-Gesellschaft für Physikalische Chemie

Gesellschaft Deutscher Chemiker e.V.

Universität Hannover

ISBN 3-934178-46-4